

ABSTRACT

Title of Document:

SYNTHESIS AND APPLICATION OF
DOUBLE CAVITY CUCURBITURILS

James B. Wittenberg, Ph.D., 2012

Directed By:

Professor, Lyle Isaacs
Department of Chemistry and Biochemistry

Molecular containers are a unique set of compounds that are able to recognize and associate with other molecules. It is these molecular recognition properties that has resulted in a large number of research groups studying such phenomena. The cucurbit[n]uril (CB[n]) family of macrocyclic hosts are well known for their high binding affinities and selectivity towards guests, particularly ammonium compounds, in water. Synthesizing new types of CB[n] hosts will lead to new and exciting applications for these exceptional molecular receptors.

Chapter 1 introduces the concept and importance of noncovalent interactions. A review of cucurbit[n]uril chemistry, including the *nor-seco*-cucurbit[n]urils and glycoluril hexamer, is covered. The potential applications of the double cavity host, *bis-nor-seco*-cucurbit[10]uril (*bis-ns*-CB[10]), and of the mono-functionalized CB[6] derivatives recently synthesized are discussed. The wide range of applications incorporating CB[8] as a host for ternary complexes is also reviewed.

Chapter 2 describes the synthesis of a new double cavity host (**II-1**) derived from bis-*ns*-CB[10]. Host **II-1** is synthesized by the double bridging reaction of bis-*ns*-CB[10] with **II-2** under acidic conditions. Host **II-1** binds a variety of aliphatic and aromatic ammonium ions (**II-3–II-17**) in water as the corresponding ternary complexes. Conducting the bridging reaction in the presence of guest **II-4** delivers [3]rotaxane **II-1•II-4₂** by a clipping process, the first published rotaxane of a cucurbituril prepared *via* a clipping mechanism.

Chapter 3 describes the synthesis and potential application of two new double cavity hosts (**III-1** and **III-2**) synthesized through condensation of two equivalents of glycoluril hexamer (**III-3**) with one equivalent of tetra-aldehydes **III-4** and **III-5**, respectively. Host **III-1** has been shown to bind four different PEG derivatives (**III-16₃₀₀**, **III-16₁₀₀₀**, **III-16₃₃₅₀**, **III-16₁₀₀₀₀**) in D₂O, and the degree of polymerization was measured by diffusion ordered spectroscopy (DOSY). The highly symmetrical and rigid host **III-2** binds to synthesized guests **III-20** – **III-23** to form discrete complexes and supramolecular ladders.

SYNTHESIS AND APPLICATION OF DOUBLE CAVITY CUCURBITURILS

By

James B. Wittenberg

Dissertation submitted to the Faculty of the Graduate School of the
University of Maryland, College Park, in partial fulfillment
of the requirements for the degree of
Doctor of Philosophy
2012

Advisory Committee:

Professor Lyle Isaacs, Chair

Professor Daniel Falvey

Professor Andrei Vedernikov

Professor Steven Rokita

Associate Professor Volker Briken, Dean's Representative

© Copyright by
James B. Wittenberg
2012

Dedication

To my parents George and Cindy Wittenberg,
and to my fiancée Stefanie.

Acknowledgements

I would like to thank my Ph.D. advisor Professor Lyle Isaacs for all of the time and effort he has put forth in guiding me through my graduate career. I have learned more about chemistry and how to be a successful scientist than I ever thought I would. Through his teachings and support I feel as though I am well prepared to be a successful researcher and scientist throughout my professional career.

I would like to thank two undergraduate professors of mine, Professors Ron Hess and Tom Rutledge. Thank you Professor Hess for your advice and guidance both in the classroom and in the lab. Thank you Professor Rutledge for inspiring me to pursue a Ph.D. in chemistry.

I would like to thank the former Isaacs group members for teaching me essential laboratory techniques and answering all my questions during the initial stages of my graduate research. I would especially like to thank Dr. Derick Lucas for not only his scientific help and input but also for his continued friendship. Also, thank you Matt Costales for being a very valuable undergraduate research assistant and teammate. Matt was a great mentee for many years.

I would like to thank the current Isaacs group members not only for making our lab a great place to work but also for all the collaborative efforts and input. Thank you to Dr. Yiu-Fai Lam and Dr. Yinde Wang for your expert NMR advice.

Finally, I would like to thank my parents, George and Cindy Wittenberg, and my soon to be wife, Dr. Stefanie Sherrill, for all of their support, understanding, and encouragement they have given me throughout my graduate school career. I could not have done it without you.

Table of Contents

| | |
|---|-----|
| Dedication..... | ii |
| Acknowledgements..... | iii |
| Table of Contents..... | iv |
| List of Tables..... | vi |
| List of Figures..... | vii |
| Chapter 1: Formation of Ternary Complexes and Dynamic Materials Through Noncovalent Interactions..... | 1 |
| 1.1 Introduction..... | 1 |
| 1.2 Popular Molecular Containers..... | 2 |
| 1.3 Some Applications of Molecular Receptors..... | 3 |
| 1.4 Synthesis and Recognition Properties of Cucurbit[n]urils..... | 8 |
| 1.5 Nor-seco-cucurbit[n]urils..... | 13 |
| 1.5.1 <i>Nor-seco-cucurbit[6]uril</i> | 14 |
| 1.5.2 <i>Bis-nor-seco-cucurbit[10]uril</i> | 15 |
| 1.6 Glycoluril Hexamer (I-33)..... | 18 |
| 1.6.1 CB[6] Derivatives Synthesized From Hexamer..... | 20 |
| 1.7 Ternary Complexes Using Cucurbit[8]uril..... | 23 |
| 1.7.1 CB[8] Molecular Loop Lock..... | 24 |
| 1.7.2 CB[8] Induced Self-assembly..... | 25 |
| 1.7.3 CB[8] Polymers..... | 28 |
| 1.7.4 CB[8] Induced Heterodimerization of Functionalized Proteins..... | 31 |
| 1.8 Summary and Conclusions..... | 32 |
| Chapter 2: A Clipped [3]Rotaxane Derived from <i>Bis-nor-seco-cucurbit[10]uril</i> | 34 |
| 2.1 Introduction..... | 34 |
| 2.2 Scale-up Synthesis of Bis-ns-CB[10]..... | 35 |
| 2.3 Synthesis of Host II-1..... | 36 |
| 2.4 Characterization of Host II-1..... | 37 |
| 2.5 Physical Properties of Host II-1 Studied by X-Ray Crystallography..... | 38 |
| 2.6 Molecular Recognition Properties of Host I Studied by ¹ H NMR Spectroscopy..... | 40 |
| 2.7 Formation of a [3]Rotaxane..... | 42 |
| 2.8 Mechanistic Study on the Formation of [3]Rotaxane II-1•II-4 ₂ | 43 |
| 2.9 Conclusions..... | 44 |
| Chapter 3: Higher Order Complexes Formed from Cucurbit[6]uril Dimers..... | 45 |
| 3.1 Introduction..... | 45 |
| 3.2 Synthesis of Two Cucurbit[6]uril Dimer Hosts..... | 45 |
| 3.3 X-Ray Crystal Structure and Physical Properties of Host III-1..... | 48 |
| 3.4 Supramolecular Polymer Formation..... | 50 |
| 3.4.1 Synthesis of Poly(ethylene glycol) Guests Bearing Two Hexanediamine Units..... | 51 |
| 3.4.2 Attempted Formation of Supramolecular Polymers Between Host III-1 and Guests III-16 Studied by Diffusion Ordered Spectroscopy..... | 52 |

| | | |
|--------------|--|-----|
| 3.5 | Supramolecular Ladder Formation..... | 59 |
| 3.5.1 | Design and Synthesis of III-20 – III-23 as Oligovalent Guests for Formation of Ladder Polymers with Double Cavity Host III-2..... | 60 |
| 3.6 | Conclusions..... | 78 |
| Chapter 4: | Summary and Future Work..... | 79 |
| 4.1 | Summary..... | 79 |
| 4.2 | Future Work..... | 80 |
| Appendix 1 | | 84 |
| Appendix 2 | | 122 |
| Bibliography | | 191 |

List of Tables

Chapter 1

Table I-1. Binding constants measured for some guests that form 1:1 complexes with CB[n].

Chapter 3

Table III-1. Diffusion Coefficients obtained by DOSY NMR (600 MHz, D₂O, 298 K).

Table III-2. Diffusion Coefficients obtained by DOSY NMR (600 MHz, D₂O, 298 K).

List of Figures

Chapter 1

- Figure I-1.** Chemical structures of crown ethers, calixarenes, and cyclodextrins.
- Figure I-2.** Recognition properties of cucurbiturils.
- Figure I-3.** Typical guests that form inclusion complexes with CB[n] hosts.
- Figure I-4.** Chemical structures of the *nor-seco*-cucurbit[n]urils.
- Figure I-5.** a) Representation of the relative size difference of the top and bottom portals in *ns*-CB[6] and b) the synthesis of mono-functionalized CB[6] *via ns*-CB[6].
- Figure I-6.** MMFF minimized molecular models for complexes a) bis-*ns*-CB[10]•**I18**₂ (n = 6) and b) bis-*ns*-CB[10]•**29**₂ where the non-bonded H₂C•••CH₂ distance was measured.
- Figure I-7.** Three possible binding motifs, or diastereomers, for bis-*ns*-CB[10] with two guests.

Chapter 2

- Figure II-1.** ¹H NMR spectra (400 MHz, D₂O, RT) recorded for: (a) **II-1**•**II-3**₂ (5 mM), (b) a mixture of **II-1** (5 mM) and **II-5** (n = 4) (10mM), (c) a mixture of **II-1** (5 mM) and **II-5** (n = 5) (10 mM), (d) a mixture of **II-1** (5 mM) and **II-5** (n = 6) (10 mM) and (e) a mixture of **II-1** (5 mM) and **II-5** (n = 7) (10 mM).
- Figure II-2.** Cross-eyed stereoview of the crystal structure of **II-1**•**II-3**₂. Color code: C, gray; H, white; N, blue; O, red; H-bonds, yellow-red striped.
- Figure II-3.** ¹H NMR spectrum (400 MHz, D₂O, RT) recorded for **II-1**•**II-4**₂.

Chapter 3

- Figure III-1.** ^1H NMR spectra (400 MHz, D_2O , RT) of a) guest **III-6** ($n = 6$), b) complex **III-1•III-6** ($n = 6$)₂, and c) complex **III-2•III-6** ($n = 6$)₂.
- Figure III-2.** A cross-eyed stereoview of the crystal structure of host **III-1** as the “P” enantiomer. Color code: C, gray; H, white; N, blue; O, red.
- Figure III-3.** A cross-eyed stereoview of the crystal packing of host **III-1**. Color code: C, gray; H, white; N, blue; O, red.
- Figure III-4.** A view of the crystal packing and H-bonding of **III-2** in the (a) x-z plane and the (b) y-z plane. Color code: C, gray; H, white; N, blue; O, red; H-bonds, red-yellow striped.
- Figure III-5.** Plots of the change in intensity of the indicative NMR resonances in the DOSY spectra as a function of magnetic field gradient recorded (600 MHz, D_2O , 298 K) for: a) guest **III-16**₁₀₀₀₀ and b) complex **III-1•III-16**₁₀₀₀₀.
- Figure III-6.** ^1H NMR spectra (400 MHz, D_2O , RT) recorded for: a) guest **III-20**, b) complex **III-2•III-20**₂, c) guest **III-21**, d) complex **III-2₂•III-21**₂, e) guest **III-22**, and f) complex **III-2₃•III-22**₂.
- Figure III-7.** Schematic representation of the formation of the a) 2:1, b) 2:2, c) 3:2, d) and potential 4:2 host•guest complexes.
- Figure III-8.** Plots of the change in intensity of the indicative NMR resonances in the DOSY spectra as a function of magnetic field gradient recorded (600 MHz, D_2O , 298 K) for: a) guest **III-22** and b) complex **III-2₃•III-22**₂.

Figure III-9. Proposed structures of the ions observed in the ESI-MS for a) **III-21**,
b) **III-22**, and c) **III-23**.

Figure III-10. ^1H NMR spectra recorded for: a) dimer guest **III-21**, b) **III-21** and **III-2** mixed together in a 2:1 ratio, and c) **III-21** and **III-2** mixed together in a 4:1 ratio.

Figure III-11. ^1H NMR spectra recorded for trimer guest **III-22** and host **III-2** mixed together in a a) 2:1 ratio, b) 2:2 ratio, and c) 2:3 ratio.

Figure III-12. ^1H NMR spectra recorded for tetramer guest **III-23** and host **III-2** mixed together in a a) 2:2 ratio, b) 2:3 ratio, and c) 2:4 ratio.

Chapter 4

Figure IV-1. Schematic representation of a supramolecular polymer controlled by:
a) guest exchange and b) pH change.

List of Schemes

Chapter 1

- Scheme I-1.** Schematic representation of the three possible pathways to rotaxane formation: a) slipping, b) threading, and c) clipping.
- Scheme I-2.** Stimuli induced unidirectional rotation of a macrocycle in a [2]catenane.
- Scheme I-3.** Schematic representation of polymer capsule formation induced by host•guest interactions.
- Scheme I-4.** Formation of a self-assembled ladder duplex controlled by the ratio of polymer to bipyridine.
- Scheme I-5.** Synthesis of cucurbituril *via* Behrend's procedure.
- Scheme I-6.** Synthesis of CB[5] – CB[10].
- Scheme I-7.** Schematic representation of the equilibrium between discrete and polymeric complexes with bis-*ns*-CB[10].
- Scheme I-8.** Templated synthesis of glycoluril hexamer (**I-33**).
- Scheme I-9.** Mono-functionalized CB[6] derivatives synthesized *via* condensation of glycoluril hexamer (**I-33**) with *o*-phthalaldehydes (**I-30**, **I-34**, and **I-35**).
- Scheme I-10.** Fluorescence assay based on fluorescent CB[6] derivative (**I-40**) quenched by association with a metal ion.
- Scheme I-11.** Formation of a CB[6] derivative that undergoes self-assembly.
- Scheme I-12.** Formation of a ternary complex with CB[8] and methyl viologen (**I-26**) upon reduction to the radical cationic species.

Scheme I-13. CB[8] molecular loop lock (CB[8]•**I-46**) induced by redox stimulus.

Scheme I-14. Electrochemical switching and size selection of a CB[8]-assembled dendrimer.

Scheme I-15. Schematic representation of a CB[8]-induced self-assembling receptor (CB[8]•**I-49**) for peptide recognition.

Scheme I-16. CB[8] complexation-induced polymeric systems.

Scheme I-17. Supramolecular polymerization driven by CB[8]-enhanced π - π interaction.

Scheme I-18. CB[8] induced protein FRET pair dimerization.

Chapter 2

Scheme II-1. Large-scale synthesis of bis-*ns*-CB[10].

Scheme II-2. Synthesis of Host **II-1**.

Scheme II-3. Possible mechanistic paths for the formation of **II-1**•**II-4₂**.

Chapter 3

Scheme III-1. Synthesis of two CB[6] dimer hosts (**III-1** and **III-2**).

Scheme III-2. Synthesis of PEG-based polymer guests **III-16₃₀₀** – **III-16₁₀₀₀₀**.

Scheme III-3. Possible host•guest systems formed when the double cavity host (**III-1**) is mixed with the polymer divalent guest (**III-16_{MW}**).

Scheme III-4. Synthesis of the viologen-based guests **III-20** – **III-23**.

Scheme III-5. Possible intermediates in the formation of the 3:2 supramolecular ladder complex (**III-2₃**•**III-22₂**).

Scheme III-6. Possible intermediates in the formation of the proposed 4:2 supramolecular ladder complex (**III-2₄•III-23₂**).

Chapter 4

Scheme IV-1. Schematic representation of the synthesis of: a) potential new bis-*ns*-CB[10] derivatives and b) glycoluril derivatives.

List of Charts

Chapter 2

Chart II-1. Guests used in this study.

Chapter 3

Chart III-1. Guests used in this study.

List of Abbreviations

| | |
|---------------------------------|---|
| AgNO ₃ | silver nitrate |
| Å | angstrom |
| Boc | <i>tert</i> -butoxy |
| br | broad |
| CB[n] | cucurbit[n]uril |
| CHCl ₃ | chloroform |
| CH ₃ CN | acetonitrile |
| CT | charge transfer |
| <i>D</i> | diffusion coefficient |
| d | doublet |
| D ₂ O | deuterium oxide |
| CH ₂ Cl ₂ | dichloromethane |
| DLS | dynamic light scattering |
| DMF | dimethylformamide |
| DMSO | dimethylsulfoxide |
| DOSY | diffusion-ordered spectroscopy |
| ESI-MS | electrospray ionization-mass spectrometry |
| FRET | fluorescence resonance energy transfer |
| g | gram |
| GFP | green fluorescent protein |
| h | hour |
| HDA | hexanediamine |

| | |
|--------------------------------|----------------------------------|
| HCl | hydrochloric acid |
| H ₂ SO ₄ | sulfuric acid |
| Hz | hertz |
| K | kelvin |
| IR | infrared |
| ITC | isothermal titration calorimetry |
| <i>J</i> | coupling constant |
| KBr | potassium bromide |
| KOH | potassium hydroxide |
| m | multiplet |
| M | molar |
| M ⁺ | molecular ion |
| MeOH | methanol |
| MHz | megahertz |
| min | minute |
| mM | millimolar |
| MMFF | Merck molecular force field |
| M.p. | melting point |
| MV | methyl viologen |
| MW | molecular weight |
| <i>m/z</i> | mass to charge ratio |
| NaOH | sodium hydroxide |
| NaAuCl ₄ | sodium tetrachloroaurate(III) |

| | |
|---------------------------------|---------------------------------|
| Na ₂ SO ₄ | sodium sulfate |
| N(Bu) ₄ Cl | tetrabutylammonium chloride |
| NH ₄ OH | ammonium hydroxide |
| NMR | nuclear magnetic resonance |
| Np | naphthyl |
| <i>o</i> | <i>ortho</i> |
| <i>p</i> | <i>para</i> |
| PEG | poly(ethylene glycol) |
| PES | poly(ethersulfone) |
| PF ₆ | hexafluorophosphate |
| PI | poly(isoprene) |
| ppm | parts per million |
| RB | round-bottom |
| RT | room temperature |
| s | singlet |
| t | triplet |
| <i>t</i> -BuOK | potassium <i>tert</i> -butoxide |
| TFA | trifluoroacetic acid |
| THF | tetrahydrofuran |
| Trp | tryptophan |
| Ts | toluenesulfonyl |
| W | watt |
| YFP | yellow fluorescent protein |

Chapter 1: Formation of Ternary Complexes and Dynamic Materials Through Noncovalent Interactions.

1.1 Introduction.

Supramolecular chemistry encompasses the study of non-covalent interactions between two or more compounds that arrange and assemble in a specific way. It is these non-covalent interactions (i.e. hydrogen bonding, ion – dipole, dipole – dipole, $\pi - \pi$, metal coordination, hydrophobic effects, and van der Waals forces) that govern the assembly of multiple compounds into a larger architecture. It was not until the work of Lehn,¹ Cram,² and Pedersen,³ who studied the molecular recognition properties of crown ethers and cryptands as metal ion receptors – and were awarded the Nobel Prize in 1987 for their achievements – that there was a surge in supramolecular chemistry research in the hopes of mimicking the behavior of biological molecules with synthetic compounds. Since then, the amount of research devoted to supramolecular chemistry and the study of molecular recognition has exploded. Many new families of receptors, including molecular containers, have been discovered and used in a wide variety of applications. This chapter will first discuss the most widely known and used molecular containers as well as some of their unique applications. The synthesis and application of the cucurbit[n]uril family and glycoluril hexamer will then be discussed. Finally, the ability of cucurbit[8]uril to form ternary complexes and its uses will be examined.

1.2 Popular Molecular Containers.

In order to study noncovalent interactions effectively for the purpose of applying the gained knowledge on a wide variety of applications, such as catalysis, sensors, molecular machines, supramolecular polymers, and drug delivery systems, supramolecular chemists have designed and synthesized a number of receptors. Some of the most studied receptors include crown ethers, calixarenes, and cyclodextrins (Figure I-1).⁴⁻⁶ Each family of receptor possesses specific properties, namely its selectivity and affinity for an analyte, that set it apart from the next receptor. For example, crown ethers are well known to bind metal ions within their cavity due to the favorable ion – dipole interactions between the O lone pairs and the M^+ ion. Both calixarenes and cyclodextrins have a hydrophobic cavity that arises from their bowl shape structure, and both are known to bind a variety of hydrophobic small molecules and ions.

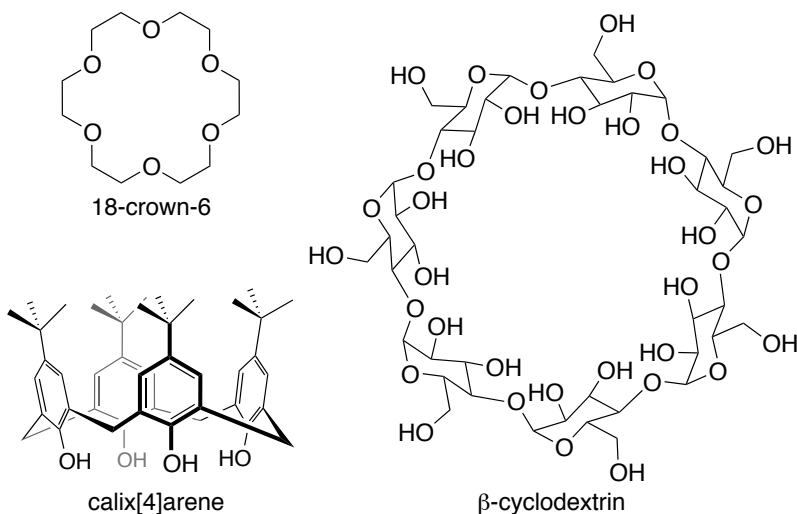


Figure I-1. Chemical structures of crown ethers, calixarenes, and cyclodextrins.

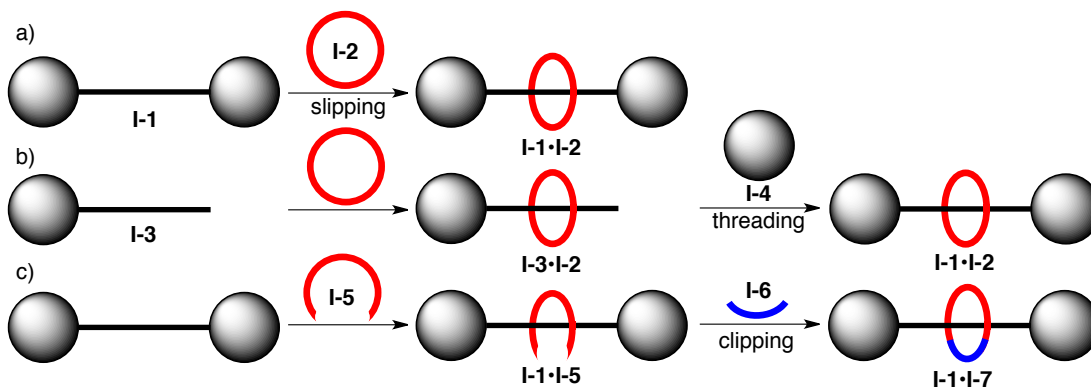
Cyclodextrins, in particular, have been widely used for industrial applications because they are inexpensive, commercially available, easily functionalized, and soluble in a variety of solvents. For example, they are used in the household product Febreze® where a functionalized β -cyclodextrin acts as the active ingredient and traps odor molecules.^{7,8} They have also been used for drug sequestration. Suggamadex is a functionalized γ -cyclodextrin known to sequester the anesthetic drug rocuronium and reverses the effects of the neuromuscular blocking agent.⁹⁻¹¹ Although cyclodextrins possess many favorable characteristics, they display only moderate molecular recognition properties, or binding affinity ($\sim 10^2$ - 10^4 M⁻¹) and selectivity. Many research groups have worked with various molecular containers to improve on the benchmark set by cyclodextrins. A large number of new hosts with very interesting properties have been reported in recent years.¹²⁻¹⁵

1.3 Some Applications of Molecular Receptors.

Molecular receptors can be utilized in a wide variety of applications as described earlier. The surface of their potential in real-life applications has only been scratched. There are many research groups inventing new supramolecular molecules to perform new tasks. Old molecular receptors, such as cyclodextrins, are being applied in new and inventive ways as well. This section highlights a number of examples of applications of some molecular receptors.

Artificial molecular machines are unique supramolecular assemblies that can perform machine-like motions when exposed to an external stimulus, such as light, redox, or pH change.¹⁶ Designing and synthesizing nano-sized machines has gained

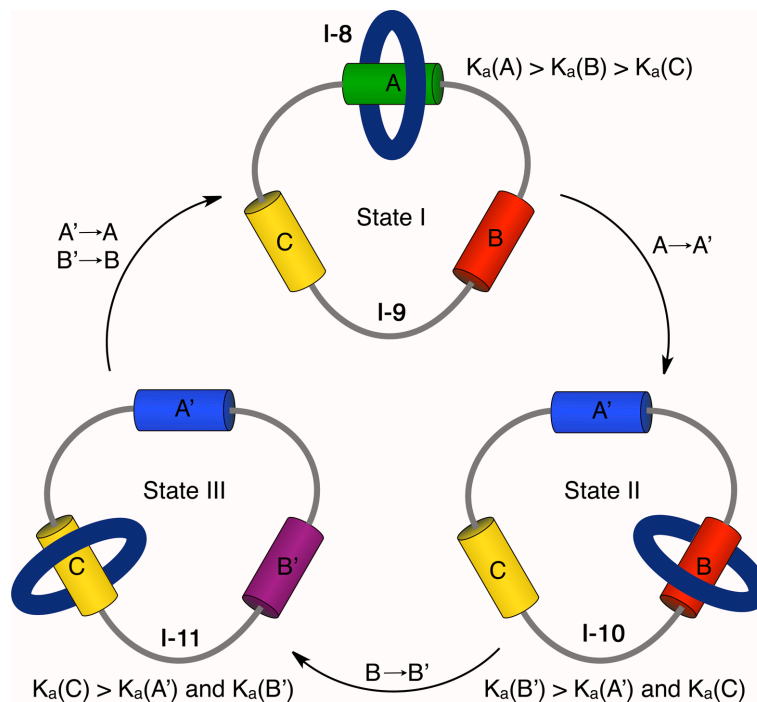
great interest due to their potential applications. One popular approach is the formation of rotaxanes, or mechanically interlocked molecules. Molecular motion can be implemented through rotaxanes in the form of shuttling, threading/dethreading, and rotational motions. Rotaxanes can be synthesized in three ways: (a) a preformed macrocycle (**I-2**) is slipped of one end of a dumbbell-shaped rod (**I-1**) to form **I-1•I-2**, (b) a preformed macrocycle (**I-2**) is threaded onto a rod containing only one bulky end-group (**I-3**) to form **I-3•I-2** then capped with another bulky group (**I-4**) to form **I-1•I-2**, and (c) an incomplete macrocycle (**I-5**) can associate around the center of a dumbbell-shaped rod (**I-1**) then clipped in place with **I-6** to form the complete macrocycle (**I-7**) and the rotaxane **I-1•I-7** (Scheme I-1).



Scheme I-1. Schematic representation of the three possible pathways to rotaxane formation: a) slipping, b) threading, and c) clipping.

Catenanes are a specific type of rotaxane where two or more macrocycles are interconnected. They are synthesized through the clipping mechanism shown above (Scheme I-1c) but in the place of the dumbbell rod is the other macrocycle. This specific synthetic route makes them more challenging to create. However, some very interesting molecular motors made of catenanes have been reported, specifically from

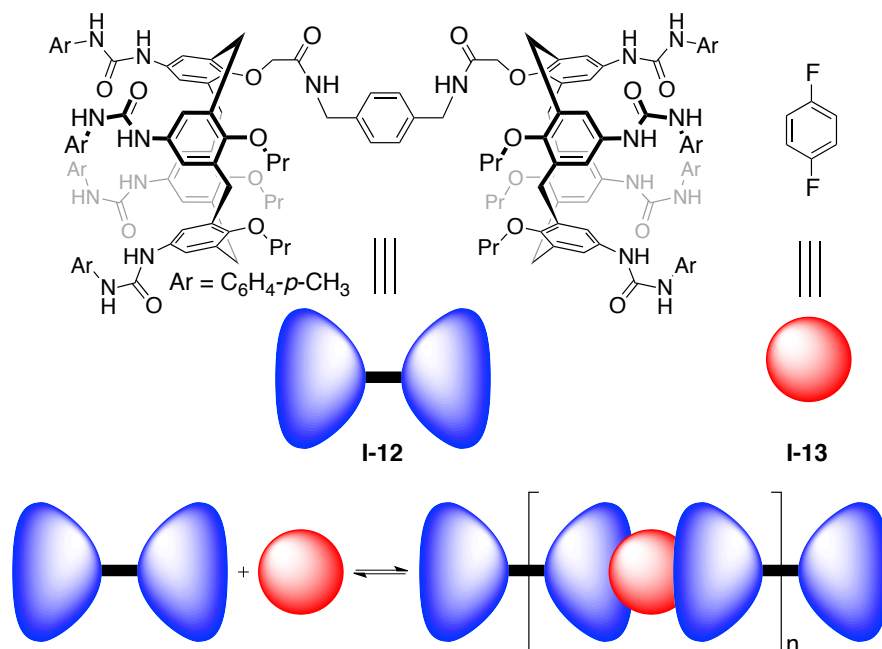
the Leigh group.^{12,13} In 2003, Leigh and co-workers synthesized a [2]catenane (**I-8**•**I-9**), or a catenane involving two macrocycles, in which one macrocycle rotated around the second macrocycle (Scheme I-2).¹² The larger of the two macrocycles (**I-9**) possessed three different binding sites, each site with a different binding affinity towards the smaller macrocycle. In State 1, the binding affinity is greatest towards station A. Upon photo isomerization of A into A' (**I-10**) the binding affinity is reduced to below the affinity for station B, and the smaller macrocycle slides to bind station B. Similarly, upon photo isomerization of station B to B' (**I-11**) the binding affinity is reduced to below the affinity for station C, and the macrocycle slides again to bind station C. Once A' and B' are returned to their original isomer state (**I-9**) the macrocycle slides to bind station A again, and the process can be repeated.



Scheme I-2. Stimuli induced unidirectional rotation of a macrocycle in a [2]catenane.

Supramolecular polymers present an attractive field of research due to their dynamic nature and ability to respond to external stimuli that can enhance or discourage the monomeric units to remain intact.^{17,18} It is the noncovalent interactions that govern the mechanical properties of the resulting polymeric materials. Therefore, the controlling the noncovalent interactions allows for control over the physical properties of the material.

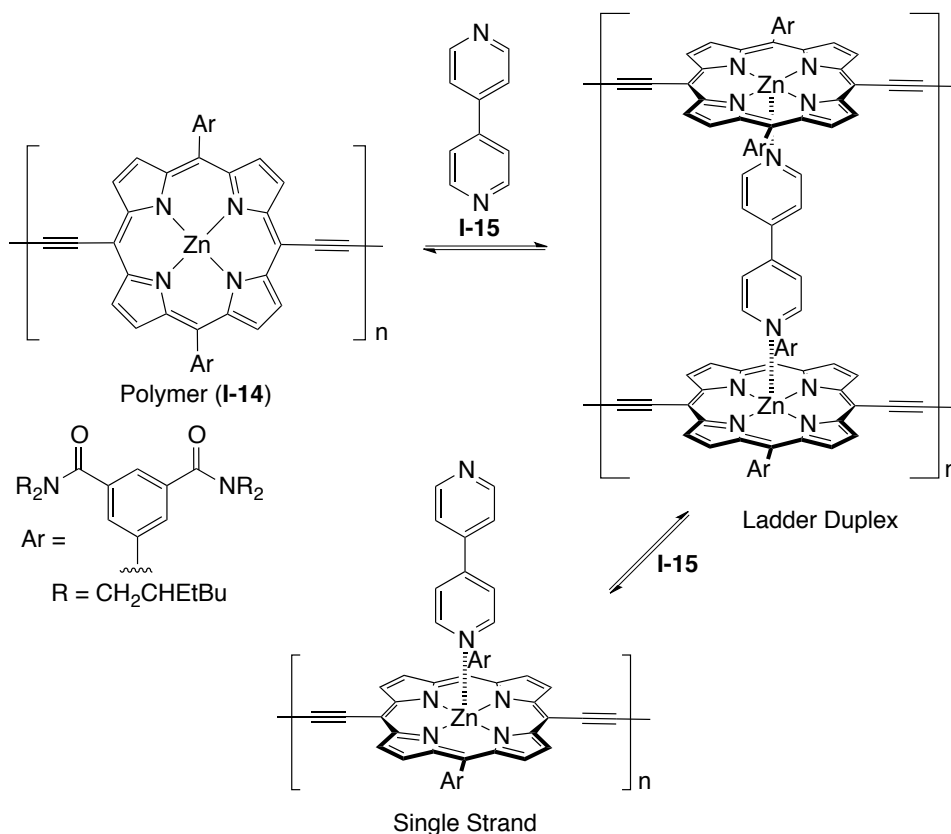
There are many molecular receptors that have been used to create a variety of supramolecular polymers. One example, shown in Scheme I-3, reported by Rebek and co-workers involves the formation of polycaps, or polymer capsules.¹⁴ The molecular receptor was constructed from two calix[4]arenes functionalized with ureidyl groups along the upper rims and covalently connected through an aromatic linker (**I-12**). In solution, two capsules interact through H-bonding of the ureidyl groups, as seen by downfield-shifting of the ureidyl H-atoms in the ¹H NMR spectrum. However, when *p*-difluorobenzene (**I-13**) is introduced to the system it creates an inclusion complex with the calix[4]arene capsule (**I-12•I-13**), and the equilibrium is driven towards the formation of a polymeric material, or polycaps, evidenced by ¹H NMR.



Scheme I-3. Schematic representation of polymer capsule formation induced by host•guest interactions.

Noncovalent interactions can also be used to control the physical properties of preformed polymeric materials. If the polymer is susceptible to noncovalent interactions from a second compound then the properties of the initial polymer will be altered, and a number of new polymeric materials may arise by controlling the stoichiometry between the two materials. In 2002, the Anderson group reported on a self-assembled double-strand conjugated porphyrin polymer ladder (Scheme I-4).¹⁵ A preformed zinc porphyrin-based conjugated polymer (**I-14**), known to be used in optical applications, was the starting material chosen for this experiment. Upon addition of one 4,4'-bipyridyl (**I-15**) for every two porphyrin units, **I-15** coordinates with two Zn-centers to undergo self-assembly and form a ladder polymer duplex. This ladder duplex displayed an amplification of optical nonlinearity by one full order

of magnitude due to the rigidity of the ladder duplex over the original polymer. Interestingly, the ladder can be broken up into a single strand upon addition of excess **I-15**, where every zinc porphyrin in **I-14** is coordinated to one **I-15**.

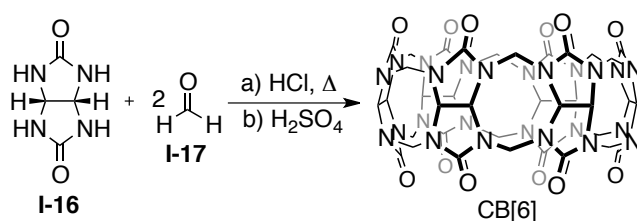


Scheme I-4. Formation of a self-assembled ladder duplex controlled by the ratio of polymer to bipyridine.

1.4 Synthesis and Recognition Properties of Cucurbit[n]urils.

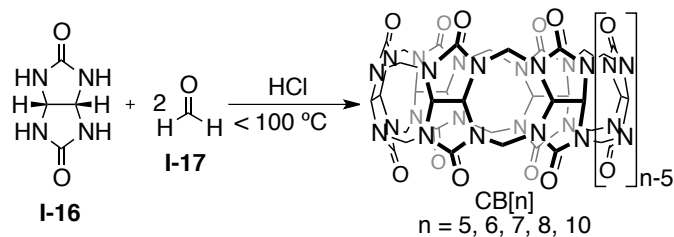
In 1905, Behrend and co-workers reported on a condensation reaction between one equivalent glycoluril (**I-16**) and two equivalents formaldehyde (**I-17**) in concentrated HCl which resulted in a polymeric substance that was dubbed

“Behrend’s polymer.”¹⁹ A crystalline solid was obtained upon recrystallization from concentrated H₂SO₄. It was discovered that this crystalline material was able to form complexes with materials such as KMnO₄, AgNO₃, and NaAuCl₄. However, the chemical structure of this interesting compound remained unknown for the next 75 years. In 1981, Mock took a closer look at the material that was first discovered by Behrend, and after obtaining the X-ray crystallographic data determined that the compound was a highly symmetrical macrocyclic structure composed of six glycoluril units and 12 methylene bridges that resembled a pumpkin, thus naming the compound “cucurbituril” after *cucurbitaceae*, or the gourd family (Scheme I-5).²⁰



Scheme I-5. Synthesis of cucurbituril *via* Behrend’s procedure.

Since Mock’s discovery of cucurbituril, now known as cucurbit[6]uril (CB[6]) where 6 represents the number of glycoluril units that make up the macrocycle, there have been many research groups focused on the development of the field of cucurbiturils. Due to the pioneering work of Mock,^{21,22} Buschmann,^{23,24} Day,²⁵ Kim,^{26,27} and Isaacs²⁸⁻³¹ the isolation of CB[5], CB[6], CB[7], CB[8], and CB[10], which can be synthesized using concentrated HCl as the solvent at temperatures less than 100 °C (Scheme I-6), has been established as well as a clear understanding of the mechanism of formation of the cucurbit[n]urils and their acyclic glycoluril oligomer intermediates.



Scheme I-6. Synthesis of CB[5] – CB[10].

The cucurbit[n]uril macrocycles possess some unique structural properties that set them apart from other typical molecular containers, such as cyclodextrins and calixarenes, in terms of their binding capability. There are two highly electrostatically negative carbonyl portals lining the top and bottom of the structure that are excellent sites for H-bonding, and ion–dipole interactions to occur with a guest molecule. The C-shaped glycoluril units also form a sizeable cavity in the center of the structure that can accommodate hydrophobic moieties of various guest molecules. Figure I-2 demonstrates the favorable interactions that can occur between the cucurbit[n]uril host and a guest to form an inclusion complex.

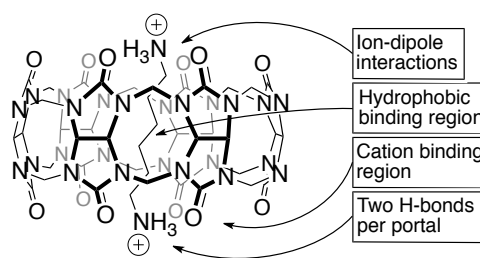


Figure I-2. Recognition properties of cucurbiturils.

Cucurbiturils are ideally situated to form strong host•guest complexes with alkyl and aryl ammonium guests.²¹⁻²⁴ Due to the variety of CB[n] host size, where the portal diameters range from 2.4 – 11.0 Å and the cavity volumes range from 82 –

>500 Å,³² CB[n]s can bind to a wide variety of guests with high affinity and high selectivity (Figure I-3). A number of binding constants are listed in Table I-1 for a various CB[n]•guest complexes.^{21,33,34} The rigid structure of cucurbiturils enhances the selectivity and binding ability for a specific size host. For example, CB[7] is able to bind to compound **I-27** with a binding constant of $3 \times 10^{15} \text{ M}^{-1}$, which is on the scale of avidin-biotin affinity. The binding constant measured for CB[7]•**I-22** is $4.2 \times 10^{12} \text{ M}^{-1}$. However, the binding constant for CB[8]•**I-22** decreases to $8.2 \times 10^8 \text{ M}^{-1}$, and no cavity binding occurs between CB[6] and **I-22** due to the difference in host cavity volume.

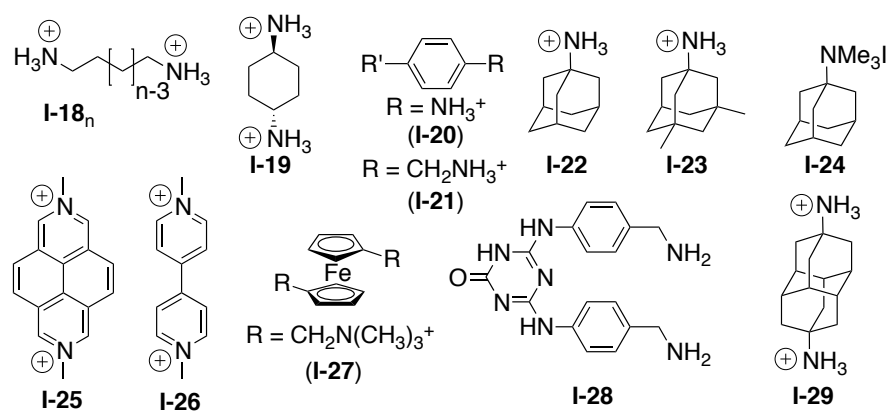


Figure I-3. Typical guests that form inclusion complexes with CB[n] hosts.

Table I-1. Binding constants measured for some guests that form 1:1 complexes with CB[n].

| Guest | CB[6] (M^{-1}) | CB[7] (M^{-1}) | CB[8] (M^{-1}) |
|---------------------|--------------------|----------------------|----------------------|
| I-18 (n = 4) | 1.5×10^5 | - | - |
| I-18 (n = 5) | 2.4×10^6 | - | - |
| I-18 (n = 6) | 2.8×10^6 | 9.0×10^7 | - |
| I-19 | 1.4×10^6 | 2.3×10^8 | - |
| I-20 | 1860 | 2.1×10^6 | - |
| I-21 | 550 | 1.8×10^9 | - |
| I-22 | - | 4.2×10^{12} | 8.2×10^8 |
| I-23 | - | 2.5×10^4 | 4.3×10^{11} |
| I-24 | - | 1.7×10^{12} | 9.7×10^{10} |
| I-25 | - | 3.8×10^7 | 6.4×10^8 |
| I-26 | - | 1.3×10^7 | 1.1×10^5 |
| I-27 | - | 3.0×10^{15} | - |
| I-28 | - | 1.7×10^7 | 5.8×10^{10} |

There are many favorable features to the cucurbit[n]uril family that can be utilized for a wide variety of applications.^{27,32} There are some limitations, however, such as poor solubility and lack of functionalization that have hindered its use in industrial applications. The following sections describe the synthesis, characterization, and applications of some new members of the CB[n] family that possess some unique physical properties and focus on decreasing the limitations of traditional CB[n] macrocycles.

1.5 *Nor-seco-cucurbit[n]urils.*

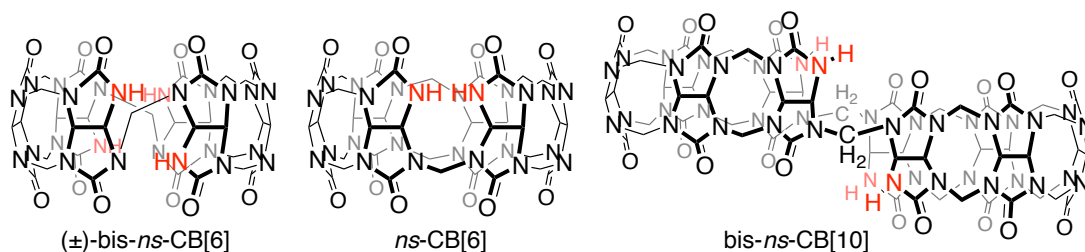


Figure I-4. Chemical structures of the *nor-seco-cucurbit[n]urils*.

In recent years, a number of new cucurbituril host derivatives have been synthesized that lack one or more methylene bridges (Figure I-4). A normal cucurbituril condensation reaction requires two equivalents of formaldehyde (**I-17**) for every glycoluril (**I-16**). However, by starving the reaction mixture of less than two equivalents of **I-17** per unit **I-16** under the right reaction conditions one is able to synthesize such unique CB[n] derivatives. (±)-Bis-*nor-seco*-CB[6] is the first chiral CB[n] ever synthesized formed from two glycoluril trimer units that are attached through two methylene bridges instead of four as in CB[6].³⁵ *Nor-seco*-CB[6] is very similar in size and shape to CB[6] but lacks only one methylene bridge between two adjacent glycolurils.³⁶ Bis-*nor-seco*-CB[10] is a unique dual cavity host formed from two staggered glycoluril pentamer units attached through two methylene bridges instead of four as in CB[10].³⁷ Since there are missing methylene bridges, the *nor-seco*-CB[n]s, or *ns*-CB[n]s, are capable of being functionalized, which had been a challenge until recently³⁸⁻⁴² and is still a major focus in current cucurbituril research.

1.5.1 *Nor-seco-cucurbit[6]uril*.

Nor-seco-cucurbit[6]uril (*ns*-CB[6]) is a unique CB[6]-sized host formed from starving the condensation reaction of formaldehyde (**I-17**).³⁶ Interestingly, due to the difference in electrostatic and steric effects felt at the top and bottom portals (Figure I-5a), *ns*-CB[6] is able to achieve diastereoselective recognition with unsymmetrical amine guests.

It was shown that *ns*-CB[6] was able to undergo further condensation with *o*-phthalaldehyde (**I-30**) under acidic conditions to yield the mono-functionalized CB[6] derivative **I-31** (Figure I-5b).³⁶ The functionalized portal is slightly larger than the unfunctionalized portal. This difference in size allows for long-chain alkylammonium guests to back-fold on itself to allow ion-dipole interactions at both portals, and thus possess diastereoselective recognition as well.

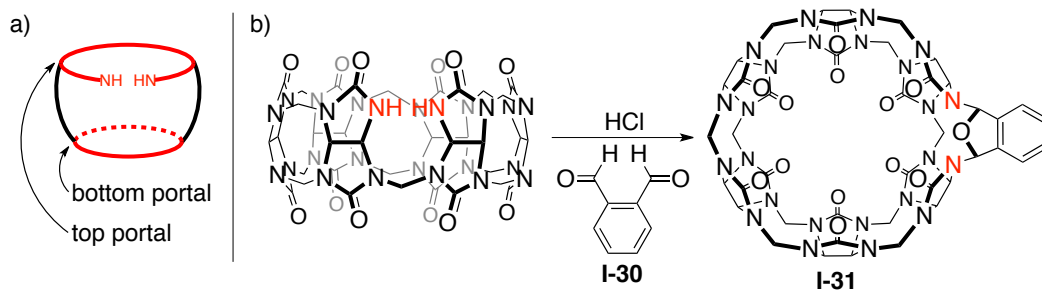


Figure I-5. a) Representation of the relative size difference of the top and bottom portals in *ns*-CB[6] and b) the synthesis of mono-functionalized CB[6] *via ns*-CB[6].

Unfortunately, there are a few drawbacks to the idea of utilizing *ns*-CB[6] as a building block for functionalized CB[6] derivatives. First and foremost, the overall yield of *ns*-CB[6] is only 3% after purification by ion-exchange chromatography. Secondly, the **I-31** is most similar in size to CB[6], which is limited to binding

narrow or small alkyl and aryl ammonium compounds and cannot accommodate larger, more interesting compounds. Finally, **I-31** is much less symmetrical after functionalization which can prove to be a challenge to analyze spectroscopically if the functionalized moiety becomes more complicated.

1.5.2 Bis-*nor-seco*-cucurbit[10]uril.

Bis-*nor-seco*-cucurbit[10]uril is also formed from starving the CB[n] reaction of formaldehyde (**I-17**).³⁷ However, unlike *ns*-CB[6], it is relatively simple to synthesize in moderate yield. It is collected as a reaction precipitate in 25% yield and requires no chromatography during purification. It was the first double cavity CB[n] to be reported and has the ability to form binary and ternary complexes depending on the size of the guest.

Bis-*ns*-CB[10] possesses the ability to expand and contract its two cavities to accommodate a larger variety of guests. This flexibility arises from the two methylene bridge connections between the two glycoluril pentamer units. As one guest enters the first cavity, which expands or contracts for a best fit of the guest, the second cavity is subsequently preorganized to allow a second identical guest molecule and thus exhibits homotropic allostery. As shown in Figure I-6, the distance observed between the two methylene bridges that connect the glycoluril pentamer units allows for a better understanding of this phenomenon. For the ternary complex of bis-*ns*-CB[10]•**I-18**₂ (n = 6) a distance of only 5.61 Å is observed while for bis-*ns*-CB[10]•**I-29**₂ the distance is stretched to 9.22 Å.

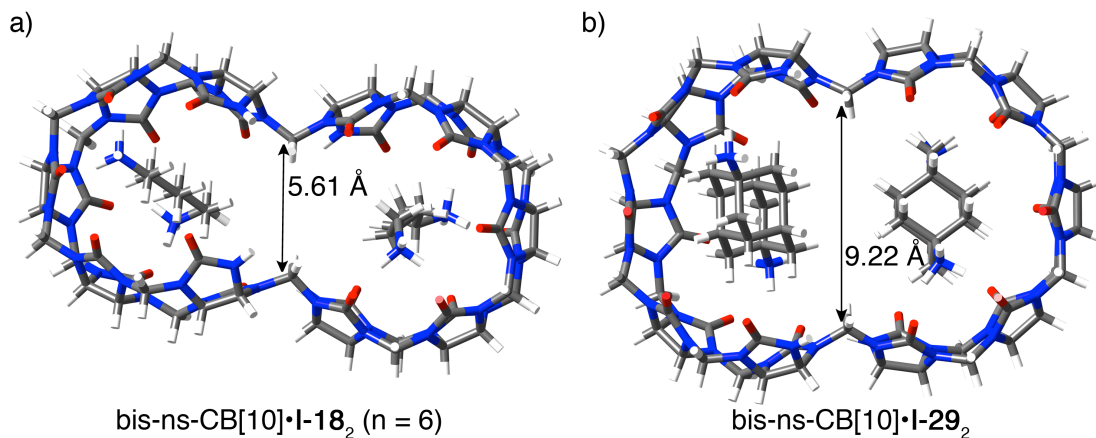


Figure I-6. MMFF minimized molecular models for complexes a) $\text{bis-ns-CB[10]}\cdot\text{I-18}_2$ ($n = 6$) and b) $\text{bis-ns-CB[10]}\cdot\text{I-29}_2$ where the non-bonded $\text{H}_2\text{C}\cdots\text{CH}_2$ distance was measured.

The orientation of the guests included in bis-ns-CB[10] can vary as well. There are three diastereomers, depicted in Figure I-7, that are possible.³⁷ First, the guests can be oriented in a way that the majority of the guest, or the binding region, is positioned at the top and bottom of the dual cavity host, termed top-top. Second, one guest can be oriented near the top while the second is oriented in the same direction as the first or near the center of the host, noted as top-center. Third, both guests can be oriented towards the center of the host, noted as center-center.

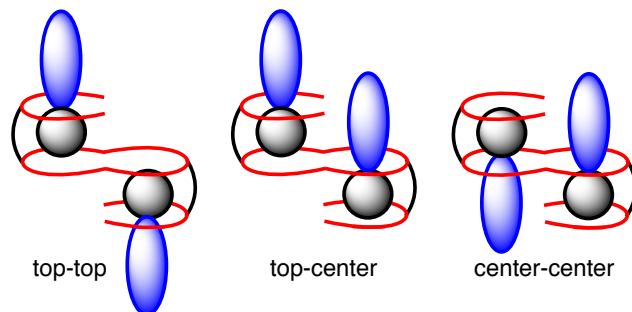
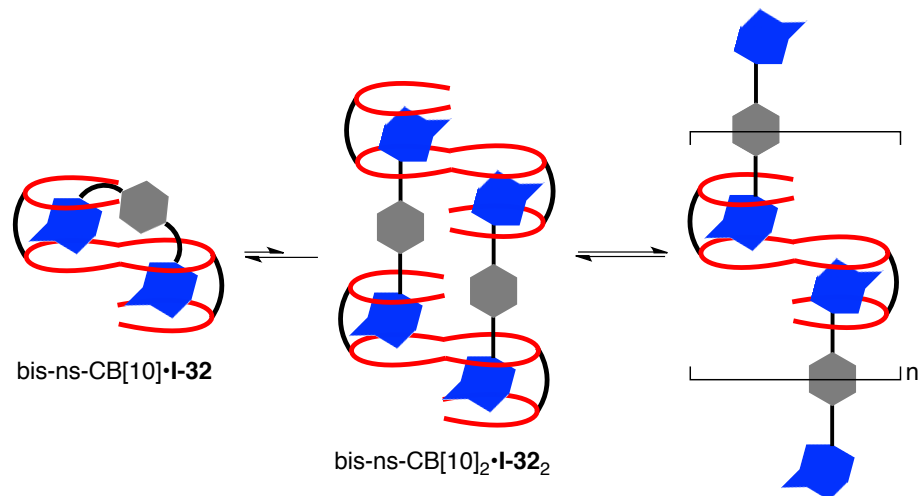


Figure I-7. Three possible binding motifs, or diastereomers, for bis-*ns*-CB[10] with two guests.

As a dual cavity host, bis-*ns*-CB[10] was thought to be an ideal building block for a non-covalent polymeric system. The idea was to synthesize a guest (**I-32**) with identical terminal groups that are able to bind bis-*ns*-CB[10], and take advantage of its homotropic allosteric properties, to promote supramolecular polymerization.⁴³ Isaacs and co-workers synthesized a number of guests that contained guest moieties at the terminus known to bind to bis-*ns*-CB[10] with large binding constants. In the presence of the dual cavity host the guests would bind in a top-top orientation, thus promoting polymerization (Scheme I-7). Unfortunately, the discrete complexes, notably 1:1 (bis-*ns*-CB[10]•**I-32**) and 2:2 (bis-*ns*-CB[10]₂•**I-32**₂), as depicted in Scheme I-7, were favored due to the entropic advantages.



Scheme I-7. Schematic representation of the equilibrium between discrete and polymeric complexes with *bis-ns-CB[10]*.

Isaacs and co-workers synthesized a similar guest but with a longer biphenyl linker in the hopes of preventing the smaller discrete complexes. Although it was successful in preventing the 1:1 complex, the 2:2 complex was favored instead of a longer polymeric complex. Unfortunately, it is difficult to prevent discrete complex formation, or cyclization, with a system utilizing a guest with two binding motifs and is a common challenge in forming supramolecular polymers.¹⁸

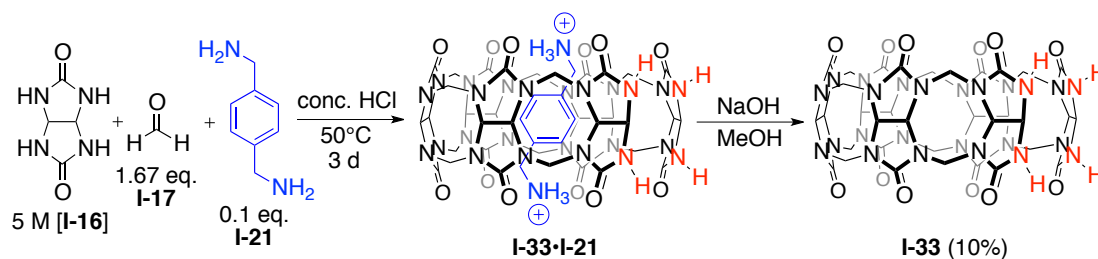
1.6 Glycoluril Hexamer (I-33).

The Isaacs group has completed extensive research on the mechanistic understanding of the formation of cucurbiturils.³¹ The condensation between **I-16** and **I-17** initially leads to the formation of a mixture of methylene bridged glycoluril oligomers. Once a desirable length of oligomer is formed, i.e. six glycoluril units, the

oligomer may undergo cyclization to form the cucurbituril macrocycle, CB[6], which is irreversible and therefore drives the reaction to completion. The initial methylene bridge formations, however, are reversible. This creates a challenge if one wants to isolate a specific glycoluril oligomer because a mixture of multiple oligomers is formed when the condensation reaction is starved of **I-17**.

The glycoluril oligomers, dimer – hexamer, have been synthesized from a single condensation reaction between **I-16** and less than two equivalents of **I-17**.³¹ Each was isolated by ion-exchange chromatography and characterized. However, the yield of the oligomers was considerably low, i.e. 1% for hexamer. The Isaacs group envisioned using hexamer (**I-33**) as a building block for mono-functionalized CB[6] derivatives but needed a direct synthetic route to its formation.

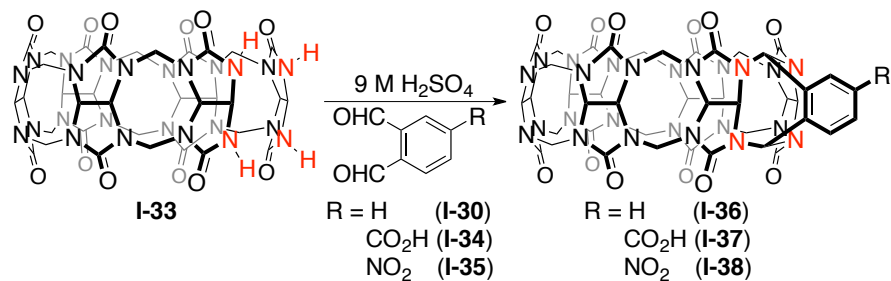
Fortunately, in 2011, Isaacs and co-workers synthesized **I-33** in one pot starting with **I-16**, **I-17**, and **I-21** as a templating agent (Scheme I-8).⁴⁰ Templates are well known to aid macrocyclic formation and have proven to be useful in the synthesis of various molecular receptors.⁴⁴ Cucurbiturils form tight complexes with amine compounds. **I-21** binds to CB[6], but it is known that it binds with higher affinity to **I-33**.⁴⁵ This is due to the acyclic nature of **I-33**, which can expand its cavity to better fit **I-21** than the rigid CB[6] macrocycle can. The presence of **I-21** within **I-33** actually hinders the formation of CB[6] when the complex is subjected to **I-17** in acidic conditions. When **I-21** is placed in the reaction mixture with **I-16** and **I-17** the **I-33•I-21** complex is isolated as a reaction precipitate. Upon washing the complex under basic conditions free **I-33** is isolated in 10% yield.



Scheme I-8. Templated synthesis of glycoluril hexamer (**I-33**).

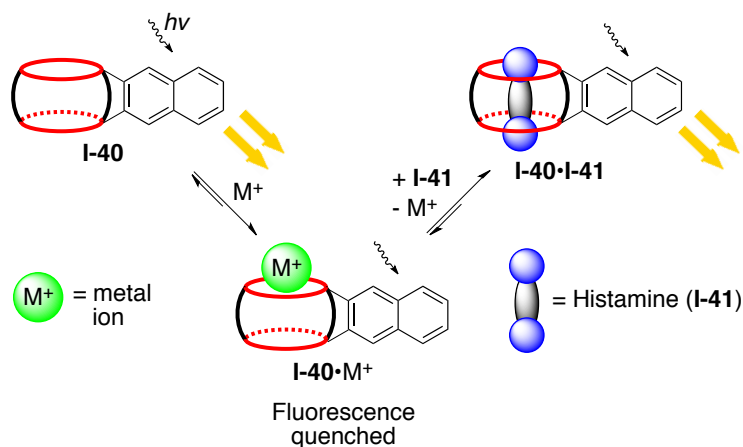
1.6.1 CB[6] Derivatives Synthesized From Hexamer.

Previous work by Isaacs and co-workers used *ns*-CB[6] as a starting material in the synthesis of the mono-functionalized CB[6] (**I-31**) by condensation of a phthalaldehyde (**I-30**) with the free ureidyl nitrogens.³⁶ However, the **I-31** proved to be difficult to synthesize and purify, and the functionalized moiety destroyed the symmetry of the two portals thus inducing new recognition properties. In the case of hexamer (**I-33**), there are two bridging points that must undergo condensation to form the desired cyclized product, and would therefore lead to a more symmetrical host with the recognition properties similar to CB[6]. In H₂SO₄ at room temperature **I-33** reacts with various phthalaldehydes (**I-30**, **I-34**, and **I-35**) to form the desired CB[6] derivatives (**I-36**, **I-37**, and **I-38**), respectively (Scheme I-9).^{40,46} Two derivatives of with very high potential for further functionalization containing a carboxylic acid moiety (**I-37**) and a nitro moiety (**I-38**) were synthesized. All the products were isolated as a precipitate from the reaction mixture in good yield (56 – 83%) and did not require chromatographic purification.



Scheme I-9. Mono-functionalized CB[6] derivatives synthesized *via* condensation of glycoluril hexamer (**I-33**) with *o*-phthalaldehydes (**I-30**, **I-34**, and **I-35**).

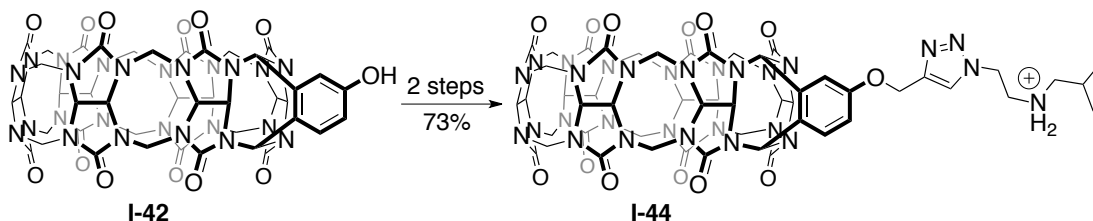
Isaacs and co-workers also synthesized a CB[6] derivative containing a naphthylene group on its posterior (**I-40**).⁴⁰ Interestingly, this host fluoresces when exposed to ultraviolet light. CB[n] containers are well known to be used in a variety of sensing applications.⁴⁷⁻⁴⁹ To test its ability as a sensor, a variety of heavy metal ions were placed in solution with **I-40** and bind to the C=O portals. Upon metal ion association with **I-40**, the fluorescence was quenched due to a heavy metal effect or paramagnetic quenching effect (Scheme I-10). When the solubilized host was treated with Eu^{3+} the fluorescence was quenched up to 60%. Intriguingly, when a strong binding biogenic ammonium guest, like histamine (**I-41**), was placed in the system, it kicks out the metal ion and forms the **I-40**•**I-41** complex due to its stronger binding affinity towards the host thus recovering fluorescence.



Scheme I-10. Fluorescence assay based on fluorescent CB[6] derivative (**I-40**) quenched by association with a metal ion.

Recently, Isaacs and co-workers have synthesized a CB[6] derivative containing a hydroxy moiety (**I-42**) on the posterior utilizing the hexamer condensation with a phthalaldehyde (**I-43**) as described previously.⁴⁶ This is not the first CB[6] with a hydroxy moiety, however. Previous to the compound synthesized by Isaacs and co-workers, Kim³⁸ and Scherman⁵⁰ published their syntheses on the formation of hydroxylation performed on a preformed CB[6] macrocycle. However, controlling the amount of hydroxy groups incorporated, in the case of Kim's compound, and a challenging purification procedure, in the case of Scherman's compound, showcase the advantages of this new mono-functionalized CB[6] derivative (**I-42**) that is isolated without chromatographic purification on the gram scale. Using **I-42** as a starting material, they were able to synthesize in two steps a CB[6] derivative covalently attached to an isopropylamine group (**I-44**), a known tight binding compound to CB[6] (Scheme I-11). An interesting observation was seen when **I-44** was dissolved in D₂O and analyzed by ¹H NMR spectroscopy and

Diffusion Ordered Spectroscopy (DOSY). Host **I-44** self-assembled into a cyclic [c2] daisy chain. Furthermore, subsequent addition of spermine (**I-45**), which binds with higher affinity to the host cavity than does isopropylamine, interrupted the self-assembly and a 1:1 binding motif (**I-44**•**I-45**) was established.

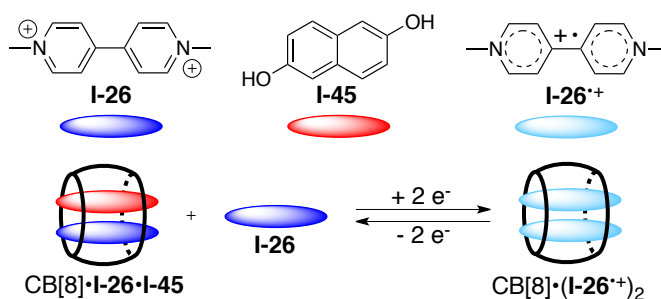


Scheme I-11. Formation of a CB[6] derivative (**I-44**) that undergoes self-assembly.

1.7 Ternary Complexes Using Cucurbit[8]uril.

Cucurbit[8]uril is a relatively large macrocycle similar in size to γ -cyclodextrin. It is large enough to actually form a ternary complex, or a complex comprised of one host and two guests. It was first discovered by Kim and co-workers in 2000 that CB[8] can form a ternary complex with 2,6-bis(4,5-dihydro-1*H*-imidazol-2-yl)naphthalene to form a 1:2 host•guest complex.²⁶ In 2001, they discovered that CB[8] can form stable ternary complexes with two different guests, methyl viologen (**I-26**) and 2,6-dihydroxynaphthalene (**I-45**), to form a 1:1:1 host•guest complex (Scheme I-12).⁵¹ The electron-poor **I-26** first enters the CB[8] to form a 1:1 complex followed by the electron-rich **I-45** to form the stable 1:1:1 ternary charge transfer (CT) complex. However, when the ternary complex is subjected to a reducing agent and excess **I-26** is in solution, **I-26** is converted to the radical cation **I-26^{•+}** and a new ternary complex CB[8]•(**I-26^{•+}**)₂ is formed (Scheme I-12).⁵² With the

introduction of an oxidizing agent **I-26**⁺ is converted back into **I-26**, the complex is broken up, and the initial 1:1:1 complex is reformed. This chemical-stimuli-induced interchangeable host-guest complexation has led to a vast amount of research and is highlighted in the following sections.

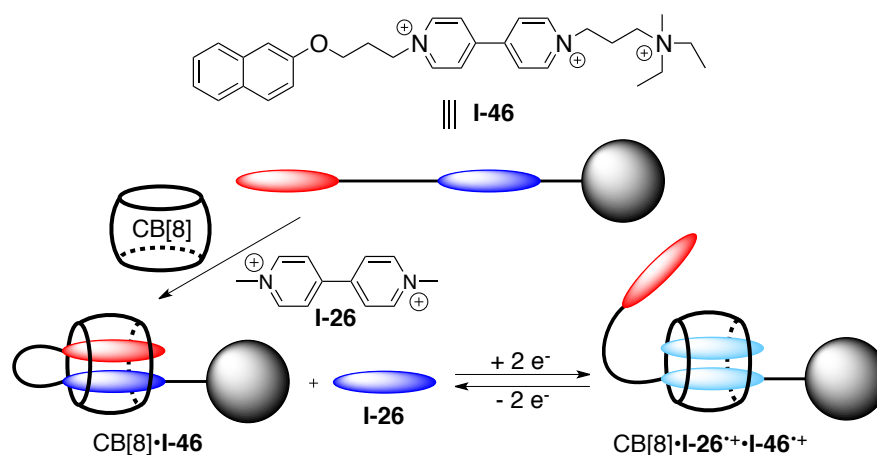


Scheme I-12. Formation of a ternary complex with CB[8] and methyl viologen (**I-26**) upon reduction to the radical cationic species.

1.7.1 CB[8] Molecular Loop Lock.

Cucurbiturils have been used in a wide variety of molecular machines. Since CB[8] can form ternary complexes the scope of possibilities for exciting molecular machines is quite large. In 2005, Kim and co-workers reported on a reduction-oxidation driven molecular loop lock system using CB[8].⁵² Knowing that CB[8] forms stable charge-transfer (CT) complexes with naphthalene (Np) and methyl viologen (**I-26**), they set out to synthesize a specific guest that contained a naphthalene group covalently attached to a methyl viologen group through an alkyl chain linker. A bulky terminal group known to not fit through the CB[8] cavity was attached to the opposite side of the methyl viologen. As expected, the CT complex (**CB[8]•I-46**) was formed when both CB[8] and the guest (**I-46**) were placed in

solution forming a looped lock structure (Scheme I-13). When a reducing agent was entered into the system along with excess **I-26**, **I-26** and the methyl viologen moiety (MV^{2+}) of **I-46** underwent a $1 e^-$ reduction to form **I-26⁺** and MV^{+} , respectively. The change to MV^{+} disrupted the CT complex and formed the $CB[8] \cdot (I-26^{+})_2$ complex, thus “unlocking” the loop. In the presence of an oxidizing agent, the unlocked system would return to a loop lock upon formation of **I-26** which subsequently formed the CT complex with $CB[8]$.

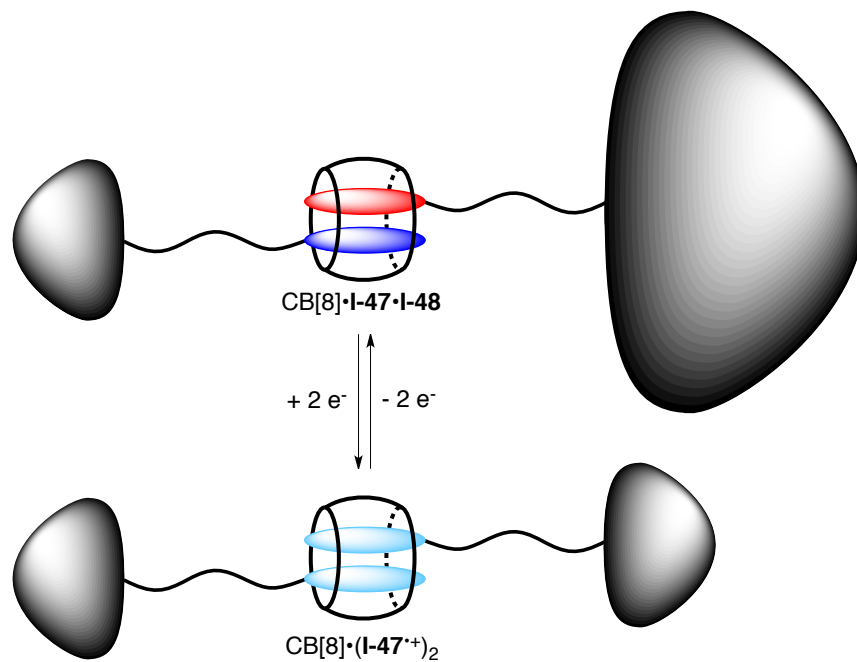


Scheme I-13. $CB[8]$ molecular loop lock ($CB[8] \cdot I-46$) induced by redox stimulus.

1.7.2 $CB[8]$ Induced Self-assembly.

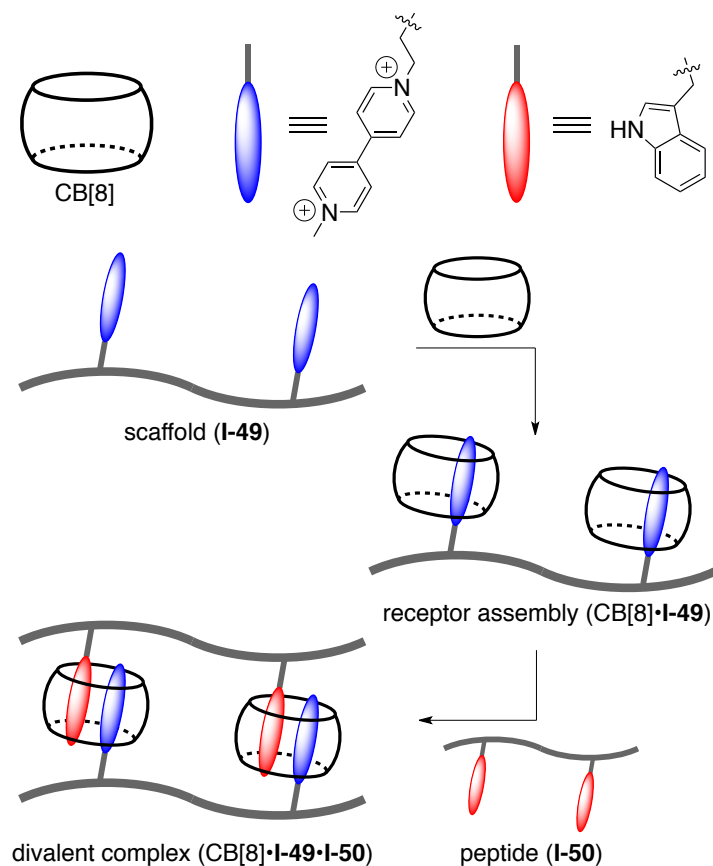
The self-assembly of preformed dendrimers is an efficient way to create large interesting nanostructures. One can double the size of the dendritic system by simply bringing two smaller dendrimers together. A non-covalent assembly would also allow for a triggered release of the components. In 2004, Kaifer and co-workers demonstrated the ability to bring two dendrimers together by forming a reversible CT complex with $CB[8]$.⁵³ Then in 2006, they reported on a new set of self-assembled

dendrimers where the size of the dendritic system was controlled.⁵⁴ A number of dendrimers were synthesized, ranging from G1 – G3, where one set included a MV^{2+} (π -acceptor) group (**I-47**) and the other a dialkoxybenzene (π -donor) group (**I-48**). When one of each type of dendrimer was placed in solution with CB[8] a CT complex was observed ($CB[8]\cdot I-47\cdot I-48$). As expected, upon electrochemical reduction of the MV^{2+} groups in **I-47** to MV^{+} the CT complex was destroyed and a homodimeric dendrimer species ($CB[8]\cdot(I-47^+)_2$) was formed (Scheme I-14). A number of combinations of dendrimers would be able to undergo self-assembly in the presence of CB[8] and the size of the overall assembly could be controlled electrochemically.



Scheme I-14. Electrochemical switching and size selection of a CB[8]-assembled dendrimer.

CB[8] has also been used for multivalent recognition of peptides. CB[8] is known to bind a variety of amino acid residues.^{49,55} Its use in biomimetic systems can therefore be applied to recognition of peptides and proteins. In 2009, the Urbach group reported on a self-assembled receptor, incorporating CB[8] and a methyl viologen scaffold (**I-49**), able to recognize a target peptide containing tryptophan (Trp) residues (**I-50**) (Scheme I-15).⁵⁶ Peptide-based scaffolds containing one, two, or three MV²⁺ groups were synthesized along with the respective scaffolds containing one, two, or three Trp residues. In water, CB[8] underwent complexation with the **I-49** to first form the receptor assembly (CB[8]•**I-49**). In the presence of the receptor assembly, **I-50** was recognized by the receptor and formed multiple ternary complexes to ultimately form the multivalent complex CB[8]•**I-49**•**I-50**. It was determined by isothermal calorimetry (ITC) that the binding affinity increases 31 – 280-fold due to multivalency relative to the monovalent complex. Interestingly, the Trp residues can be observed by UV-Vis spectroscopy and therefore allow for a simple method for quantitation of the extent of valency. This system allows for studies of structure-activity relationships in multivalent complexes due to its simple design and synthetic approach as well as the range of analytical techniques that can be applied.

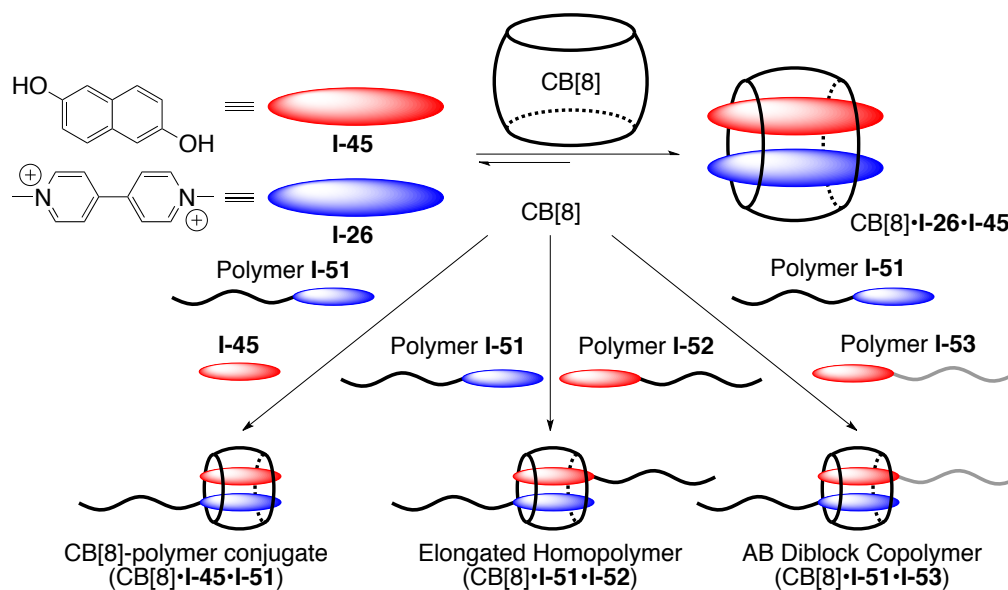


Scheme I-15. Schematic representation of a CB[8]-induced self-assembling receptor (CB[8]•I-49) for peptide recognition.

1.7.3 CB[8] Polymers.

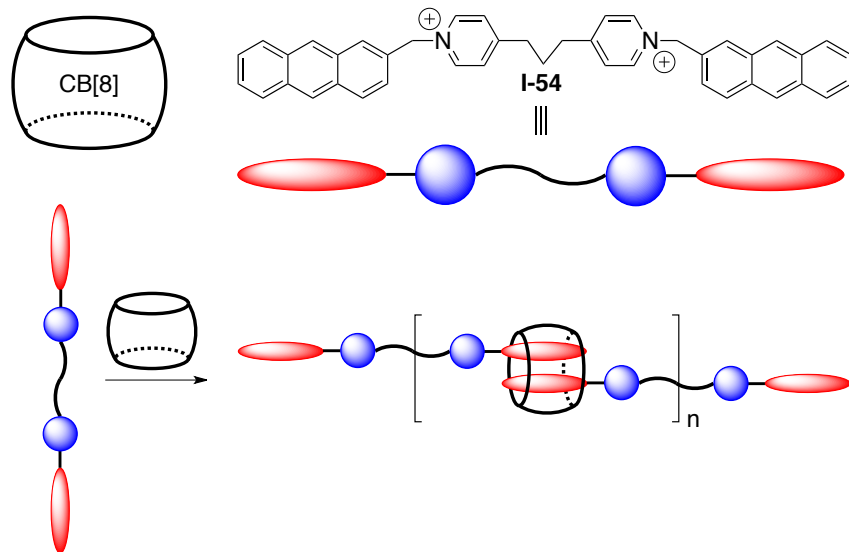
Supramolecular polymers have become an increasingly researched field. They have gained so much attention due the dynamic nature and stimuli responsiveness of the materials in forming the non-covalent polymer systems.¹⁷ As seen in the previous examples, CB[8] forms ternary complexes. If a polymeric monomer contains a binding moiety at the terminus one can envision an elongation of the polymer through the formation of a CB[8]-mediated complex.

In 2008, the Scherman group formed supramolecular block copolymers in water by utilizing CT complexes with CB[8].⁵⁷ Linear polymers were prepared containing terminal guest moieties suitable for encapsulation by CB[8]. Two polymers were synthesized from Poly(ethylene glycol) (PEG) and terminated with methyl viologen (**I-51**) and 2-naphthol (**I-52**). A third polymer was synthesized from *cis*-1,4-poly(isoprene) (PI) and was terminated with 2-naphthol (**I-53**). Three polymeric systems were investigated (Scheme I-16). In the presence of CB[8] and dihydroxynaphthalene (**I-45**), **I-51** formed the polymer conjugate CT complex CB[8]•**I-45**•**I-51**. When both **I-51** and **I-52** were in the presence of CB[8], an elongated homopolymer (CB[8]•**I-51**•**I-52**) was observed. Finally, when **I-51** and **I-53** were in the presence of CB[8], an AB block copolymer (CB[8]•**I-51**•**I-53**) was observed.



Scheme I-16. CB[8] complexation-induced polymeric systems.

With a host that binds two guests it is also possible to envision a system with a guest that has identical terminal groups that bind to the host in a 1:2 ratio. Under the correct conditions, the host-guest interaction would induce polymerization. In 2011, the Zhang group reported on a water-soluble supramolecular polymer based on CB[8]-enhanced π - π interaction.⁵⁸ Zhang and co-workers synthesized a guest that contained an anthracene terminal group adjacent to a pyridinium moiety at both ends of the molecule (**I-54**). Similar to the CB[8]•Np₂ complexes, anthracene also forms 1:2 complexes with CB[8] due to an enhanced π - π interaction when encapsulated. The pyridinium moiety is within close proximity to the C=O portal for favorable ion-dipole interactions. When **I-54** is dissolved in water and exposed to CB[8] the monomers assemble in a head to tail fashion forming a supramolecular polymer (Scheme I-17). Using dynamic light scattering (DLS) the hydrodynamic radius of the resulting polymer was calculated to be 45 nm. In comparison, the 1:2 complex of CB[8] and a monovalent guest containing only one anthracene and pyridinium unit was calculated to have a hydrodynamic radius of 1-3 nm. Typically, discrete complexes would be favored in these types of systems as described earlier with bis-*ns*-CB[10]. However, cyclization is prevented in this system for two reasons: (1) the short propylidene linker prevents a 1:1 complex due to steric hindrance, and (2) there is a charge repulsion between the two positively charged pyridinium moieties that does not allow a 2:2 complex to form.

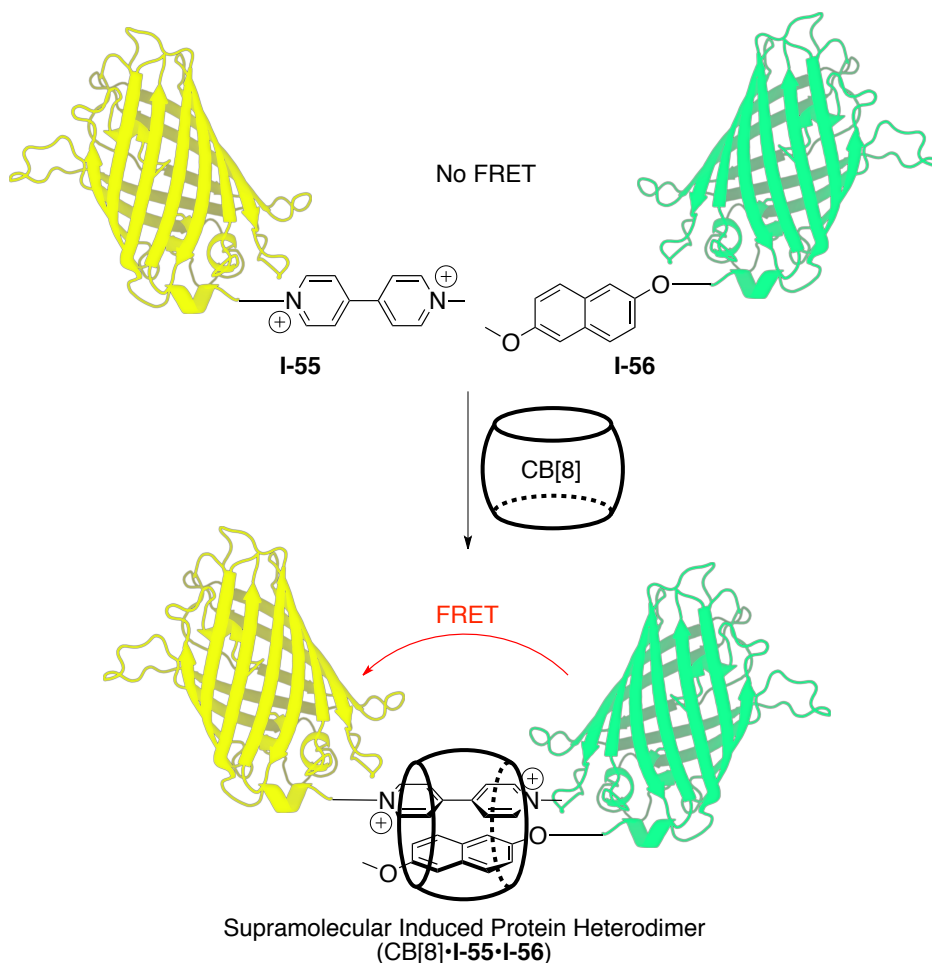


Scheme I-17. Supramolecular polymerization driven by CB[8]-enhanced π - π interaction.

1.7.4 CB[8] Induced Heterodimerization of Functionalized Proteins.

Supramolecular chemistry approaches for biological applications is an attractive field since the inspiration behind supramolecular chemistry stems from biological molecules and their interactions.⁵⁹ CB[8] has been used in biological systems as well. The Brunsveld group recently reported on a CB[8] induced protein FRET pair dimerization (Scheme I-18).⁶⁰ The protein FRET (Fluorescence Resonance Energy Transfer) pair of cyan and yellow fluorescent protein (CFP and YFP) was used in this study. Each was functionalized with a methyl viologen group (**I-55**) and a methoxynaphthol group (**I-56**), respectively. In the absence of CB[8], no FRET was observed by fluorescence spectroscopy from the protein pair. However, in the presence of CB[8], the protein pair formed a heterodimer through the CB[8]•**I-55**•**I-56** CT complex. As a consequence of the dimerization, the proximity of the two

proteins was close enough to induce FRET and was clearly observed by fluorescence spectroscopy from the increase in the YFP emission.



Scheme I-18. CB[8] induced protein FRET pair dimerization.

1.8 Summary and Conclusions.

Since the discovery of CB[6] in 1981 by Mock cucurbituril chemistry growth has been massive. A variety of sizes of cucurbituril macrocycles have been synthesized, characterized, and made commercially available (CB[5], CB[6], CB[7], and CB[8]). Although they have limitations with respect to solubility and

functionalization, they have been used for a wide range of applications including sensors, molecular machines, biomimetic systems, and supramolecular polymers.

CB[8] has been involved in some interesting systems due to its ability to form ternary complexes and include two guests within its cavity. The formation of these ternary complexes allow for facile formation of molecular machines, supramolecular polymers, and protein dimerization. However, it is limited in its uses due to poor solubility and because the ternary complexes require specific pairs of guests. Bis-*ns*-CB[10] is a unique dual cavity cucurbituril that is able to form ternary complexes as well. It is made up of two glycoluril pentamer units that can expand and contract their cavity to fit a wide range of guests. However, this ability diminishes its selectivity towards guests, a favorable trait of most cucurbiturils.

In the following chapters, new double cavity cucurbituril derivatives will be discussed in detail. Their synthesis, characterization, and potential applications will be addressed. The formation of ternary complexes is quite intriguing, and the possibilities for potential application and formation of dynamic materials is enormous.

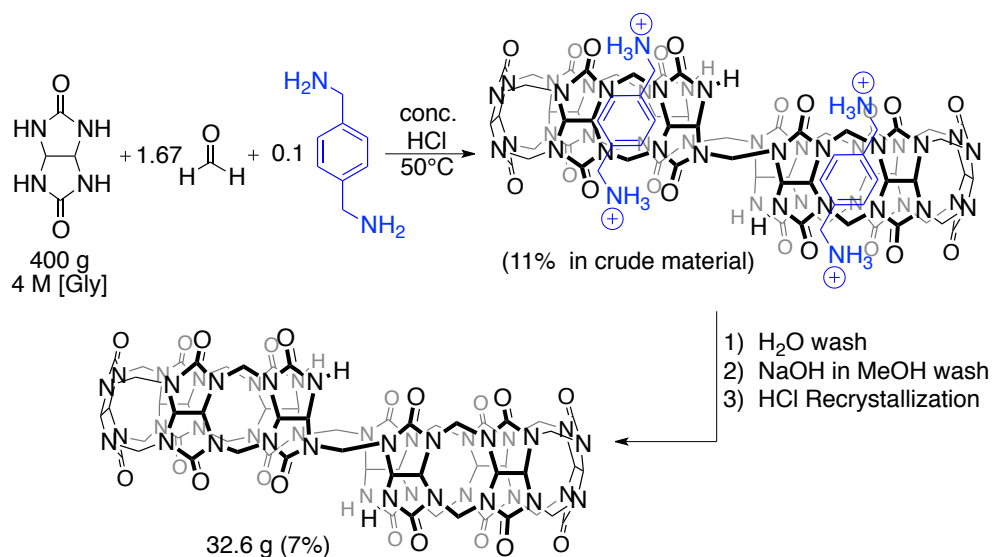
Chapter 2: A Clipped [3]Rotaxane Derived from Bis-*nor-seco*-cucurbit[10]uril

2.1 Introduction.

Interest in the cucurbit[n]uril (CB[n])^{32,61} family of molecular containers has surged in recent years due to the availability of a homologous series of hosts (CB[n], n = 5, 6, 7, 8, 10)^{20,25,26,30,62} that undergo high affinity and high selectivity binding processes in water.^{21,33,34} For example, CB[n] have been used to create a variety of molecular machines,^{52,63,64} chemical sensors,⁶⁵⁻⁶⁹ supramolecular polymers/macromolecules,^{54,70-73} and biomimetic systems.⁷⁴⁻⁷⁶ In several of these systems, the CB[n] rotaxanes or pseudorotaxanes that played key roles were prepared by stoppering, slippage, and intracavity 3 + 2 cycloaddition.⁷⁷⁻⁷⁹ In contrast, some of the most complex molecular machines rely on clipping of macrocycles onto preformed threads or rings.^{12,13} Such clipping processes have not been demonstrated with CB[n] systems because of insufficient synthetic ability to control CB[n] macrocyclization. Over the years, the Isaacs group has developed a thorough understanding of the mechanism of CB[n] formation^{31,35-37,80,81} that has allowed us to prepare *nor-seco*-CB[n] compounds which lack one or more bridging CH₂-groups and therefore possess potentially reactive ureidyl NH groups. In this study we use bis-*ns*-CB[10] as a starting material for the preparation of macrotricyclic host **II-1**, investigate its recognition properties toward ammonium guests in water, and prepare [3]rotaxane **II-1•II-4₂** by a clipping process that has not been previously demonstrated for CB[n]-type macrocycles.

2.2 Scale-up Synthesis of Bis-*ns*-CB[10].

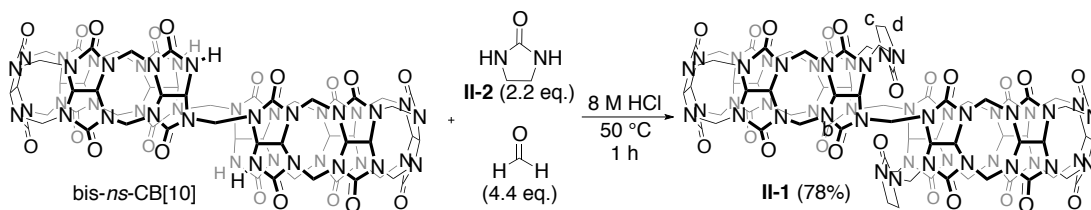
Previously, we have reported that the reaction of glycoluril (1.42 g, 1 equiv., 2.5 M) and paraformaldehyde (1.67 equiv.) in conc. HCl at 50 °C delivers bis-*ns*-CB[10] as an insoluble precipitate (0.238 g, 15%).³⁷ We found that this reaction is very sensitive to many variables including the initial mixing of the solid reagents with the HCl solvent, the nature of the reaction vessel, and the nature of the vessel closure. Given the high sensitivity of this reaction, it is perhaps unsurprising that we have been unable to scale-up this reaction to the 10 or 100 g levels; reactions on this scale typically deliver large amounts of CB[6] as product. Since the CB[n] forming reaction is a cyclo-oligomerization reaction³¹ whose fundamental condensation steps respond to changes in concentration over the millimolar to molar range,⁸⁰ we reasoned that it would be worthwhile to perform the **II-3** templated reaction at various concentrations of glycoluril. For example, when the reaction is conducted using 400 g of glycoluril with [glycoluril] = 4 M, the reaction mixture remains homogeneous and ¹H NMR analysis of the crude reaction mixture reveals the presence of bis-*ns*-CB[10] in 11% yield (Scheme II-1). The more soluble impurities including glylcoluril hexamer, CB[6], and *ns*-CB[6] were removed by washing with H₂O. Decomplexation of bis-*ns*-CB[10]•**II-3**₂ by washing with 0.1 M NaOH in MeOH followed by recrystallization from HCl delivered bis-*ns*-CB[10] (32.6 g, 7% yield).



Scheme II-1. Large-scale synthesis of bis-*ns*-CB[10].

2.3 Synthesis of Host II-1.

Initially, we intended to take advantage of the stability of bis-*ns*-CB[10] under basic conditions (e.g. DMSO, *t*-BuOK, RT) to prepare functionalized and solubilized derivatives by reaction with suitable electrophiles but were uniformly unsuccessful. Eventually, we determined that it is possible to functionalize bis-*ns*-CB[10] under sufficiently mild acidic conditions that preserve the bis-*ns*-CB[10] skeleton. Heating bis-*ns*-CB[10] with CH₂O and imidazolidone (**II-2**) at 50 °C in 8 M HCl for 1 h results in the formation of **II-1** as an insoluble precipitate in 78% yield (Scheme II-2).



Scheme II-2. Synthesis of Host **II-1**.

2.4 Characterization of Host **II-1**.

Host **II-1** is poorly soluble in aqueous solution which precluded spectroscopic determination of its structure. However, the **II-1•II-3**₂ complex is nicely soluble in D₂O which allowed us to measure its ¹H NMR spectrum (Figure II-1a) and determine its molecular formula by ESI-MS. Host **II-1** is comprised of 10 glycolurils, 22 CH₂-groups, and two imidazolidone units. The symmetry equivalent aryl H-atoms (H_a) of guest **II-3** become non-equivalent in the **II-1•II-3**₂ complex and appear as a pair of doublets at 6.82 and 6.66 ppm which suggests that host **II-1** maintains the C_{2h}-symmetry of the bis-*ns*-CB[10] starting material. A sharp singlet appears surprisingly far downfield at 6.60 ppm (vide infra) which is attributable to the central bridging CH₂-groups (H_b) of **II-1**. Based on the molecular formula and the symmetry properties of **II-1•II-3**₂ we tentatively assigned the structure of **II-1** as shown in Scheme II-2.

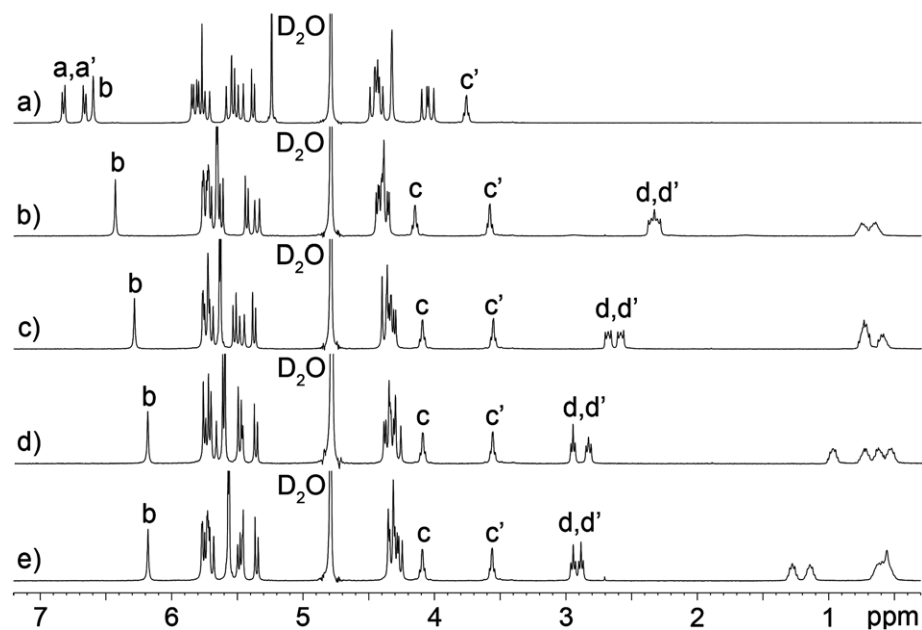


Figure II-1. ^1H NMR spectra (400 MHz, D_2O , RT) recorded for: (a) **II-1**•**II-3**₂ (5 mM), (b) a mixture of **II-1** (5 mM) and **II-5** ($n = 4$) (10mM), (c) a mixture of **II-1** (5 mM) and **II-5** ($n = 5$) (10 mM), (d) a mixture of **II-1** (5 mM) and **II-5** ($n = 6$) (10 mM) and (e) a mixture of **II-1** (5 mM) and **II-5** ($n = 7$) (10 mM).

2.5 Physical Properties of Host **II-1** Studied by X-Ray Crystallography.

Fortunately, we were able to obtain single crystals of **II-1** as its **II-1**•**II-3**₂ complex and solve its crystal structure (Figure II-2). The X-ray crystal structure of **II-1**•**II-3**₂ displayed a number of interesting features. First, the bridging imidazolidone units are inverted with the C=O groups pointing towards the central bridging CH_2 -groups; the $\text{C}=\text{O}\cdots\text{H}_2\text{C}$ distance amounts to only 2.35 Å. The bridging CH_2 -groups are located in the deshielding lone pair region of the C=O group which provides an explanation for their large chemical shift (6.60 ppm). The geometry of the bridging units is reminiscent of that observed for hemicucurbit[6]uril and

bambus[6]uril.^{82,83} Second, the distance between the two central CH₂-groups is 4.5 Å which is smaller than the corresponding distance observed in the crystal structure of bis-*ns*-CB[10]•**II-3**₂ (5.1 Å).³⁷ We attribute this shorter CH₂•••CH₂ distance in **II-1**•**II-3**₂ to the geometrical constraints of the bridging imidazolidone units which lock the host into a more rigid, macrotricyclic structure. Third, the diameter of the ureidyl C=O portals of **II-1** averages 6.9 Å which is similar to the value measured for CB[6] (6.8 Å) which accounts for the similar guest size preferences of host **II-1** relative to CB[6] noted below. There are four N–H•••O H-bonds (N–H•••O distances = 1.930, 2.108, 2.181, 2.234 Å; N–H•••O angles = 170, 161, 132, 125°, respectively), or two per portal between **II-3** and **II-1**.⁸⁴ Overall, host **II-1** is structurally similar to double cavity host bis-*ns*-CB[10] but the bridging imidazolidone rings rigidify the structure and make each cavity of **II-1** more similar in size to that of CB[6].

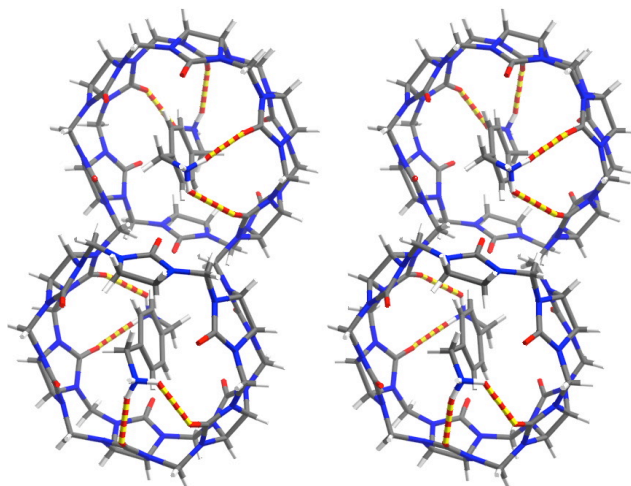


Figure II-2. Cross-eyed stereoview of the crystal structure of **II-1**•**II-3**₂. Color code: C, gray; H, white; N, blue; O, red; H-bonds, yellow-red striped.

2.6 Molecular Recognition Properties of Host **1** Studied by ^1H NMR

Spectroscopy.

Initially, we sought to determine the effective volume of each cavity of **1** by studying its recognition property toward a series of ammonium ions (**5**($n = 6$), **3**, **6**, **7**, **8**, and **9**) of increasing size (Chart II-1). We observed the formation of ternary complexes (**1**•guest₂) with slow exchange for **5**($n = 6$), **3**, **6**, and **7** and intermediate exchange with methyl viologen (**8**), but did not observe an inclusion complex for adamantaneammonium (**9**). This allowed us to estimate the size of each cavity of **1** as being similar in size to that of CB[6] which also rejects guest **9**. Unlike bis-*ns*-CB[10], which has the ability to expand its cavity to accommodate larger guests, the bridging imidazolidone units of **1** rigidify its structure and make it selective for smaller guests. Encouraged by the clean ternary complex formation with slow exchange on the chemical shift timescale observed for guests **3**, **5** ($n = 6$), **6**, and **7** we decided to study the influence of diamine length (**5**(n), $n = 4-10$) on guest binding. Figure II-2b-e shows the ^1H NMR spectra recorded for **1**•**5**(n)₂ ($n = 4, 5, 6, 7$). A notable feature of the spectra is the large difference in chemical shift (~ 0.5 ppm) for the diastereotopic CH₂-groups (H_c and H_{c'}) of the bridging imidazolidone. We attribute this difference to an H-bonding/electrostatic interaction of H_c but not H_{c'} to the ureidyl C=O portal of **1** (Figure II-2). Interesting trends are observed in the chemical shifts for H_b of host **1** and H_d of guests. The trend observed for H_d can be easily rationalized because the CH₂-NH₃⁺ groups of **5** ($n = 4$) and **5** ($n = 5$) are located within the shielding internal cavity of **1** whereas for **5** ($n = 6$) and **5**($n = 7$) they are located near

the deshielding region of the ureidyl C=O portals.²¹ We believe that the upfield shift observed for (CH₂)_b as the guest gets longer is due to a change in orientation of the imidazolidone C=O group and the deshielding effect of its lone pairs with respect to (CH₂)_b.

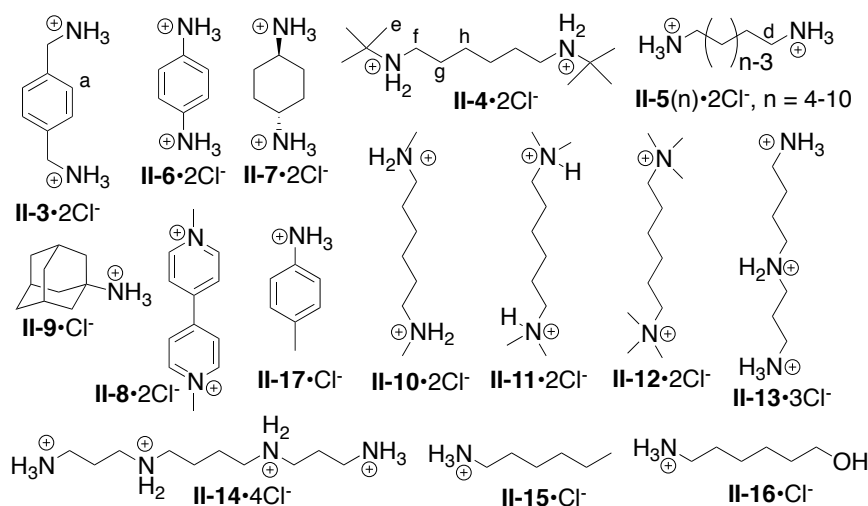


Chart II-1. Guests used in this study.

The ESI shows the ¹H NMR recorded for ternary complexes of **II-1** with guests **II-10–II-17** (see Appendix 1). The methylated and dimethylated guests **II-10** and **II-11** form soluble stable complexes **II-1•II-10**₂ and **II-1•II-11**₂ that show slow exchange kinetics on the NMR time scale whereas quaternary ammonium **II-12** forms a less stable complex with faster exchange kinetics. As might be expected, tetracationic spermine (**II-14**) cleanly forms the **II-1•II-14**₂ complex whereas tricationic spermidine (**II-13**) forms a mixture of diastereomeric complexes with stoichiometry **II-1•II-13**₂ which reflects the top-center dissymmetry of host **II-1**.³⁷ Finally, we did not observe the formation of soluble complexes upon stirring solid **II-1** with **II-5** or **II-17**, although ¹H NMR spectroscopy indicates a depletion of free **II-15** and **II-17**

from solution which suggests the formation of insoluble complexes with **II-1**. Overall, host **II-1** behaves as a double cavity CB[n]-type host that is complementary to narrow di-, tri- and tetramines.

2.7 Formation of a [3]Rotaxane.

One of the most prized architectures in supramolecular chemistry are the rotaxanes many of which function as molecular machines. Although a variety of CB[n] (pseudo)rotaxanes have been prepared by stoppering or slippage it would be desirable to develop clipping processes, or processes involving an incomplete macrocycle associated around a dumbbell-shaped guest then clipped in place to form the completed macrocycle, that might allow more complex architectures to be constructed. We found that stirring a mixture of bis-*ns*-CB[10], **II-4**, CH₂O and **II-2** at 50 °C in 8 M HCl for 1 h delivers **II-1•II-4₂** as an insoluble precipitate in 69% yield.

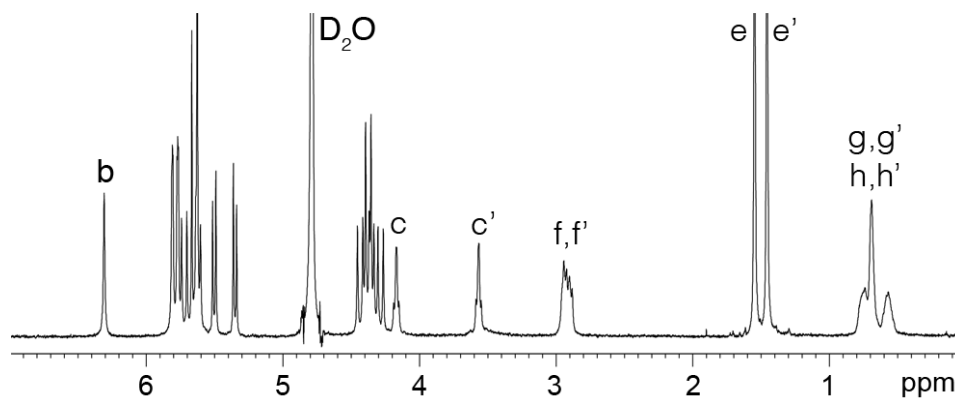


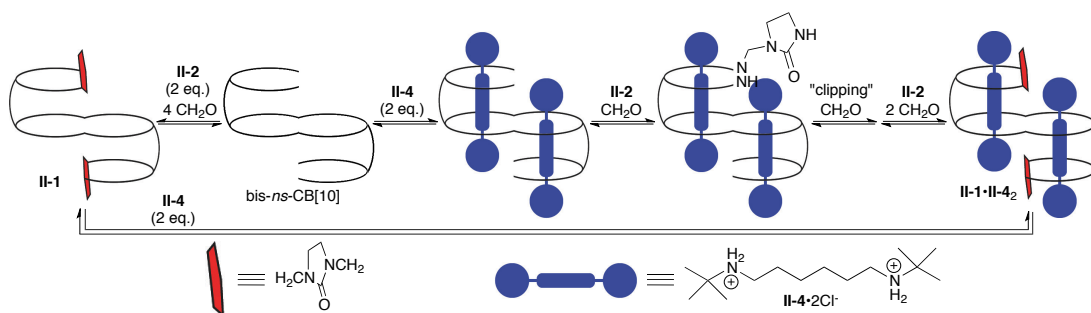
Figure II-3. ¹H NMR spectrum (400 MHz, D₂O, RT) recorded for **II-1•II-4₂**.

Figure II-3 shows the ¹H NMR spectrum recorded for [3]rotaxane **II-1•II-4₂** in D₂O. Integration of the resonances for **II-1** versus **II-4** allowed us to determine the

1:2 host•guest stoichiometry whereas the downfield shifts observed for H_e (1.34 - 1.46, 1.55 ppm) and the upfield shifts for the hexylene chain (1.4–1.7 - 0.85–0.50 ppm) establish the binding geometry shown in Scheme II-3. Two experiments confirm that **II-1•II-4**₂ is a [3]rotaxane: (1) treatment of **II-1•II-4**₂ with 0.1 M NaOH in MeOH does not dissociate the complex, and (2) stirring **II-1•II-4**₂ with **II-3** (10 equiv.) or **II-5** (n = 6) (10 equiv.) in D₂O at 50 °C does not result in guest exchange.

2.8 Mechanistic Study on the Formation of [3]Rotaxane **II-1•II-4**₂.

Scheme II-3 shows two mechanistic possibilities for the formation of [3]rotaxane **II-1•II-4**₂. In the first pathway, bis-*ns*-CB[10] reacts with **II-2** and CH₂O to give **II-1** which undergoes a slippage process with 2 equiv. **II-4** to yield **II-1•II-4**₂. The second pathway proceeds via complex bis-*ns*-CB[10]•**II-4**₂ which then undergoes a clipping process to deliver **II-1•II-4**₂. Three experiments strongly suggest that the clipping pathway is dominant: (1) preformed bis-*ns*-CB[10]•**II-4**₂ complex reacts rapidly with **II-2** and CH₂O to give **II-1•II-4**₂, (2) heating a mixture of **II-1•II-4**₂ and **II-5** (n=6) at 50 °C in D₂O does not result in the formation of **II-1•II-5** (n = 6)₂ which means that slippage processes of **II-4** with **II-1** do not occur, and (3) heating a mixture of **II-1** and **II-4** in D₂O (50 °C) does not deliver **II-1•II-4**₂. However, heating a mixture of **II-1** and **II-4** under acidic conditions (8 M HCl, 50 °C) does deliver **II-1•II-4**₂ because the presence of acid causes reversible opening of the imidazolidone bridges.



Scheme II-3. Possible mechanistic paths for the formation of **II-1•II-4₂**.

2.9 Conclusions.

In summary, we have prepared host **II-1** by a double bridging reaction between **II-2** and bis-*ns*-CB[10]. Host **II-1** has been characterized crystallographically which allows us to rationalize its affinity toward narrow diammonium ions (e.g. **II-5**(*n*), *n* = 4–10). [3]Rotaxane **II-1•II-4₂** is formed by the first clipping process involving a CB[*n*]-type host. We expect that such clipping of CB[*n*]-type macrocycles onto preformed axles or rings will result in CB[*n*]-based molecular machines of higher complexity than could otherwise be prepared.

Chapter 3: Higher Order Complexes Formed from Cucurbit[6]uril Dimers.

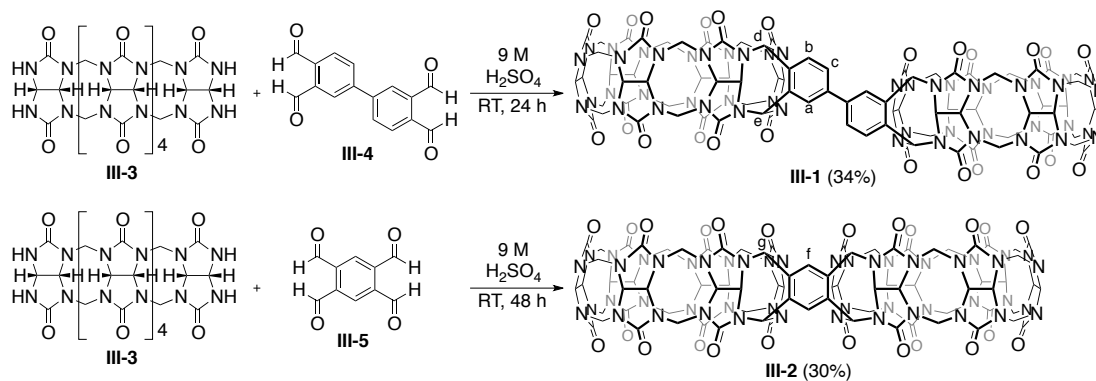
3.1 Introduction.

In 2011 and early 2012, the Isaacs group reported that di-aldehydes undergo condensation with glycoluril oligomers under acidic conditions to yield monofunctionalized CB[6] derivatives.^{40,46,80} We envisioned the possibility of creating CB[6] dimer hosts under similar conditions to the synthesis of the monofunctionalized CB[6] derivatives when a tetra-aldehyde was used in place of an *o*-phthalaldehyde.

3.2 Synthesis of Two Cucurbit[6]uril Dimer Hosts.

Tetra-aldehyde **III-4** was synthesized following a literature procedure⁸⁵, and **III-5** was synthesized *via* a modification of the synthesis reported in the literature⁸⁶ (see Appendix 2). Stirring two equivalents of glycoluril hexamer (**III-3**) in the presence of one equivalent of **III-4** in 9 M H₂SO₄ at RT for 24 h results in the formation of host **III-1** as a white solid in 34% yield after purification by DowexTM ion-exchange column chromatography and recrystallization from TFA/H₂O (Scheme III-1). Interestingly, host **III-1** is soluble (~ 8 mM) in 0.2 M Na₂SO₄. However, when **III-1** is complexed with guest **III-6** (*n* = 6)₂, the NMR resonances for the host are sharper and more dispersed (Figure III-1b). We were also able to determine molecular formula of **III-1** by ESI-MS from the **III-1**•**III-6** (*n* = 6)₂ complex. Host

III-2 was synthesized in a similar fashion. Stirring two equivalents of glycoluril hexamer (**III-3**) in the presence of one equivalent of **III-5** in 9 M H₂SO₄ at RT for 48 h results in the formation of host **III-2** as a white insoluble precipitate in 30% yield (Scheme III-1). Unlike host **III-1**, host **III-2** is insoluble in all solvents studied as the free host. Similar to host **III-1**, the complex **III-2**•**III-6** ($n = 6$)₂ is nicely soluble in D₂O and allowed us to measure its ¹H NMR spectrum (Figure III-1c) and determine its molecular formula by ESI-MS.



Scheme III-1. Synthesis of two CB[6] dimer hosts (**III-1** and **III-2**).

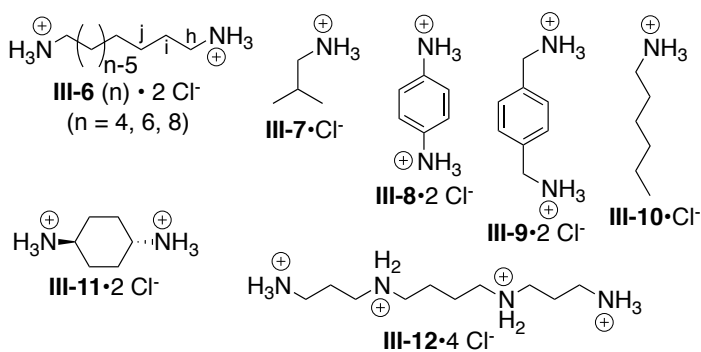


Chart III-1. Guests used in this study.

Because hosts **III-1** and **III-2** are poorly soluble in D₂O, formation of their host•guest complexes involves stirring an excess of solid host with a solution of guest. Accordingly, a variety of guests (Chart III-1) were stirred with hosts **III-1** and **III-2** in D₂O which results in the formation of 1:2 host:guest complexes as determined by integration of the ¹H NMR spectra recorded. Based on the size of the guests that were successfully complexed, we were able to estimate the size of the cavities of **III-1** and **III-2** to be similar to CB[6] and very similar to the CB[6] derivatives previously synthesized by Isaacs and co-workers.^{40,46} The complexes formed with guest **III-6** (n = 6) (Figure III-1) display some interesting characteristics. Due to the biphenyl linkage, the two portals per cavity in host **III-1** are not equivalent. The methine protons on **III-1** (H_d and H_e) appear as two separate singlets in the ¹H NMR spectrum (Figure IIIb). On the other hand, the two portals per cavity in host **III-2** are equivalent. As expected based on symmetry arguments, the methine protons on **III-2** (H_g) appear as one singlet in the ¹H NMR spectrum (Figure IIIc).

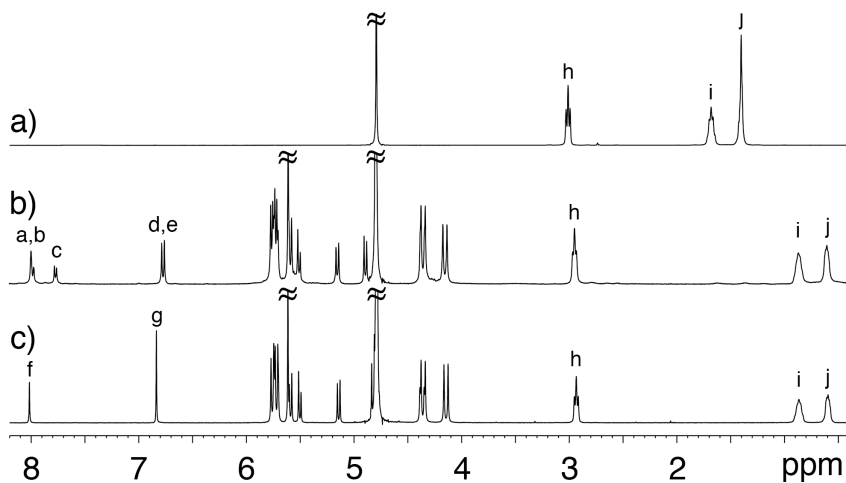


Figure III-1. ¹H NMR spectra (400 MHz, D₂O, RT) of a) guest **III-6** (n = 6), b) complex **III-1•III-6** (n = 6)₂, and c) complex **III-2•III-6** (n = 6)₂.

3.3 X-Ray Crystal Structure and Physical Properties of Host III-1.

Fortunately, we were able to obtain single crystals of **III-1** as the free host and solve its crystal structure by X-ray crystallography. Figure III-2 shows a cross-eyed stereoview of the structure of **III-1**. There is a torsional angle (36°) observed within the biphenyl moiety of the compound. The cavities of **III-1** display a very similar shape to related CB[6] derivatives that have been prepared previously and studied previously by MMFF calculations.^{40,46} The macrocyclic cavities of **III-1** display an ellipsoidal deformation along their equator caused by the *o*-xylylene functional group on the exterior of the cavity. As displayed in Figure III-2, the diameter across the cavity between the methine bridge C-atom and the methylene bridge C-atom directly across (distance a) is 10.8 Å whereas the other pairs of methylene bridge C-atom diameters (distances b and c) are only 9.2 Å and 9.3 Å. The presence of the *o*-xylylene group results in a substantial (1.5-1.6 Å) ellipsoidal deformation of the cavity. Related structural distortions are known from the literature to result in a preference for flatter guests.^{87,88}

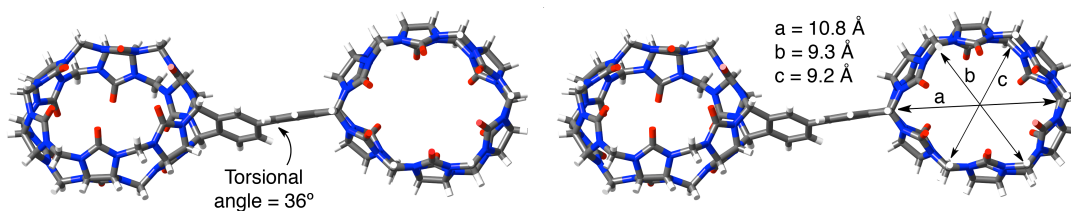


Figure III-2. A cross-eyed stereoview of the crystal structure of host **III-1** as the “P” enantiomer. Color code: C, gray; H, white; N, blue; O, red.

Interestingly, as shown in Figure III-3, there are two enantiomers observed in the crystal lattice. One can identify the two enantiomers by focusing on the bond between the two aromatic rings in the biphenyl moiety. The front and back hosts in Figure III-3 are in a counter-clockwise orientation, or an “M” orientation, whereas the left and right hosts staggered between the front and back are in a clockwise orientation, or a “P” orientation. There are four C–H•••O H-bonds (2 C–H•••O H-bonds: C–H•••O distance = 2.421 Å, C–H•••O angle = 155°; 2 C–H•••O H-bonds: C–H•••O distance = 2.474 Å, C–H•••O angle = 114°)⁸⁹ between two hosts of the opposite orientation (Figure III-4). The H-bonds are formed between the staggered hosts and are best shown along the x-z plane and y-z plane (Figure III-4). The sheets of H-bonded hosts grow in the x-z plane, and the hosts stack along the z-axis.

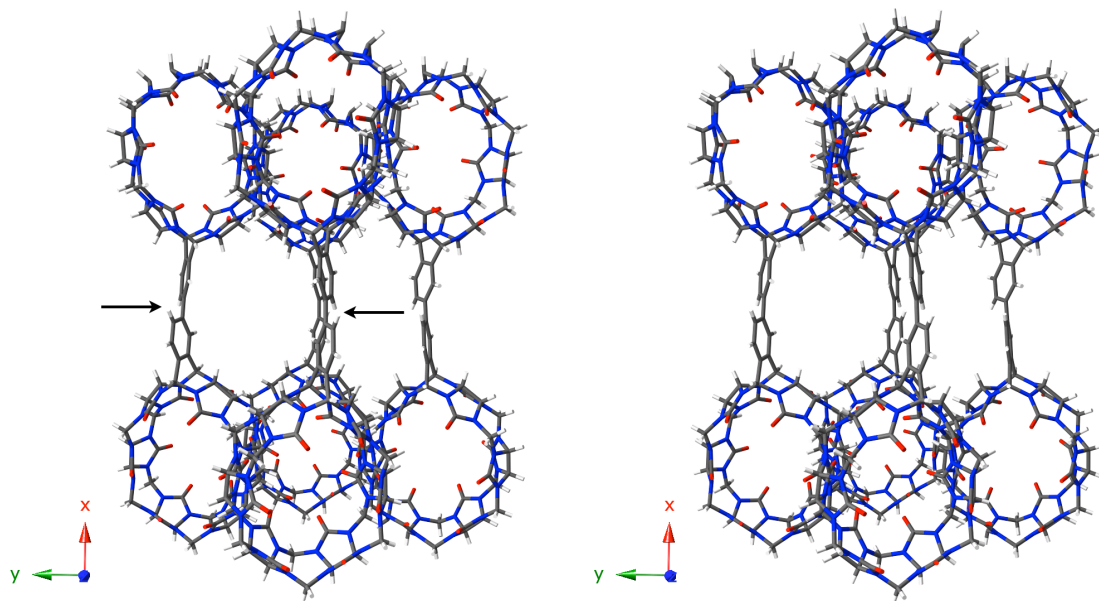


Figure III-3. A cross-eyed stereoview of the crystal packing of host **III-1**. Color code: C, gray; H, white; N, blue; O, red.

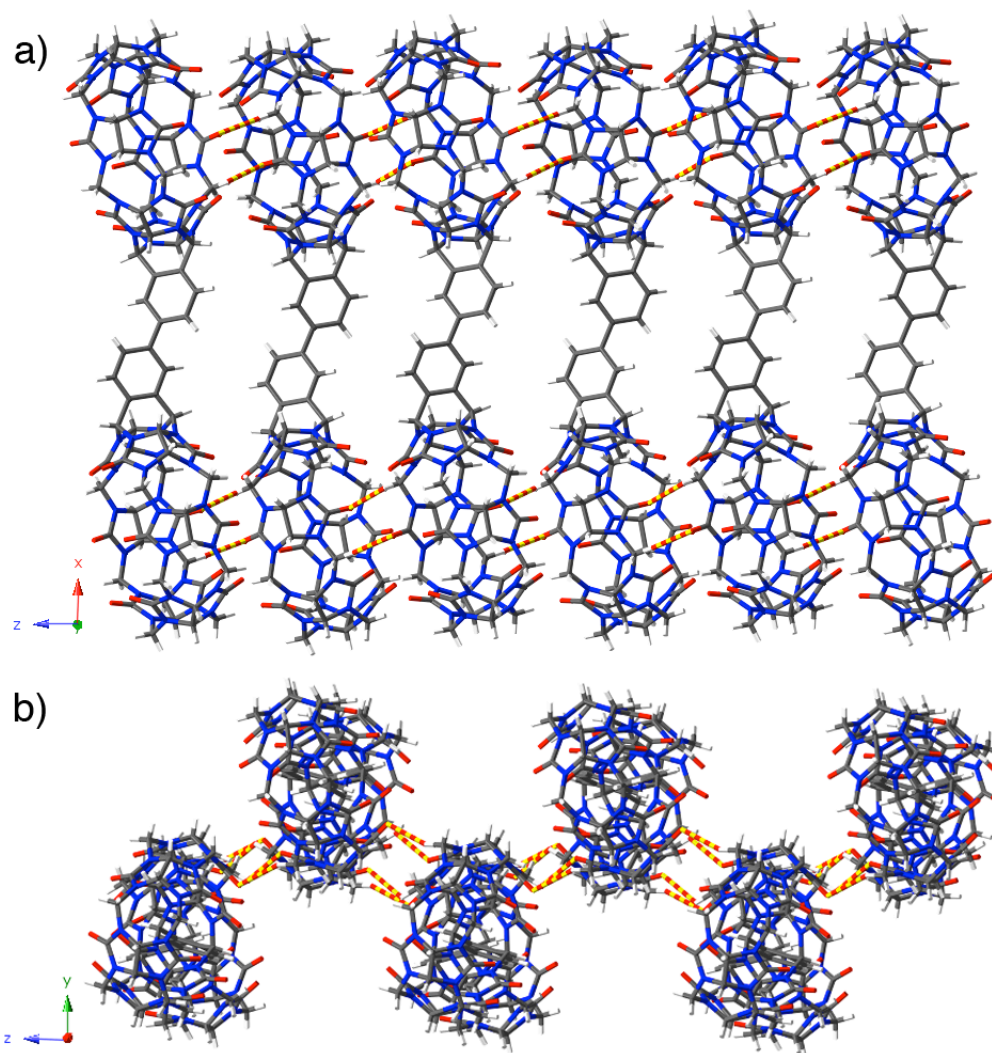


Figure III-4. A view of the crystal packing and H-bonding of **III-2** in the (a) x-z plane and the (b) y-z plane. Color code: C, gray; H, white; N, blue; O, red; H-bonds, red-yellow striped.

3.4 Supramolecular Polymer Formation.

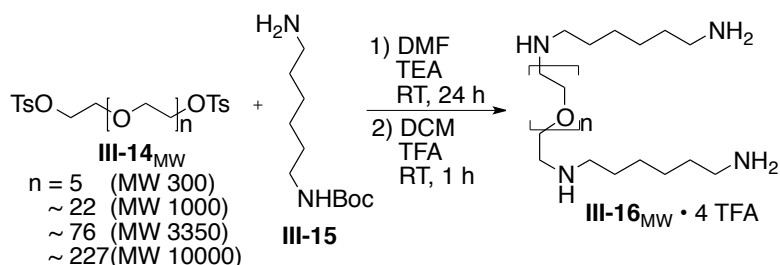
Since host **III-1** was soluble in a saline solution in H₂O we hoped that we could induce polymerization of a ditopic oligomeric or polymeric guest compound where **III-1** would act as a ditopic host. In such a system, the degree of

polymerization can, in theory, be controlled by the stoichiometry of host-to-guest. When host (guest) is present in excess it endcaps the growing polymer chain; for example a 0.9:1.0 host:guest ratio gives a maximum degree of oligomerization of 10. Supramolecular polymers are also responsive to various stimuli, such as pH, temperature, or redox.^{17,18} In our case with CB[n] host•guest chemistry involved, our supramolecular polymers could be controlled by a change in pH to decrease the binding affinity of the guest, or by addition of a competing guest for the CB[n] cavity. Both circumstances would allow us to control the polymerization (de-polymerization) of the system.

3.4.1 Synthesis of Poly(ethylene glycol) Guests Bearing Two Hexanediamine Units.

Poly(ethylene glycol) (PEG) was chosen as a building block for our polymeric guests because of its solubility in aqueous media and its well known functionalization chemistry at the terminal positions.⁹⁰⁻⁹² Since hexanediamine (HDA, **III-6** (n = 6)) was already shown to be a good guest ($K_a = 1.4 \pm 0.3 \times 10^7 \text{ M}^{-1}$)⁴⁰ for previously synthesized *o*-xylylene derived CB[6] hosts, it was chosen to be the terminal moieties on the PEG derivatives. Accordingly, PEG₃₃₅₀ (avg. MW 3350, Sigma-Aldrich, Part # 202444) was first reacted with excess *p*-toluenesulfonyl chloride (TsCl, **III-13**) in the presence of NaOH in THF to form the (TsO)₂PEG₃₃₅₀ derivative (**III-14**₃₃₅₀) as shown in Scheme III-2. Compound **III-14**₃₃₅₀ was then reacted with N-Boc-1,6-hexanediamine (**III-15**) in the presence of triethylamine in DMF to give the crude Boc-protected (HDA)₂PEG₃₃₅₀ derivative. The crude material was subsequently

stirred in a mixture of dichloromethane and trifluoroacetic acid to remove the Boc-protecting group to yield the crude (HDA)₂PEG₃₃₅₀ derivative (**III-16**₃₃₅₀) as its trifluoroacetate salt (Scheme III-1). The crude material was dissolved in a minimal amount of H₂O and purified by size-exclusion chromatography (SEC, Sephadex G25) to give **III-16**₃₃₅₀ in 30% yield. In an analogous fashion different molecular weight PEGs (PEG_{MW}, MW = 300, 1000, and 10000) were used as starting materials to synthesize **III-16**₃₀₀, **III-16**₁₀₀₀, and **III-16**₁₀₀₀₀.



Scheme III-2. Synthesis of PEG-based polymer guests **III-16**₃₀₀ – **III-16**₁₀₀₀₀.

3.4.2 Attempted Formation of Supramolecular Polymers Between Host **III-1** and Guests **III-16** Studied by Diffusion Ordered Spectroscopy.

Diffusion Ordered Spectroscopy (DOSY) is an NMR technique used to obtain the diffusion coefficient, which is determined by plotting the signal intensity versus the gradient strength and is expressed as an area per time for a given molecule.⁹³ The Stokes-Einstein Equation (Equation 1) relates the diffusion coefficient (D) to the hydrodynamic radius (R) of a spherical molecule, where k_b is Boltzmann's constant, T is temperature, and η is viscosity. Theoretically, the ratio of the diffusion coefficients

for two species is inversely proportional to the cube root of their volumes (V), or their molecular weights (MW) assuming both species can be treated as uniform spherical species (Equation 4).

$$D = \frac{k_b T}{6\pi\eta R} \quad (1)$$

$$\frac{D_1}{D_2} = \frac{R_2}{R_1} \quad (2)$$

$$\text{For a sphere, } V = \frac{4}{3}\pi R^3 \therefore R = \sqrt[3]{\frac{4}{3}\pi V} \quad (3)$$

$$\frac{D_1}{D_2} = \frac{\sqrt[3]{V_2}}{\sqrt[3]{V_1}} \approx \frac{\sqrt[3]{MW_2}}{\sqrt[3]{MW_1}} \quad (4)$$

The equation above (Equation 4) works well for systems that assume spherical shapes in solution. PEGs, however, tend to exist in multiple conformations in aqueous solution depending on the concentration and temperature of the solution.⁹⁴⁻⁹⁶ In order to determine the correlation between the diffusion coefficient of PEGs and their molecular weight, Shimada and co-workers measured the diffusion coefficient for uniform PEG oligomers.⁹⁷ They determined the scaling factor of the diffusion coefficient against the molecular weight for a given PEG molecule to be -0.43 (Equation 5). Using this relationship we can then correlate the ratio of the diffusion coefficients of a free guest and a host•guest complex to their molecular weight (Equation 6). We have used both models to estimate the degree of supramolecular oligomerization as described below.

$$D \propto MW^{-0.43} \quad (5)$$

$$\frac{D_1}{D_2} = \frac{MW_1^{-0.43}}{MW_2^{-0.43}} \quad (6)$$

In an attempt to form supramolecular polymers, we separately dissolved host **III-1** and guest **III-16**₁₀₀₀₀ in 0.1 M Na₂SO₄ solution in D₂O. The concentration of each stock solution was calculated by spiking each sample with a known amount of **III-9** and comparing the integration of the peaks of the host (guest) to the integration of the peaks of **III-9**. The host and guest were then mixed together in a 1:1 molar ratio to obtain a concentration of 2 mM each in solution. In order to determine the relative size of the system in solution, DOSY NMR was used to analyze the host (**III-2**), guest (**III-16**₁₀₀₀₀), and host•guest mixture (**III-1**)_n•(**III-16**₁₀₀₀₀)_m. An example of the data obtained by DOSY is shown in Figure III-4. The diffusion coefficient (*D*) obtained for free **III-16**₁₀₀₀₀ was determined to be $(30.6 \pm 2.7) \times 10^{-12} \text{ m}^2 \text{ s}^{-1}$ (Figure III-5a) while the complex **III-1**_n•(**III-16**₁₀₀₀₀)_m was determined to be $(6.00 \pm 0.06) \times 10^{-12} \text{ m}^2 \text{ s}^{-1}$ (Figure III-5b).

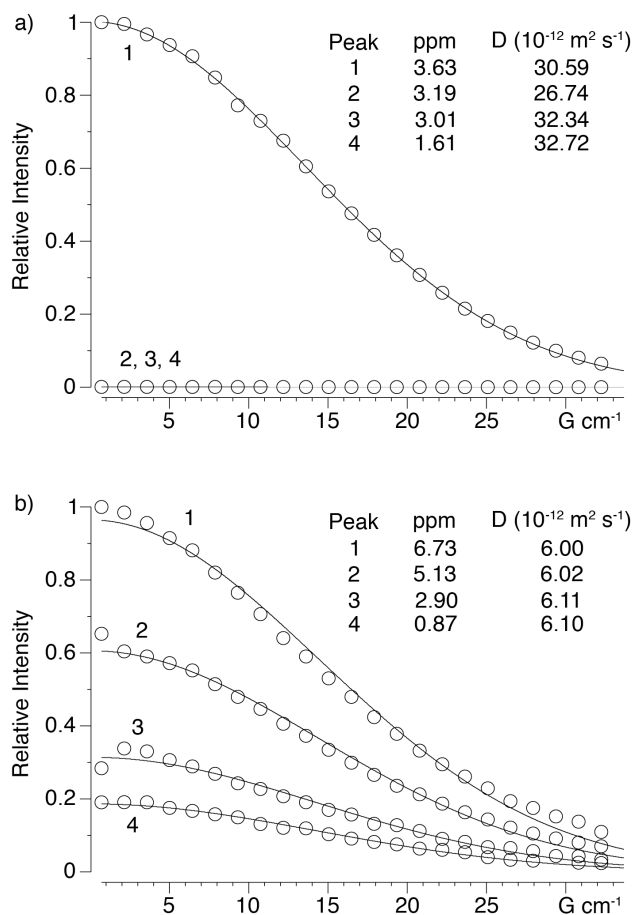


Figure III-5. Plots of the change in intensity of the indicative NMR resonances in the DOSY spectra as a function of magnetic field gradient recorded (600 MHz, D_2O , 298 K) for: a) guest **III-16**₁₀₀₀₀ and b) complex **(III-1)_n•(III-16)**₁₀₀₀₀_m.

In an analogous manner, diffusion coefficients were obtained for the other PEG derivatives (**III-16**) as the free guest and as the material obtained from equimolar mixtures ($\sim 2 \text{ mM}$) with host **III-1** (Table III-1). The diffusion coefficients obtained were then compared to the host (as the **III-1•III-6** ($n = 6$)₂ complex) and the free guests to estimate the size increase of the obtained supramolecular polymer and the degree of polymerization (Table III-1). Based on the spherical model using

Equation 4 to solve for the molecular weight of the host•guest complex, we determined the average complex:guest molecular weight ratio for each system. For the $(\mathbf{III-16}_{300})_n \cdot (\mathbf{III-1})_m$ system a complex:guest molecular weight ratio of 1.67 was calculated, in other words a total of 1.67 host•guest units comprise one oligomeric unit in solution. Complex:guest molecular weight ratios for the $(\mathbf{III-16}_{1000})_n \cdot (\mathbf{III-1})_m$, $(\mathbf{III-16}_{3350})_n \cdot (\mathbf{III-1})_m$, and $(\mathbf{III-16}_{10000})_n \cdot (\mathbf{III-1})_m$ systems were calculated in a similar manner and determined to be 2.31, 4.12, and 109.63, respectively. Based on this model, it is clear that the shorter PEG derivatives ($\mathbf{III-16}_{300} - \mathbf{III-16}_{3350}$) form smaller oligomeric complexes with low degrees of oligomerization whereas the longest PEG derivative ($\mathbf{III-16}_{10000}$) most likely forms a long-chain polymer. However, this model is based on the idea that host and guest are of similar structure and volume which is not true. Therefore, we also determined complex:guest molecular weight ratios for the host•guest systems by solving for the molecular weight of the complexes using the PEG model (Equation 6). For the $(\mathbf{III-16}_{300})_n \cdot (\mathbf{III-1})_m$ system a complex:guest molecular weight ratio of 1.03 was determined. Complex:guest molecular weight ratios for the $(\mathbf{III-16}_{1000})_n \cdot (\mathbf{III-1})_m$, $(\mathbf{III-16}_{3350})_n \cdot (\mathbf{III-1})_m$, and $(\mathbf{III-16}_{10000})_n \cdot (\mathbf{III-1})_m$ systems were calculated in a similar manner and determined to be 1.52, 2.70, and 36.54, respectively. Clearly, the values obtained using the PEG model are very different from the values obtained using the spherical model. However, similar results overall are observed. Again, we can conclude that the shorter PEG derivatives ($\mathbf{III-16}_{300} - \mathbf{III-16}_{3350}$) form short oligomers whereas the longest PEG derivative ($\mathbf{III-16}_{10000}$) forms a long-chain polymer.

Table III-1. Diffusion Coefficients obtained by DOSY NMR (600 MHz, D₂O, 298 K).

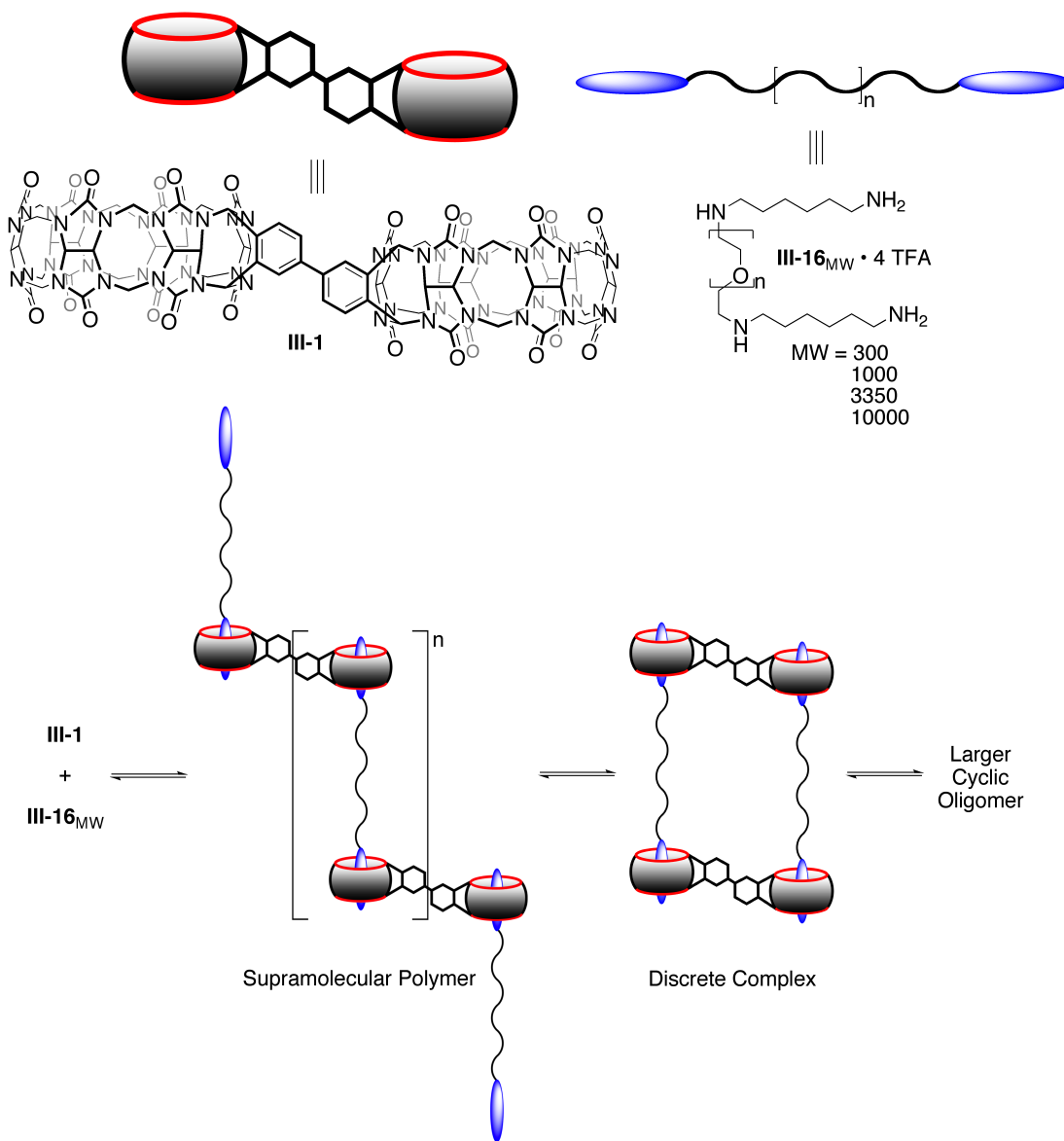
| Host | Guest | $D_{\text{complex}}^{[a]}$ | $D_{\text{free guest}}^{[a]}$ |
|--------------|--------------------------------|----------------------------|-------------------------------|
| CB[6] | III-6 (n = 6) | 348.8 | - |
| III-1 | III-6 (n = 6) | 224.8 | - |
| - | III-16 ₃₀₀ | - | 282.6 |
| III-1 | III-16 ₃₀₀ | 136.7 | - |
| - | III-16 ₁₀₀₀ | - | 168.5 |
| III-1 | III-16 ₁₀₀₀ | 90.6 | - |
| - | III-16 ₃₃₅₀ | - | 104.5 |
| III-1 | III-16 ₃₃₅₀ | 55.7 | - |
| - | III-16 ₁₀₀₀₀ | - | 30.6 |
| III-1 | III-16 ₁₀₀₀₀ | 6.0 | - |

[a] Units are: $\times 10^{-12} \text{ m}^2 \text{ s}^{-1}$

We decided to study the time dependence of supramolecular polymer (**III-16**₁₀₀₀₀)_n•(**III-1**)_m in more detail to see the interplay of the kinetics versus the thermodynamics of the system. To determine the time dependence, the host and guest were first mixed in an equimolar ratio with a concentration of 2 mM for both host and guest. After 30 min, the diffusion coefficient was determined by DOSY NMR to be $(6.6 \pm 0.3) \times 10^{-12} \text{ m}^2 \text{ s}^{-1}$. A minimum diffusion coefficient of $(6.0 \pm 0.2) \times 10^{-12} \text{ m}^2 \text{ s}^{-1}$ was obtained after 4 hrs. After 5 days the diffusion coefficient had increased to $(6.8 \pm 0.2) \times 10^{-12} \text{ m}^2 \text{ s}^{-1}$ and after 14 days to $(8.1 \pm 0.3) \times 10^{-12} \text{ m}^2 \text{ s}^{-1}$. The overall change in diffusion coefficient over time is minor; however, after 14 days the oligomer length was calculated to have decreased from a 36-mer to a 22-mer based on the PEG model. We can attribute this slow decrease in oligomerization to the k_{off} for the (**III-1**)_n•(**III-16**₁₀₀₀₀)_m complex. Based on literature reports, we know

that hexanediamine is very slow to escape the cavity of CB[6].^{21,22} Therefore, the equilibrium for our supramolecular polymer is reached after many days.

Scheme III-3 depicts the potential supramolecular polymerization when host **III-1** and guest **III-16_{MW}** are mixed together in solution in a 1:1 molar ratio. There are other possibilities, however, such as a 2:2 discrete complex or a larger cyclic oligomer with an n:n host:guest ratio. Based on the diffusion coefficients measured by DOSY all host•guest pairs except for **III-1_n•(III-16₁₀₀₀₀)_m** form short oligomeric (or cyclic) complexes rather than undergo polymerization. In the case of **III-1_n•(III-16₁₀₀₀₀)_m**, however, we obtain a supramolecular polymer.



Scheme III-3. Possible host•guest systems formed when the double cavity host (**III-1**) is mixed with the polymer divalent guest (**III-16_{MW}**).

3.5 Supramolecular Ladder Formation.

Although we were able to show evidence for some polymerization occurring, it was not to the extent we were hoping for (i.e. >50-mer), nor were there any interesting physical changes (gelation)⁷¹ observed. Instead of attempting to form

supramolecular polymers we decided to focus our attention on the formation of some unique discrete complexes comprised of our CB[6] dimer hosts, namely supramolecular ladders. A number of supramolecular ladder structures have been synthesized utilizing noncovalent interactions in their formation.^{15,98-100} These systems showcase the utility and strength of noncovalent interactions to form highly ordered complexes. Most examples, however, utilize metal coordination chemistry. We were interested in assemblies involving our double cavity hosts and organic guests to showcase their recognition and assembly properties.

3.5.1 Design and Synthesis of III-20 – III-23 as Oligovalent Guests for Formation of Ladder Polymers with Double Cavity Host III-2.

In order to create a ladder structure we envisioned a narrow guest able to slip through the CB[6]-sized cavity easily with multiple tight binding sites held together through a rigid linker (Figure III-7). To satisfy our requirements we turned to viologen-containing compounds. Substitution reactions involving the terminal N-atoms of 4,4'-bipyridyl (**III-17**) are well known.¹⁰¹⁻¹⁰³ There are also many reports using viologen compounds as guests for macrocyclic chemical applications.¹⁰³⁻¹⁰⁷

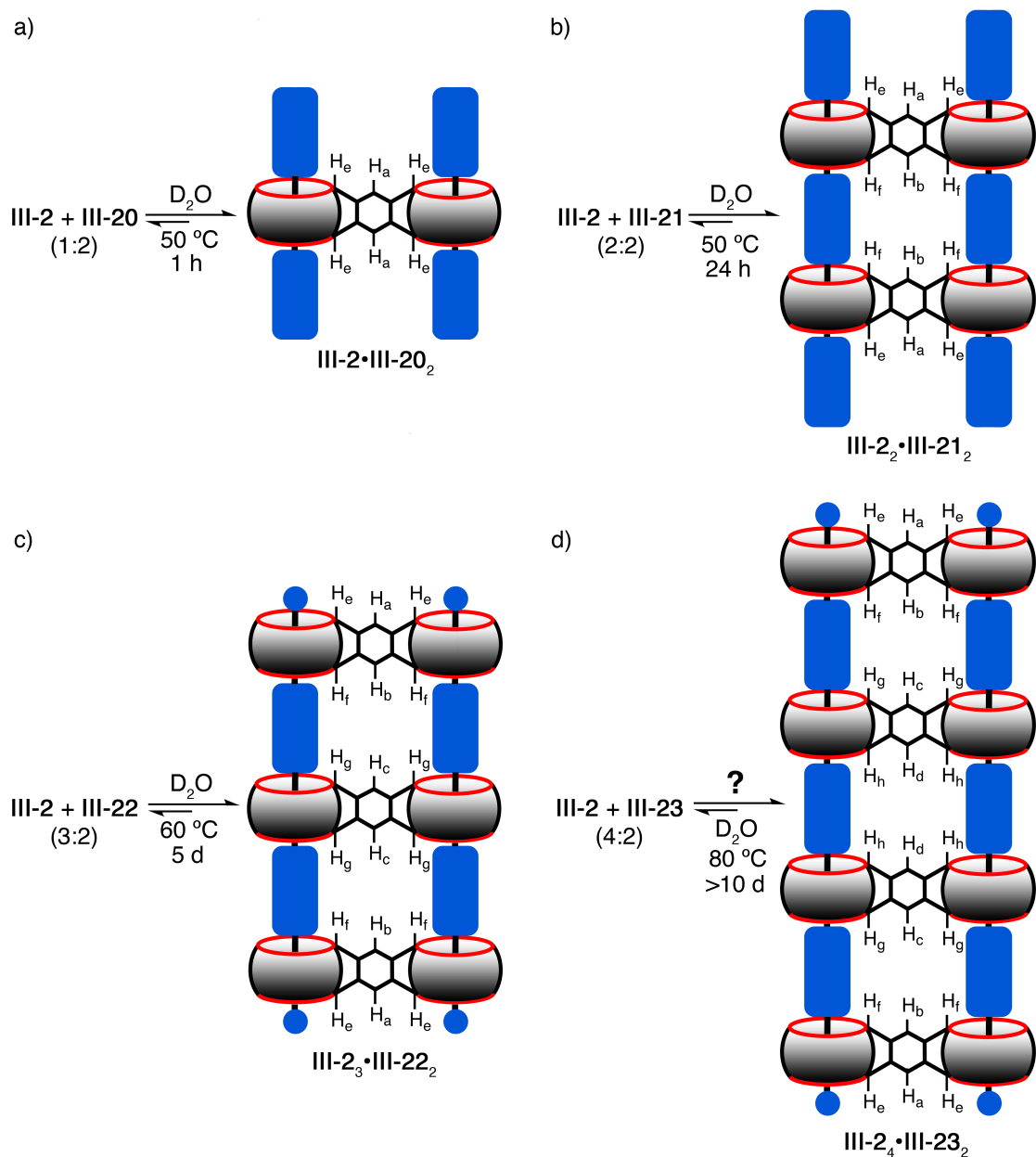
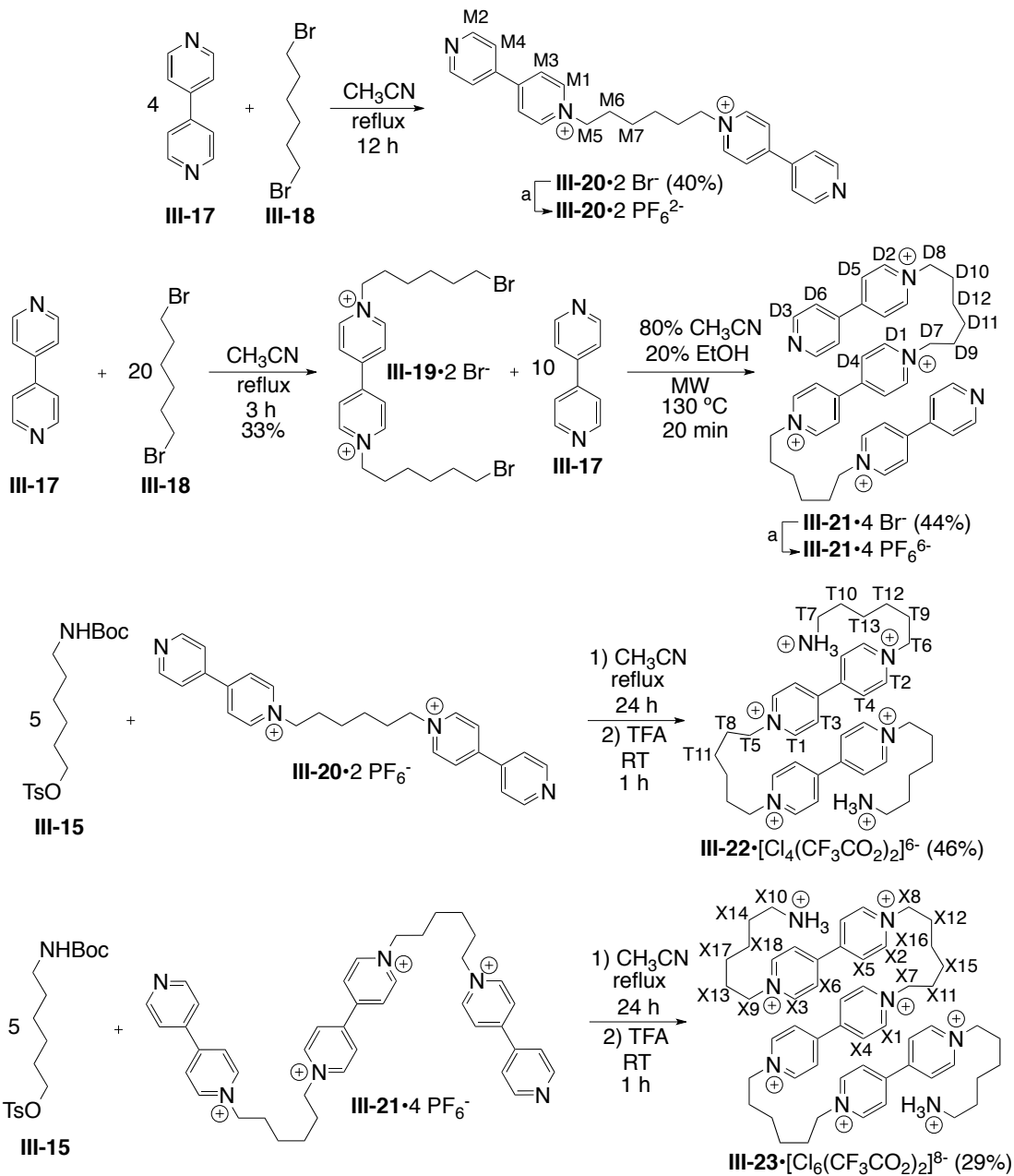


Figure III-7. Schematic representation of the formation of the a) 2:1, b) 2:2, c) 3:2, d) and potential 4:2 host•guest complexes.

We synthesized the known compound (**III-20**) following a literature procedure¹⁰⁸ which would act as our monovalent guest (Scheme III-4). Compound **III-21** was synthesized using a microwave reactor. With a microwave reactor we

were able to react the starting materials, which were not completely soluble at the boiling point of the solvent, together at temperatures above the boiling point of the solvent. These S_N2-type reactions can also be accomplished in minutes rather than hours or days. Compound **III-19** was dissolved in 20% EtOH in CH₃CN with excess **III-17** and reacted at 130 °C for 20 min. under microwave irradiation to give **III-21** in 44% yield. Trivalent guest **III-22** was synthesized using compound **III-20** as a starting material. Compound **III-20** was first converted to the •PF₆ salt for two reasons: (1) it increases its solubility in CH₃CN, and (2) bromide (Br⁻) is known to attack the C-atom adjacent to the viologen which can cause undesirable substitution patterns and a mixture of products.¹⁰¹ It was then reacted with excess **III-15**¹⁰⁹ to afford the boc-protected product (**III-24**). Compound **III-24** was subsequently stirred in CH₂Cl₂ and TFA to remove the boc protecting group and form **III-22** in 46% yield after washing with isopropanol. In a similar fashion tetravalent guest **III-23** was synthesized in 29% overall yield by using **III-21**•PF₆ as a starting material.



Scheme III-4. Synthesis of the viologen-based guests **III-20** – **III-23**. ^aCounterion exchange is described in detail in Appendix 2.

We envisioned **III-2** would have the ability to form supramolecular ladder complexes with a guest that possessed multiple binding sites since it is a very rigid and highly symmetrical double cavity host. Indeed, when **III-2** is stirred with a

solution of guest **III-20** in D₂O we observe the formation of a complex by ¹H NMR with a host:guest ratio of 1:2 (Figure III-6b). For the **III-2•III-20**₂ complex we observe a downfield shift for all the viologen protons and an upfield shift for the methylene protons of the guest resonances, indicating that **III-2** binds to the hexyldiammonium moiety of **III-20** as expected. The resonances corresponding to the aromatic H-atoms (H_f) and the axial methine H-atoms (H_g) on **III-2** were most useful in determining the type of assembly between host and guest. There is only one singlet present for the aromatic H-atoms (H_f) and one singlet of the methine H-atoms (H_g) for the host, indicating a symmetrical top and bottom of the host for the 1:2 complex (Figure III-6a). In an analogous fashion, we observe complexes formed for guests **III-21** and **III-22** with host:guest ratios of 2:2 and 3:2, respectively, as shown by ¹H NMR in Figure III-6d,f. Similar to **III-2•III-20**, we know that **III-2** binds to the hexyldiammonium moiety of guest **III-21** (Figure III-6d) because of the upfield chemical shift change of these guest resonances. However, we noticed a difference in the diagnostic resonances for the host when **III-2** complexed with **III-21** to form **III-2**₂**•III-21**₂. We now observe four diagnostic singlets for the host; two for the aromatic H-atoms (H_{f,f'}) and two for the methine H-atoms (H_{g,g'}). The presence of two singlets each is indicative of a reduction in host symmetry within the **III-2**₂**•III-21**₂ assembly. The top and bottom of the host are now in different chemical environments and would most likely be due to a 2:2 host•guest assembly (Figure III-7b). When **III-2** complexed with **III-22** we again determined that **III-2** was bound to the hexylammonium moiety of the guest based on the upfield chemical shift change of the hexyl chain resonances (Figure III-6f). The diagnostic host resonances,

however, were split into two singlets for the aromatic H-atoms and three singlets for the methine H-atoms. We would expect three singlets for each region for a 3:2 complex because of the central mirror plane running through the middle of the **III-23**•**III-22**₂ assembly (Figure III-7c). It is clear that one singlet in the aromatic H-atom region is double the intensity of the other due to an overlap of two resonances so the observed spectrum is consistent with the formulation of the complex (**III-2**)₃•(**III-22**)₂ (Figure III-7c). Unfortunately, when tetramer guest **III-23** forms a complex with **III-2** in D₂O the resonances become very broad and lose their resolution even after heating the mixture at 80 °C for over 10 days (Figure III-6h). Although it is clear that a complex is formed and the ratio of host:guest is 4:2, we are unable to identify the diagnostic resonances for the 4:2 complex. This is most likely due to a mixture of host•guest complexes instead of the desired 4:2 supramolecular ladder complex.

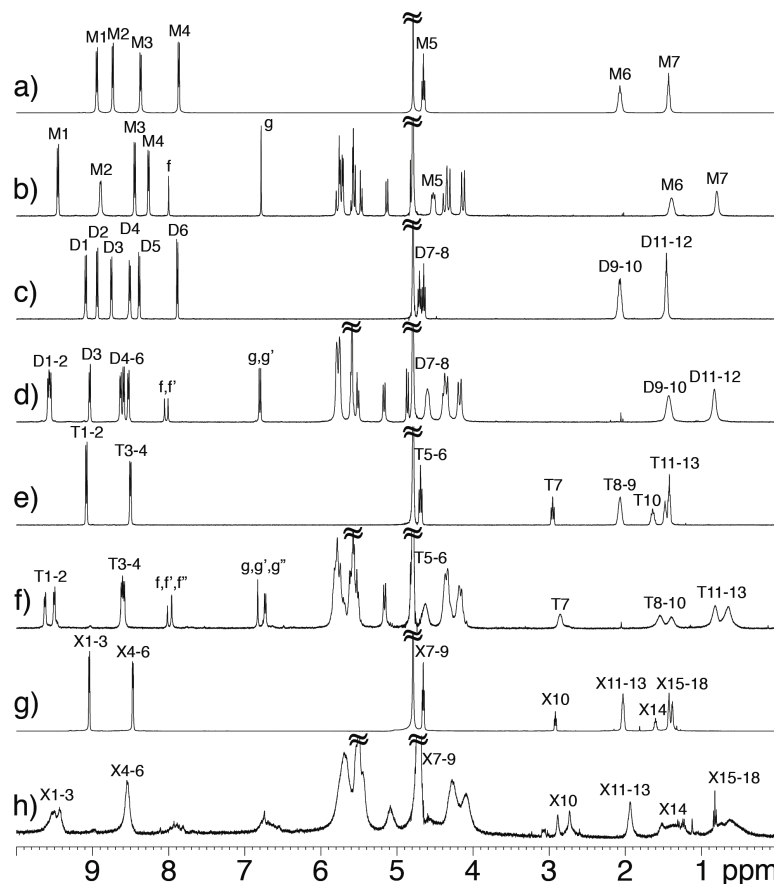


Figure III-6. ^1H NMR spectra (400 MHz, D_2O , RT) recorded for: a) guest **III-20**, b) complex **III-2**•**III-20**₂, c) guest **III-21**, d) complex **III-2**₂•**III-21**₂, e) guest **III-22**, f) complex **III-2**₃•**III-22**₂, g) guest **III-23**, and h) complex **III-2**₄•**III-23**₂.

Although the relative stoichiometry of the complexes described above are determined by the ratios of compounds used, we wanted further evidence to determine the absolute stoichiometry of each assembly since, for example, relative NMR integration for a 1:1 complex would be the same as for 2:2 or n:n complexes. We, therefore, performed diffusion-ordered spectroscopy (DOSY) in order to obtain a relative size of hosts **III-1** and **III-2**, guests **III-20** – **III-23**, and the proposed host•guest complexes **III-2**•**III-20**₂, **III-2**₂•**III-21**₂, **III-2**₃•**III-22**₂, and **III-2**₄•**III-23**₂.

The diffusion coefficients were measured using multiple resonances for **III-20** and **III-2•III-20₂** and averaged to give values of $(386.9 \pm 2.8) \times 10^{-12}$ and $(188.0 \pm 3.1) \times 10^{-12} \text{ m}^2 \text{ s}^{-1}$, respectively. The diffusion coefficients were measured for all viologen guests (**III-20** – **III-23**) and their host•guest complexes with **III-2** (Table III-2). Sample DOSY spectra shown below were recorded for free guest **III-22** (Figure III-8a) and the complex **III-2₃•III-22₂** (Figure III-8b). The diffusion coefficients of the host•guest complexes **III-2•III-20₂** and **III-2₂•III-21₂** were then compared to each other using the spherical model (Equation 4). According to the spherical model, the diffusion coefficient for a dimeric species should be 79% the value of the diffusion coefficient measured for the monomer. As expected, the diffusion coefficient for **III-2₂•III-21₂** is exactly 79% the value of the diffusion coefficient for **III-2•III-20₂**. According to the spherical model, the diffusion coefficient for a trimeric species should be 69% the value of the diffusion coefficient measured for the monomer and 87% the value of the dimer. Interestingly, the diffusion coefficient for **III-2₃•III-22₂** is 73% the value of the monomer and 93% the value of the dimer. The difference is slightly less than expected; however, this can be attributed to the structural differences between the ammonium-terminated trimer and the viologen-terminated monomer and dimer. The diffusion coefficient for a tetrameric species should theoretically be 63%, 79%, and 91% the values of the monomer, dimer, and trimer, respectively. The diffusion coefficient for proposed **III-2₄•III-23₂** complex is 52%, 66%, and 71% the value of the diffusion coefficients measured for the complexes **III-2•III-20₂**, **III-2₂•III-21₂**, and **III-2₃•III-22₂**, respectively. Since the diffusion coefficient is lower than expected for the 4:2

complex we surmise that one or more than one larger, more complicated structural recognition motif is present in solution, which would account for the broadening of the ^1H NMR resonances as seen in Figure III-6h.

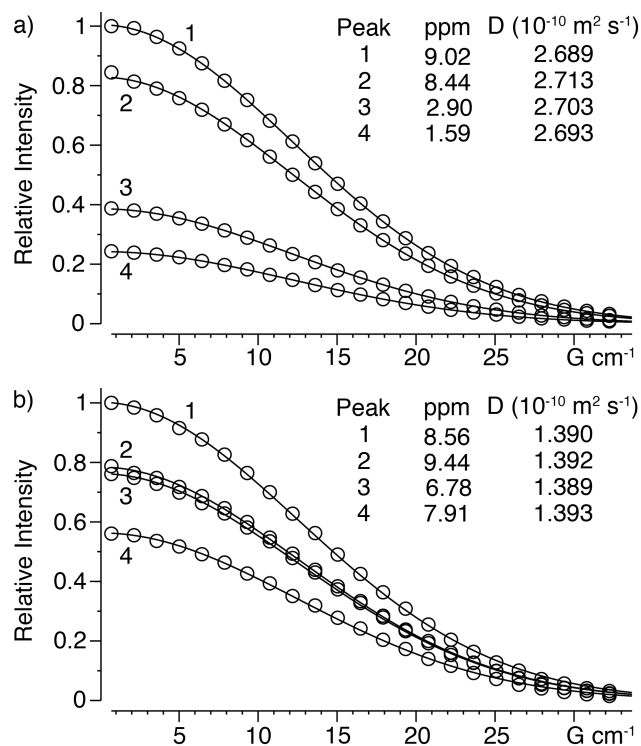


Figure III-8. Plots of the change in intensity of the indicated NMR resonances in the DOSY spectra as a function of magnetic field gradient recorded (600 MHz, D_2O , 298 K) for: a) guest **III-22** and b) complex **III-23•III-22₂**.

Table III-2. Diffusion Coefficients obtained by DOSY NMR (600 MHz, D₂O, 298 K).

| Host | Guest | $D_{\text{complex}}^{[a]}$ | $D_{\text{free guest}}^{[a]}$ |
|--------------|----------------------|----------------------------|-------------------------------|
| CB[6] | III-6 (n = 6) | 348.8 | - |
| III-1 | III-6 (n = 6) | 223.6 | - |
| III-2 | III-6 (n = 6) | 224.8 | - |
| - | III-20 | - | 386.9 |
| III-2 | III-20 | 188.0 | - |
| - | III-21 | - | 290.2 |
| III-2 | III-21 | 147.9 | - |
| - | III-22 | - | 269.4 |
| III-2 | III-22 | 137.7 | - |
| - | III-23 | - | 206.9 |
| III-2 | III-23 | 98.0 | - |

[a] Units are: $\times 10^{-12} \text{ m}^2 \text{ s}^{-1}$

In the previous section we used the results of DOSY spectroscopy to infer the absolute stoichiometry of the assemblies formed between mixtures of dual cavity host **III-2** and monomer – tetramer guests **III-20** – **III-23**. Because of the uncertainty that exists in the interpretation of DOSY measurements we decided to perform electrospray ionization mass spectrometry (ESI-MS) measurements. Initially, we measured the ESI-MS spectra for guests **III-20** – **III-23**. For monomer guest **III-20** – which contains one hexanediammonium binding site and exists as a dication – we observe a molecular ion $[\text{M}]^{2+}$ at m/z 198.1. For dimer guest **III-21** – which contains two hexanediammonium binding sites and exists as a tetracation – we do not observe the $[\text{M}]^{4+}$ ion by ESI-MS. On the contrary, the dominant ion detected can be assigned to the $[\text{M} - 2\text{H}]^{2+}$ ion at m/z 317.2. We can rationalize the formation of this $[\text{M} - 2\text{H}]^{2+}$ ion by the α -cleavages of two H^+ from the C-atoms adjacent to the quaternary N-atoms of the bipyridinium units (Figure III-9a). We believe that such losses of H^+

atoms are favorable because of the resonance structure shown which results in neutralization of a positively charged N-atom (Figure III-9a). In an analogous way, we observed the molecular ions for trimer **III-22** and tetramer **III-23** at m/z 297.3 ($[M-4H]^{2+}$) and m/z 278.8 ($[M-5H]^{3+}$), respectively (Figure III-9b and c).

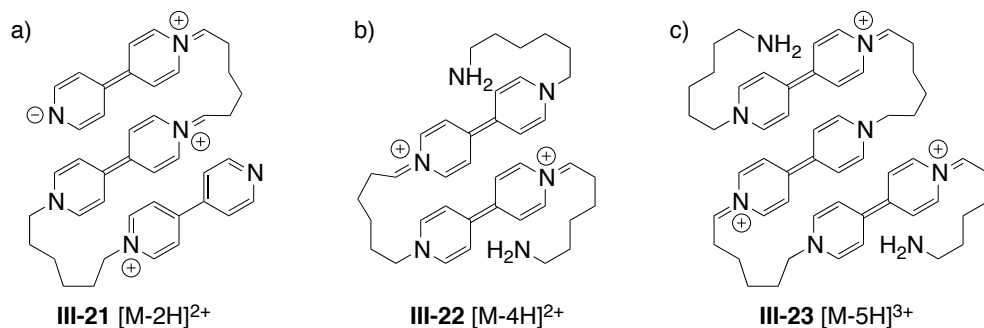


Figure III-9. Proposed structures of the ions observed in the ESI-MS for a) **III-21**, b) **III-22**, and c) **III-23**.

After having investigated the ESI-MS behavior of **III-20** – **III-23** alone, we decided to look at the ESI-MS spectra of their complexes with dual cavity host **III-2**. For the **III-2**•**III-20**₂ complex, we observe the molecular ion ($[M]^{4+}$) at m/z 714.0. For the complex formed by mixture equimolar amounts of **III-2** and **III-21**, we observe an ion at m/z 1107.3 which can be assigned to the octacationic 2:2 complex **III-2**₂•**III-21**₂ present as the $[M+3Br]^{5+}$ ion in the ESI-MS. Although the observation of the 5⁺ state with Br⁻ counterions is somewhat surprising given the propensity of **III-21** to undergo successive losses of H⁺ we rationalize the result by the well known preference of cucurbit[n]uril compounds to bind viologen dications which should suppress the loss of H⁺ to give a monocationic species. Unfortunately, we were not

able to observe diagnostic ions in the ESI mass spectra recorded **III-2**₃•**III-22**₂ or 4:2 mixtures of **III-2** and **III-23**.

Earlier in this dissertation we showed the ¹H NMR spectra recorded for 2:2, 3:2, and 4:2 mixtures of double cavity host **III-2** with guests **III-21** – **III-23** (Figure III-6). Our inability to observe the 4:2 complex **III-2**₂•**III-23**₄ by ¹H NMR spectroscopy suggested that a different structural recognition motif might be operating in this situation and therefore, we decided to investigate the behavior of these systems as a function of host:guest stoichiometry. For example, the ¹H NMR spectrum of **III-2**₂•**III-21**₂ (Figure III-10) remains unchanged even in the presence of excess guest **III-21** (2 equiv. excess) which indicates that this 2:2 assembly possesses high thermodynamic stability probably formed in a cooperative self-assembly process.

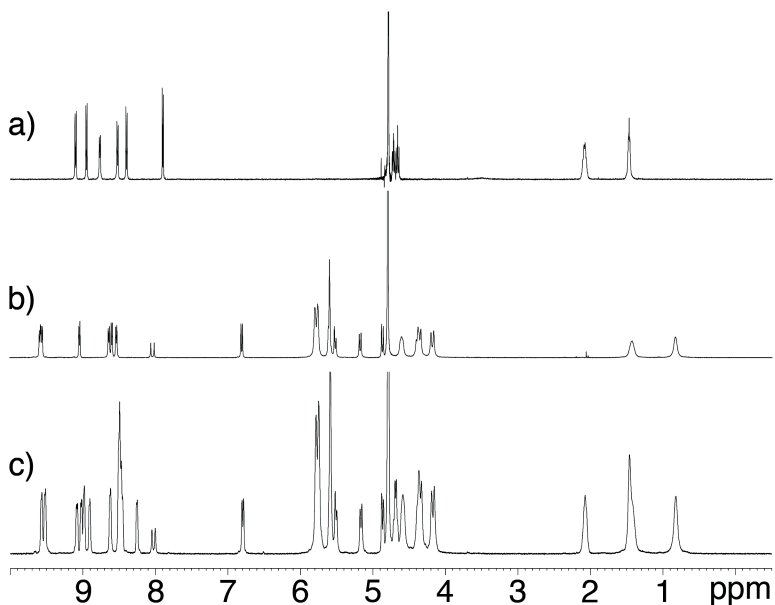


Figure III-10. ¹H NMR spectra recorded for: a) dimer guest **III-21**, b) **III-21** and **III-2** mixed together in a 2:1 ratio, and c) **III-21** and **III-2** mixed together in a 4:1 ratio.

Very interestingly, when we prepared a 1:2 mixture of double cavity host **III-2** and trimer guest **III-23** we recorded a simple ^1H NMR spectrum that displays two resonances for the aromatic ($\text{H}_{\text{a,b}}$) and two resonances for the methine ($\text{H}_{\text{e,f}}$) groups of **III-2** as well as upfield shifting of some of the protons on the hexanediammonium group (Figure III-11a). Excess free guest **III-22** is also observed by ^1H NMR. These observations suggest the formation of a fairly stable complex containing equimolar amounts of host **III-2** and trimeric guest **III-22**. Based on number of resonances observed in the ^1H NMR for $\text{H}_{\text{a,b}}$ and $\text{H}_{\text{e,f}}$ and through the use of symmetry arguments we can suggest the formation of the folded 1:1 complex **III-2•III-22** (Scheme III-5) or isomer 2 of the possible 2:2 complexes (**III-2₂•III-22₂**) (Scheme III-5). Isomer 1 would have four methine resonances and two aromatic resonances, and isomer 3 would have four methine resonances and four aromatic resonances. In order to determine which of the two species was formed we studied the complex by DOSY NMR and ESI-MS. We determined the diffusion coefficient to be $(190.6 \pm 2.1) \times 10^{-12} \text{ m}^2 \text{ s}^{-1}$, which suggests that the complex is smaller than the 3:2 complex and most likely the 1:1 complex. Further confirmation of the 1:1 complex was obtained by the ESI-MS spectrum and observation of the molecular ion ($[\text{M}]^{4+}$) at m/z 666.7. When a 2:2 mixture of **III-2** and **III-22** was prepared a more complex spectrum was obtained that displayed at least five resonances for aromatic ($\text{H}_{\text{a-d}}$) and four resonances for methine ($\text{H}_{\text{e-h}}$) groups of **III-2** (Figure III-11b). We suggest that under these conditions that the 1:1 complex and all three isomers of the possible 2:2 complexes

may be present in solution (Figure III-12). Unfortunately, there is no hard evidence to suggest that one intermediate is favored over the other possibilities. Finally, as described above, when a 3:2 mixture of dual cavity host **III-2** and trimer guest **III-22** is heated at 60 °C for 5 days we observe the formation of the three-rung ladder complex **III-2₃•III-22₃** (Figure III-11c).

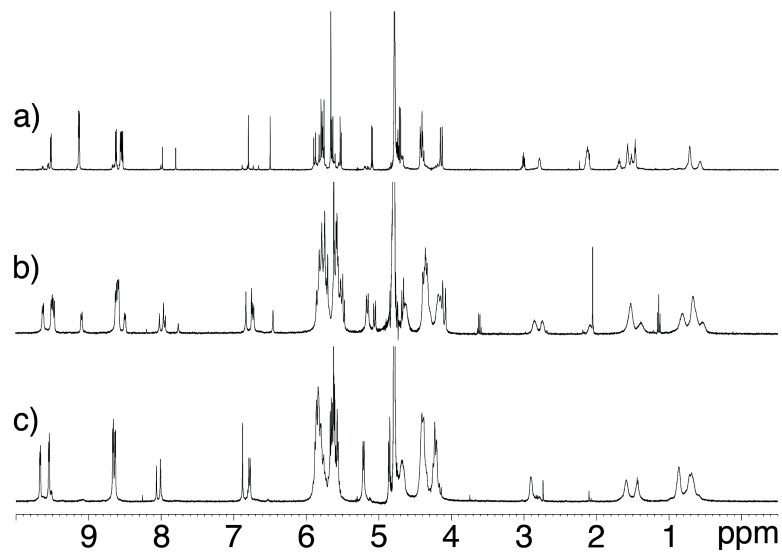
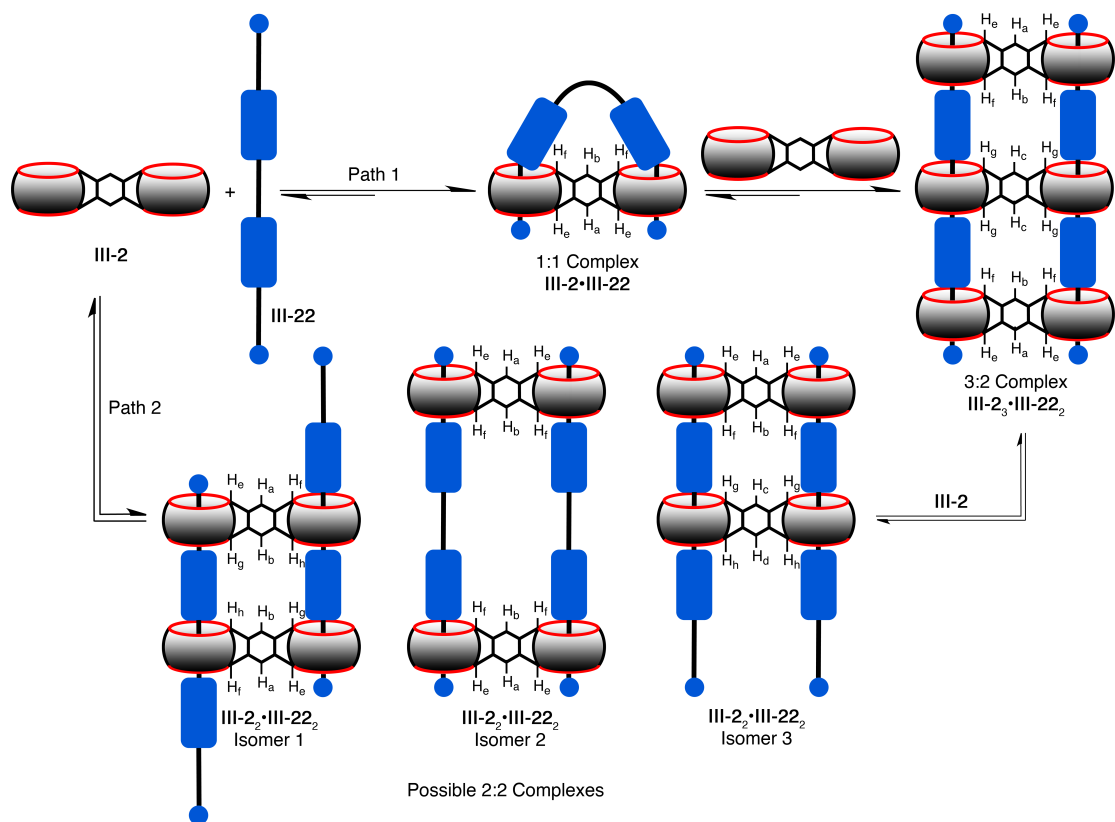


Figure III-11. ¹H NMR spectra recorded for trimer guest **III-22** and host **III-2** mixed together in a) 2:1 ratio, b) 2:2 ratio, and c) 2:3 ratio.



Scheme III-5. Possible intermediates in the formation of the 3:2 supramolecular ladder complex **III-2₃•III-22₂**.

The situation for the double cavity host **III-2** and tetrameric guest **III-23** is equally interesting. For example, the ¹H NMR spectrum recorded for an equimolar mixture of **III-2** and **III-23** shows four resonances for the methine (H_{e-h}) and two resonances for the aromatic (H_{a,b}) protons of host **III-2** as well as excess free guest **III-22** (Figure III-12a). Based on symmetry considerations, one possible complex that would display this number of resonances is the self-threaded 1:1 complex **III-2•III-23** (Scheme III-6) that is analogous to the self-threaded 1:1 complex (**III-2•III-22**) formed described above for trimer **III-22**. Other possibilities that would also have four methine resonances and two aromatic resonances include isomer 5 or

isomer 7 of the possible 2:2 complexes (**III-2**₂•**III-23**₂) shown in Scheme III-6. Isomers 1 and 4 would have only two methine resonances and two aromatic resonances. Isomers 2 and 3 would have four methine resonances and four aromatic resonances, Isomer 6 would potentially have eight methine resonances and four aromatic resonances. The diffusion coefficient was measured for the equimolar mixture ($(168.3 \pm 9.2) \times 10^{-12} \text{ m}^2 \text{ s}^{-1}$) and suggests that the 1:1 complex is formed and not the 2:2 complexes, which would have diffusion coefficients closer to that of the 4:2 complex. Unfortunately, unlike the 1:1 complex observed between host **III-2** and trimer guest **III-22**, we were unable to detect the molecular ion peak for the 1:1 complex **III-2**•**III-23** by ESI-MS. When one equivalent of host **III-2** is added to the 2:2 mixture, we observe a much more complicated ¹H NMR spectrum (Figure III-12b). There are approximately seven resonances for the methine (H_{c-l}) and four resonances for the aromatic (H_{a-d}) protons of host **III-2**. We suggest that the large number of resonances is not due to one major intermediate but to a mixture of multiple intermediates that may be comprised of the 1:1 complex, any of the seven isomers of the possible 2:2 complexes, and possibly even other complexes with a 3:2 host:guest ratio. The diffusion coefficient measured for this mixture ($(130.1 \pm 13.5) \times 10^{-12} \text{ m}^2 \text{ s}^{-1}$) suggests a mixture of components averaging larger than the 1:1 complex but smaller than the 4:2 complex. Finally, we observe a host•guest complex with a 4:2 ratio upon addition of one equivalent of host **III-2** to the previous mixture (Figure III-12c). The spectrum becomes even more complicated and the signals become very broad. Clearly, there are many possible host•guest complexes and a combination of multiple complexes would explain the broadness of the spectrum. As stated before,

the diffusion coefficient measured for this mixture as well as the host:guest ratio measured by integration suggests a complex close to that of the expected 4:2 supramolecular ladder.

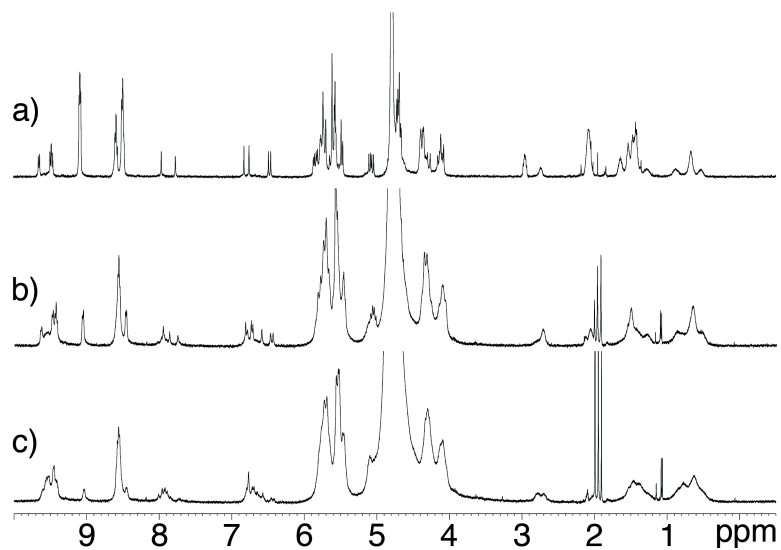
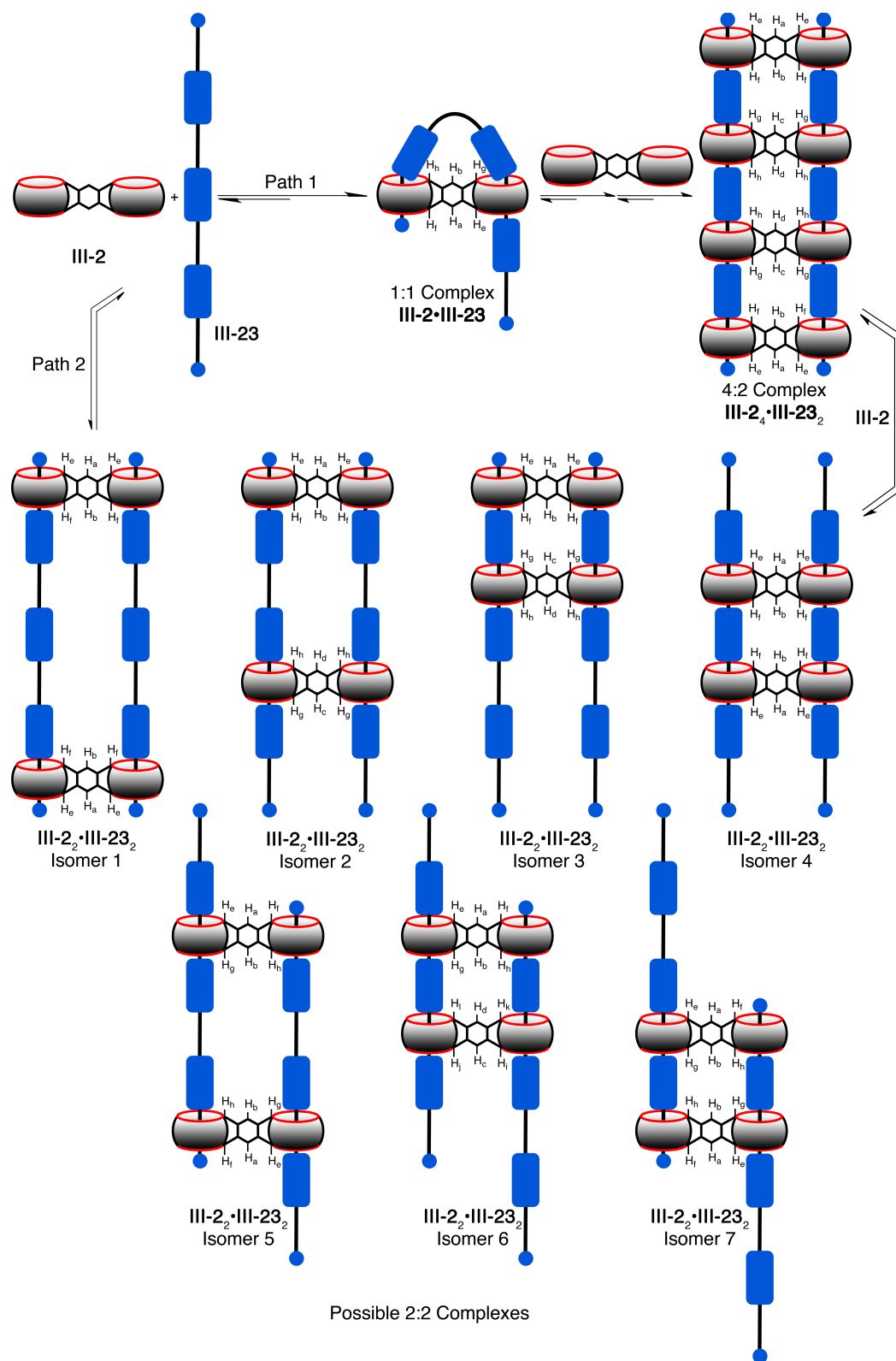


Figure III-12. ^1H NMR spectra recorded for tetramer guest **III-23** and host **III-2** mixed together in a) 2:2 ratio, b) 2:3 ratio, and c) 2:4 ratio.



Scheme III-6. Possible intermediates in the formation of the proposed 4:2 supramolecular ladder complex **III-2₄·III-23₂**.

3.6 Conclusions.

In summary, we have synthesized two new double cavity cucurbit[6]uril dimer hosts (**III-1** and **III-2**) through condensation of two glycoluril hexamer units (**III-3**) with an aromatic tetra-aldehyde (**III-4** and **III-5**). Four PEG derivatives (**III-16_{MW}**) were synthesized in order to study polymerization, by measuring the diffusion coefficient using DOSY NMR, of the PEG derivatives when complexed with an equimolar ratio of host **III-1** in aqueous solution. All shorter PEG derivatives (**III-16₃₀₀**, **III-16₁₀₀₀**, and **III-16₃₃₅₀**) formed short oligomeric (or cyclic) complexes with host **III-1**, whereas the longest PEG derivative (**III-16₁₀₀₀₀**) formed a moderately sized long-chain polymer (>36-mer). Four viologen-containing multivalent guests (**III-20** – **III-23**) were synthesized in order to create supramolecular ladder structures with host **III-2**. The complexes were analyzed using DOSY NMR and ESI-MS. All evidence suggests that we have created the 1:2, 2:2, and 3:2 supramolecular ladders. Unfortunately, there is a lack of evidence for the formation of the 4:2 complex. However, we have showcased two unique double cavity cucurbituril hosts and their potential to create some interesting host•guest systems.

Chapter 4: Summary and Future Work.

4.1 Summary.

The field of supramolecular chemistry is ever evolving, and new and interesting molecular receptors are being synthesized all the time. Chemists have the ability to tailor a molecular receptor for a single purpose or application. Other receptors, such as cyclodextrins, can be used for a wide variety of applications. However, they lack the selectivity and binding affinity that can be very useful for certain applications. Cucurbituril molecular containers are selective and display high binding affinity towards their guests but lack good solubility characteristics and are difficult to functionalize. Fortunately, recent research has led to a number of new cucurbituril derivatives that display good solubility, contain functionality, and maintain their selectivity and high binding affinity.

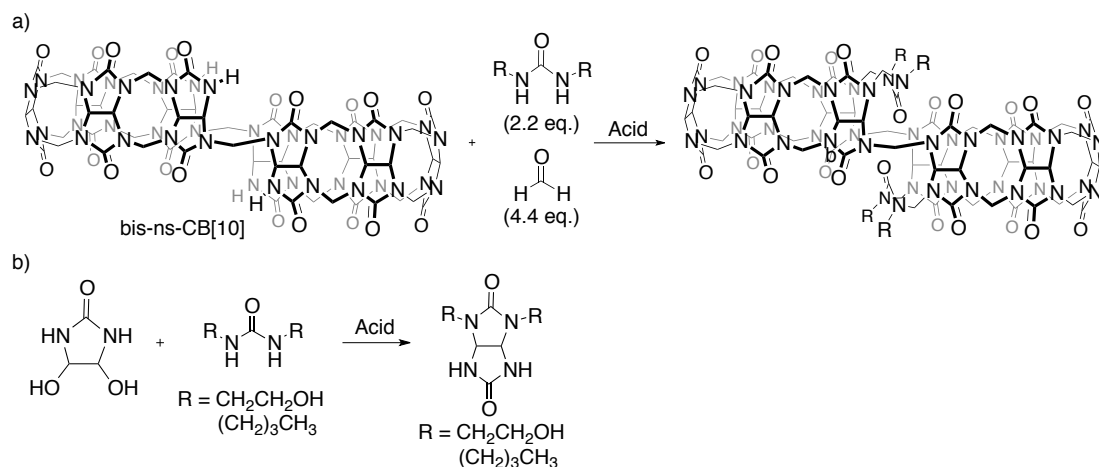
In this body of work, double cavity cucurbiturils were investigated due to their unique ability to bind and sequester two guest molecules simultaneously. The ability to form ternary complexes has been shown to lead to many intriguing applications. However, only two cucurbiturils synthesized and published previous to this body of work (CB[8] and bis-*ns*-CB[10]) were capable of forming ternary complexes.

In Chapter 2, a new double cavity host (**II-1**) was synthesized starting from bis-*ns*-CB[10]. Host **II-1** is more rigid, thus more selective towards its guests than bis-*ns*-CB[10]. We also demonstrated its ability to form a [3]rotaxane, and the first rotaxane *via* clipping using a cucurbituril host. In Chapter 3, two new double cavity

hosts (**III-1** and **III-2**) were synthesized starting from glycoluril hexamer (**III-3**). Host **III-1** displayed moderate solubility in a Na₂SO₄ aqueous solution. Therefore, we attempted to form supramolecular polymers in aqueous solution through the polymerization of PEG derivatives (**III-16**_{MW}). Once the PEG chain was long enough (**III-16**₁₀₀₀₀) we observed a >36-mer oligomer based on the diffusion coefficients measured by DOSY NMR. The highly symmetrical host **III-2** was used to create supramolecular ladders in aqueous solution. Multivalent viologen-containing guests (**III-20** – **III-23**) were synthesized, and we observed the formation of the 1:2, 2:2, and 3:2 host•guest supramolecular ladders based on the diffusion coefficients obtained by DOSY NMR and ESI-MS analysis.

4.2 Future Work.

The synthesis of host **II-1** discussed in Chapter 2 incorporated ethyleneurea (**II-2**) as the bridge for the bis-*ns*-CB[10] derivative. Using similar reaction conditions for the formation of **II-1** and some urea-containing molecule, we will be able to form a new family of double cavity hosts based on bis-*ns*-CB[10] (Scheme IV-1a). Of particular interest are functionalized glycoluril derivatives that have the potential to enhance solubility and/or functionality to the bis-*ns*-CB[10] derivatives. We have successfully synthesized two potentially interesting functionalized glycolurils (Scheme IV-1b). Unfortunately, we have yet to isolate the corresponding bis-*ns*-CB[10] derivatives.



Scheme IV-1. Schematic representation of the synthesis of: a) potential new bis-*ns*-CB[10] derivatives and b) glycoluril derivatives.

Hosts **III-1** and **III-2** discussed in Chapter 3 are the first cucurbituril hosts comprised of two covalently attached CB[6] macrocycles. Although we showed that **III-1** has the ability to polymerize a guest that incorporates binding moieties at the terminus, it was not to the extent we imagined. There is a great deal of room to optimize the system and use host **III-1** in the formation of a supramolecular polymer. However, the system may or may not utilize PEG derivatives similar to the system studied in Chapter 3. PEGs are known to change their conformation and aggregate in aqueous solution, and therefore may not be ideal candidates for such a system. Ideally, we want to create a supramolecular polymer that can be controlled by some sort of stimuli, such as guest exchange (Figure IV-1a) or pH change (Figure IV-1b).

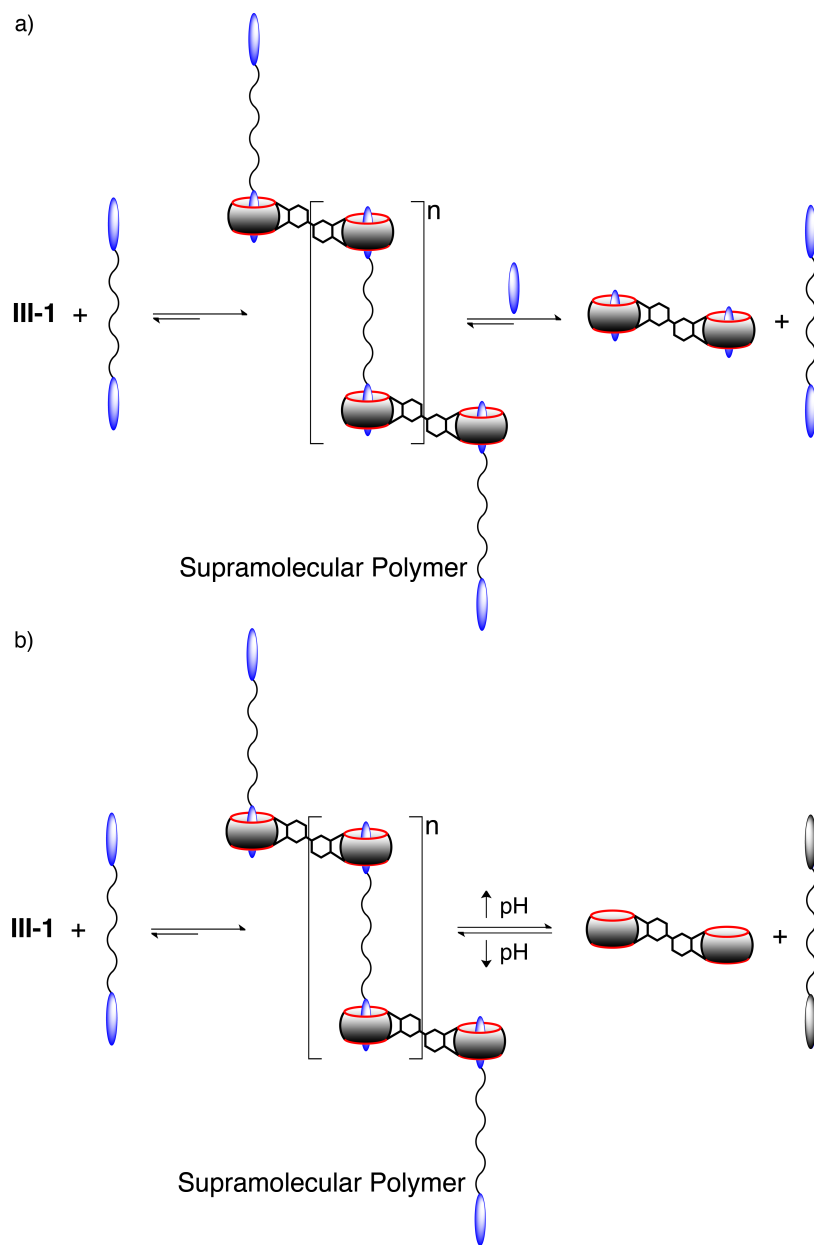


Figure IV-1. Schematic representation of a supramolecular polymer controlled by: a) guest exchange and b) pH change.

Host **III-2** was used to create some interesting host•guest complexes with the multivalent viologen guests (**III-20** – **III-23**). Due to solubility constraints, host **III-2** would not make a good candidate for the supramolecular polymer project. Therefore,

host **III-2** should be used in the formation of other unique host•guest complexes. CB[8], for example, is utilized in many types of applications, as described in Chapter 1. Host **III-2** could be implemented into many similar applications. A major advantage to using host **III-2** would be the ability to use a variety guests rather than be limited to methyl viologen and naphthalene or anthracene containing compounds.

Appendix 1

A Clipped [3]Rotaxane Derived From Bis-*nor-seco*-Cucurbit[10]uril

Supplementary Information

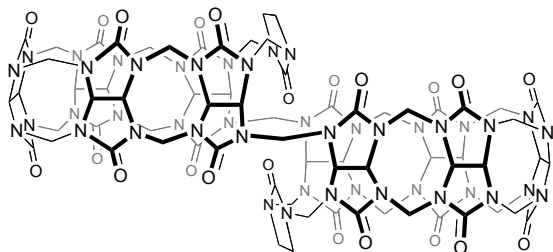
*by James B. Wittenberg, Matthew G. Costales, Peter Y. Zavalij, and Lyle Isaacs**

*Department of Chemistry and Biochemistry, University of Maryland, College Park,
MD 20742*

| Table of Contents | Pages |
|--|--------------|
| General experimental details | 85 |
| Synthetic procedures and characterization data | 85 – 88 |
| ¹ H and ¹³ C NMR spectra of new compounds | 89 – 94 |
| ¹ H NMR spectra recorded for selected II-1 •guest complexes | 95 – 114 |
| ¹ H NMR spectra recorded for II-1 • II-4 ₂ experiments | 115 – 117 |
| Details of the X-ray Crystal Structure of II-1 • II-3 ₂ | 118 – 122 |

General Experimental. Starting materials were purchased from commercial suppliers were used without further purification. Bis-*ns*-CB[10] is known in the literature.¹ Melting points were measured on a Meltemp apparatus in open capillary tubes and are uncorrected. TLC analysis was performed using pre-coated plastic plates from Merck. IR spectra were recorded on a JASCO FT/IR 4100 spectrometer and are reported in cm^{-1} . ^1H NMR spectra were measured on a Bruker DRX-400 instrument operating at 400 MHz. ^{13}C NMR spectra were measured on a Bruker DRX-500 instrument operating at 500 MHz (125 MHz for ^{13}C NMR). Mass spectrometry was performed using a JEOL AccuTOF electrospray instrument (ESI).

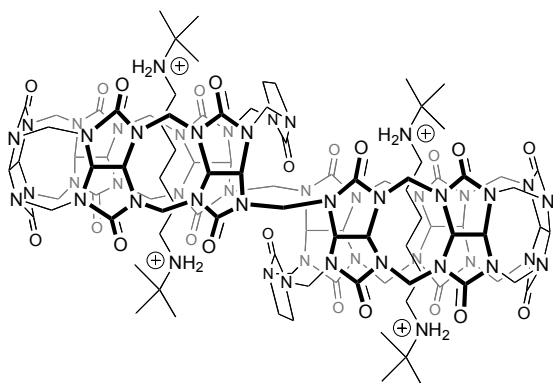
Synthetic Procedures and Characterization.



Compound **II-1**: To a solution of bis-*ns*-CB[10] (100.0 mg, 0.061 mmol) in HCl (8 M, 0.53 mL) in a 1 dram glass vial was added **II-2** (13.0 mg, 0.134 mmol)

and then CH_2O (8.0 mg, 0.269 mmol). The vial was then sealed with a screw cap. The mixture was stirred and heated at 50 °C for 1 h. The precipitate was collected by vacuum filtration. The precipitate was then washed with HCl (8 M, 0.5 mL) and H_2O (3×1.0 mL) and dried under high vacuum to yield **II-1** as a white solid (89.0 mg, 0.048 mmol, 78%). M.p. > 300 °C. IR (cm^{-1}): 1734s, 1463m, 1378m, 1258s, 1219s, 966m, 796s, 758m. ^1H NMR (400 MHz, D_2O , as **1•3**₂, RT): 6.82 (d, $J = 8.1$, 4H), 6.66 (d, $J = 8.1$, 4H), 6.60 (s, 4H), 5.84 (d, $J = 6.0$, 4H), 5.80 (d, $J = 6.0$, 4H), 5.77 (s, 4H), 5.73 (d, $J = 14.4$, 4H), 5.56 (d, $J = 16.4$, 4H), 5.53 (d, $J = 9.0$, 4H), 5.47 (d, $J =$

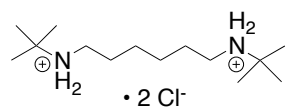
15.6, 4H), 5.38 (d, $J = 9.0$, 4H), 5.30-5.20 (m, 8H), 4.55-4.35 (m, 16H), 4.33 (s, 8H), 4.08 (d, $J = 15.6$, 4H), 4.03 (d, $J = 15.6$, 4H), 3.76 (dd, $J = 6.8, 8.4$, 4H). ^{13}C NMR (125 MHz, D_2O , **3** as guest, RT, 1,4-dioxane as internal standard): δ 160.69, 160.20, 158.13, 157.52, 157.17, 157.03, 156.09, 133.21, 132.40, 126.57, 124.99, 71.63, 70.52, 70.28, 70.09, 66.98, 56.65, 51.50, 51.36, 51.31, 47.19, 44.46, 42.50, 41.94. MS (ESI, **3** as guest): m/z 711 ($[\text{M}\cdot\mathbf{3}_2+3\text{H}]^{3+}$).



Compound **II-1•II-4₂**: To a solution of bis-*ns*-CB[10] (100.0 mg, 0.061 mmol) in HCl (8 M, 0.53 mL) in a 1 dram glass vial was added **II-4** (37.0 mg, 0.122 mmol) and the reaction was stirred at RT until homogeneous. To the reaction

mixture was added **II-2** (13.0 mg, 0.134 mmol) and CH_2O (8.0 mg, 0.269 mmol). The vial was then sealed with a screw cap. The mixture was stirred and heated at 50 °C for 1 h. The precipitate was collected by vacuum filtration. The precipitate was stirred with MeOH (5.0 mL), collected by centrifugation, and dried under high vacuum to yield **II-1•4₂** as a white solid (98.0 mg, 0.040 mmol, 69%). M.p. > 300 °C. IR (cm^{-1}): 3459br, 1726s, 1471, 1322m, 1257m, 1223s, 1184s, 1142m, 966s, 848m, 797s, 760m. ^1H NMR (400 MHz, D_2O , RT): 6.31 (s, 4H), 5.85-5.75 (m, 12H), 5.72 (d, $J = 15.6$, 4H), 5.67 (s, 4H), 5.63 (s, 8H), 5.62 (d, $J = 15.6$, 4H) 5.51 (d, $J = 9.4$, 4H), 5.35 (d, $J = 9.4$, 4H), 4.43 (d, $J = 15.6$, 4H), 4.40-4.30 (m, 12H), 4.28 (d, $J = 15.6$, 4H), 4.17 (dd, $J = 7.2, 8.6$, 4H), 3.57 (dd, $J = 7.2, 8.6$, 4H), 3.0-2.80 (m, 8H),

1.55 (s, 18H), 1.46 (s, 18H), 0.75-0.60 (m, 12H), 0.60-0.50 (m, 4H). ^{13}C NMR (125 MHz, D_2O , RT, 1-4-dioxane as internal reference): δ 164.08, 160.30, 159.58, 158.45, 156.98, 156.85, 156.66, 156.39, 71.57, 70.60, 70.53, 70.37, 67.02, 57.21, 56.24, 51.56, 51.33, 47.39, 44.49, 42.06, 41.66, 26.96, 26.82, 25.93, 25.86, 25.54. MS (ESI): m/z 772.3 ($[\text{M}+3\text{H}]^{3+}$).



Compound **II-4** • 2 Cl⁻: To a stirring and refluxing solution of *t*-butylamine (10.0 g, 41.0 mmol) in THF (7.0 mL) in a 3-neck RB flask was added a solution of 1,6-dibromohexane (18.0 g, 246.1 mmol) in THF (8.0 mL) dropwise. The reaction mixture was stirred at reflux for 3 h at which point a solution of KOH (5.5 g, 98.4 mmol) in H_2O (3.3 mL) was added. The reaction mixture was stirred at reflux for 14 h then cooled to RT. The KBr salt produced from the reaction was filtered off, and the filtrate was concentrated by rotary evaporation to give a crude oil. The crude oil was dissolved in toluene (30.0 mL) and the mixture was concentrated by rotary evaporation and dried under high vacuum. The crude waxy solid was purified by column chromatography (4:1 $\text{CHCl}_3/\text{MeOH}$, 2% NH_4OH , $R_f = 0.25$) to yield **II-4** as a waxy solid (7.5 g, 32.9 mmol, 80%). The spectroscopic data (^1H NMR and ^{13}C NMR) matches that reported in the literature.² Compound **II-4**•2HCl was obtained by adding **II-4** (7.5 g, 32.9 mmol) to H_2O (100.0 mL) followed by the addition of conc. HCl until pH = 2. The homogeneous mixture was then concentrated by rotary evaporation and dried under high vacuum to yield **II-4**•2HCl as a white solid (9.8 g, 98%). M.p. > 300 °C. IR (cm^{-1}): 3514s, 3465s, 3069m, 2978s, 2870m, 2803s, 2482m, 2437m, 1641m, 1598s,

1482m, 1447s, 1409s, 1382s, 1257m, 1216s, 997s, 877m, 794m. ¹H NMR (400 MHz, D₂O, RT): 2.99 (t, 4H), 1.63 (p, 4H), 1.43 (p, 4H), 1.34 (s, 18H). ¹³C NMR (125 MHz, D₂O, RT, 1,4-dioxane as internal reference): δ 56.94, 41.28, 26.08, 25.50, 24.96. MS (ESI): *m/z* 229.3 ([M+H]¹⁺).

Sample ¹H NMR experiment for the formation of complex **II-1•II-3**₂: To a solution of **II-3** (2.1 mg, 0.01 mmol) in D₂O (1.0 mL) in a 1 dram glass vial was added an excess of solid **II-1** (11.0 mg, 0.006 mmol) and stirred at RT overnight. The heterogeneous mixture was filtered through a 0.2 μm PES (polyethersulfone) filtering device into an NMR tube. The ¹H NMR spectra were recorded at RT.

References

- 1) Huang, W. -H.; Liu, S.; Zavalij, P. Y.; Isaacs, L. *J. Am. Chem. Soc.* **2006**, *128*, 14744-14745.
- 2) Nagel, M.; Hany, R.; Lippert, T.; Molberg, M.; Nuesch, F. A.; Rentsch, D. *Macromol. Chem. Phys.* **2007**, *208*, 277-286.

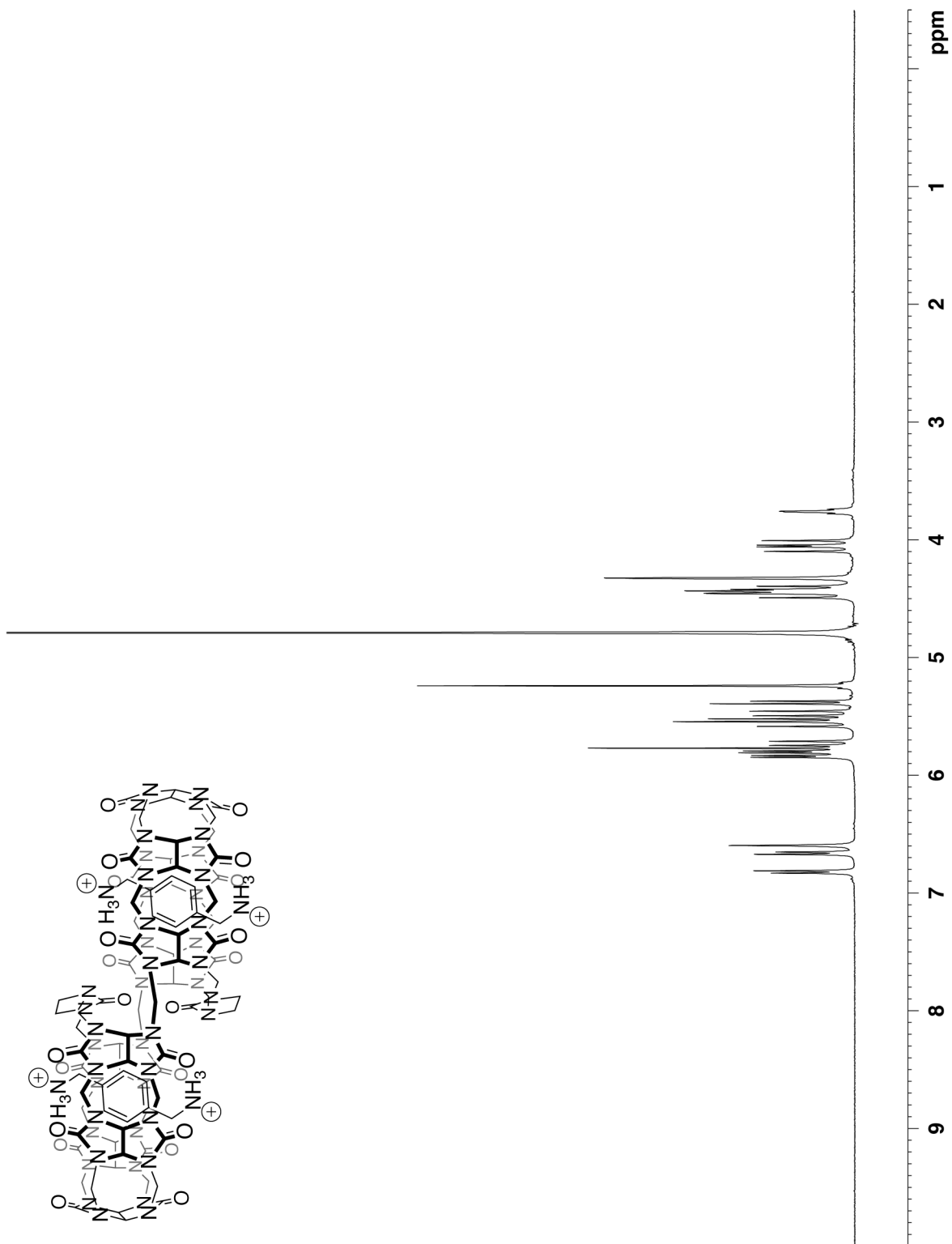


Figure II-S1. ^1H NMR spectrum (400 MHz, D_2O , RT) recorded for a mixture of *p*-xylenediammonium dihydrochloride and **II-1** (2:1 ratio).

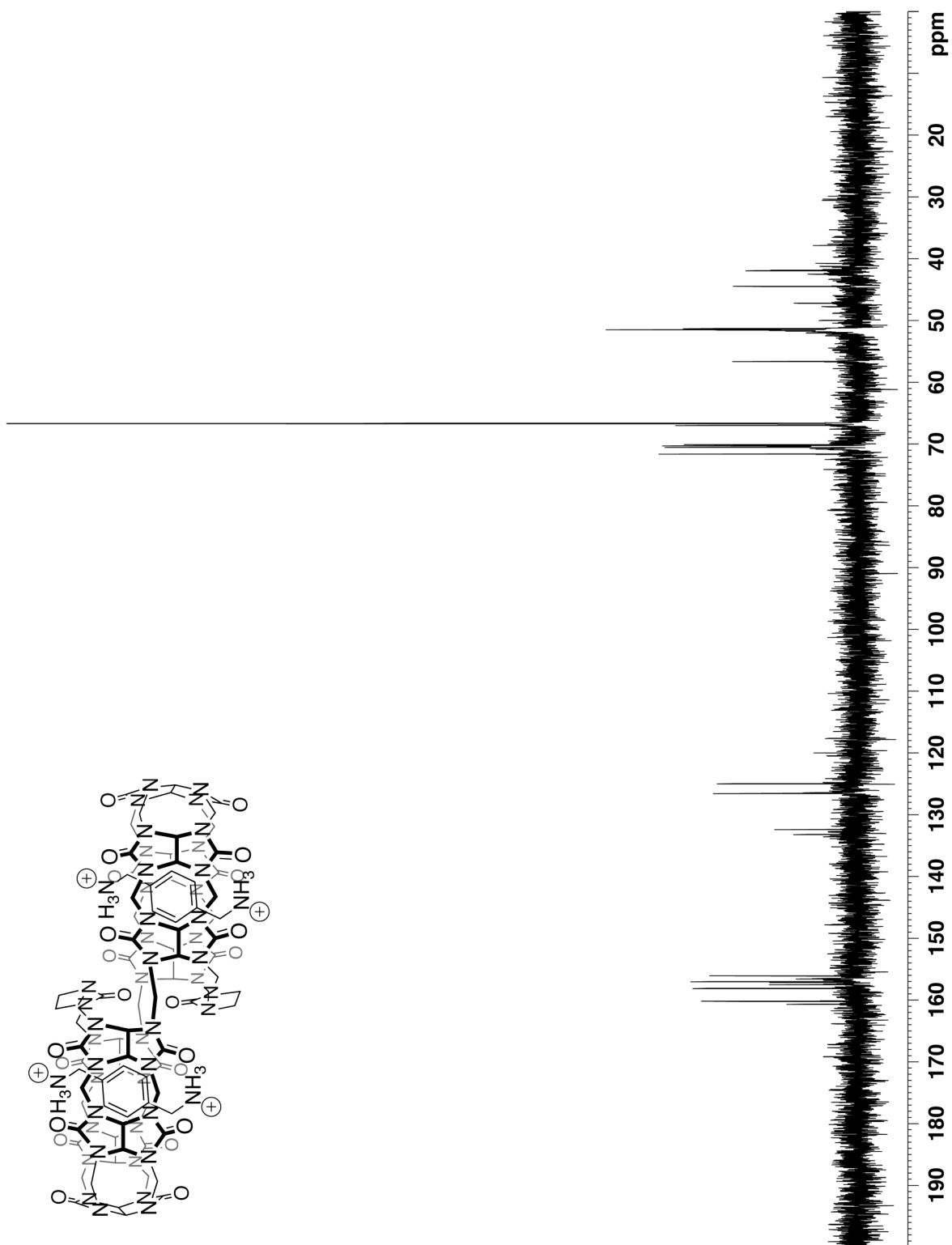


Figure II-S2. ^{13}C spectrum (125 MHz, D_2O , 1,4-dioxane as internal reference, RT) recorded for a mixture of *p*-xylenediammonium dihydrochloride and **II-1** (2:1 ratio).

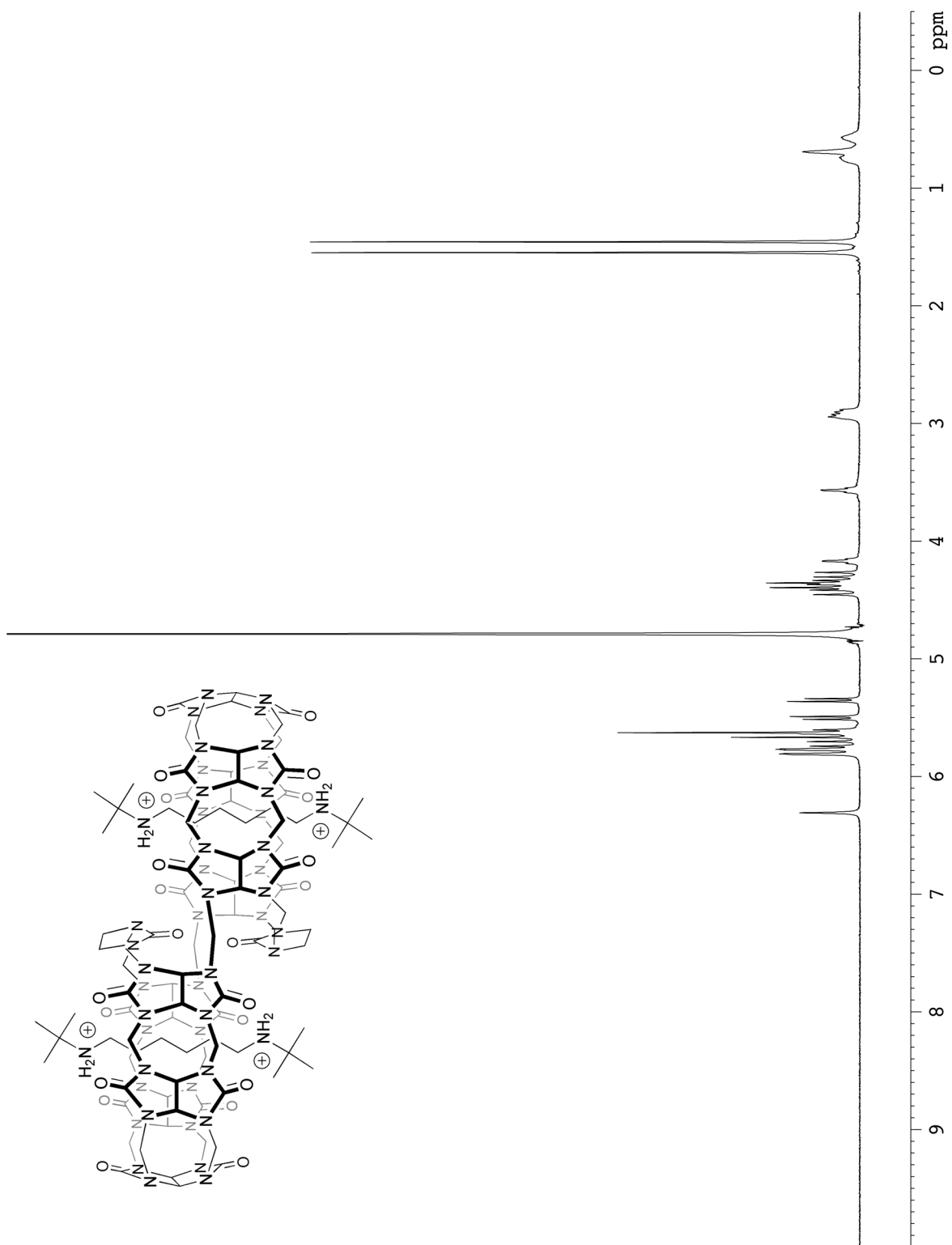


Figure II-S3. ¹H NMR spectrum (400 MHz, D₂O, RT) recorded for [3]rotaxane **II-1•II-4₂**.

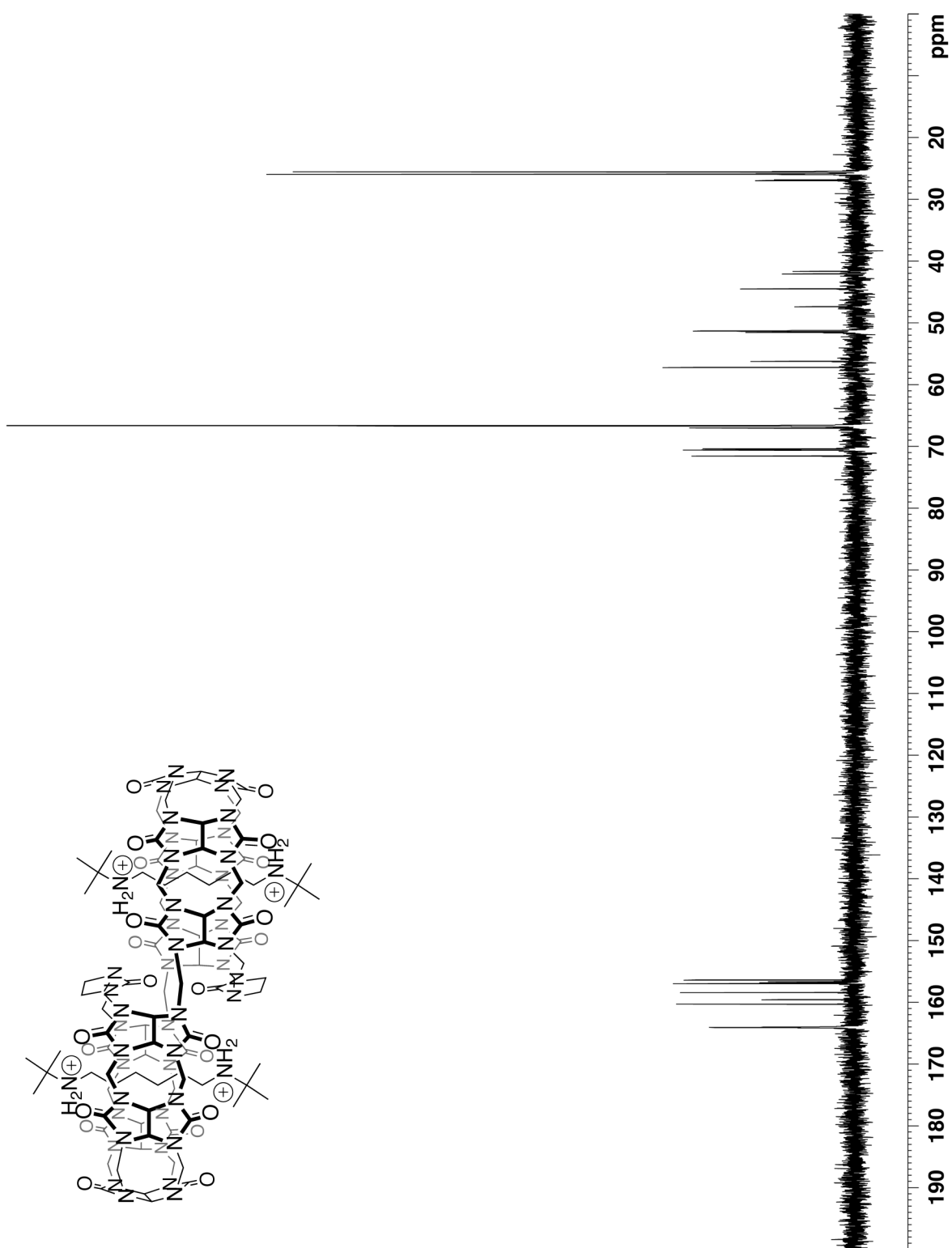


Figure II-S4. ¹³C Spectrum (125 MHz, D₂O, 1,4-dioxane as internal reference, RT) recorded for [3]rotaxane **II-1•II-4₂**.

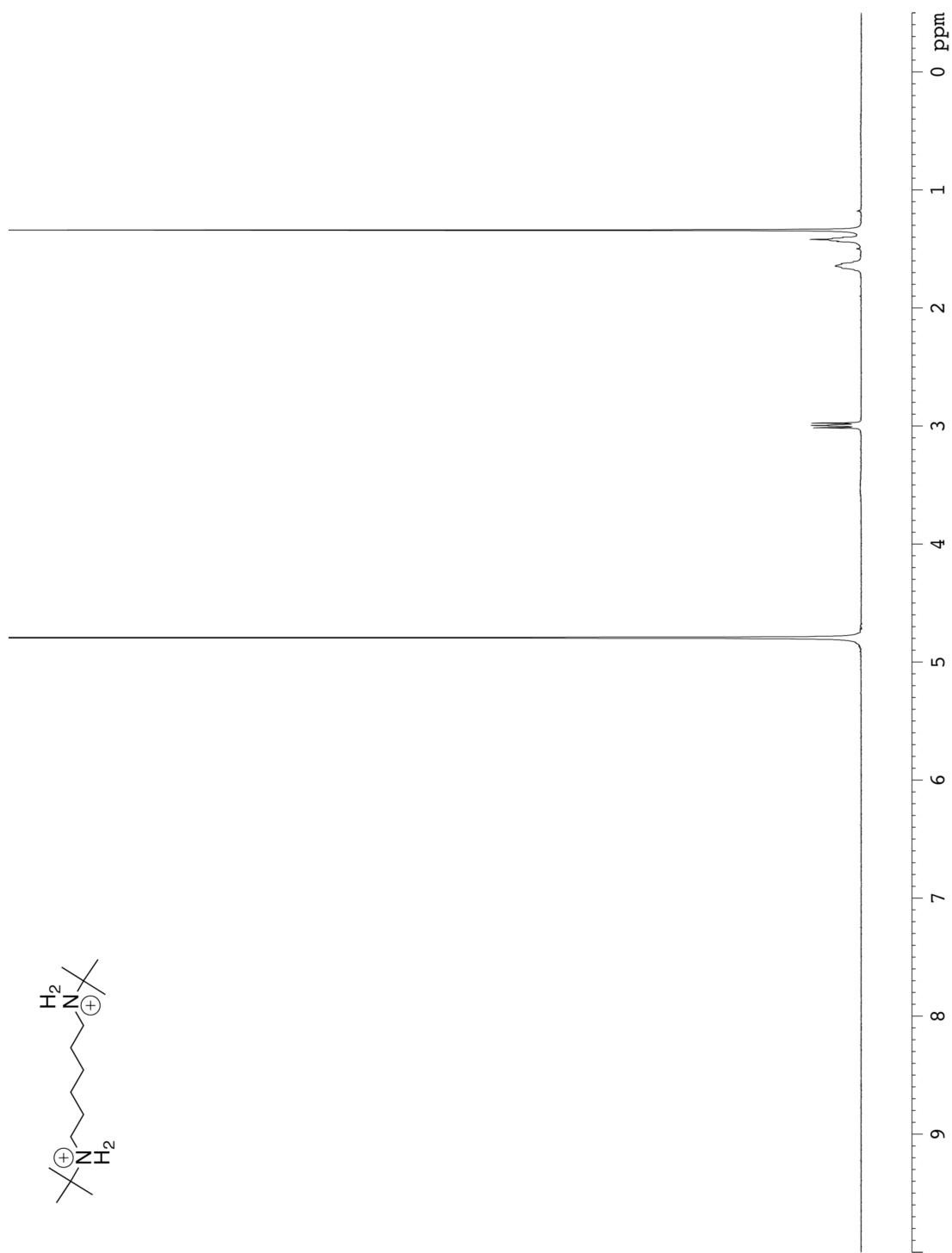


Figure II-S5. ^1H NMR spectrum (400 MHz, D_2O , RT) recorded for compound II-4•2Cl $^-$.

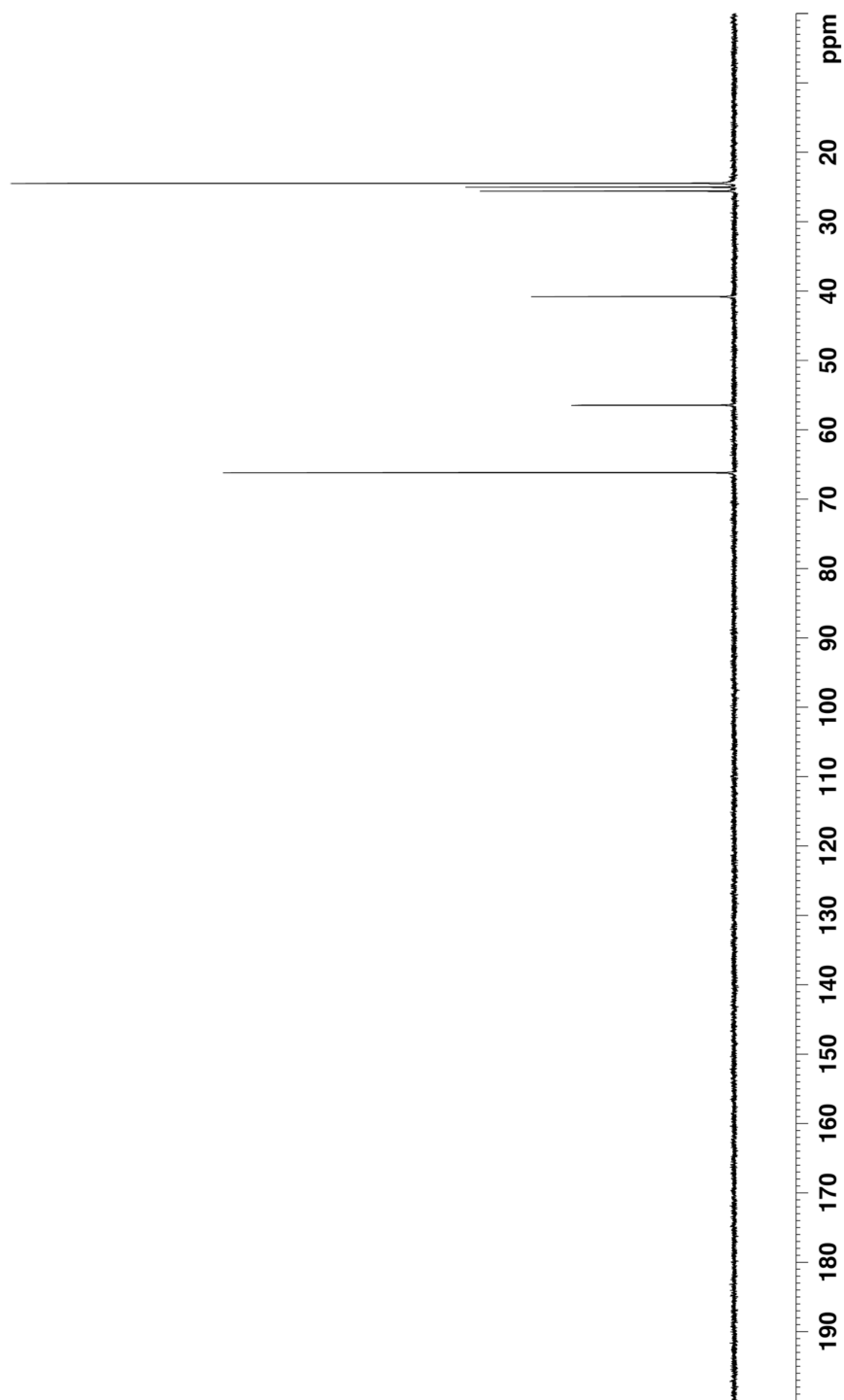
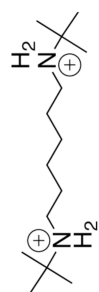


Figure II-S6. ^{13}C NMR spectrum (125 MHz, D_2O , 1,4-dioxane as internal reference, RT) recorded for compound **II-4**• 2Cl^- .

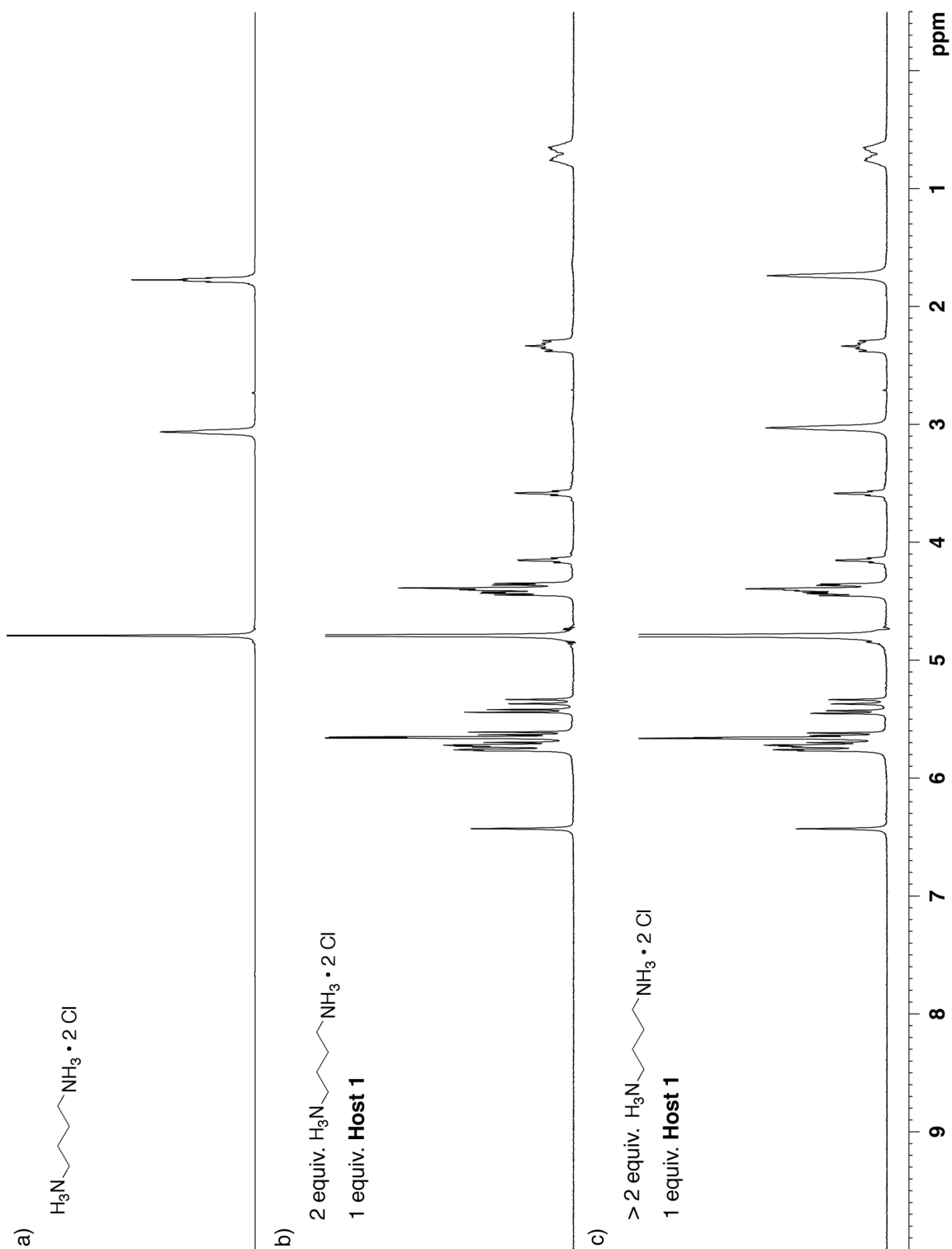


Figure II-S7. ^1H NMR spectra (400 MHz, D_2O , RT) recorded for: a) 1,4-butanediammonium dihydrochloride, b) a mixture of 1,4-butanediammonium dihydrochloride and **II-1** (2:1 ratio), and c) a mixture of 1,4-butanediammonium dihydrochloride and **II-1** (>2:1 ratio).

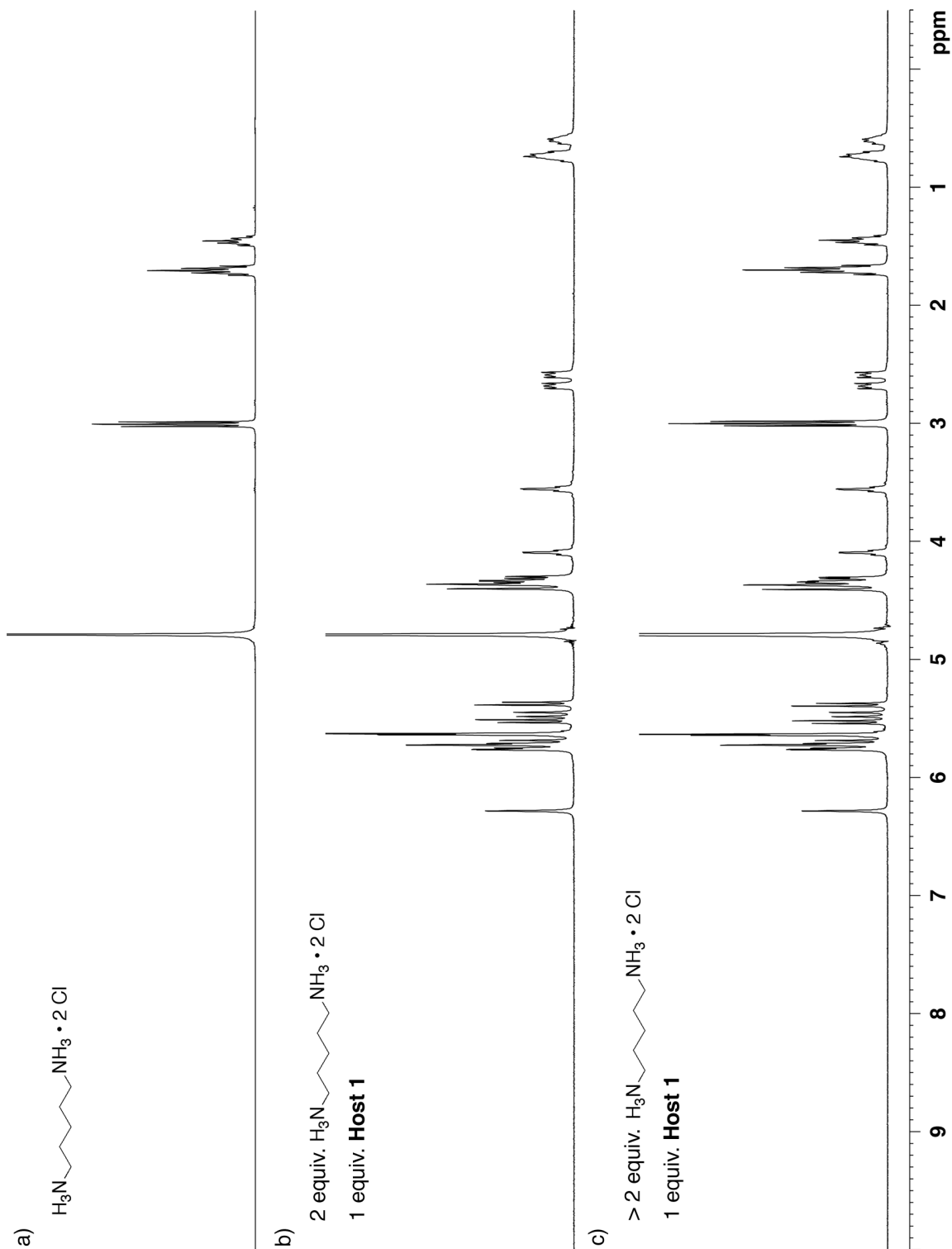


Figure II-S8. ^1H NMR spectra (400 MHz, D_2O , RT) recorded for: a) 1,5-pentanediammonium dihydrochloride, b) a mixture of 1,5-pentanediammonium dihydrochloride and **II-1** (2:1 ratio), and c) a mixture of 1,5-pentanediammonium dihydrochloride and **II-1** (>2:1 ratio).

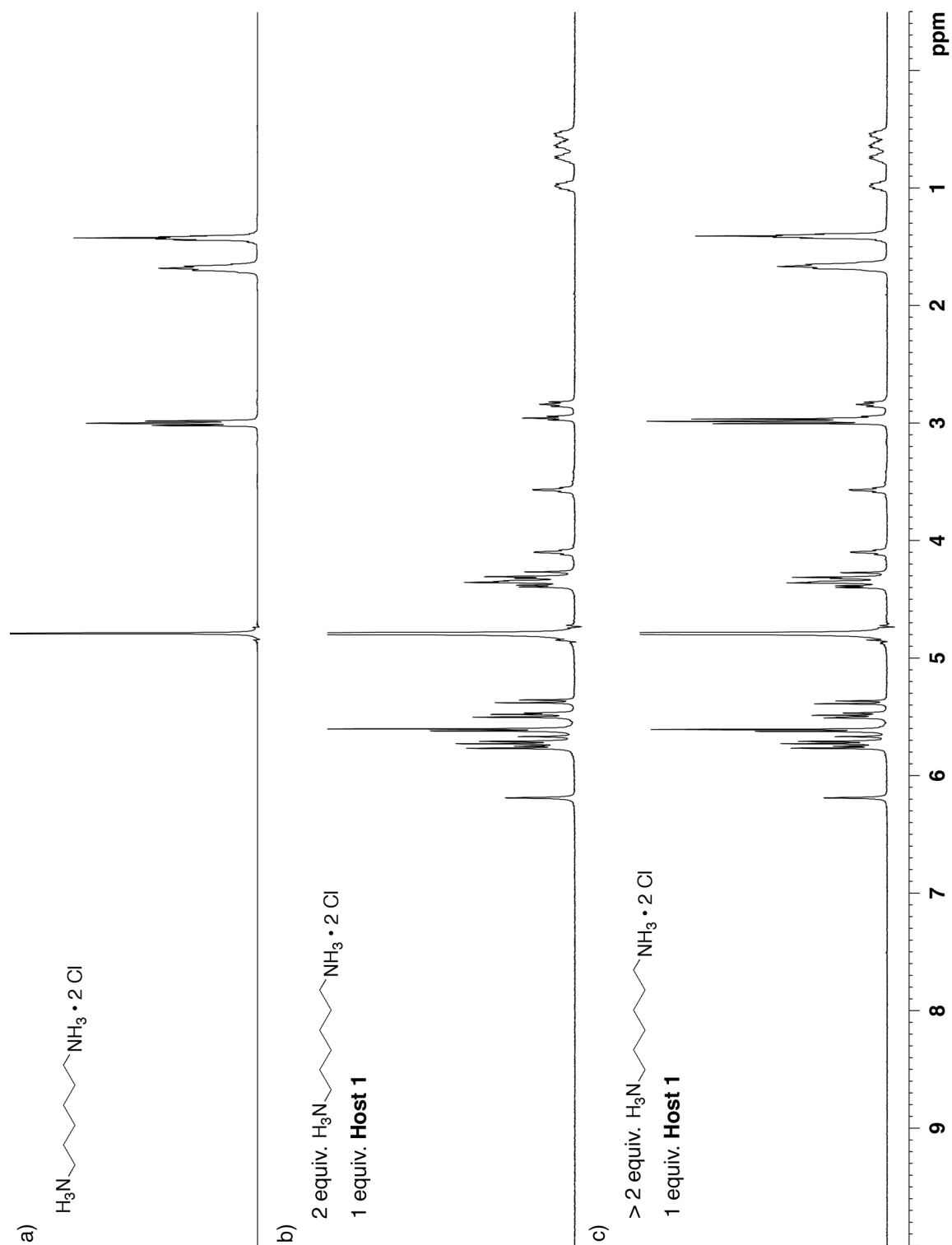


Figure II-S9. ^1H NMR spectra (400 MHz, D_2O , RT) recorded for: a) 1,6-hexanediammonium dihydrochloride, b) a mixture of 1,6-hexanediammonium dihydrochloride and **II-1** (2:1 ratio), and c) a mixture of 1,6-hexanediammonium dihydrochloride and **II-1** (>2:1 ratio).

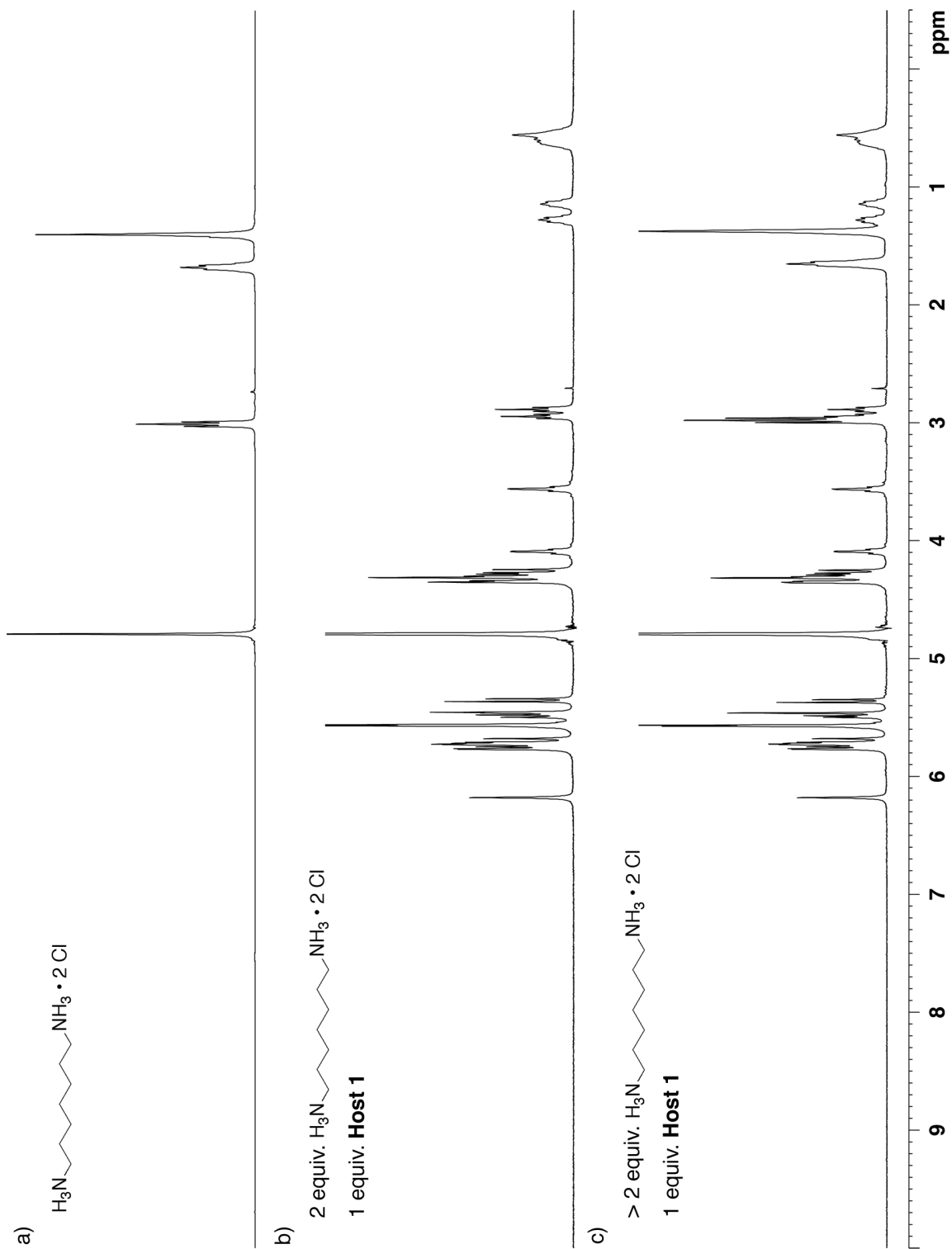


Figure II-S10. ^1H NMR spectra (400 MHz, D_2O , RT) recorded for: a) 1,7-heptanediammonium dihydrochloride, b) a mixture of 1,7-heptanediammonium dihydrochloride and **II-1** (2:1 ratio), and c) a mixture of 1,7-heptanediammonium dihydrochloride and **II-1** (>2:1 ratio).

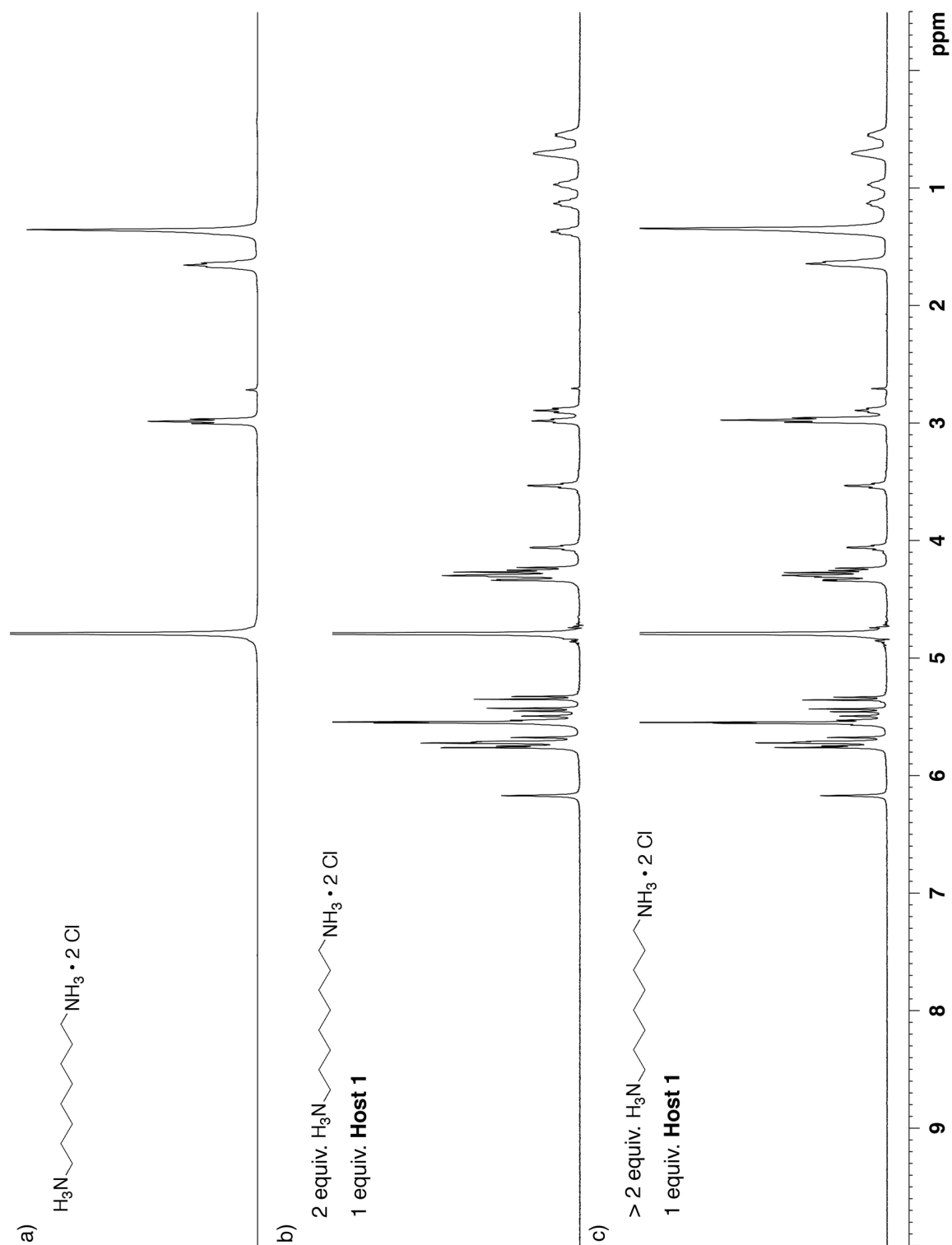


Figure II-S11. ^1H NMR spectra (400 MHz, D_2O , RT) recorded for: a) 1,8-octanediammonium dihydrochloride, b) a mixture of 1,8-octanediammonium dihydrochloride and **II-1** (2:1 ratio), and c) a mixture of 1,8-octanediammonium dihydrochloride and **II-1** (>2:1 ratio).

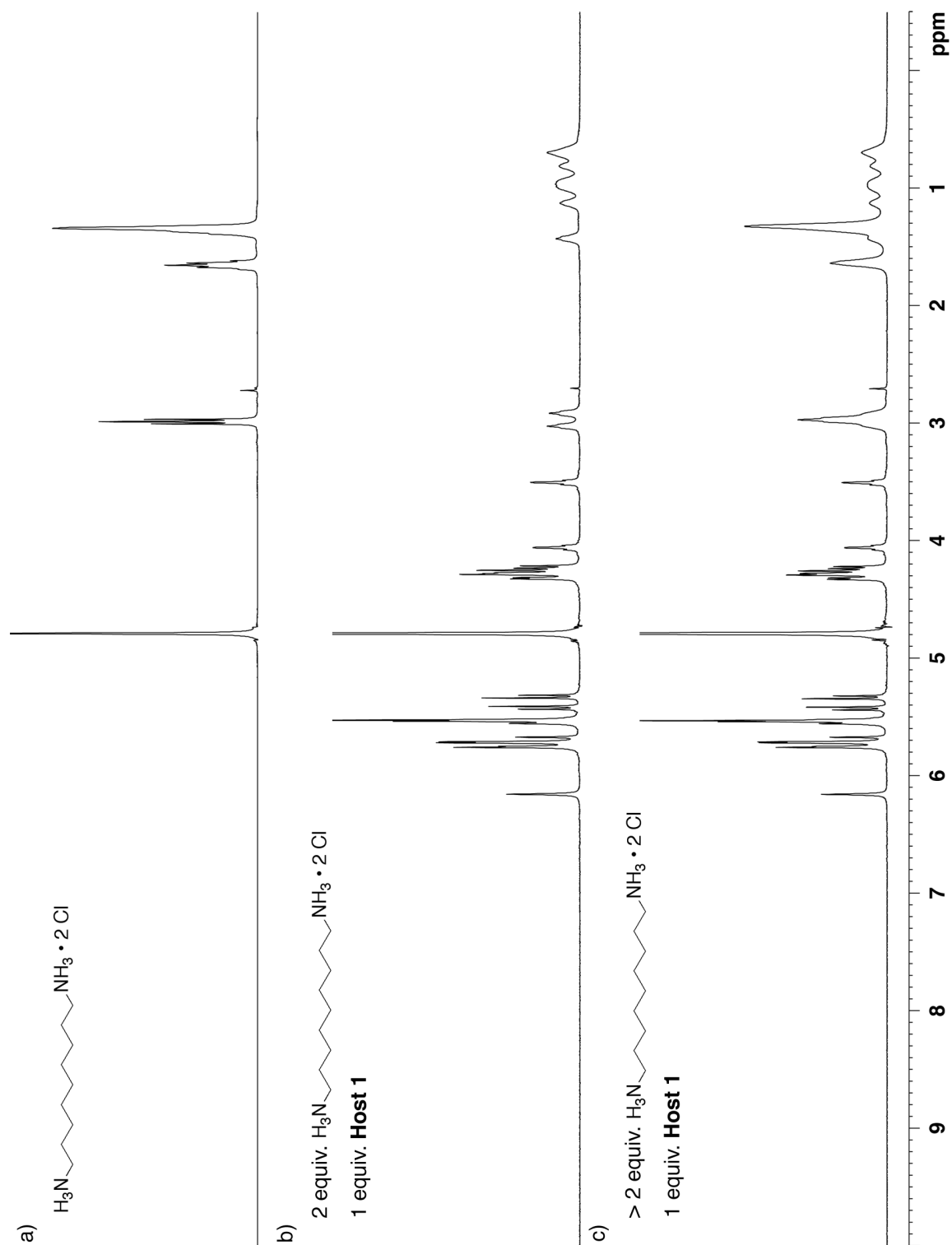


Figure II-S12. ^1H NMR spectra (400 MHz, D_2O , RT) recorded for: a) 1,9-nonanediammonium dihydrochloride, b) a mixture of 1,9-nonanediammonium dihydrochloride and **II-1** (2:1 ratio), and c) a mixture of 1,9-nonanediammonium dihydrochloride and **II-1** (>2:1 ratio).

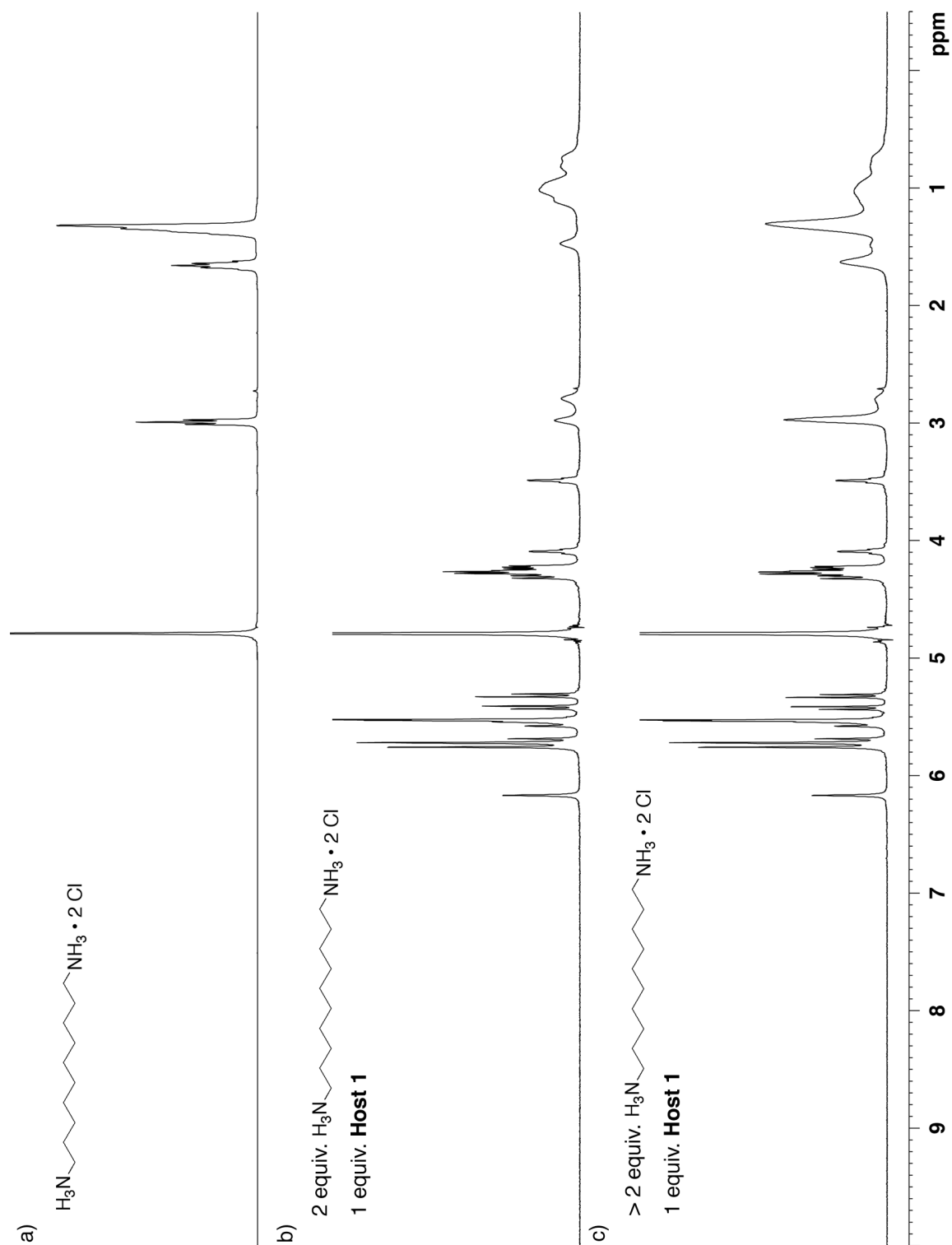


Figure II-S13. ^1H NMR spectra (400 MHz, D_2O , RT) recorded for: a) 1,10-decanediammonium dihydrochloride, b) a mixture of 1,10-decanediammonium dihydrochloride and **II-1** (2:1 ratio), and c) a mixture of 1,10-decanediammonium dihydrochloride and **II-1** (>2:1 ratio).

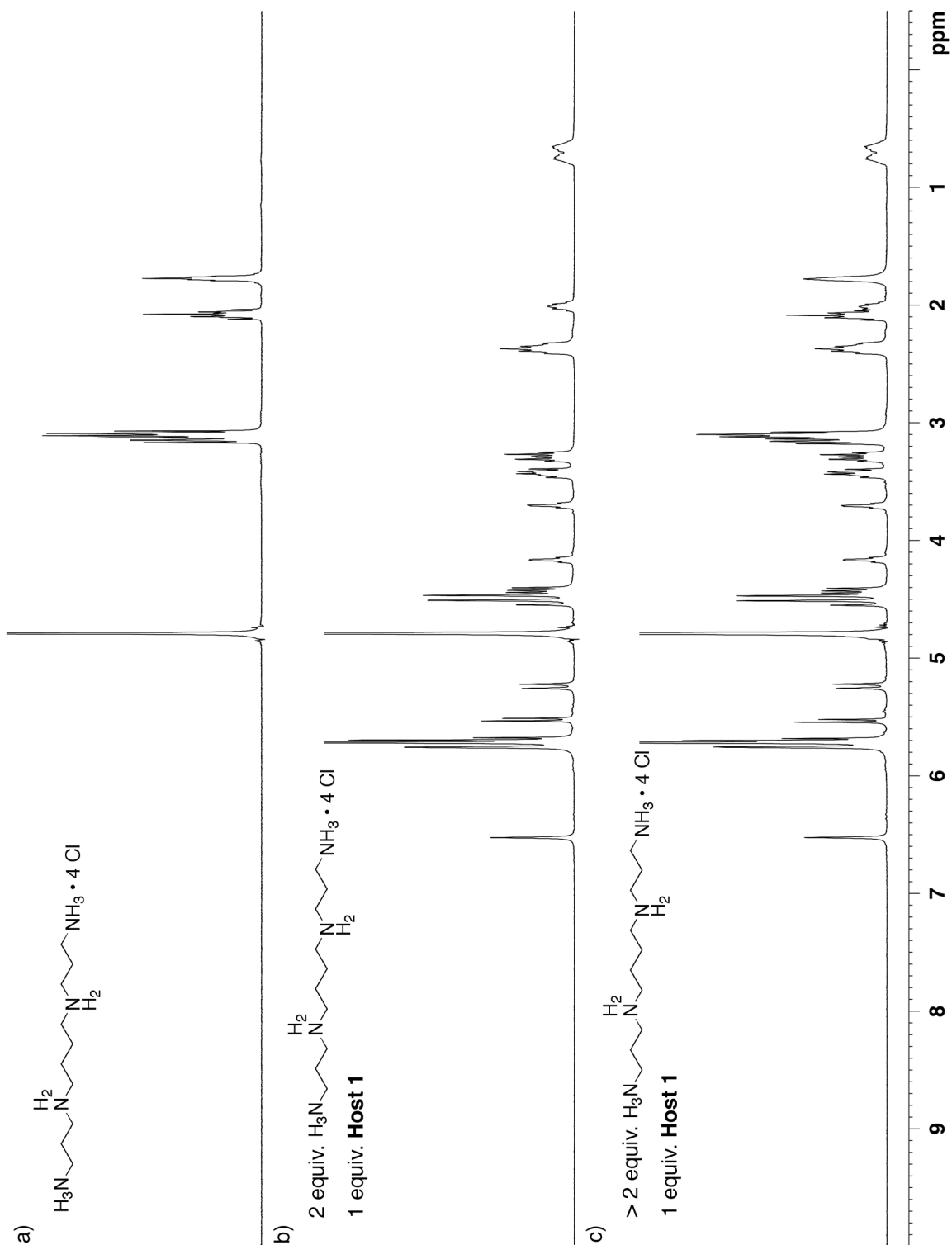


Figure II-S14. ^1H NMR spectra (400 MHz, D_2O , RT) recorded for: a) spermine tetrahydrochloride, b) a mixture of spermine tetrahydrochloride and **II-1** (2:1 ratio), and c) a mixture of spermine tetrahydrochloride and **II-1** (>2:1 ratio).

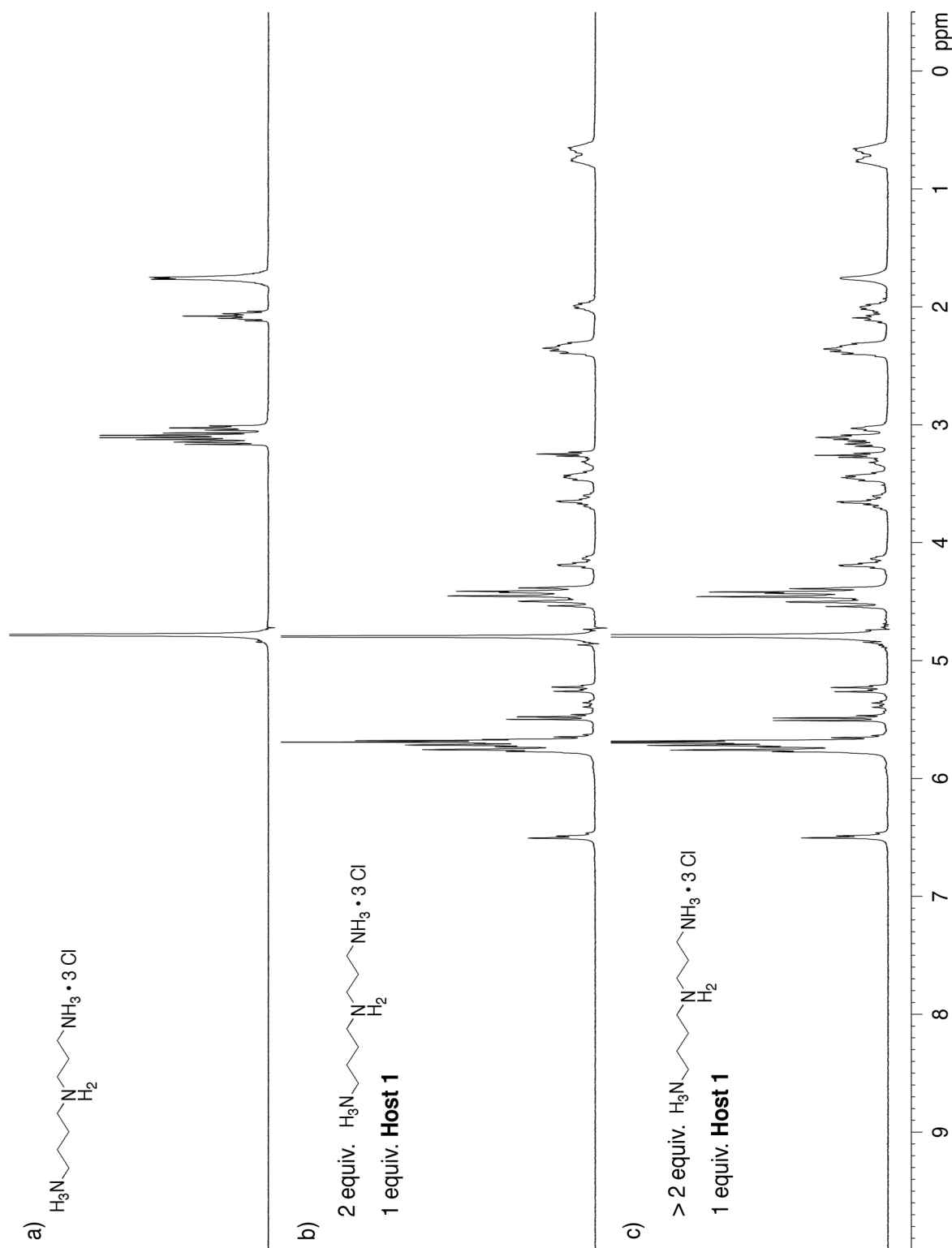


Figure II-S15. ^1H NMR spectra (400 MHz, D_2O , RT) recorded for: a) spermidine trihydrochloride, b) a mixture of spermidine trihydrochloride and **II-1** (2:1 ratio), and c) a mixture of spermidine trihydrochloride and **II-1** (>2:1 ratio).

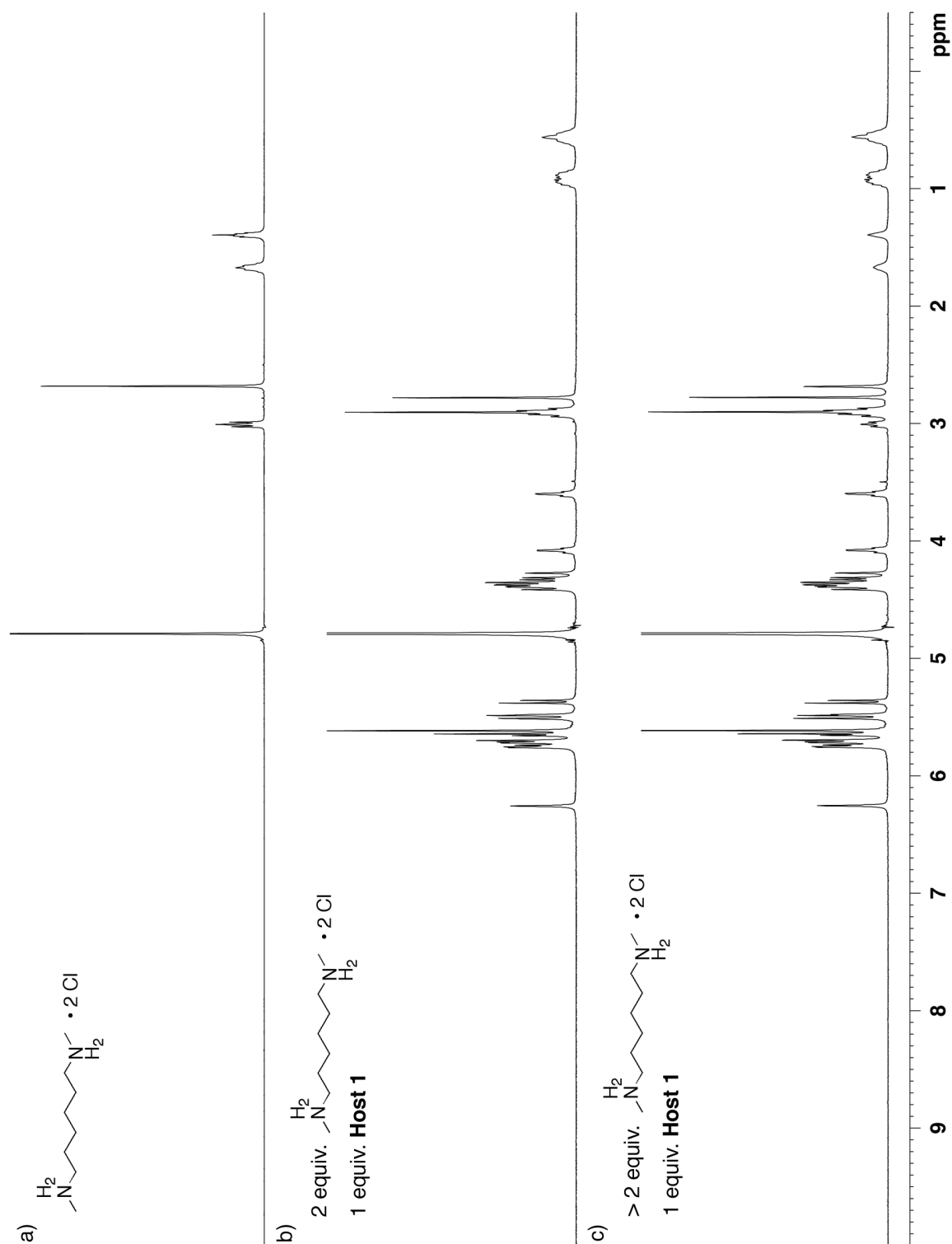


Figure II-S16. ^1H NMR spectra (400 MHz, D_2O , RT) recorded for: a) $\text{N,N}'$ -dimethyldiammonium dihydrochloride, b) a mixture of $\text{N,N}'$ -dimethyldiammonium dihydrochloride and **II-1** (2:1 ratio), and c) a mixture of $\text{N,N}'$ -dimethyldiammonium dihydrochloride and **II-1** (>2:1 ratio).

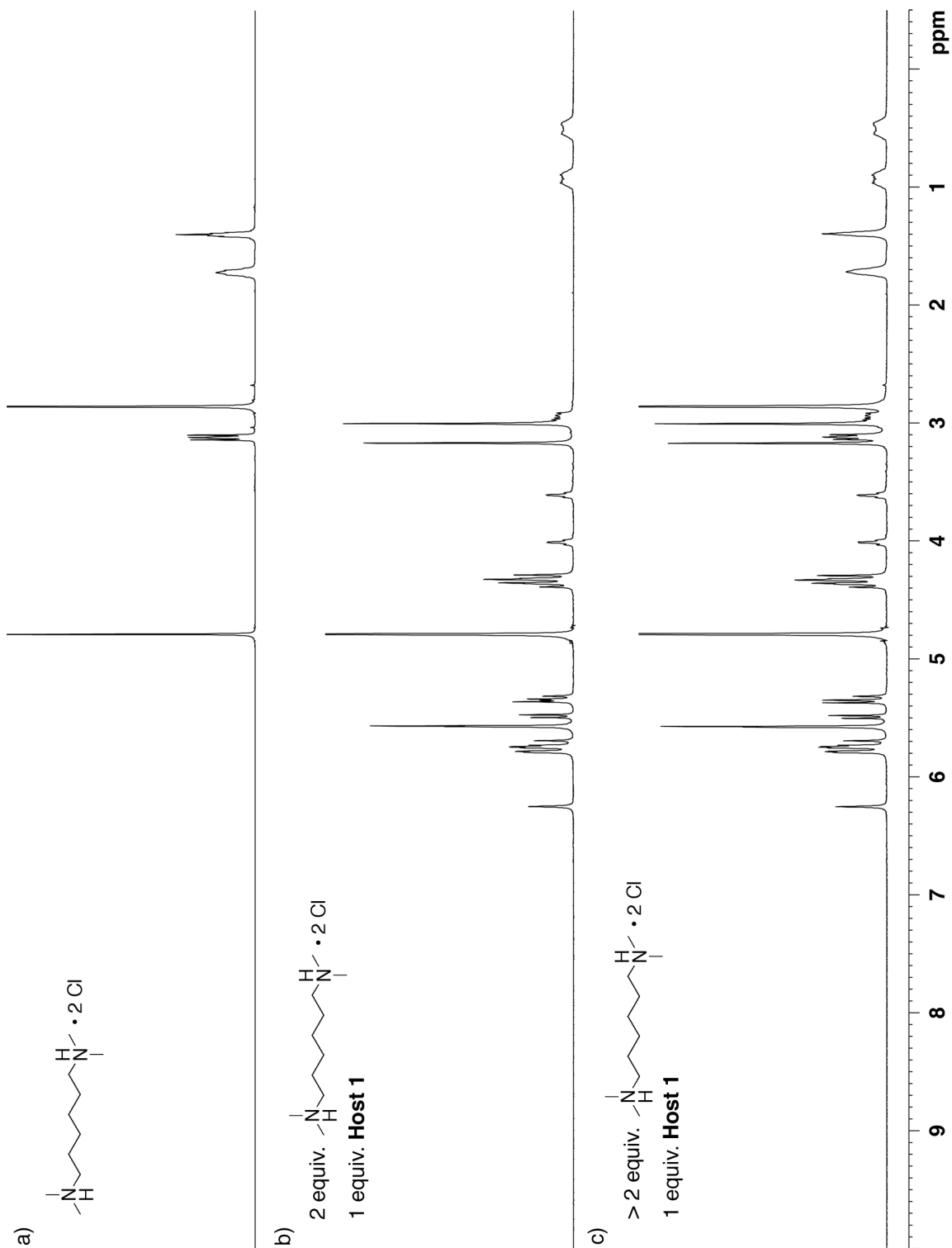


Figure II-S17. ^1H NMR spectra (400 MHz, D_2O , RT) recorded for: a) N,N,N',N' -tetramethyldiammonium dihydrochloride, b) a mixture of N,N,N',N' -tetramethyldiammonium dihydrochloride and **II-1** (2:1 ratio), and c) a mixture of N,N,N',N' -tetramethyldiammonium dihydrochloride and **II-1** (>2:1 ratio).

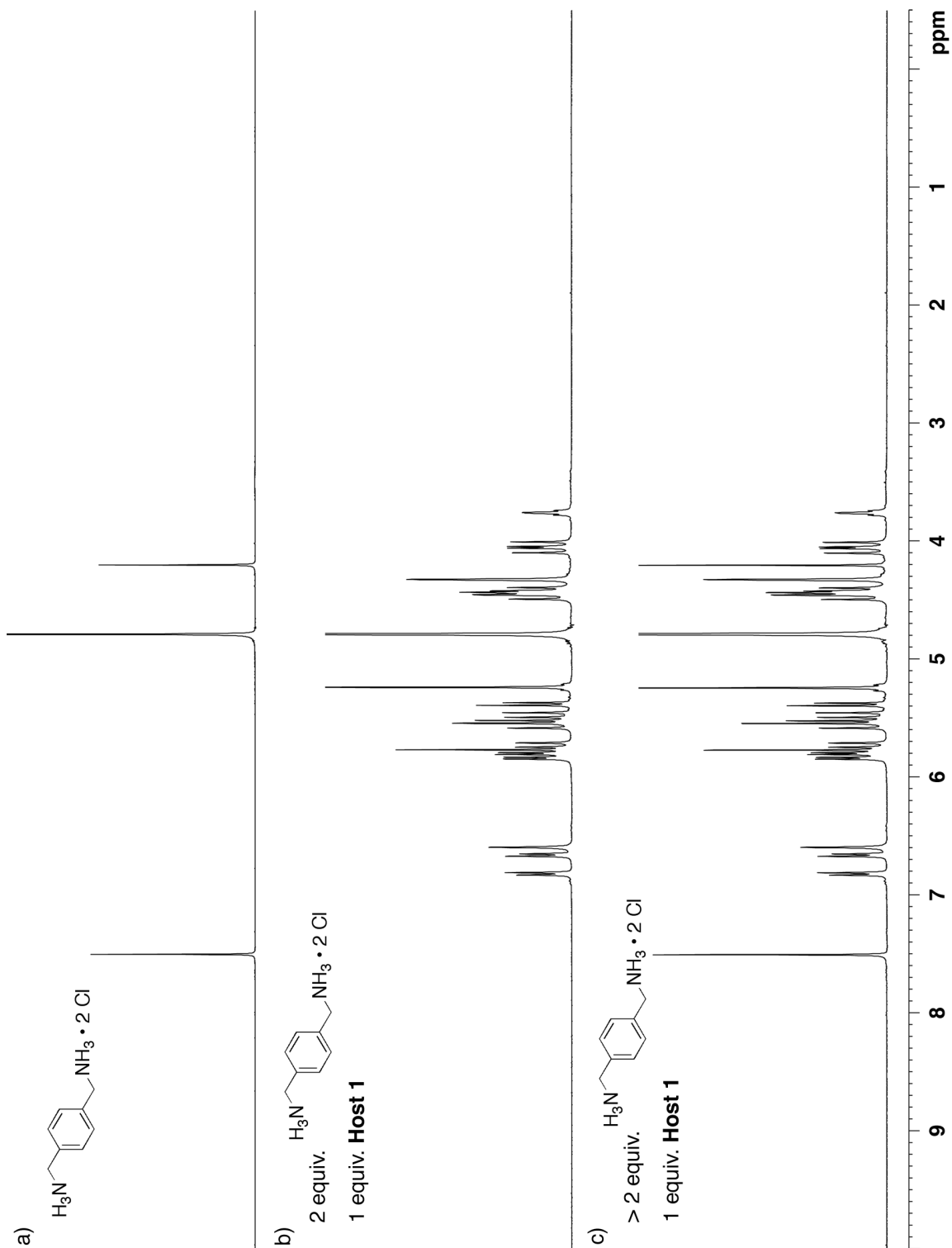


Figure II-S18. ^1H NMR spectra (400 MHz, D_2O , RT) recorded for: a) *p*-xylenediammonium dihydrochloride, b) a mixture of *p*-xylenediammonium dihydrochloride and **II-1** (2:1 ratio), and c) a mixture of *p*-xylenediammonium dihydrochloride and **II-1** (>2:1 ratio).

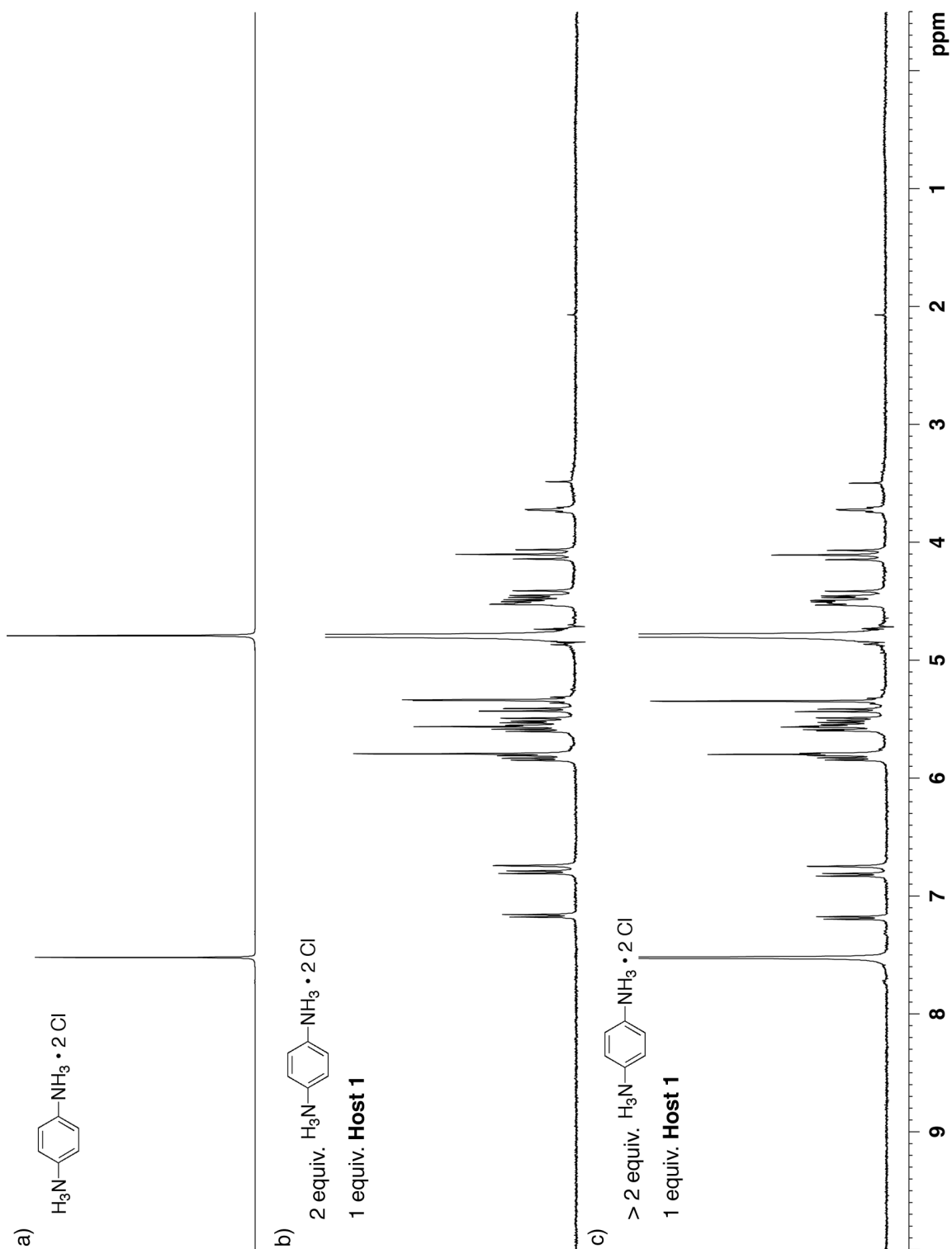


Figure II-S19. ^1H NMR spectra (400 MHz, D_2O , RT) recorded for: a) *p*-phenylenediammonium dihydrochloride, b) a mixture of *p*-phenylenediammonium dihydrochloride and **II-1** (2:1 ratio), and c) a mixture of *p*-phenylenediammonium dihydrochloride and **II-1** (>2:1 ratio).

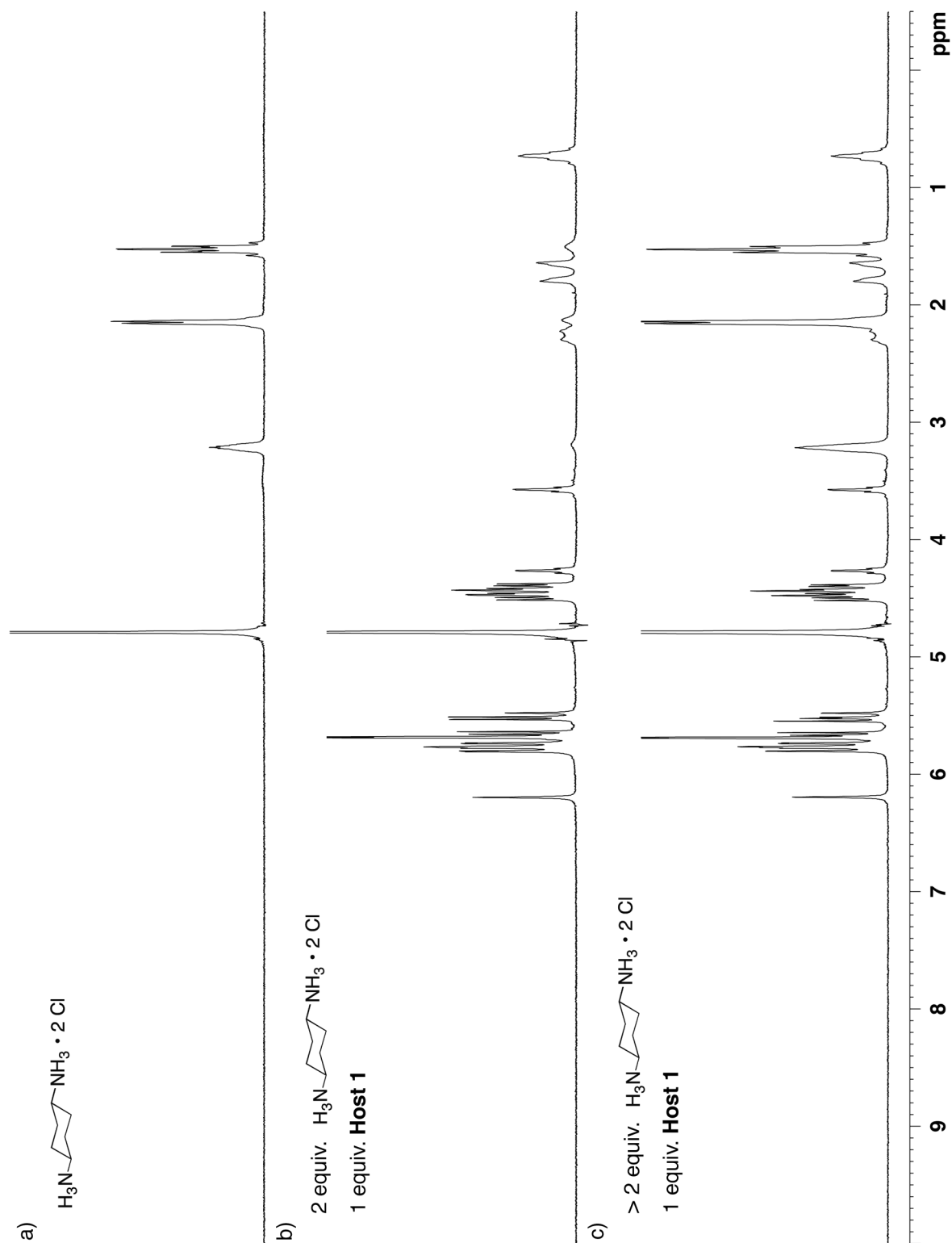


Figure II-S20. ^1H NMR spectra (400 MHz, D_2O , RT) recorded for: a) 1,4-cyclohexanediammonium dihydrochloride, b) a mixture of 1,4-cyclohexanediammonium dihydrochloride and **II-1** (2:1 ratio), and c) a mixture of 1,4-cyclohexanediammonium dihydrochloride and **II-1** (>2:1 ratio).

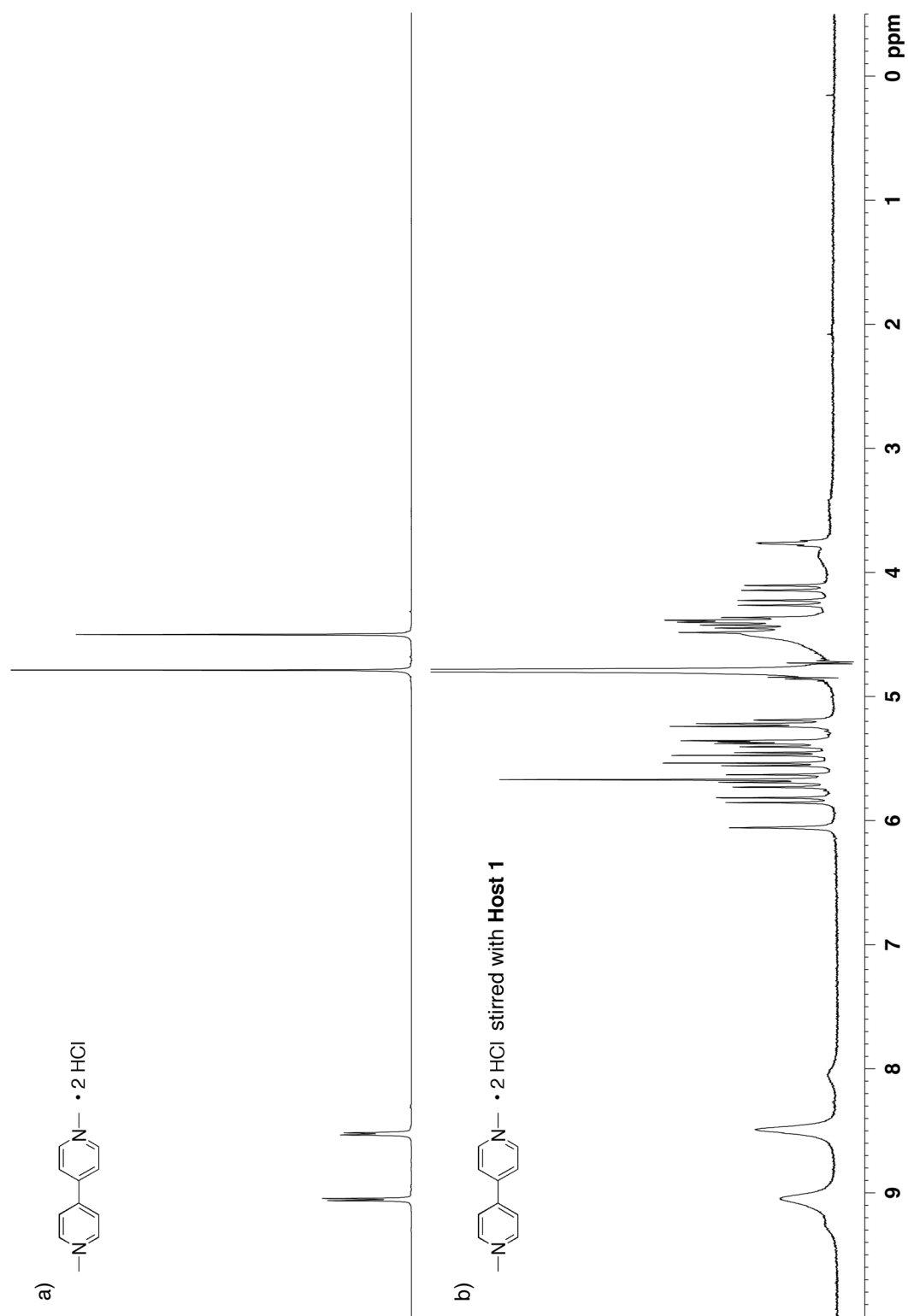


Figure II-S21. ¹H NMR spectra (400 MHz, D₂O, RT) recorded for: a) methyl viologen and b) a mixture of methyl viologen and **II-1** (2:1 ratio).



Figure II-S22. ^1H NMR spectra (400 MHz, D_2O , RT) recorded for: a) a solution obtained by stirring hexamethonium chloride (1 mM) with an excess of solid **II-1** followed by filtration and b) a solution obtained by stirring hexamethonium chloride (10 mM) with an excess of solid **II-1** followed by filtration.

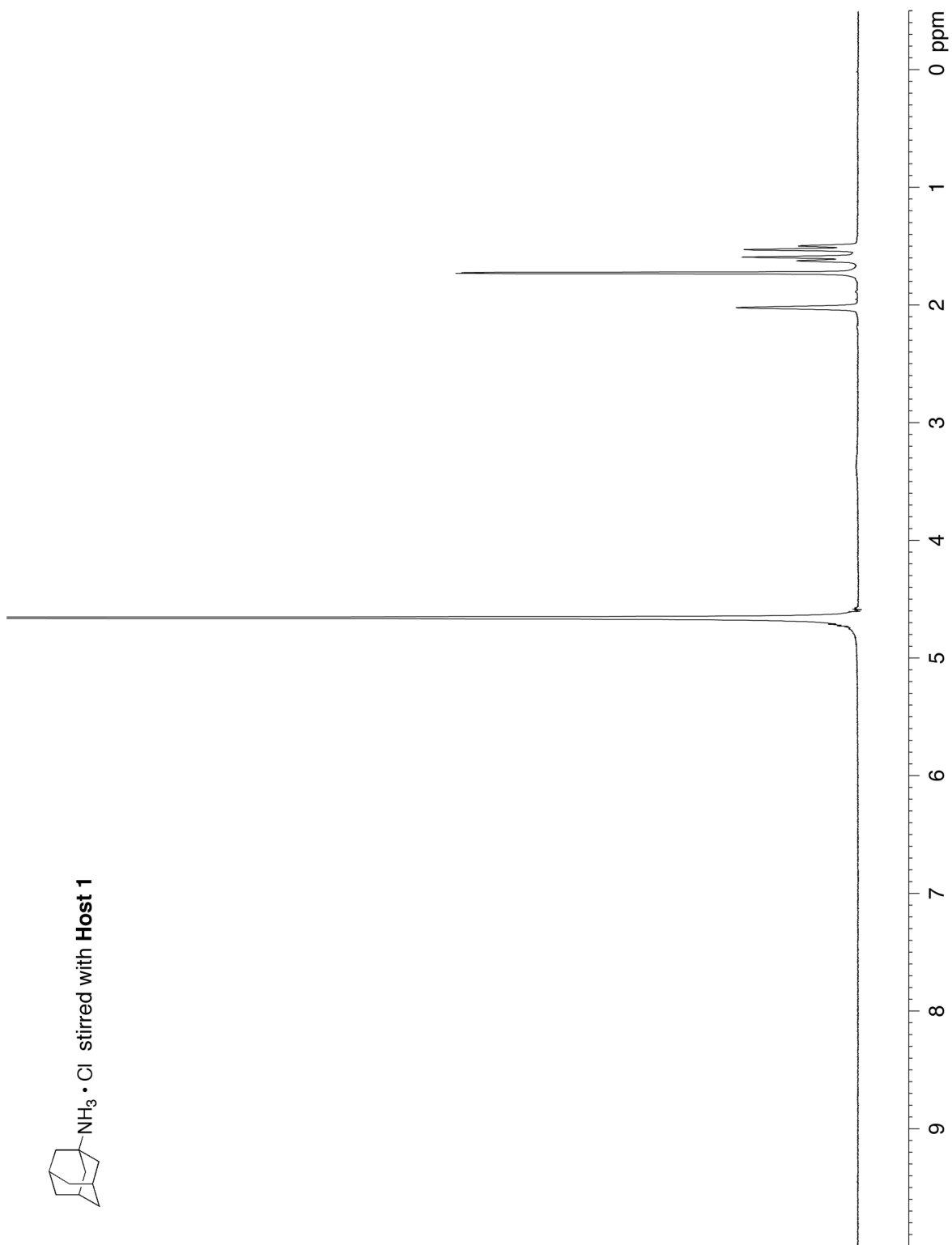


Figure II-S23. ¹H NMR spectrum (400 MHz, D₂O, RT) recorded for a solution obtained by stirring 1-adamantaneamine hydrochloride (10 mM) with an excess of solid **II-1** followed by filtration.

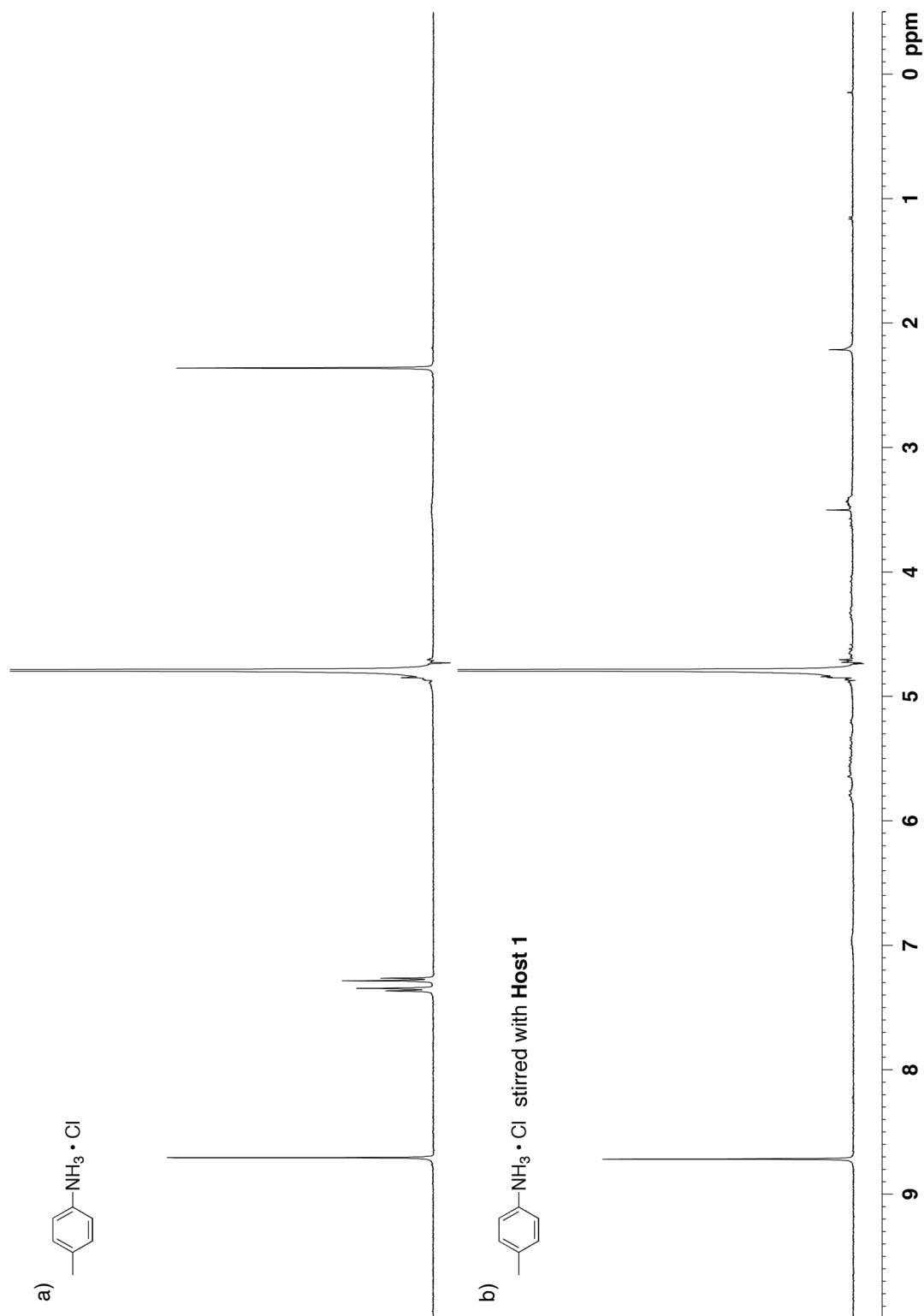


Figure II-S24. ¹H NMR spectrum (400 MHz, D₂O, RT, 1,3,5-tribenzenetricarboxylic acid as internal standard) recorded for: a) *p*-toluidine hydrochloride and b) a solution obtained by stirring *p*-toluidine hydrochloride (10 mM) with an excess of solid **II-1** followed by filtration.

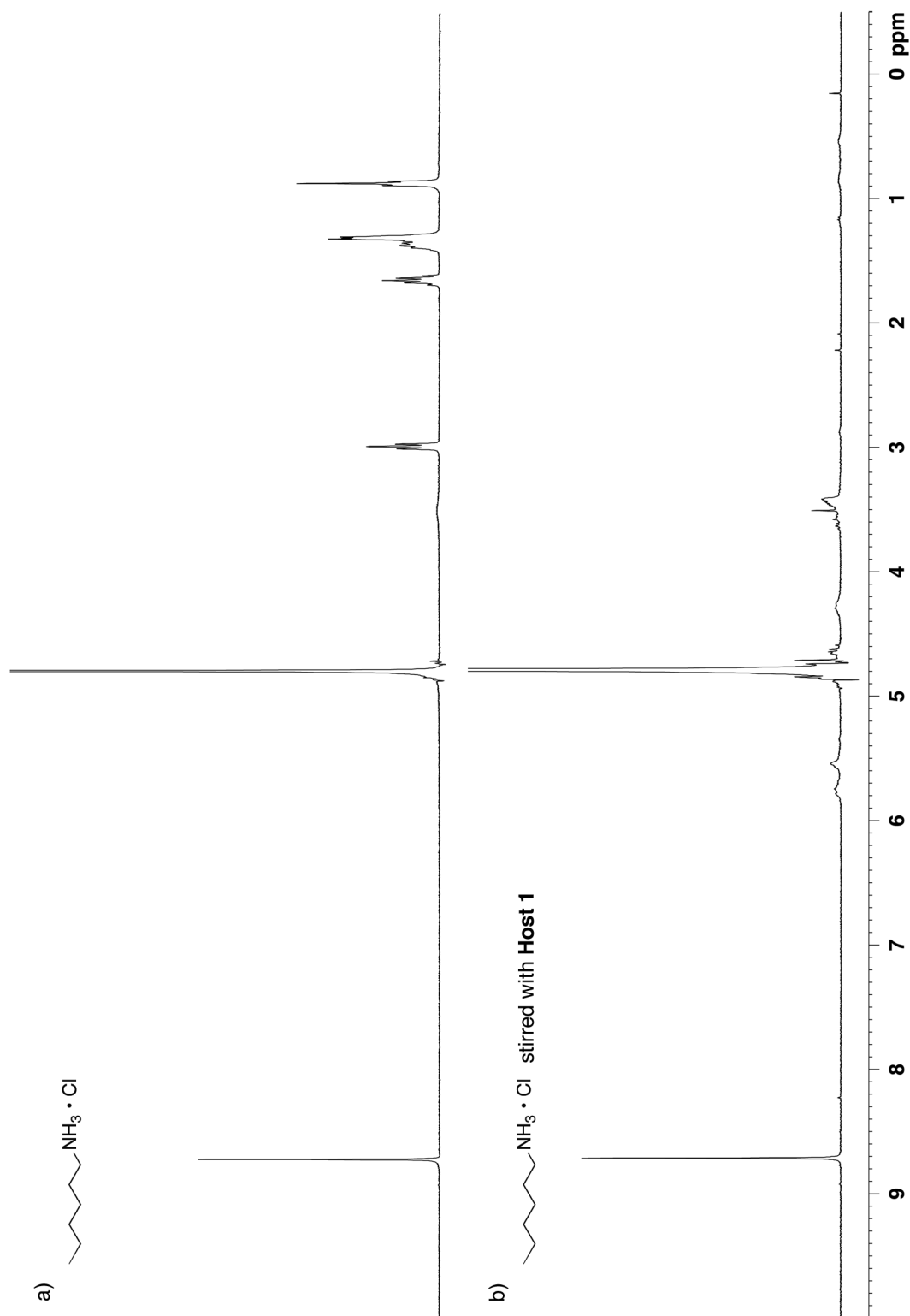


Figure II-S25. ^1H NMR spectrum (400 MHz, D_2O , RT, 1,3,5-tribenzenetricarboxylic acid as internal standard) recorded for: a) hexylammonium hydrochloride and b) a solution obtained by stirring hexylammonium hydrochloride (10 mM) with an excess of solid **II-1** followed by filtration.

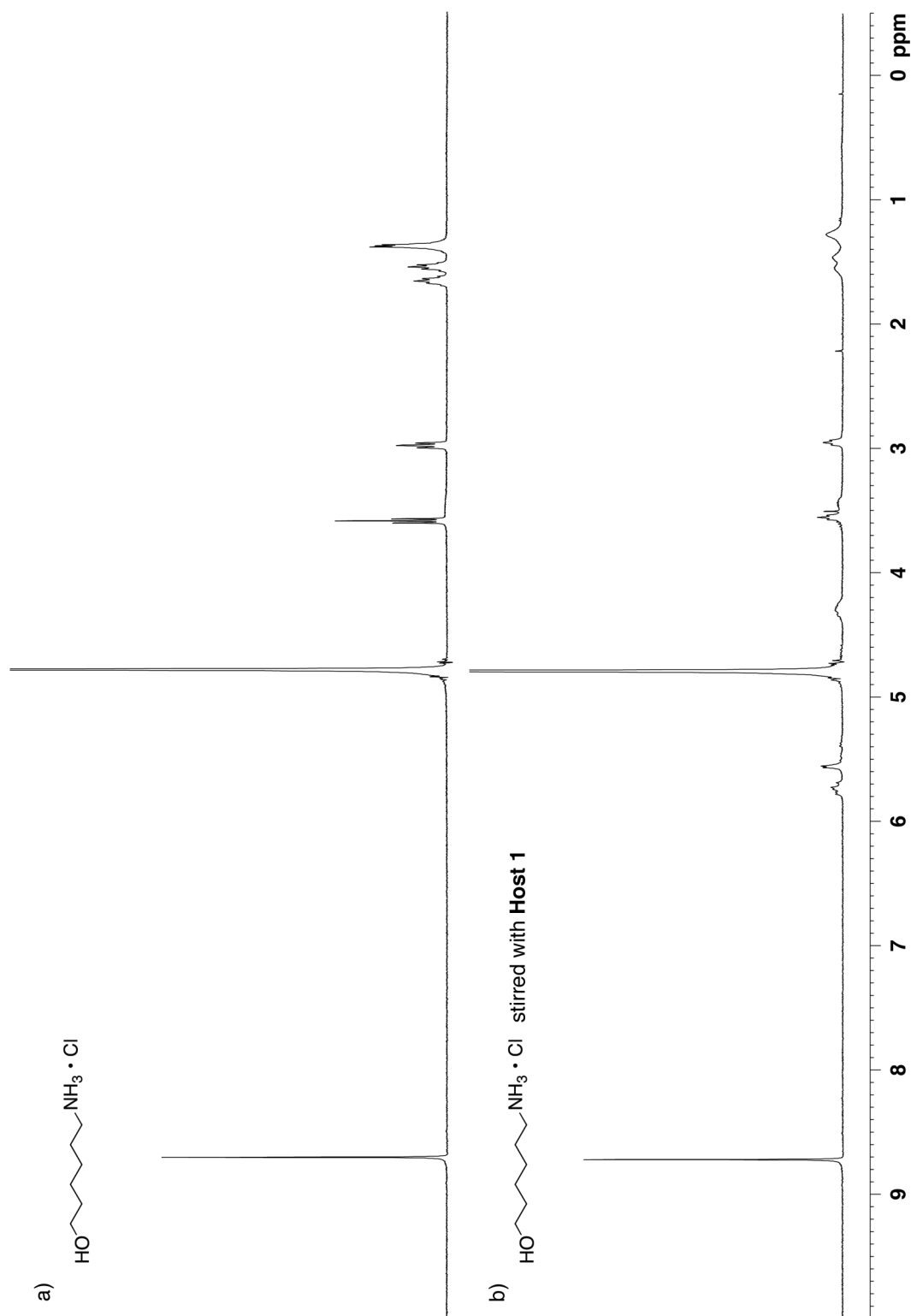


Figure II-S26. ^1H NMR spectrum (400 MHz, D_2O , RT, 1,3,5-tribenzenetricarboxylic acid as internal standard) recorded for: a) aminohexanol hydrochloride and b) a solution obtained by stirring aminohexanol hydrochloride (10 mM) with an excess of solid **II-1** followed by filtration.

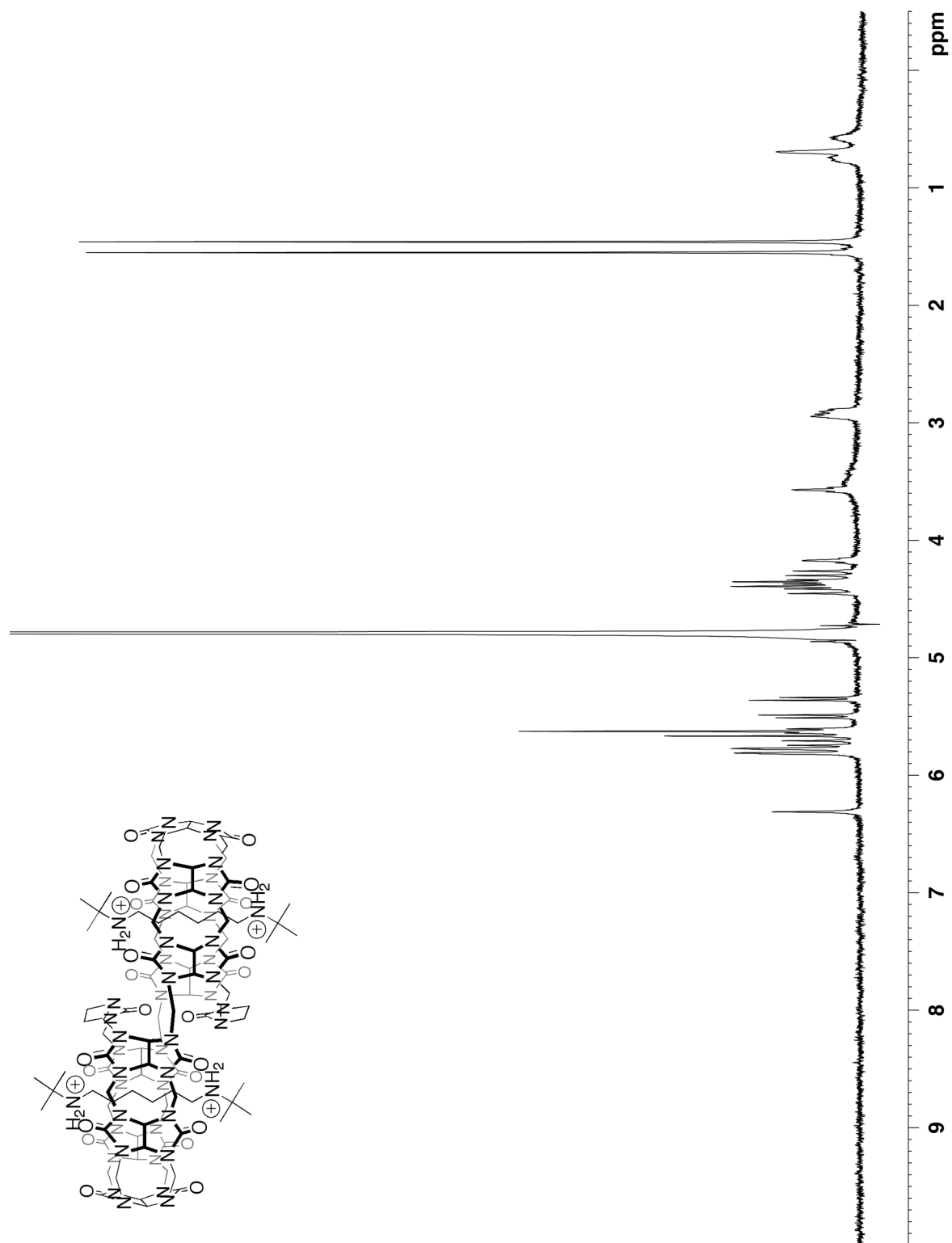


Figure II-S27. ^1H NMR spectrum (400 MHz, D_2O , RT) recorded for $\text{II-1}\cdot\text{II-4}_2$ after washing with 0.1 M NaOH in MeOH to induce removal of II-4 .

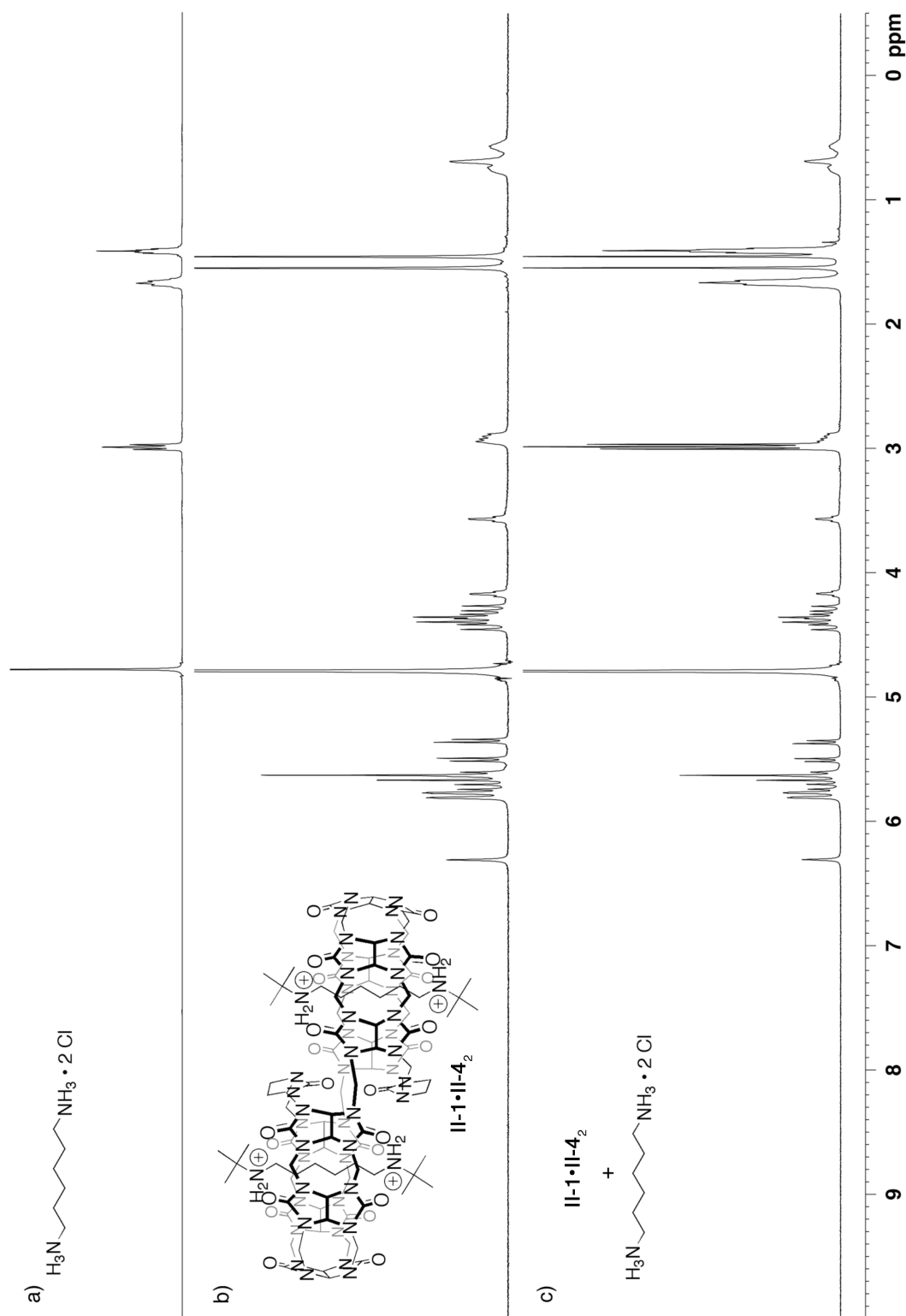


Figure II-S28. ^1H NMR spectrum (400 MHz, D_2O , RT) recorded for: a) 1,6-hexanediammonium dihydrochloride, b) $\text{II-1} \cdot \text{II-4}_2$, and c) a solution of 1,6-hexanediammonium dihydrochloride (20 mM) and $\text{II-1} \cdot \text{II-4}_2$ (2 mM).

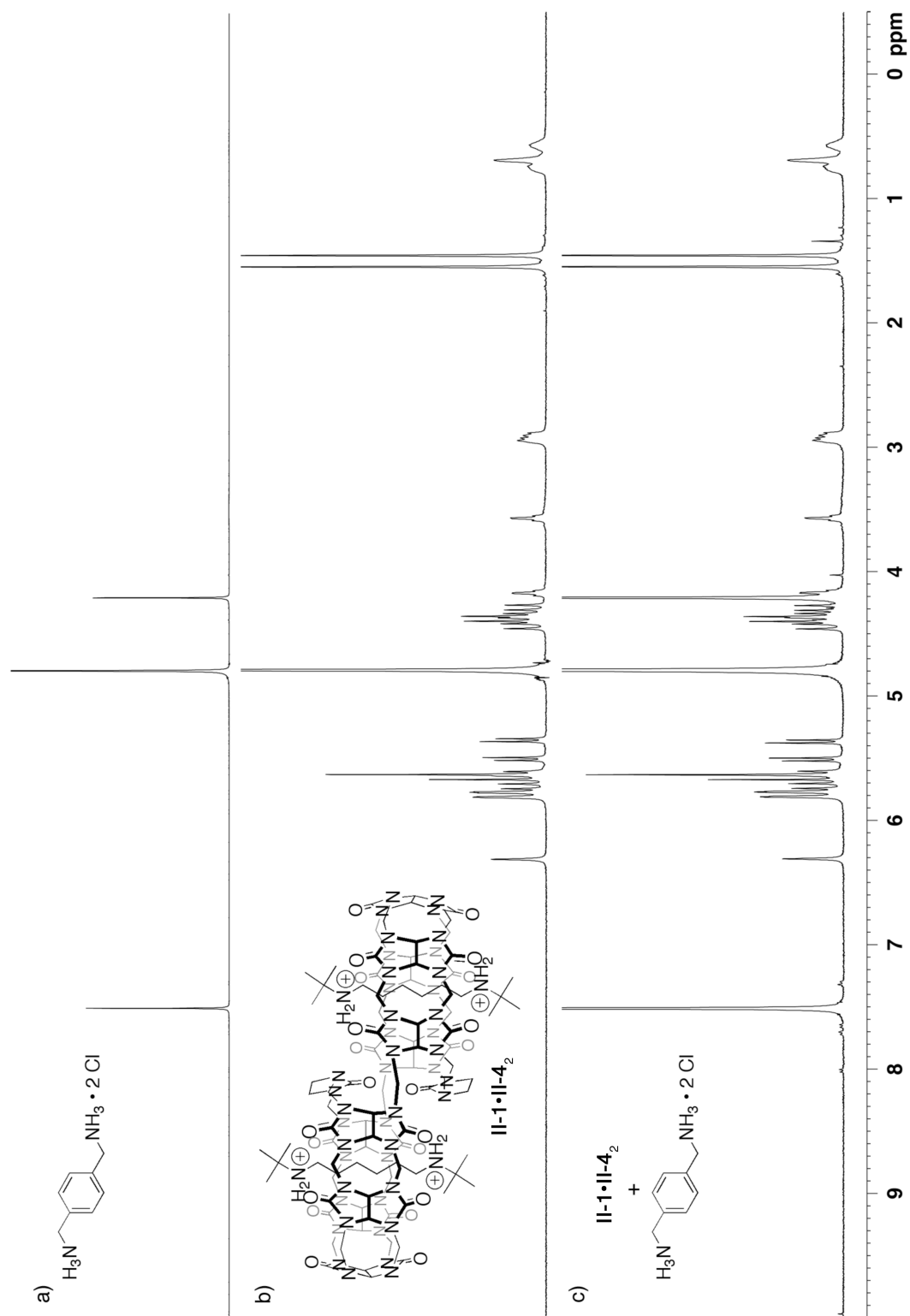
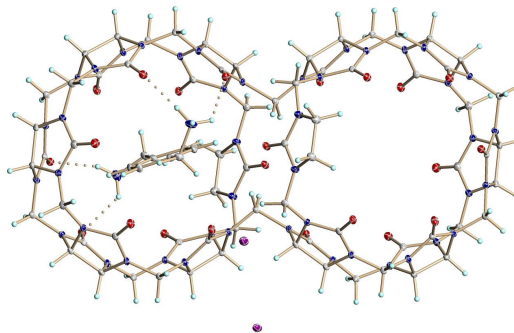


Figure II-S29. ^1H NMR spectrum (400 MHz, D_2O , RT) recorded for: a) *p*-xylenediammonium dihydrochloride, b) $\text{II-1}\cdot\text{II-4}_2$, and c) a solution of *p*-xylenediammonium dihydrochloride (20 mM) and $\text{II-1}\cdot\text{II-4}_2$ (2 mM).

Details of the crystal structure of II-1.

A colorless prism of $[(C_{68}H_{72}N_{44}O_{22})\langle(C_8H_{14}N_2)_2\rangle]I_4 \cdot 18H_2O$, approximate dimensions $0.21 \times 0.24 \times 0.37$ mm³, was used for the X-ray



crystallographic analysis. The X-ray intensity data were measured at 250(2) K on a three-circle diffractometer system equipped with Bruker Smart Apex II CCD area detector using a graphite monochromator and a MoK α fine-focus sealed tube ($\lambda = 0.71073$ Å). The detector was placed at a distance of 6.000 cm from the crystal.

A total of 1330 frames were collected with a scan width of -0.30° an exposure time of 20 sec/frame using Apex2 (Bruker, 2005). The total data collection time was 10 hours. The frames were integrated with Apex2 software package using a narrow-frame integration algorithm. The integration of the data using a Monoclinic unit cell yielded a total of 40898 reflections to a maximum θ angle of 27.50° , of which 13130 were independent (completeness = 99.5%, $R_{int} = 3.09\%$, $R_{sig} = 3.53\%$) and 10224 were greater than $2\sigma(I)$. The final cell dimensions of $a = 13.690(2)$ Å, $b = 13.972(2)$ Å, $c = 30.064(4)$ Å, $\alpha = 90^\circ$, $\beta = 93.1108(19)^\circ$, $\gamma = 90^\circ$, $V = 5742.3(15)$ Å³, are based upon the refinement of the XYZ-centroids of 15779 reflections with $2.2 < \theta < 28.2^\circ$ using Apex2 software. Analysis of the data showed 0 % decay during data collection. Data were corrected for absorption effects with the Semi-empirical from equivalents method using SADABS (Sheldrick, 1996). The minimum and maximum transmission coefficients were 0.674 and 0.779.

The structure was solved and refined using the SHELXS-97 (Sheldrick, 1990) and SHELXL-97 (Sheldrick, 1997) software in the space group $P2_1/n$ with $Z = 2$ for the formula unit $[(C_{68}H_{72}N_{44}O_{22}) \cdot (C_8H_{14}N_2)_2]I_4 \cdot 18H_2O$. The final anisotropic full-matrix least-squares refinement on F^2 with 862 variables converged at $R_1 = 4.60\%$ for the observed data and $wR_2 = 9.94\%$ for all data. The goodness-of-fit was 1.000. The largest peak on the final difference map was $1.323 \text{ e}^-/\text{\AA}^3$ and the largest hole was $-1.156 \text{ e}^-/\text{\AA}^3$. On the basis of the final model, the calculated density was 1.715 g/cm^3 and $F(000)$, 3016 e^- .

Comments:

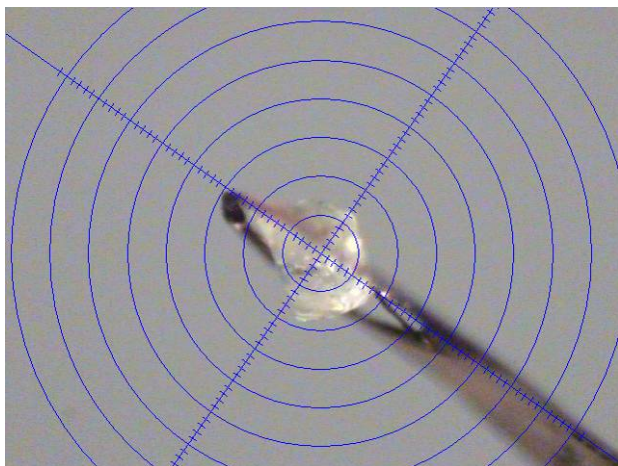
- Data quality: very good
- Disorder: 1 or 9 water molecules is disordered in two positions (O9w and O10w); another molecule (O6w) has one H atom disordered in two alternative positions
- H-atoms: constrained geometry as riding on attached atom (A) for C-H and N-H and soft restrains on distances & angle to attached atom (A) for H2O;
 $U_{\text{iso}}(\text{H})=1.5U_{\text{iso}}(\text{A})$ for CH_3 and H_2O and $1.2U_{\text{iso}}(\text{A})$ for other groups
- Residual density: near heavy atoms

Disorder-Order phase transition observed during the experiment:

At first crystal structure was indexed in a monoclinic system, sp.gr. $P2_1/n$, $a = 14.901(9)$, $b = 14.231(8)$, $c = 29.591(18) \text{ \AA}$, $\beta = 96.712(9)^\circ$, $V = 6232(11) \text{ \AA}^3$. The

structure determination revealed the same structure as reported one. However all the water molecules except one and one of two iodine ions were disordered as well as one ammonium group in the guest molecule. Analyses of the frames showed that crystal was changing during the data collection. Therefore after experiment was finished a new data collection was undertaken. It revealed that even so symmetry is unchanged but cell dimensions are noticeable different $a = 13.690(2)$, $b = 13.972(2)$, $c = 30.064(4)$, $\beta = 93.1108(19)^\circ$, $V = 5742.3(15) \text{ \AA}^3$. The crystal structure determination showed the same composition and type of structure including guest-host system. However guest molecule, both iodine ions, and most of the water molecules are fully ordered.

Thus the title compound undergoes disorder to order phase transition at 250 K which takes about 10 hours for completion.



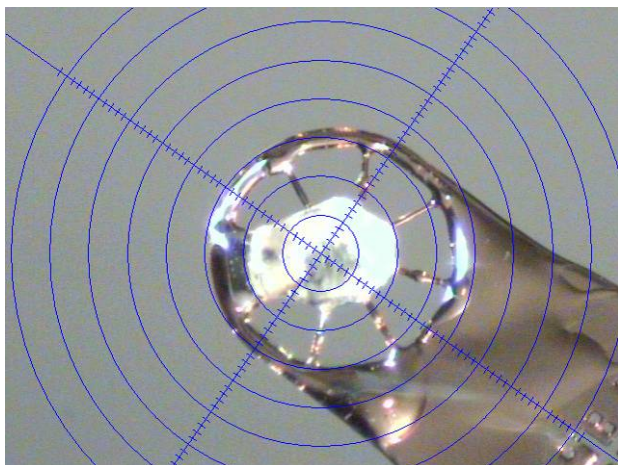


Table II-S1. Crystal data and structure refinement for UM#1946.

| | |
|---------------------------------------|---|
| X-ray lab book No. | 1946 |
| Crystal ID | Isaacs/Wittenberg JW-3-138 @250K |
| Empirical formula | $[(C_{68}H_{72}N_{44}O_{22}) \cdot (C_8H_{14}N_2)_2]I_4 \cdot 18H_2O$ |
| Formula weight | 2966.01 |
| Temperature | 250(2) K |
| Wavelength | 0.71073 Å |
| Crystal size | 0.37×0.24×0.21 mm ³ |
| Crystal habit | colorless prism |
| Crystal system | Monoclinic |
| Space group | P21/n |
| Unit cell dimensions | $a = 13.690(2)$ Å $\alpha = 90^\circ$ $b = 13.972(2)$ Å $\beta = 93.1108(19)^\circ$ $c = 30.064(4)$ Å $\gamma = 90^\circ$ |
| Volume | 5742.3(15) Å ³ |
| Z | 2 |
| Density, ρ_{calc} | 1.715 g/cm ³ |
| Absorption coefficient, μ | 1.192 mm ⁻¹ |
| F(000) | 3016 e ⁻ |
| Diffractometer | Bruker Smart Apex II CCD area detector |
| Radiation source | fine-focus sealed tube, MoK α |
| Detector distance | 6.000 cm |
| Data collection method | ω and ϕ scans |
| Total frames | 1330 |
| Frame size | 512 pixels |
| Frame width | -0.30° |
| Exposure per frame | 20 sec |
| Total measurement time | 10 hours |
| θ range for data collection | 2 to 27.50° |
| Index ranges | $-17 \leq h \leq 17, -17 \leq k \leq 18, -39 \leq l \leq 38$ |
| Reflections collected | 40898 |
| Independent reflections | 13130 |
| Observed reflection, $I > 2\sigma(I)$ | 10224 |
| Coverage of independent reflections | 99.5 % |
| Variation in check reflections | 0 % |
| Absorption correction | Semi-empirical from equivalents |

| | | | |
|--------------------------------|-------------------------|--|---|
| Max. and min. transmission | | SADABS (Sheldrick, 1996) | 0.779 and 0.674 |
| Structure solution technique | | direct | |
| Structure solution program | | SHELXS-97 (Sheldrick, 1990) | |
| Refinement technique | | Full-matrix least-squares on F^2 | |
| Refinement program | | SHELXL-97 (Sheldrick, 1997) | |
| Function minimized | | $\Sigma w(F_o^2 - F_c^2)^2$ | |
| Data / restraints / parameters | | | 13130 / 48 / 862 |
| Goodness-of-fit on F^2 | | | 1.260 |
| Δ/σ_{\max} | | | 0.001 |
| Final R indices: | $R_1, I > 2\sigma(I)$ | | 0.0460 |
| | $wR_2, \text{all data}$ | | 0.0994 |
| | R_{int} | | 0.0309 |
| | R_{sig} | | 0.0353 |
| Weighting scheme | | $w = 1/[\sigma^2(F_o^2) + (0.01P)^2 + 24.22P]$, $P = [\max(F_o^2, 0) + 2F_o^2]/3$ | |
| Largest diff. peak and hole | | | 1.323 and -1.156 $\bar{e}/\text{\AA}^3$ |

$$R_1 = \Sigma ||F_o| - |F_c|| / \Sigma |F_o|, \quad wR_2 = [\Sigma w(F_o^2 - F_c^2)^2 / \Sigma w(F_o^2)]^{1/2}$$

Appendix 2

Higher Order Complexes Formed from Cucurbit[6]uril Dimers

Supporting Information

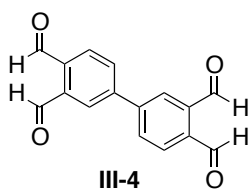
by James B. Wittenberg, Peter Y. Zavalij, and Lyle Isaacs*

Department of Chemistry and Biochemistry, University of Maryland, College Park,
MD 20742

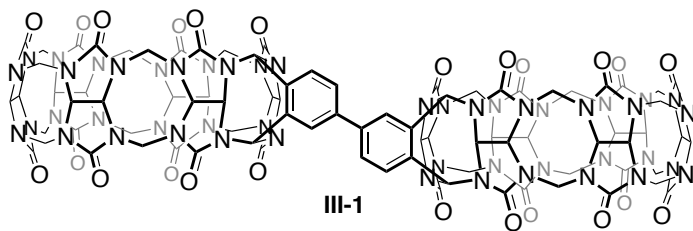
| Table of Contents | Pages |
|--|-----------|
| General experimental details | 124 |
| Synthetic procedures and characterization data | 124 – 138 |
| ¹ H and ¹³ C NMR spectra of new compounds | 139 – 172 |
| ¹ H NMR spectra recorded for selected III-1 •guest complexes | 173 – 180 |
| ¹ H NMR spectra recorded for selected III-2 •guest complexes | 181 – 186 |
| ¹ H NMR spectra recorded for III-2 • III-20 | 187 |
| Details of the X-ray Crystal Structure of III-1 | 188 – 190 |

General Experimental. Starting materials were purchased from commercial suppliers were used without further purification. Glycoluril hexamer (**III-3**) was synthesized following a known procedure in the literature.¹ Compound **III-15** was synthesized following a literature procedure.² Microwave reactions were performed using a CEM Discover microwave reactor with a maximum microwave power of 300 W. Melting points were measured on a Meltemp apparatus in open capillary tubes and are uncorrected. TLC analysis was performed using pre-coated plastic plates from Merck. IR spectra were recorded on a JASCO FT/IR 4100 spectrometer and are reported in cm^{-1} . ^1H , ^{13}C , and DOSY NMR spectra were measured on 400 MHz, 500 MHz, and 600 MHz instruments (100 MHz, 125 MHz, and 200 MHz for ^{13}C NMR, respectively). Mass spectrometry was performed using a JEOL AccuTOF electrospray instrument (ESI).

Synthetic Procedures and Characterization.

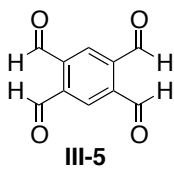


Compound **III-4**: Compound **III-4** was synthesized following a known procedure in the literature.³ ^1H NMR (400 MHz, CDCl_3 , RT): 10.69 (s, 2H), 10.58 (s, 2H), 8.29 (d, $J = 1.8$, 2H), 8.14 (d, $J = 7.9$, 2H), 8.08 (dd, $J = 7.9, 1.8$, 2H). ^{13}C NMR (125 MHz, DMSO, RT): δ 193.0, 192.6, 142.5, 137.1, 135.9, 132.1, 130.9, 129.0.



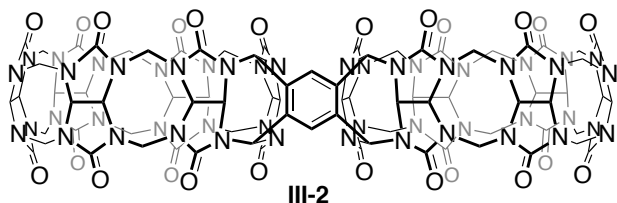
Compound **III-1**: To a solution of **III-3** (1.00 g, 1.03 mmol) in H₂SO₄ (9 M, 10.30 mL) in a 20 mL glass

vial was added **III-4** (0.14 g, 0.51 mmol). The vial was then sealed with a screw cap and stirred at RT for 24 h. The reaction mixture was poured into stirring MeOH (100 mL), which gave a white precipitate, and was stirred for 1 h. The solid was collected by centrifugation then dried under high vacuum. The crude solid (1.12 g) was purified by Dowex ion-exchange column chromatography using a gradient solvent system (50% formic acid, 50% 2-6 M HCl) giving 0.45 g of approximately 90% pure material. Final purification was completed by recrystallization from TFA/H₂O (5.0 mL) to yield **III-1** as an off-white solid (0.37 g, 0.17 mmol, 34%). M.p. > 300 °C. IR (cm⁻¹): 1716s, 1459m, 1374w, 1319w, 1234m, 1174s, 962s, 794s, 757m. ¹H NMR (400 MHz, D₂O, as the complex **III-1**•**III-6** (n = 6)₂, RT): 7.99 (s, 2H), 7.98 (d, J = 7.6, 2H), 7.77 (d, J = 7.6, 2H), 6.78 (s, 2H), 6.76 (s, 2H), 5.80-5.65 (m, 20H), 5.61 (s, 8H), 5.58 (d, J = 9.2, 4H), 5.50 (d, J = 9.2, 4H), 5.15 (d, J = 9.8, 4H), 4.89 (d, J = 9.8, 4H), 4.36 (d, J = 15.6, 4H), 4.35 (d, J = 15.4, 8H), 4.15 (d, J = 15.4, 8H), 2.94 (t, J = 6.8, 8H), 0.86 (m, 8H), 0.60 (m, 8H). ¹³C NMR (125 MHz, D₂O, as the complex **III-1**•**III-6** (n = 6)₂, RT, 1,4-dioxane as external standard): δ 162.4, 162.1, 156.0, 155.8, 154.4, 130.2, 130.1, 129.8, 119.3, 117.0, 114.7, 71.3, 70.1, 69.8, 69.6, 65.0, 63.9, 63.5, 53.0, 50.9, 50.6, 39.2, 38.9, 26.3, 26.0, 25.7, 24.7. MS (ESI, as the complex **III-1**•**III-6** (n = 6)₂): m/z 593.9 ([M•**III-6** (n = 6)₂]⁴⁺).



Compound **III-5**: Compound **III-5** is known in the literature.⁴ A key step in the synthesis is the final hydrolysis of 1,3,5,7-tetramorpholino-5,7-dihydro-1*H*,3*H*-benzo[1,2-*c*:4,5-*c'*]difuran. The compound

should be heated to reflux for at least 3 min. A liquid-liquid extractor should be used for the extraction of **III-5** and should be extracted over at least 3 h. ¹H NMR (400 MHz, CDCl₃, RT): 10.63 (s, 4H), 8.55 (s, 2H). ¹³C NMR (125 MHz, DMSO, RT): δ 192.0, 139.1, 130.6.

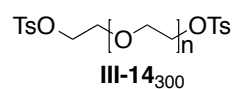


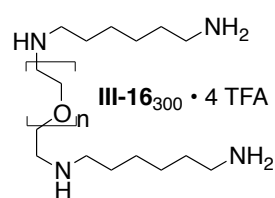
Compound **III-2**: To a solution of **III-3** (1.00 g, 1.03 mmol) in H₂SO₄ (9 M, 10.30 mL) in a 20 mL glass

vial was added **III-5** (0.10 g, 0.51 mmol). The vial was then sealed with a screw cap and stirred at RT for 48 h over which time a white insoluble solid precipitated from the reaction mixture. The precipitate was collected by centrifugation. The precipitate was then stirred with MeOH (50 mL), collected by centrifugation, and dried under high vacuum to yield **III-2** as a white solid (0.32 g, 0.16 mmol, 30%). M.p. > 300 °C. IR (cm⁻¹): 1721s, 1461s, 1375m, 1320m, 1235s, 1187s, 1045m, 963s, 796s, 759s. ¹H NMR (400 MHz, D₂O, as the complex **III-2**•**III-6** (n = 6)₂, RT): 8.04 (s, 2H), 6.86 (s, 4H), 5.80-5.70 (m, 20H), 5.64 (s, 8H), 5.61 (d, *J* = 9.0, 4H), 5.53 (d, *J* = 9.0, 4H), 5.17 (d, *J* = 10.0, 4H), 4.85 (d, *J* = 10.0, 4H), 4.39 (d, *J* = 15.6, 4H), 4.38 (d, *J* = 15.4, 8H), 4.17 (d, *J* = 15.4, 8H), 2.96 (t, *J* = 7.2, 8H), 0.89 (m, 8H), 0.62 (m, 8H). ¹³C NMR (125 MHz, D₂O, as the complex **III-2**•**III-6** (n = 6)₂, RT, 1,4-dioxane as external standard): δ 162.4, 162.1, 156.0, 155.9, 154.3, 134.1, 130.8, 119.4, 117.0,

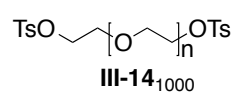
114.7, 112.4, 71.3, 70.1, 69.8, 69.6, 64.90, 63.2, 53.1, 50.9, 50.6, 39.2, 26.4, 25.8.

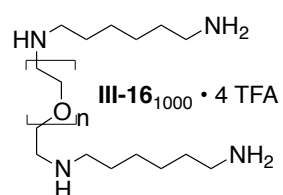
MS (ESI, as the complex **III-2**•**III-6** ($n = 6$)₂): m/z 574.9 ($[\text{M} \cdot \text{III-6} (n = 6)]^{4+}$).

 Compound **III-14**₃₀₀: Compound **III-14**₃₀₀ is known in the literature.⁵ Hexaethylene glycol (PEG₃₀₀) was purchased from Alfa Aesar, Part # L02161. ¹H NMR (400 MHz, D₂O, RT): 7.79 (d, $J = 8.0$, 4H), 7.34 (d, $J = 8.0$, 4H), 4.15 (t, $J = 4.9$, 4H), 3.68 (d, $J = 4.9$, 4H), 3.65-3.50 (m, 20H), 2.44 (s, 6H). ¹³C NMR (125 MHz, CD₃Cl, RT): δ 144.9, 133.0, 129.9, 128.0, 70.7, 70.6, 70.5, 70.4, 69.3, 68.6, 21.6.

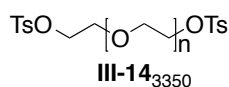
 Compound **III-16**₃₀₀ • 4 TFA: A solution of **III-15** (0.549 g, 2.54 mmol, 0.57 mL) and triethylamine (0.257 g, 2.54 mmol, 0.35 mL) in DMF (3.5 mL) was heated and stirred at 70 °C. A solution of compound **III-14**₃₀₀ (0.500 g, 0.847 mmol) in DMF (3.5 mL) was then added to the reaction mixture dropwise and stirred at 70 °C for 20 h. The reaction mixture was cooled, diluted with CH₂Cl₂ (20 mL), and then washed with NaHCO₃ soln. (20 mL) and H₂O (20 mL). The organics were isolated and concentrated by rotary evaporation then dried under high vacuum. The crude mixture was then dissolved in CH₂Cl₂ (5.0 mL) and TFA (5.0 mL) was added to the solution and stirred at RT for 1 h. The solution was then concentrated by rotary evaporation and dried under high vacuum. The crude product was purified by gel permeation chromatography (Sephadex G25, H₂O mobile phase, 3 × 30 cm column, spotted on glass plate) to yield **III-16**₃₀₀ • 4 TFA as a nearly colorless oil (0.126 g, 16%). IR

(cm^{-1}): 3322br, 2925m, 1679s, 1650s, 1626s, 1430m, 1201s, 1136s. ^1H NMR (400 MHz, D_2O , RT): 3.77 (t, $J = 5.1$, 4H), 3.70-3.65 (m, 20H), 3.24 (t, $J = 5.1$, 4H), 3.05 (t, $J = 8.0$, 4H), 2.97 (t, $J = 8.0$, 4H), 1.75-1.60 (m, 8H), 1.45-1.30 (m, 8H). ^{13}C NMR (125 MHz, D_2O , RT, 1,4-dioxane as external standard): δ 162.4, 162.2, 117.1, 114.8, 69.2, 69.1, 69.0, 64.9, 63.6, 53.4, 52.3, 46.9, 46.3, 38.9, 26.0, 26.0, 24.8, 24.7, 24.7, 24.6, 22.2. MS (ESI): m/z 479.40 (M^+).


 Compound **III-14**₁₀₀₀: To a stirring solution of PEG₁₀₀₀ (Sigma-Aldrich, Part # P3515, 1.00 g, 1.0 mmol) in THF (5.0 mL) at RT was added NaOH (0.16 g, 4.0 mmol) in H_2O (1.0 mL) and stirred for 5 m. A solution of **III-13** (0.57 g, 3.0 mmol) in THF (5.0 mL) was then added to the reaction mixture which was then stirred at RT for 20 h. The reaction mixture was slowly poured into stirring H_2O (30 mL) and stirred for 30 m. The product was then extracted from the solution with CH_2Cl_2 (3 \times 20 mL). The organics were collected and concentrated by rotary evaporation and dried under high vacuum to yield **III-14**₁₀₀₀ as a white solid (1.22 g, 93%). M.p. 37-40 $^\circ\text{C}$. IR (cm^{-1}): 3430br, 2913s, 2883s, 1730s, 1448m, 1352m, 1248m, 1174s, 1109s, 930m, 813m, 665m, 557s. ^1H NMR (400 MHz, D_2O , RT): . ^{13}C NMR (125 MHz, CD_3Cl , RT): δ 144.8, 133.1, 129.9, 128.0, 72.6, 70.7, 69.3, 68.7, 61.7, 21.7.

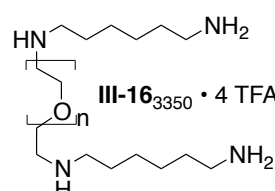

 Compound **III-16**₁₀₀₀ • 4 TFA: A solution of **III-15** (0.248 g, 1.145 mmol, 0.26 mL) and triethylamine (0.232 g, 2.29 mmol, 0.32 mL) in DMF (2.0 mL) was heated and stirred at 70 $^\circ\text{C}$. A

solution of compound **III-14**₁₀₀₀ (0.500 g, 0.382 mmol) in DMF (2.0 mL) was then added to the reaction mixture dropwise and stirred at 70 °C for 20 h. The reaction mixture was cooled, diluted with CH₂Cl₂ (15 mL), and then washed with NaHCO₃ soln. (15 mL) and H₂O (15 mL). The organics were isolated and concentrated by rotary evaporation then dried under high vacuum. The crude mixture was then dissolved in CH₂Cl₂ (3.0 mL) and TFA (3.0 mL) was added to the solution and stirred at RT for 1 h. The solution was then concentrated by rotary evaporation and dried under high vacuum. The crude product was purified by gel permeation chromatography (Sephadex G25, H₂O mobile phase, 3 × 25 cm column, spotted on glass plate) to yield **III-16**₁₀₀₀ • 4 TFA as an off-white solid (0.147 g, 23%). M.p. 260-265 °C (dec.). IR (cm⁻¹): 3448br, 2913s, 2870s, 1696s, 1643m, 1470m, 1348m, 1243m, 1200br, 987m, 961m, 835m, 726m, 652s, 622s. ¹H NMR (400 MHz, D₂O, RT): 3.78 (t, *J* = 5.0, 4H), 3.75-3.60 (m, 136H), 3.26 (t, *J* = 5.0, 4H), 3.07 (t, *J* = 7.7, 4H), 2.98 (t, *J* = 7.7, 4H), 1.75-1.60 (m, 8H), 1.45-1.35 (m, 8H). ¹³C NMR (125 MHz, D₂O, RT, 1,4-dioxane as external standard): δ 69.1, 64.8, 46.8, 46.3, 38.8, 25.9, 24.7, 24.6, 24.5.

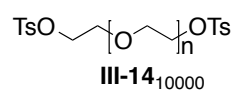


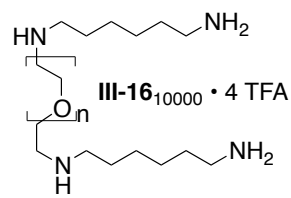
Compound **III-14**₃₃₅₀: To a stirring solution of PEG₃₃₅₀ (Sigma-Aldrich, Part # 202444, 5.00 g, 1.49 mmol) in THF (15.0 mL) at RT was added NaOH (0.239 g, 5.97 mmol) in H₂O (1.6 mL) and stirred for 5 m. A solution of **III-13** (0.854 g, 4.48 mmol) in THF (7.5 mL) was then added to the reaction mixture which was then stirred at RT for 18 h. The reaction mixture was slowly poured into stirring H₂O (100 mL) and stirred for 30 m. The product was then

extracted from the solution with CH_2Cl_2 (3×50 mL). The organics were collected and concentrated by rotary evaporation and dried under high vacuum to yield **III-14**₃₃₅₀ as a white solid (5.30 g, 97%). M.p. 37-40 °C. IR (cm^{-1}): 2945s, 2896s, 2735m, 1959m, 1470s, 1351s, 1281s, 1246s, 1113s, 959s, 847s. ^1H NMR (400 MHz, D_2O , RT): 7.86 (d, $J = 8.2$, 4H), 7.52 (d, $J = 8.2$, 4H), 4.28 (t, $J = 4.2$, 4H), 3.75-3.50 (m, 394H), 2.46 (s, 6H). ^{13}C NMR (125 MHz, CD_3Cl , RT): δ 144.8, 133.13, 129.9, 128.0, 70.6, 69.3, 68.7, 21.7.

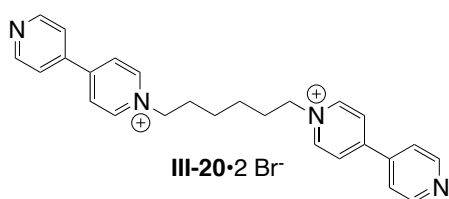

III-16₃₃₅₀ • 4 TFA: A solution of **III-15** (0.097 g, 0.448 mmol, 0.10 mL) and triethylamine (0.091 g, 0.895 mmol, 0.12 mL) in DMF (1.50 mL) was heated and stirred at 70 °C. A solution of compound **III-14**₃₃₅₀ (0.546 g, 0.149 mmol) in DMF (1.50 mL) was then added to the reaction mixture dropwise and stirred at 70 °C for 18 h. The reaction mixture was cooled, diluted with CH_2Cl_2 (15.0 mL), and then washed with NaHCO_3 soln. (15.0 mL) and H_2O (15.0 mL). The organics were isolated and concentrated by rotary evaporation then dried under high vacuum. The crude mixture was then dissolved in CH_2Cl_2 (5.0 mL) and TFA (5.0 mL) was added to the solution and stirred at RT for 1 h. The solution was then concentrated by rotary evaporation and dried under high vacuum. The crude product was purified by gel permeation chromatography (Sephadex G25, H_2O mobile phase, 3×25 cm column, spotted on glass plate) to yield **III-16**₃₃₅₀ • 4 TFA as an off-white solid (0.180 g, 30%). IR (cm^{-1}): 2942m, 2884s, 2852s, 1675m, 1471m, 1348s, 1279m, 1238m, 1148s, 1103s, 1058s, 943s, 833s. M.p. 43-46 °C. ^1H NMR (400 MHz, D_2O , RT): 3.77 (t, $J = 5.0$,

4H), 3.80-3.60 (m, 478H), 3.24 (t, $J = 5.0$, 4H), 3.05 (t, $J = 7.8$, 4H), 2.98 (t, $J = 7.8$, 4H), 1.75-1.60 (m, 8H), 1.45-1.35 (m, 8H). ^{13}C NMR (125 MHz, D_2O , RT, 1,4-dioxane as external standard): δ 70.7, 61.5, 48.5, 48.0, 40.5, 27.7, 26.4, 26.3.

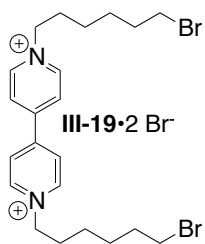

 Compound **III-14**₁₀₀₀₀: To a stirring solution of PEG₁₀₀₀₀ (Sigma-Aldrich, Part # P6667, 5.0 g, 0.50 mmol) in THF (5.0 mL) at RT was added NaOH (0.08 g, 2.0 mmol) in H_2O (0.5 mL) and stirred for 5 m. A solution of **III-13** (0.3 g, 1.5 mmol) in THF (2.5 mL) was then added to the reaction mixture which was then stirred at RT for 18 h. The reaction mixture was slowly poured into stirring H_2O (100 mL) and stirred for 30 m. The product was then extracted from the solution with CH_2Cl_2 (3 \times 50 mL). The organics were collected and concentrated by rotary evaporation and dried under high vacuum to yield **III-14**₁₀₀₀₀ as a white solid (4.5 g, 87%). M.p. 41-44 $^\circ\text{C}$. IR (cm^{-1}): 2944s, 2889s, 2742m, 1470s, 1344s, 1274s, 1239s, 1092s, 966s, 833s. ^1H NMR (400 MHz, D_2O , RT): 7.86 (d, $J = 8.2$, 4H), 7.52 (d, $J = 8.2$, 4H), 4.28 (t, $J = 4.2$, 4H), 4.80-3.45 (m, 1,210H), 2.46 (s, 6H). ^{13}C NMR (125 MHz, CD_3Cl , RT): δ 144.9, 133.2, 129.9, 128.1, 70.7, 69.4, 68.8, 21.8.


 Compound **III-16**₁₀₀₀₀ • 4 TFA: A solution of **III-15** (0.063 g, 0.291 mmol, 0.07 mL) and triethylamine (0.059 g, 0.582 mmol, 0.08 mL) in DMF (1.0 mL) was heated and stirred at 70 $^\circ\text{C}$. A solution of compound **III-14**₁₀₀₀₀ (1.0 g, 0.097 mmol) in DMF (1.0 mL) was then added to the reaction mixture dropwise and stirred at 70 $^\circ\text{C}$ for 18 h. The reaction mixture was cooled, diluted with CH_2Cl_2 (15.0 mL), and then washed with

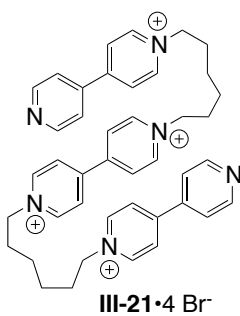
NaHCO₃ soln. (15.0 mL) and H₂O (15.0 mL). The organics were isolated and concentrated by rotary evaporation then dried under high vacuum. The crude mixture was then dissolved in CH₂Cl₂ (5.0 mL) and TFA (5.0 mL) was added to the solution and stirred at RT for 1 h. The solution was then concentrated by rotary evaporation and dried under high vacuum. The crude product was purified by gel permeation chromatography (Sephadex G50, H₂O mobile phase, 3 × 25 cm column, spotted on glass plate) to yield **III-16**₁₀₀₀₀ • 4 TFA as an off-white solid (0.228 g, 22%). IR (cm⁻¹): 3465br, 2943m, 2887s, 2800m, 2735m, 2691m, 1794m, 1691m, 1483s, 1365s, 1343s, 1274s, 1243s, 1157s, 1109s, 1052s, 965s, 943m, 843s. M.p. 42-44 °C. ¹H NMR (400 MHz, D₂O, RT): 3.76 (t, *J* = 4.8, 4H), 3.75-3.50 (m, 1,301H), 3.25 (t, *J* = 4.8, 4H), 3.07 (t, *J* = 7.8, 4H), 2.98 (t, *J* = 7.8, 4H), 1.75-1.60 (m, 8H), 1.45-1.35 (m, 8H). ¹³C NMR (125 MHz, D₂O, RT, 1,4-dioxane as external standard): δ 71.4, 69.3, 65.0, 60.1, 46.5, 24.8, 24.8.



Compound **III-20** • Br₂²⁻: Compound **III-20** • Br₂²⁻ was synthesized following a known procedure in the literature.⁶ ¹H NMR (400 MHz, D₂O, RT): 8.94 (d, *J* = 6.7, 4H), 8.73 (d, *J* = 6.3, 4H), 8.36 (d, *J* = 6.7, 4H), 7.87 (d, *J* = 6.3, 4H), 4.65 (t, *J* = 7.2, 4H), 2.15-2.00 (m, 4H), 1.50-1.35 (m, 4H). ¹³C NMR (125 MHz, D₂O, RT, 1,4-dioxane as external standard): δ 153.3, 149.5, 144.2, 142.0, 125.5, 121.9, 61.0, 29.7, 24.4. MS (ESI): *m/z* 198.1 (M²⁺).

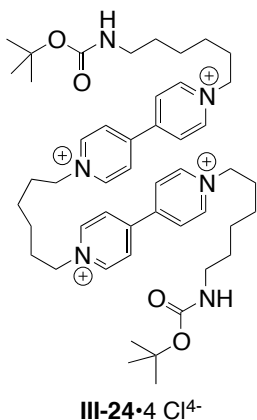


Compound **III-19** • Br₂²⁻: Compound **III-17** (0.50 g, 3.20 mmol) and compound **III-18** (10.0 mL, 15.60 g, 64.02 mmol) were dissolved in CH₃CN (45.0 mL) at RT in a RB flask. The reaction mixture was then stirred and heated to reflux for 3 h. The precipitate was then collected by vacuum filtration while the mixture was still hot. The precipitate was then washed with hot CH₃CN (3 × 20 mL) and dried under high vacuum to yield **III-19** as a yellow solid in 33% yield (1.38 g, 2.14 mmol). IR (cm⁻¹): 3109m, 3061m, 3026s, 2991s, 2970m, 2935s, 2861m, 1635s, 1557m, 1513s, 1470m, 1443m, 1378m, 1361m, 1291m, 1248m, 1239m, 1183s, 826s, 804m, 657m. M.p. 246-248 °C. ¹H NMR (400 MHz, D₂O, RT): 9.13 (d, *J* = 6.7, 4H), 8.55 (d, *J* = 6.7, 4H), 4.75 (t, *J* = 7.3, 4H), 3.5 (t, *J* = 6.6, 4H), 2.15-2.05 (m, 4H), 1.90-1.80 (m, 4H), 1.55-1.45 (m, 4H), 1.45-1.35 (m, 4H). ¹³C NMR (125 MHz, D₂O, RT, 1,4-dioxane as external standard): δ 149.5, 144.9, 126.5, 61.6, 34.5, 31.2, 29.9, 26.2, 23.9. MS (ESI): *m/z* 242.0 (M²⁺).



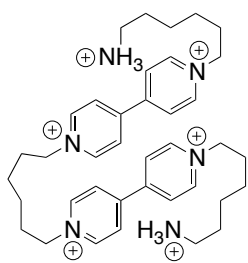
Compound **III-21** • Br₄⁴⁻: Compound **III-19** (0.100 g, 0.155 mmol) was mixed together with compound **III-17** (0.243 g, 1.550 mmol) in 20% EtOH (0.32 mL) in CH₃CN (1.25 mL) in a microwave reaction tube. A stir-bar was placed in the tube and the tube was capped. The microwave reactor was set to run for 20 min at 130 °C with a maximum power of 250 W while stirring. Upon reaction completion the precipitate was collected by vacuum filtration and washed with hot CH₃CN (3 × 5 mL) to yield **III-21** as an off-white solid in 44% (0.067 g, 0.07 mmol).

IR (cm⁻¹): 3392br, 3116m, 3087m, 3041s, 2940m, 2859m, 1636s, 1592m, 1548m, 1465m, 1443m, 1410s, 1352m, 1252m, 1221m, 1180s, 842m, 814s. M.p. 270-273 °C (dec.). ¹H NMR (400 MHz, D₂O, RT): 9.09 (d, *J* = 6.9, 4H), 8.94 (d, *J* = 6.9, 4H), 8.75 (dd, *J* = , 4H), 8.51 (d, *J* = 6.9, 4H), 8.39 (d, *J* = 6.9, 4H), 7.89 (dd, *J* = , 4H), 4.71 (t, *J* = 7.5, 4H), 4.65 (t, *J* = 7.3, 4H), 2.15-2.00 (m, 8H), 1.55-1.40 (m, 8H). ¹³C NMR (125 MHz, D₂O, RT, 1,4-dioxane as external standard): δ 153.3, 149.5, 149.5, 145.0, 144.2, 142.2, 126.5, 125.6, 122.0, 61.5, 60.9, 29.9, 29.8, 24.4, 24.3. MS (ESI), *m/z* 317.2 ([M-H₂)²⁺).

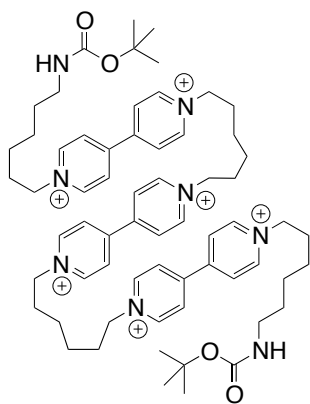


Compound **III-24** • Cl₄⁴⁻: Compound **III-20** • Br₂²⁻ was first converted to the • PF₆ salt. Compound **III-20** • Br₂²⁻ (0.250 g, 0.450 mmol) was dissolved in H₂O (5.0 mL). A conc. solution of NH₄PF₆ in H₂O (5.0 mL) was then added to the mixture. The precipitate was collected and washed with H₂O (3 × 10.0 mL) and dried under high vacuum to yield **III-20** • (PF₆)₂²⁻ as a white solid in 92% yield (0.284 g, 0.414 mmol). To a stirring solution of compound **III-20** • (PF₆)₂²⁻ (0.100 g, 0.146 mmol) in CH₃CN (2.90 mL) was added compound **III-15** (0.271 g, 0.729 mmol). The mixture was then heated to reflux and stirred for 24 h. While the mixture was hot a conc. solution of N(Bu)₄Cl in CH₃CN (5.0 mL) was added. The white precipitate was collected by centrifugation. The solid was then stirred with CH₃CN and heated to reflux at which time a conc. solution of N(Bu)₄Cl in CH₃CN (5.0 mL) was added. The mixture was stirred at reflux for 5 min. and the precipitate was collected by vacuum filtration. Final

purification was performed by stirring the solid in isopropyl alcohol (5 mL) at reflux for 5 m and collecting the precipitate by vacuum filtration to yield **III-24** • Cl₄⁴⁻ as an off-white solid (0.068 g, 50%). M.p. 233-236 °C (dec.). IR (cm⁻¹): 3421br, 3117m, 3048s, 2983s, 2926s, 2857s, 1687s, 1643s, 1557m, 1513s, 1448s, 1370s, 1278m, 1248s, 1170s, 835s, 809m, 717m, 517m. ¹H NMR (400 MHz, D₂O, RT): 9.09 (d, *J* = 6.1, 8H), 8.55-8.45 (m, 8H), 4.70 (t, *J* 6.8, 8H), 3.01 (t, *J* = .4, 4H), 2.15-2.00 (m, 8H), 1.50-1.40 (m, 8H), 1.40-1.30 (m, 26H). ¹³C NMR (125 MHz, D₂O, RT, 1,4-dioxane as external standard): δ 157.9, 149.6, 149.5, 145.0, 126.5, 126.4, 80.3, 61.7, 61.5, 39.2, 30.0, 29.9, 28.1, 27.2, 24.7, 24.4. MS (ESI) *m/z* 265.1 ([M-H]³⁺).

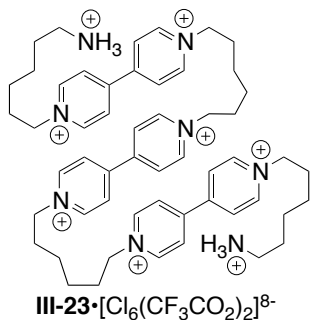


Compound **III-22** • Cl₄(CF₃CO₂)₂⁶⁻: Compound **III-24** • Cl₄⁴⁻ (0.068 g, 0.073 mmol) was dissolved in TFA (1.0 mL) and stirred at RT for 1h. The solution was concentrated by rotary evaporation and dried under high vacuum to yield **III-22** • Cl₄(CF₃CO₂)₂⁶⁻ as an off-white solid (0.064 g, 91%). M.p. 47-50 °C. IR (cm⁻¹): 3122s, 3052s, 2948m, 2865m, 1796s, 1683s, 1639s, 1561m, 1509m, 1443m, 1352m, 1204s, 1135s, 961m, 843m, 804s, 704s, 596m, 517m. ¹H NMR (400 MHz, D₂O, RT): 9.09 (d, *J* = 6.4, 8H), 8.51 (d, *J* = 6.4, 8H), 4.69 (t, *J* = 7.6, 8H), 2.96 (t, *J* = 7.6, 4H), 2.15-2.00 (m, 8H), 1.0-1.60 (m, 4H), 1.50-1.45(m, 8H), 1.45-1.40 (8H). ¹³C NMR (125 MHz, D₂O, RT, 1,4-dioxane as external standard): δ 162.4, 162.1, 161.8, 161.6, 149.5, 149.4, 144.9, 126.4, 126.4, 119.1, 116.8, 114.5, 112.2, 61.5, 61.5, 38.8, 29.9, 25.9, 24.5, 24.3. MS (ESI) *m/z* 297.3 ([M-H₄]²⁺).



III-25•6 Cl⁶⁻

Compound **III-25** • Cl₆⁶⁻: Compound **III-21** • Br₄⁴⁻ was first converted to the • PF₆ salt. Compound **III-21** • Br₄⁴⁻ (0.250 g, 0.263 mmol) was dissolved in H₂O (5.0 mL). A conc. solution of NH₄PF₆ in H₂O (5.0 mL) was then added to the mixture. The precipitate was collected and washed with H₂O (3 × 10.0 mL) and dried under high vacuum to yield **III-21** • (PF₆)₄⁴⁻ as a white solid in 90% yield (0.287 g, 0.236 mmol). To a stirring solution of compound **III-21** • (PF₆)₄⁴⁻ (0.100 g, 0.082 mmol) in CH₃CN (1.65 mL) was added compound **III-15** (0.152 g, 0.410 mmol). The mixture was then heated to reflux and stirred for 24 h. While the mixture was hot a conc. solution of N(Bu)₄Cl in CH₃CN (4.0 mL) was added. The white precipitate was collected by centrifugation. The solid was then stirred with CH₃CN and heated to reflux at which time a conc. solution of N(Bu)₄Cl in CH₃CN (4.0 mL) was added. The mixture was stirred at reflux for 5 min. and the precipitate was collected by vacuum filtration. Final purification was performed by recrystallization from ethyl alcohol (2.0 mL) to yield **III-25** • Cl₆⁶⁻ as an off-white solid (0.036 g, 35%). M.p. 243-246 °C (dec.). IR (cm⁻¹): 3417br, 3122m, 3039s, 2974m, 2935s, 2857m, 1683s, 1635s, 1561m, 1513m, 1452s, 1370m, 1252m, 1178s, 839m, 809m, 517m. ¹H NMR (600 MHz, D₂O, RT): 9.09 (d, *J* = 6.6, 12H), 8.55-8.45 (m, 12H), 4.69 (t, *J* = 3.0, 12H), 3.01 (t, *J* = 6.6, 4H), 2.15-2.00 (m, 12H), 1.50-1.45 (m, 8H), 1.45-1.40 (m, 4H), 1.40-1.30 (m, 22H). ¹³C NMR (125 MHz, D₂O, RT, 1,4-dioxane as external standard): δ 157.9, 149.6, 149.5, 144.9, 126.5, 126.4, 80.3, 61.7, 61.5, 39.2, 30.0, 29.9, 28.1, 27.2, 24.7, 24.4. MS (ESI) *m/z* 258.9 ([M-H₂)⁴⁺).



Compound **III-23** • Cl₆(CF₃CO₂)₂⁸⁻: Compound **III-25** • Cl₆⁶⁻ (0.036 g, 0.029 mmol) was dissolved in TFA (1.0 mL) and stirred at RT for 1h. The solution was concentrated by rotary evaporation and dried under high vacuum to yield **III-23** • Cl₆(CF₃CO₂)₂⁸⁻ as an off-white solid (0.031 g,

84%). M.p. 155-159 °C. IR (cm⁻¹): 3404br, 3122s, 3043s, 2948s, 2865m, 1787m, 1748s, 1678s, 1635s, 1557m, 1504m, 1470m, 1443m, 1417m, 1360m, 1304m, 1191s, 1130s, 839s, 796s, 717s, 709s. ¹H NMR (400 MHz, D₂O, RT): 9.05 (d, *J* = 3.8, 12H), 8.47 (d, *J* = 3.8, 12H), 4.66 (t, *J* = 4.8, 12H), 2.92 (t, *J* = 5.2, 4H), 2.05-1.95 (m, 12H), 1.65-1.55 (m, 4H), 1.45-1.40 (m, 8H), 1.40-1.35 (m, 8H). ¹³C NMR (125 MHz, D₂O, RT, 1,4-dioxane as external standard): δ 162.5, 162.2, 161.9, 161.6, 149.6, 145.0, 142.1, 126.5, 125.8, 119.3, 117.0, 114.7, 112.4, 61.6, 38.9, 29.9, 26.0, 24.6, 24.4. MS (ESI) *m/z* 278.8 ([M-H₅]³⁺).

References.

- 1) Lucas, D.; Minami, T.; Iannuzzi, G.; Cao, L.; Wittenberg, J.B.; Anzenbacher, Jr., P.; Isaacs, L. *J. Am. Chem. Soc.* **2011**, *133*, 17966–17976.
- 2) Arduini, A.; Bussolati, R.; Credi, A.; Faimani, G.; Garaudee, S.; Pochini, A.; Secchi, A.; Semeraro, M.; Silvi, S.; Venturi, M. *Chem. Eur. J.* **2009**, *15*, 3230-3242.

- 3) Leeming, S. W.; Anemian, R. M.; Williams, R.; Brown, B. A. Oligomeric Polyacene and Semiconductor Formulation. WO 2006/125504 A1, November 30, 2006.
- 4) Schrievers, T.; Brinker, U. H. *Synthesis*. **1988**, *4*, 330-331.
- 5) Jiang, W.; Schalley, C.A. *Beilstein J. Org. Chem.* **2010**, *6*, No. 14.
- 6) Zhang, Z.-J.; Zhang, Y.-M.; Liu, Y. *J. Org. Chem.* **2011**, *76*, 4682-468

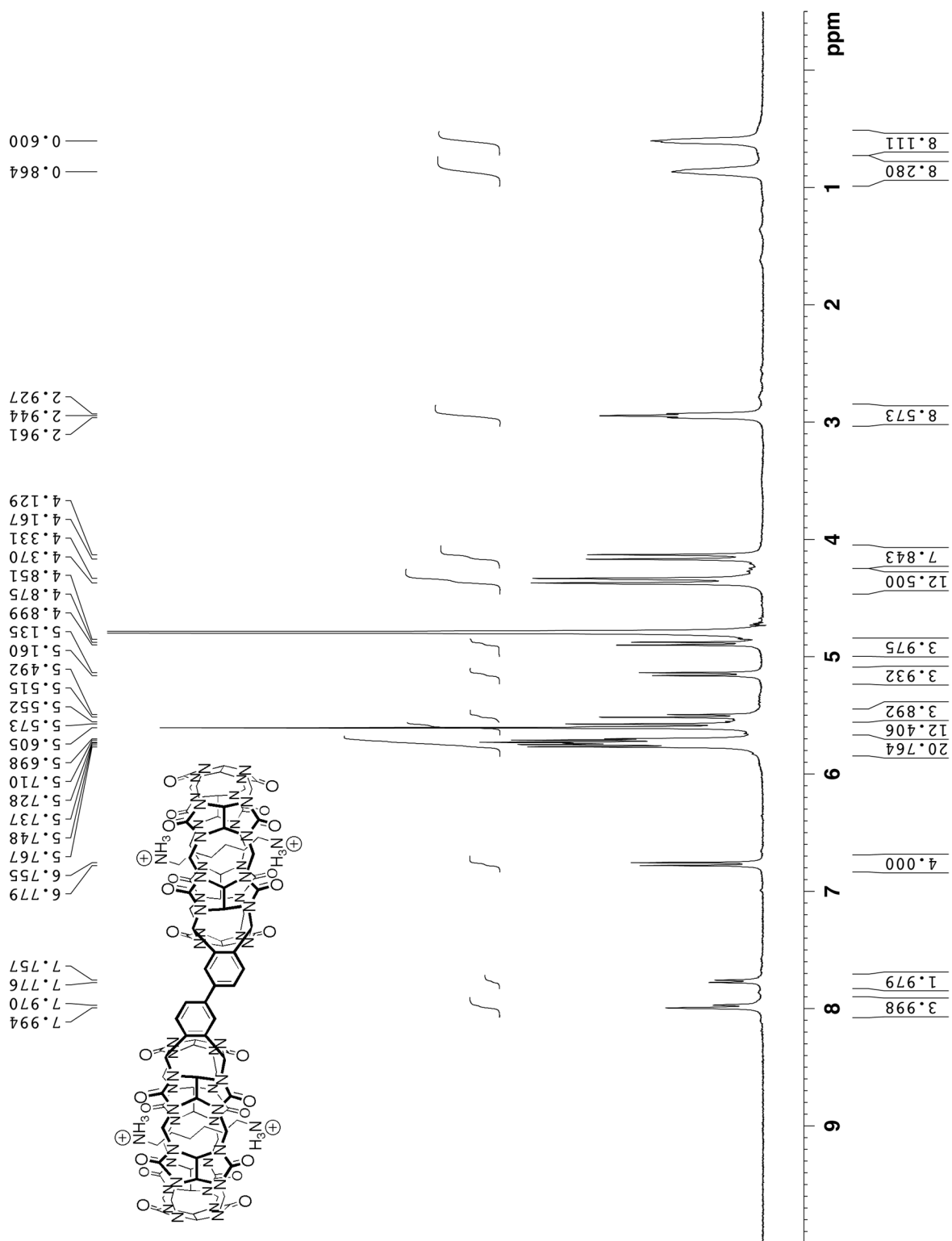


Figure III-S1. ^1H NMR spectrum (400 MHz, D_2O , RT) recorded for compound **III-1** as the complex **III-1•III-6** ($n = 6$) $_2$.

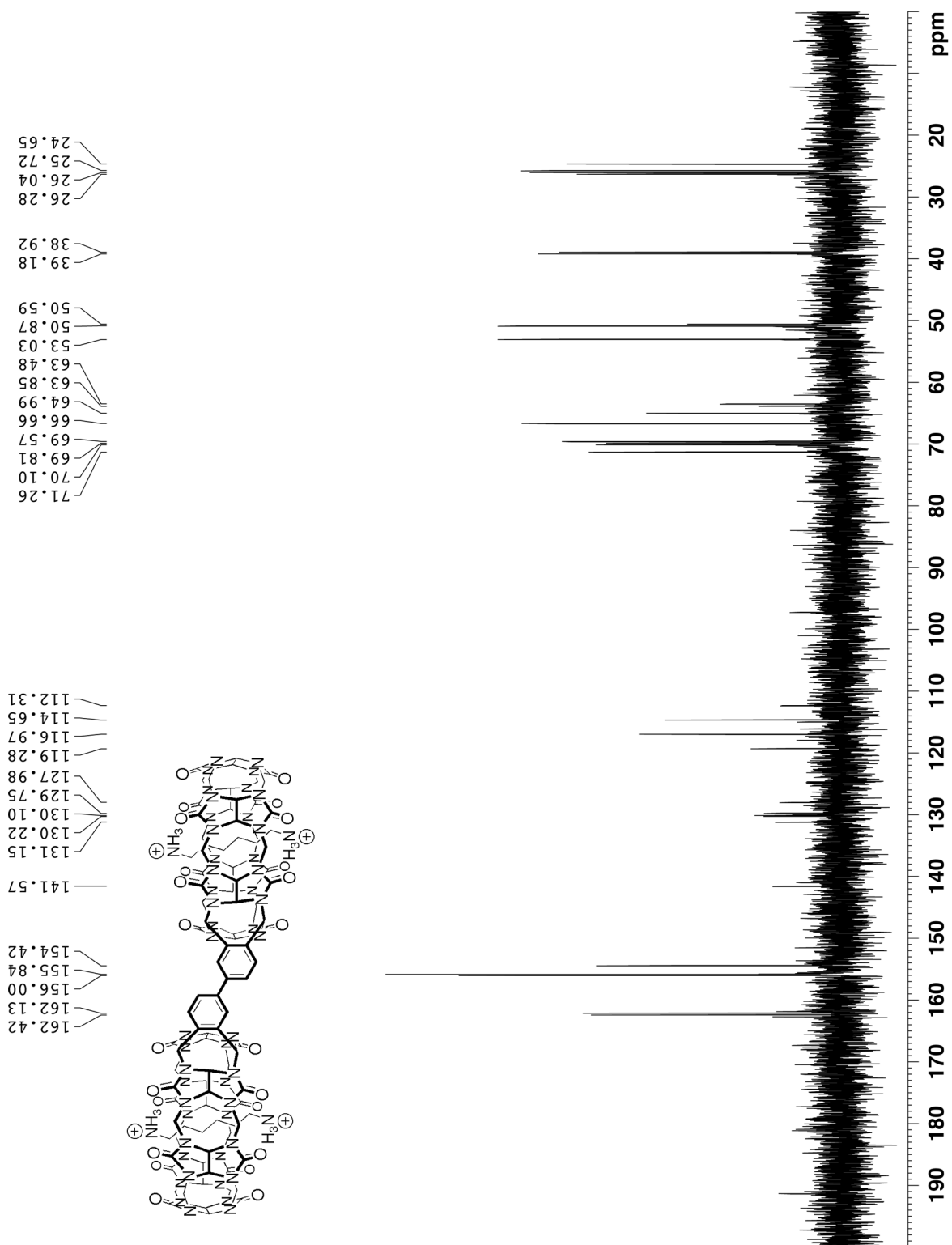


Figure III-S2. ¹³C NMR spectrum (125 MHz, D₂O, RT, 1,4-dioxane as external standard) recorded for compound **III-1** as the complex **III-1•III-6** (n = 6)₂.

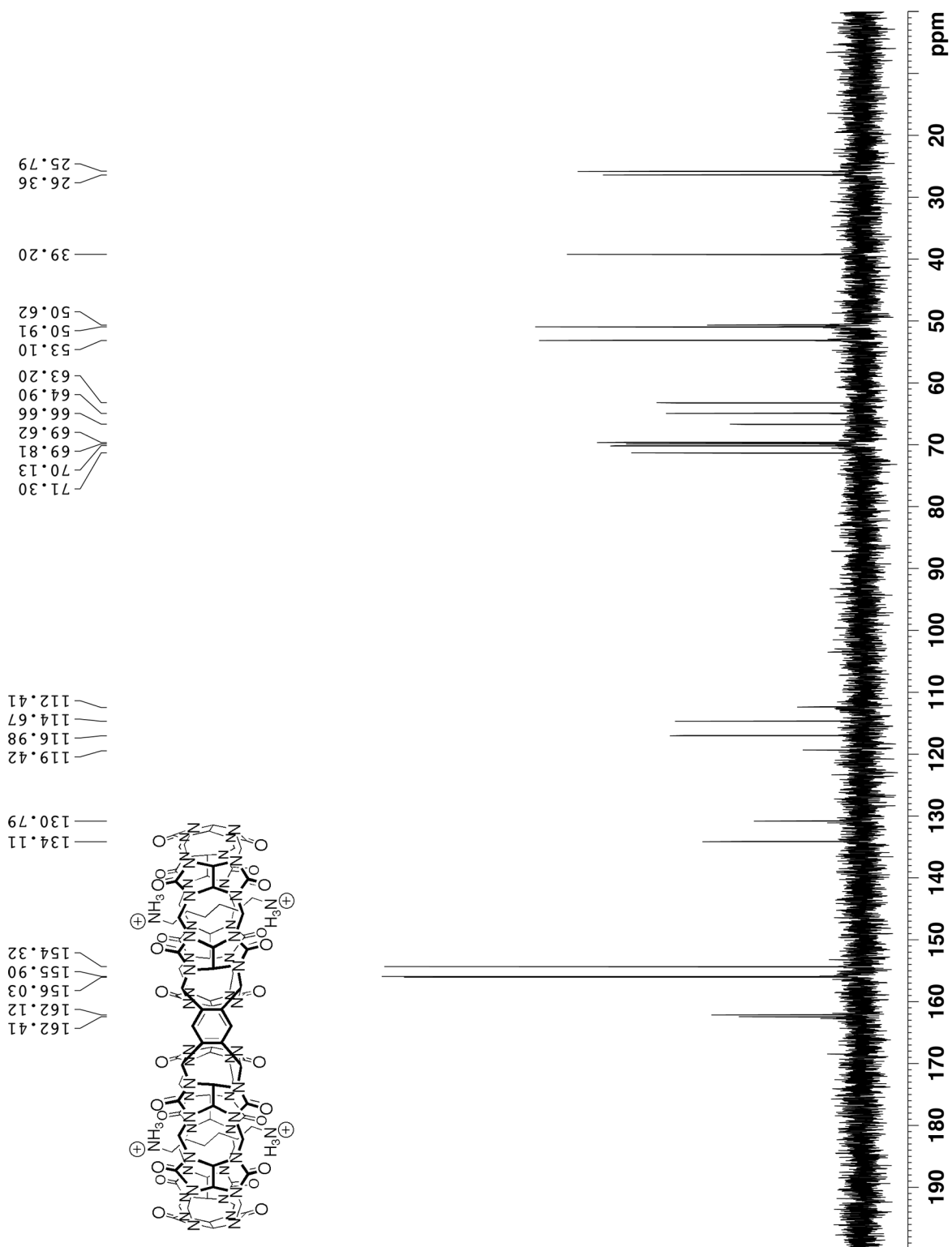


Figure III-S4. ^{13}C NMR spectrum (125 MHz, D_2O , RT, 1,4-dioxane as external standard) recorded for compound **III-2** as the complex **III-2** \cdot **III-6** ($n = 6$) $_2$.

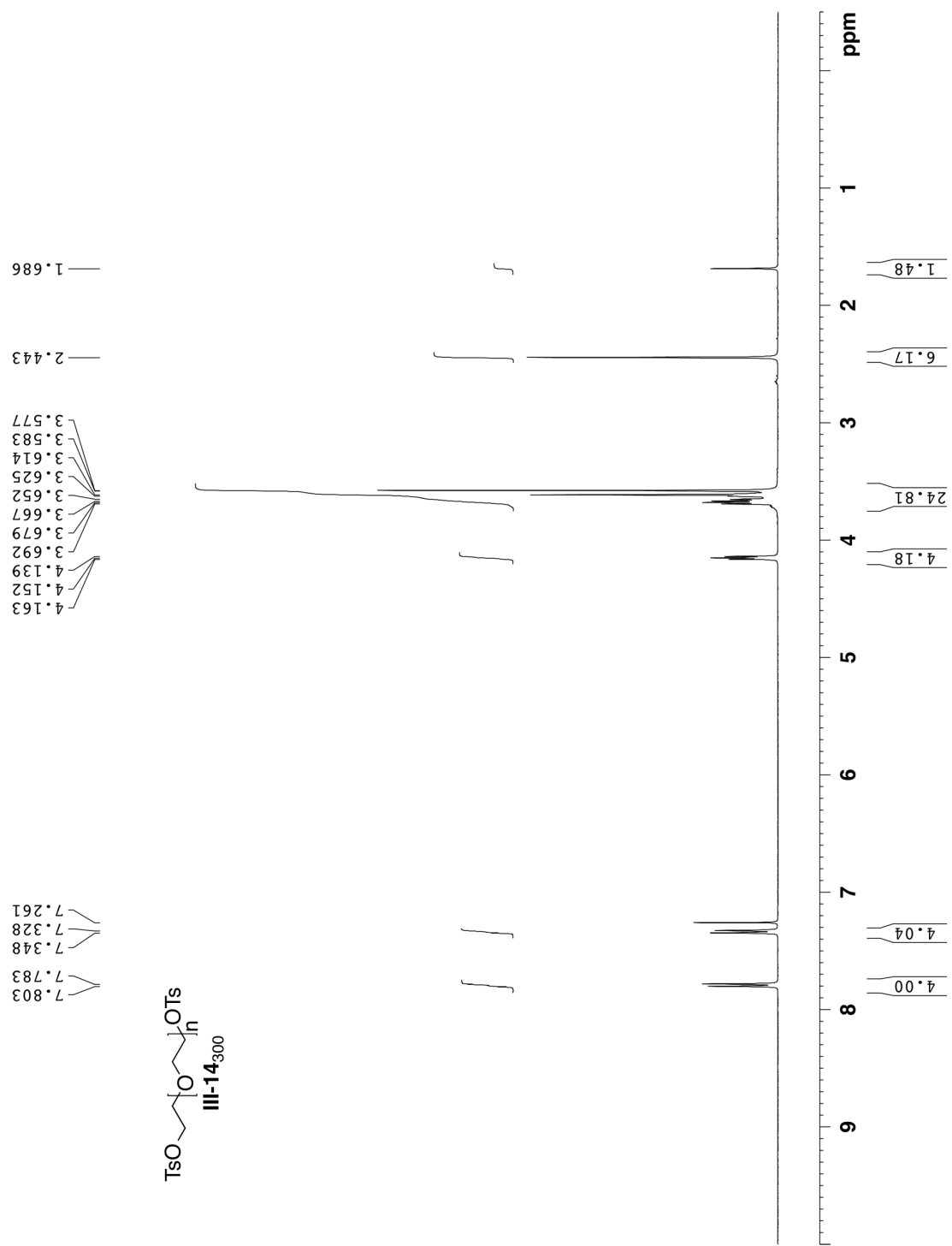


Figure III-S5. ¹H NMR spectra (400 MHz, CDCl₃, RT) recorded for **III-14₃₀₀**.

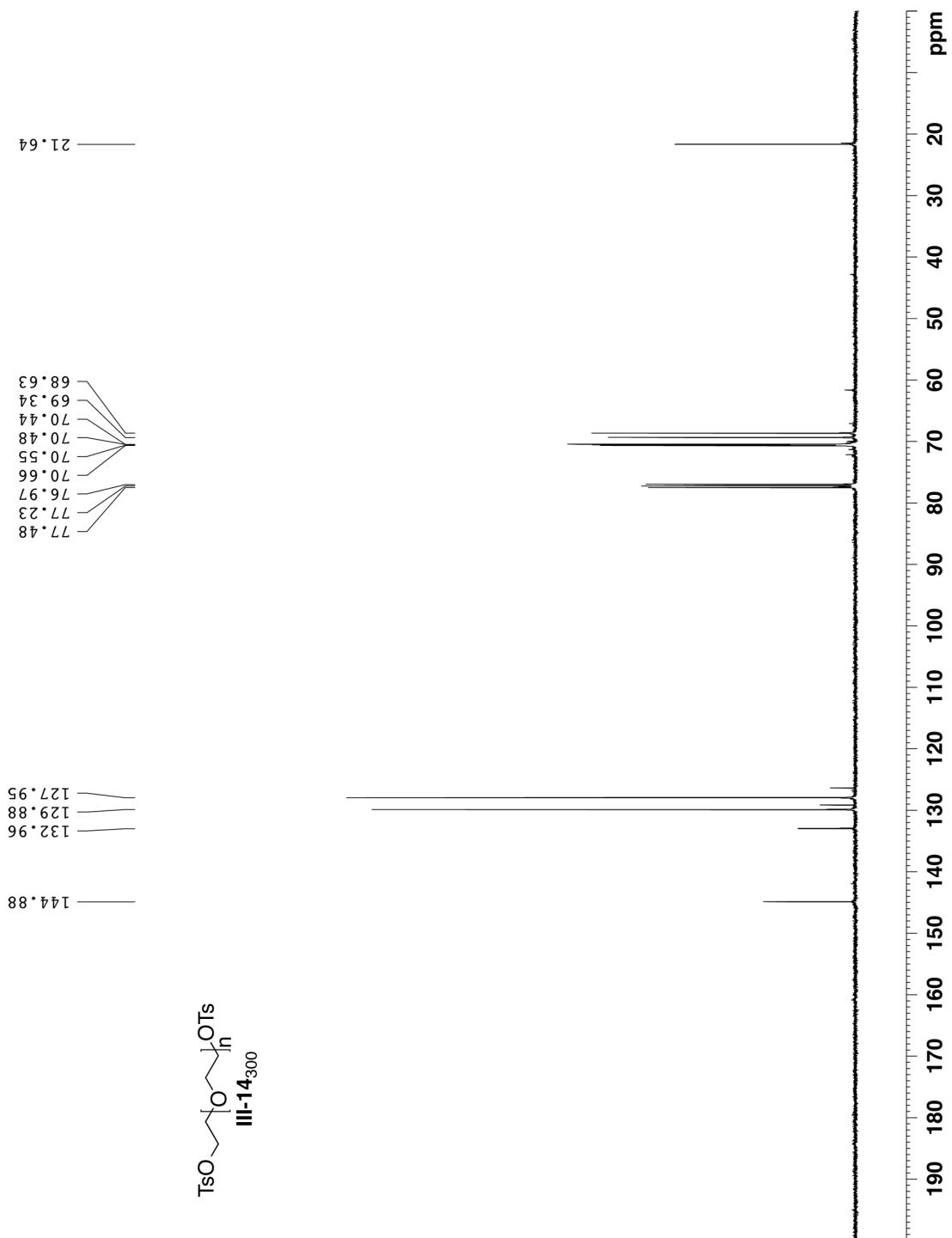


Figure III-S6. ¹³C NMR spectrum (125 MHz, CDCl₃, RT) recorded for compound III-14₃₀₀.

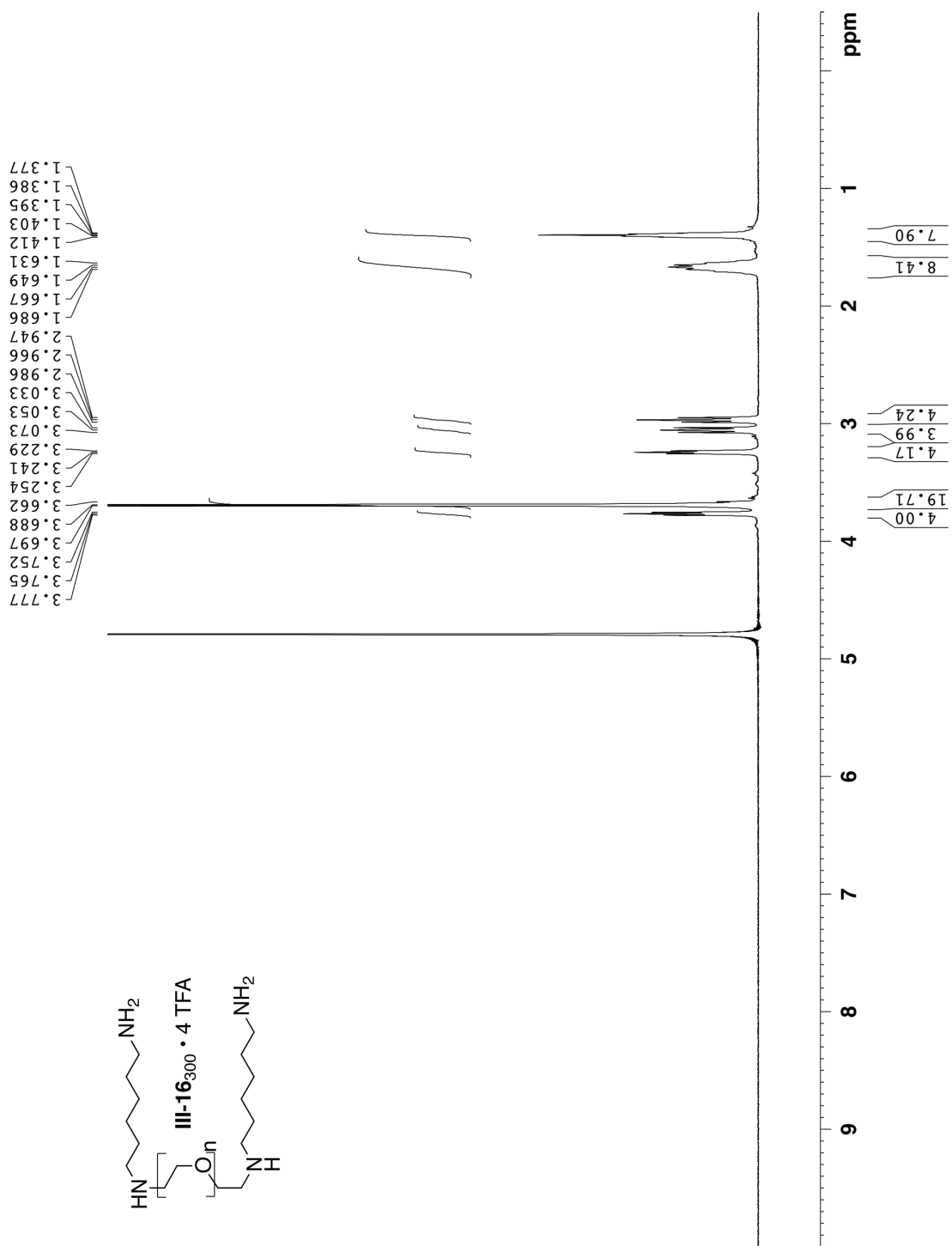


Figure III-S7. ¹H NMR spectra (400 MHz, D₂O, RT) recorded for **III-16₃₀₀ • 4 TFA**.

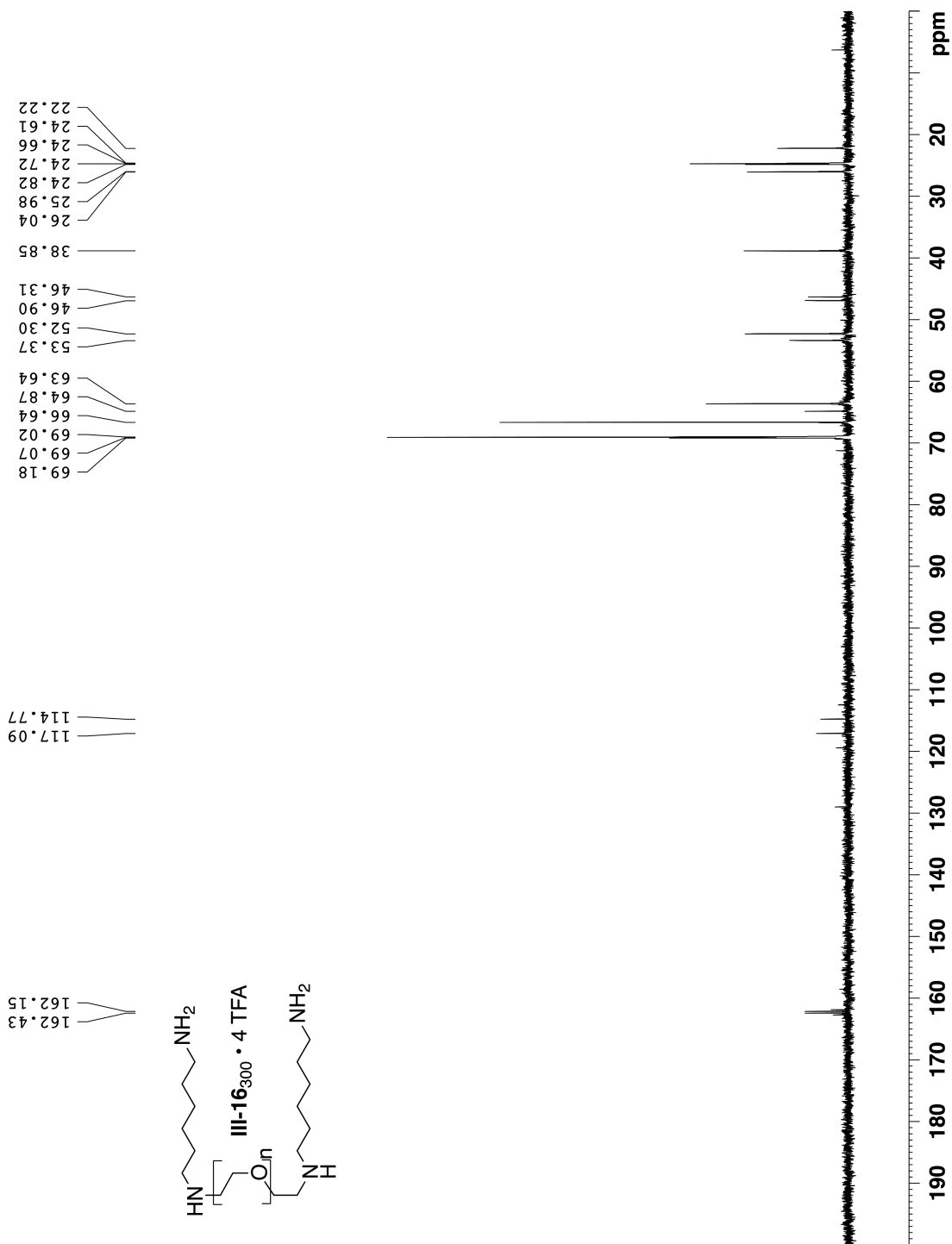


Figure III-S8. ^{13}C NMR spectrum (125 MHz, D_2O , RT, 1,4-dioxane as external standard) recorded for compound **III-16₃₀₀ • 4 TFA**.

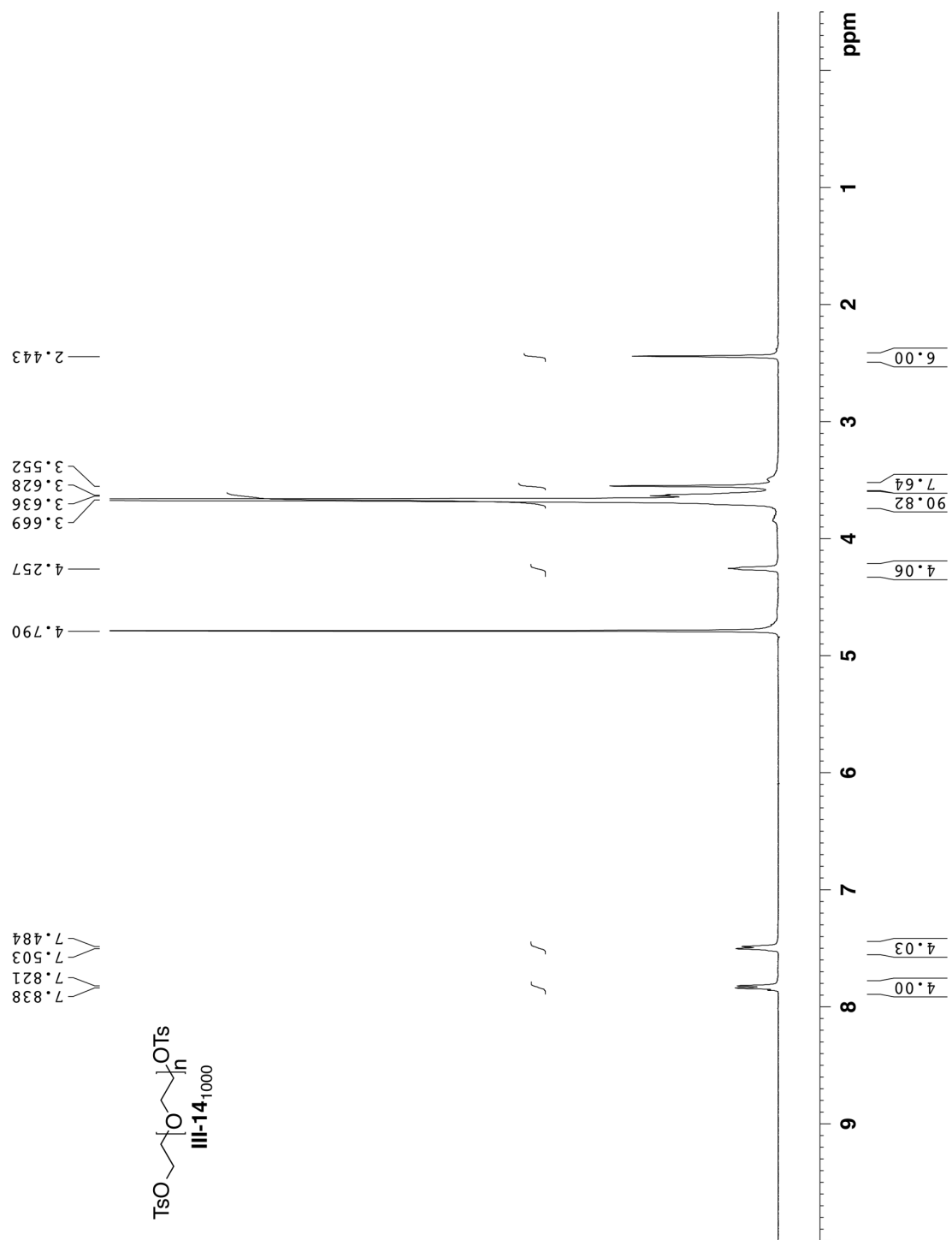


Figure III-S9. ^1H NMR spectra (400 MHz, D_2O , RT) recorded for **III-14₁₀₀₀**.

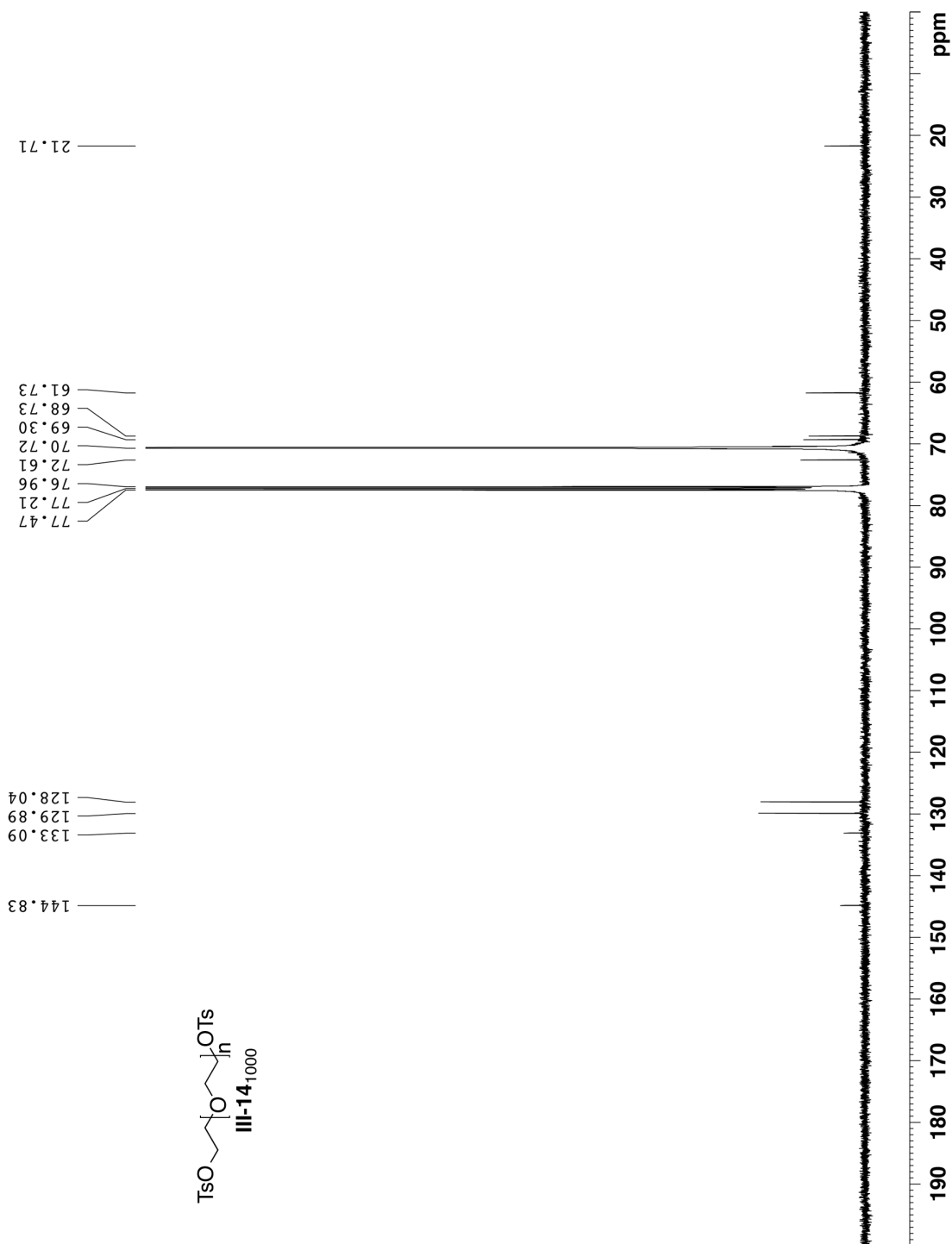


Figure III-S10. ¹³C NMR spectra (125 MHz, CDCl₃, RT) recorded for **III-14₁₀₀₀**.

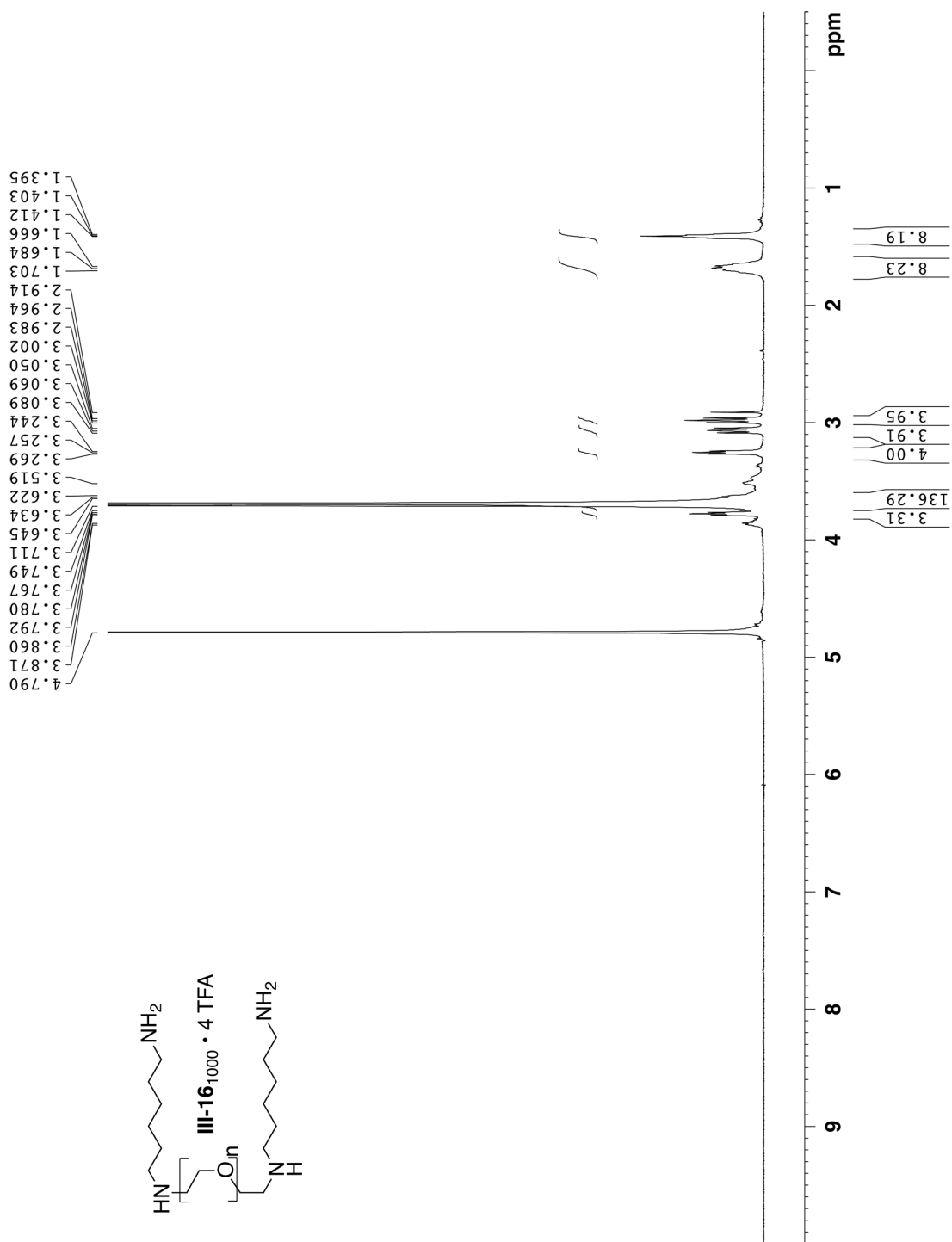


Figure III-S11. ¹H NMR spectra (400 MHz, D₂O, RT) recorded for **III-16**₁₀₀₀ • 4 TFA.

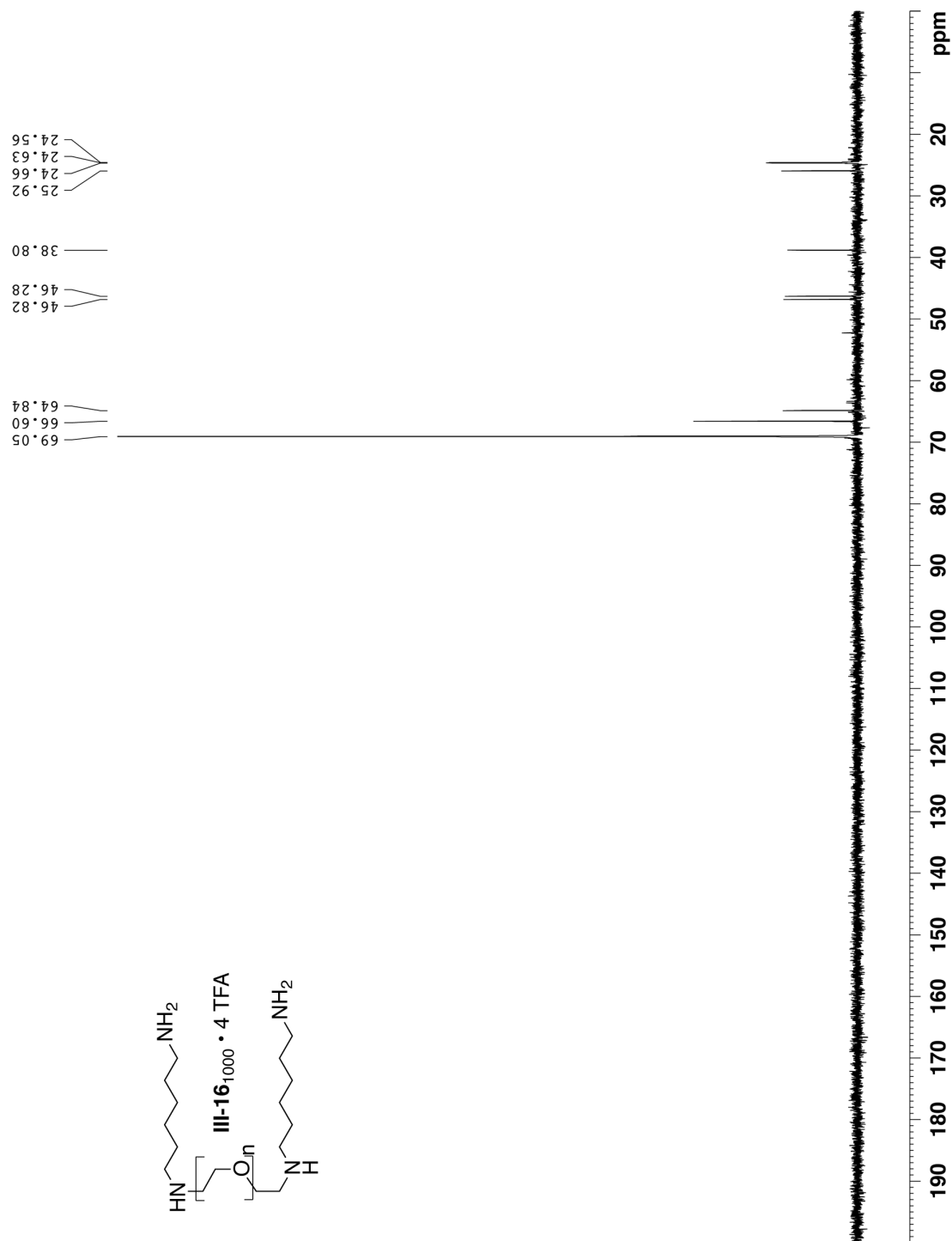


Figure III-S12. ¹³C NMR spectra (125 MHz, D₂O, RT, 1,4-dioxane as external standard) recorded for **III-16**₁₀₀₀ • 4 TFA.

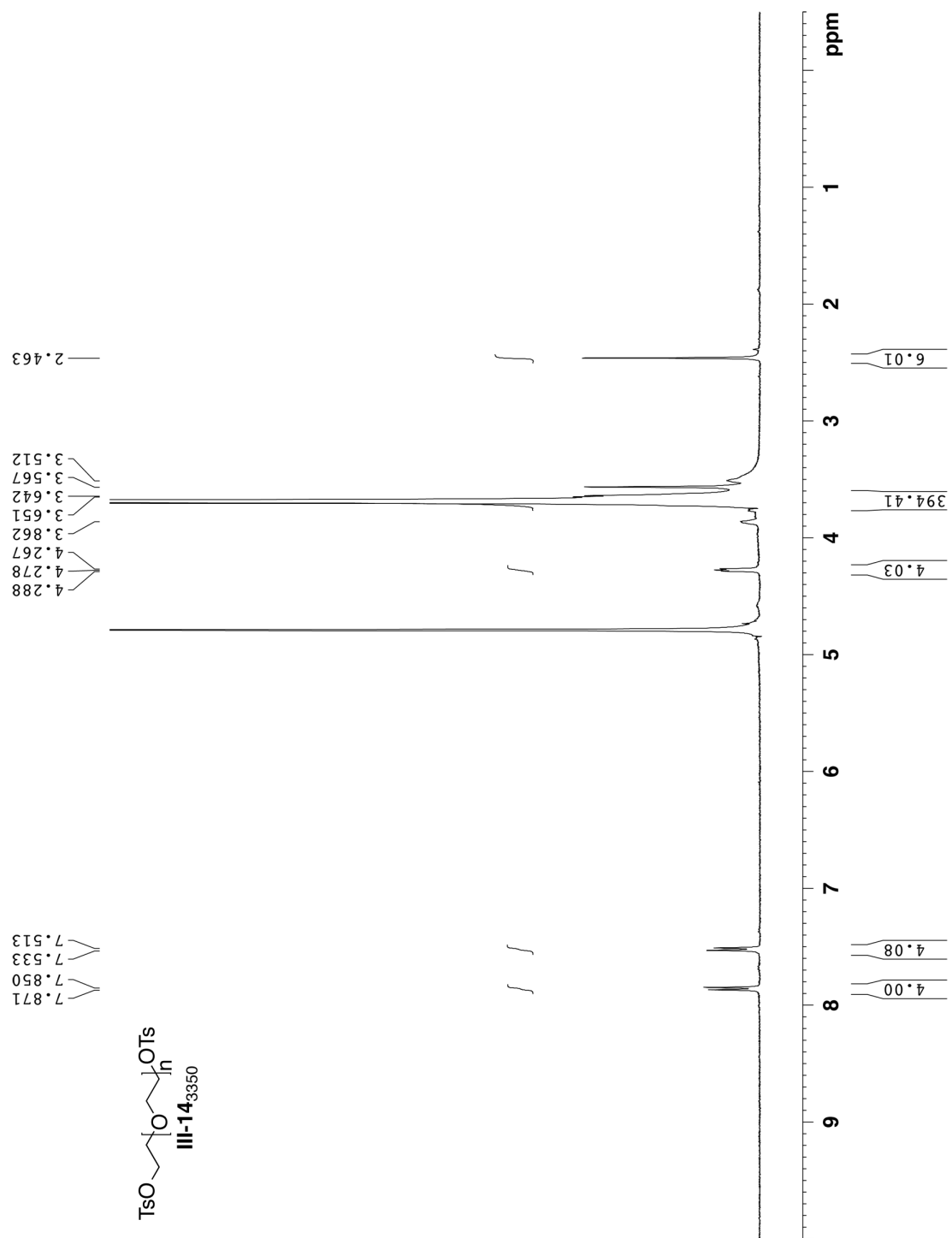


Figure III-S13. ¹H NMR spectra (400 MHz, D₂O, RT) recorded for **III-14₃₃₅₀**.

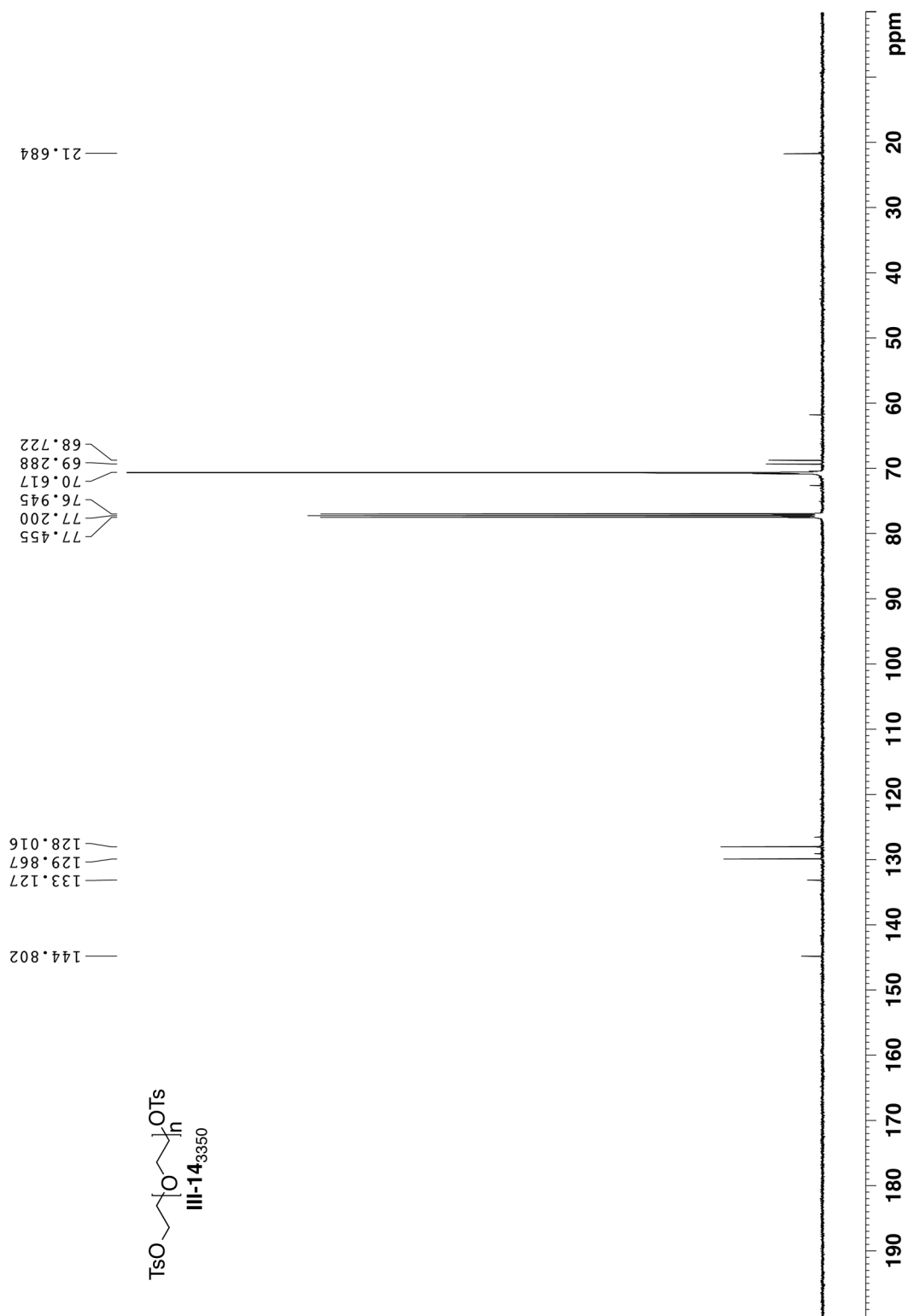


Figure III-S14. ¹³C NMR spectra (125 MHz, CDCl₃, RT) recorded for **III-14**₃₃₅₀.

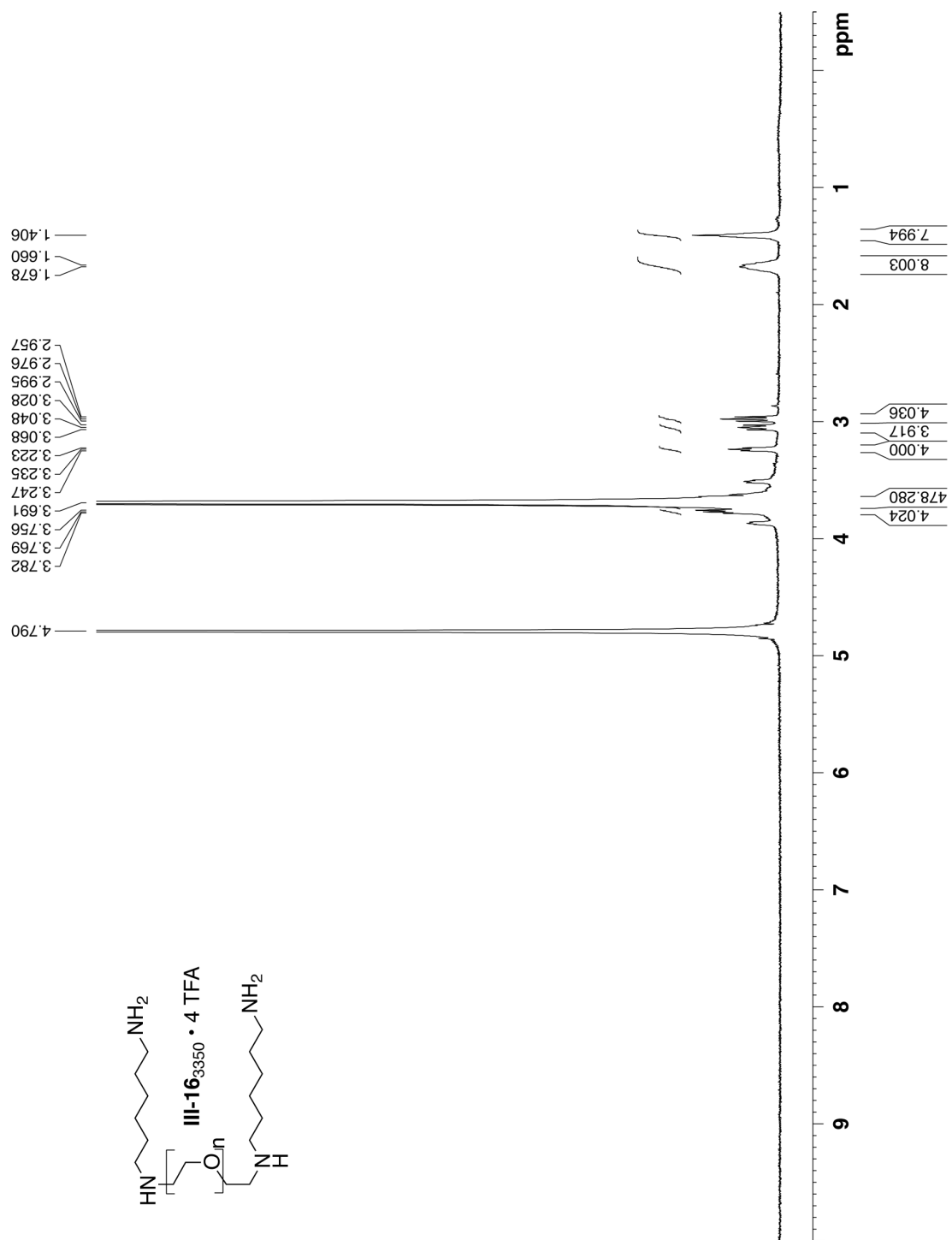


Figure III-S15. ^1H NMR spectra (400 MHz, D_2O , RT) recorded for **III-16₃₃₅₀ • 4 TFA**.

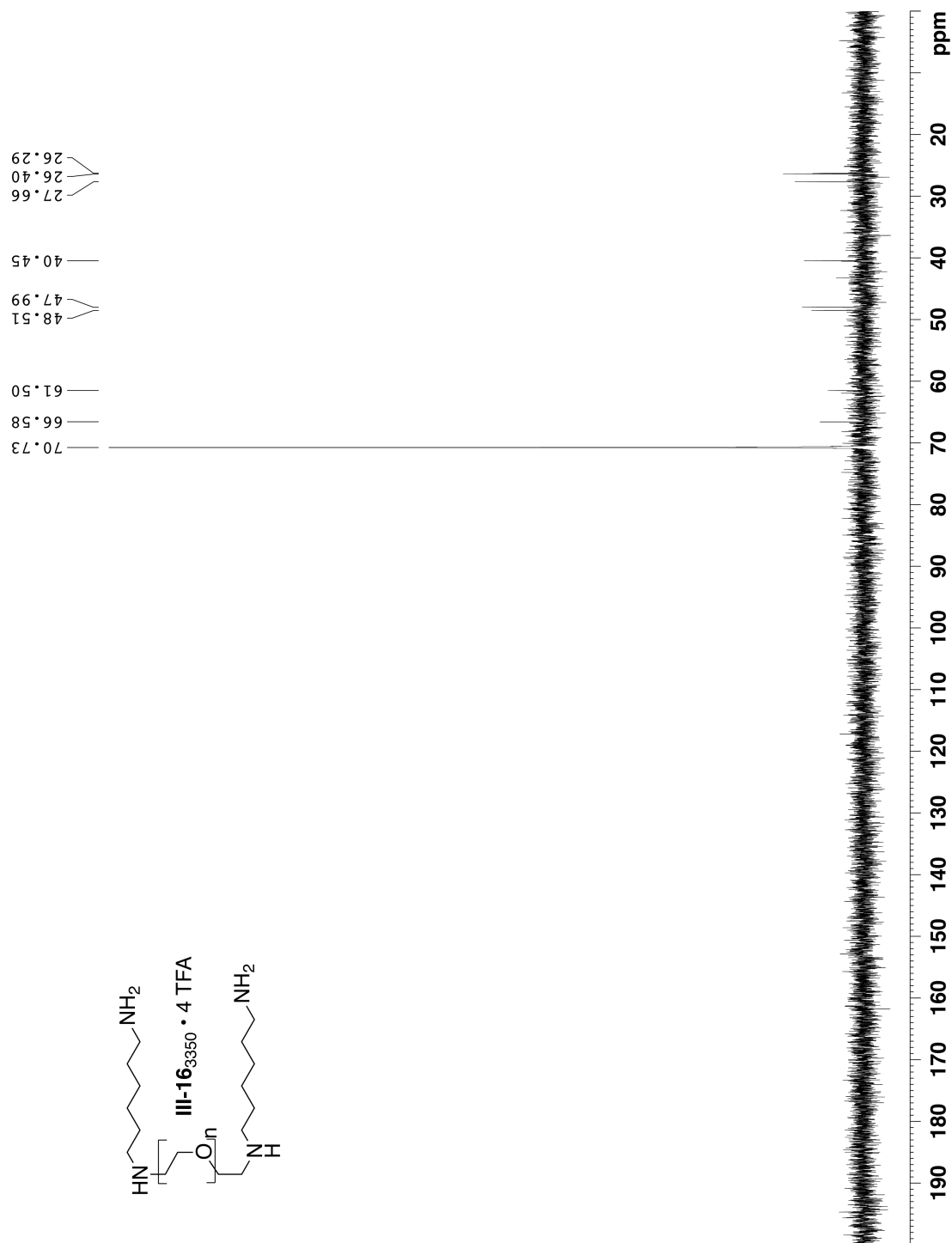


Figure III-S16. ¹³C NMR spectra (125 MHz, D₂O, RT, 1,4-dioxane as external standard) recorded for **III-16**₃₃₅₀ • 4 TFA.

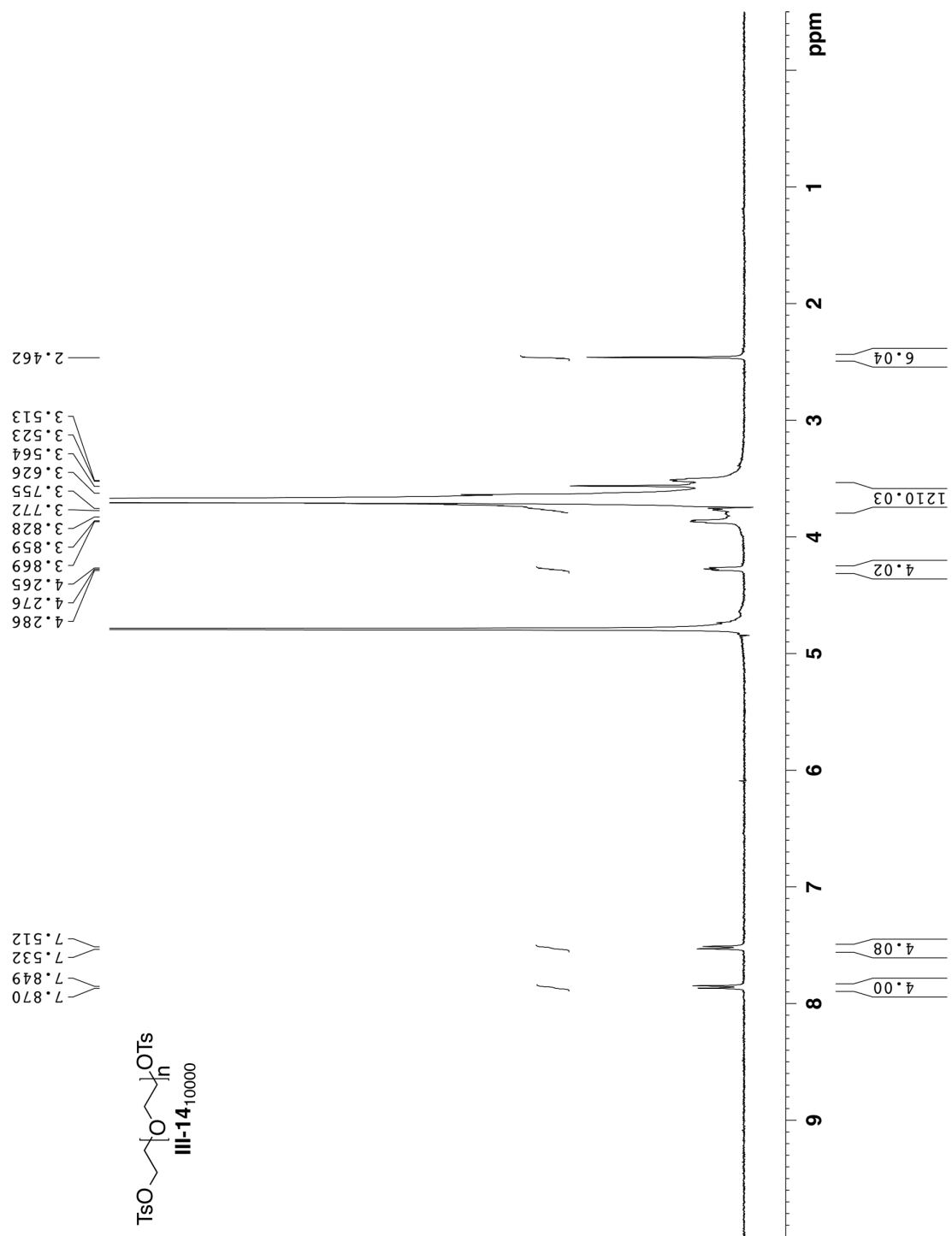


Figure III-S17. ¹H NMR spectra (400 MHz, D₂O, RT) recorded **III-14₁₀₀₀₀**.

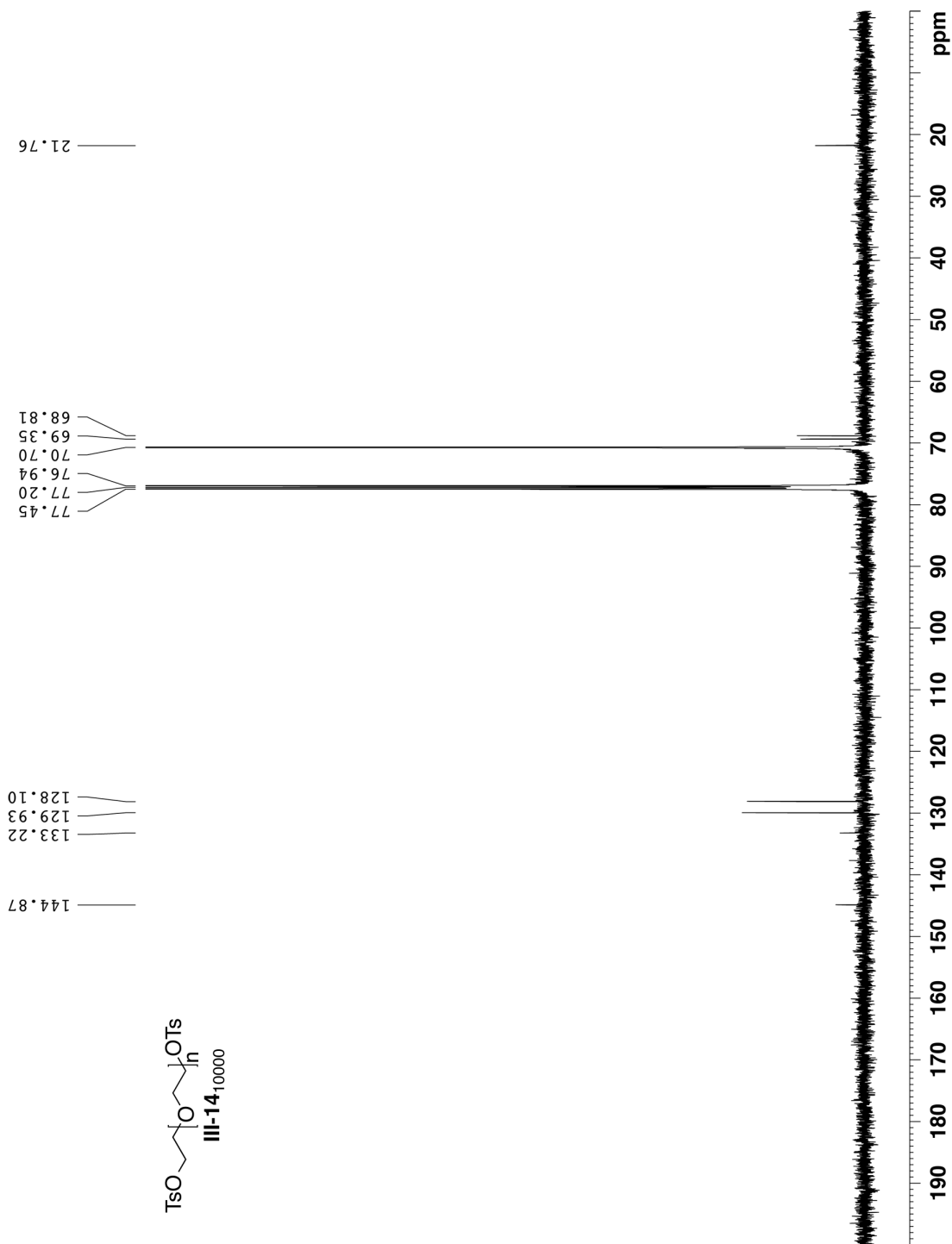


Figure III-S18. ¹³C NMR spectra (125 MHz, CDCl₃, RT) recorded for **III-14₁₀₀₀₀**.

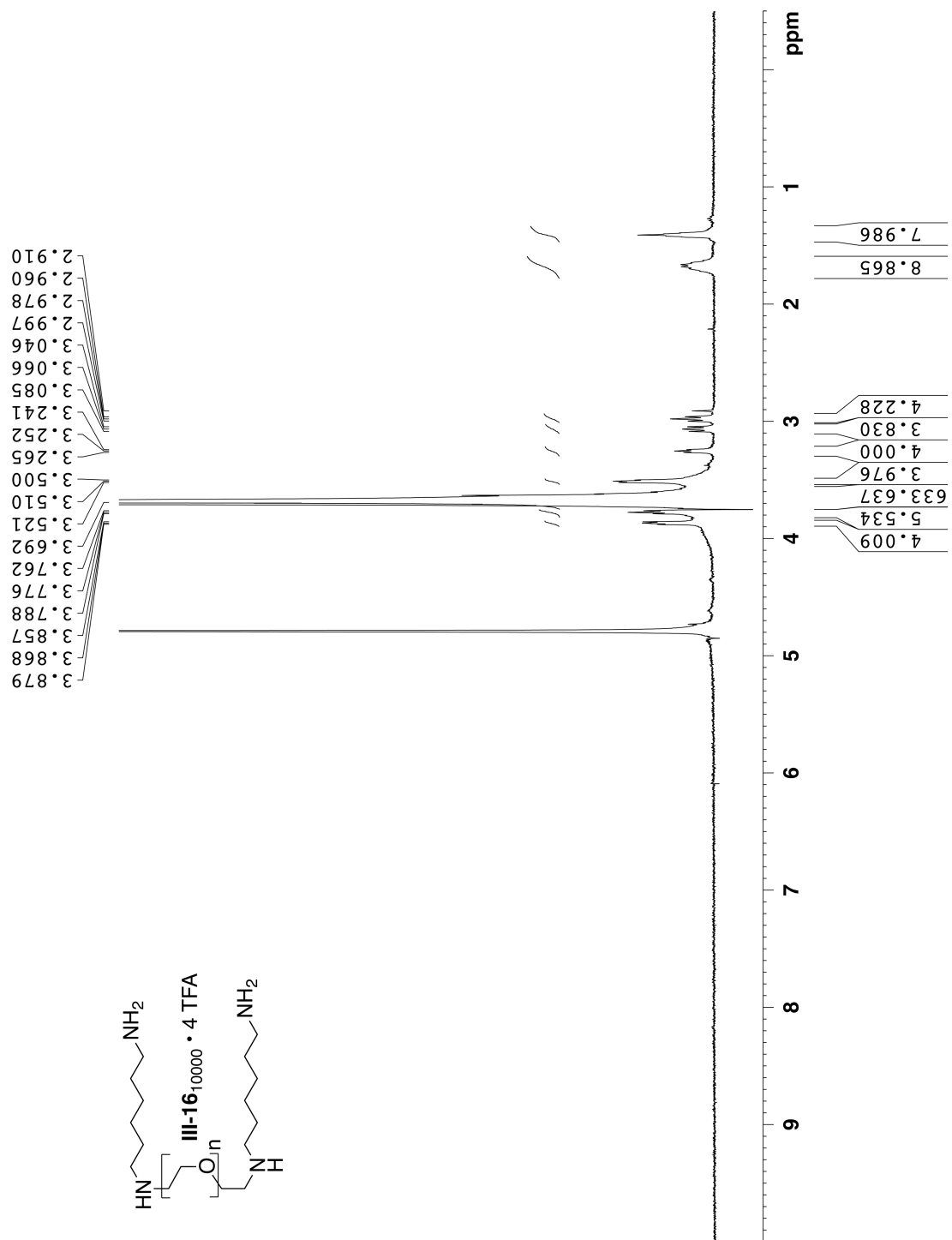


Figure III-S19. ¹H NMR spectra (400 MHz, D₂O, RT) recorded for III-16₁₀₀₀₀ • 4 TFA.

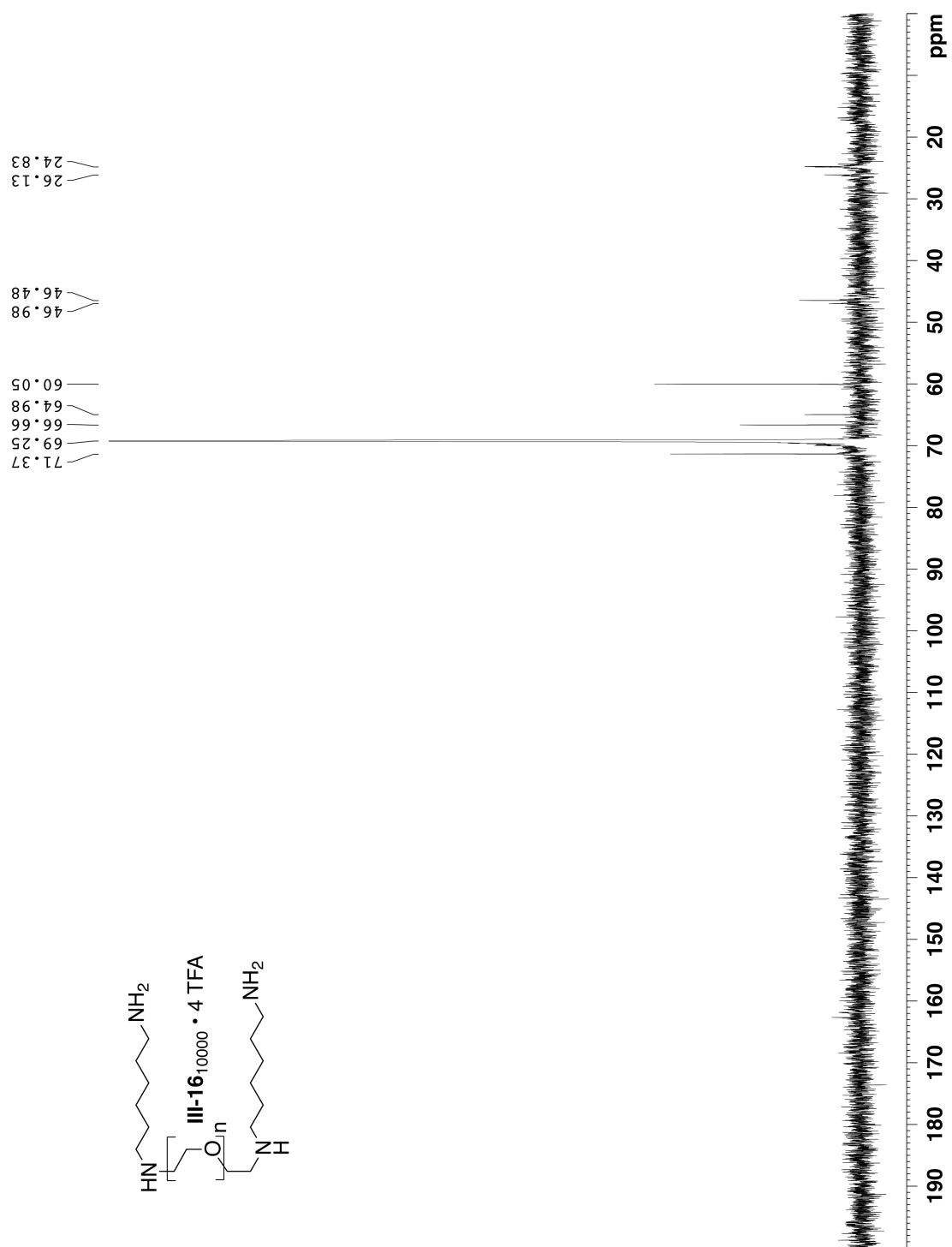


Figure III-S20. ¹³C NMR spectra (125 MHz, D₂O, RT, 1,4-dioxane as external standard) recorded for **III-16**₁₀₀₀₀ • 4 TFA.

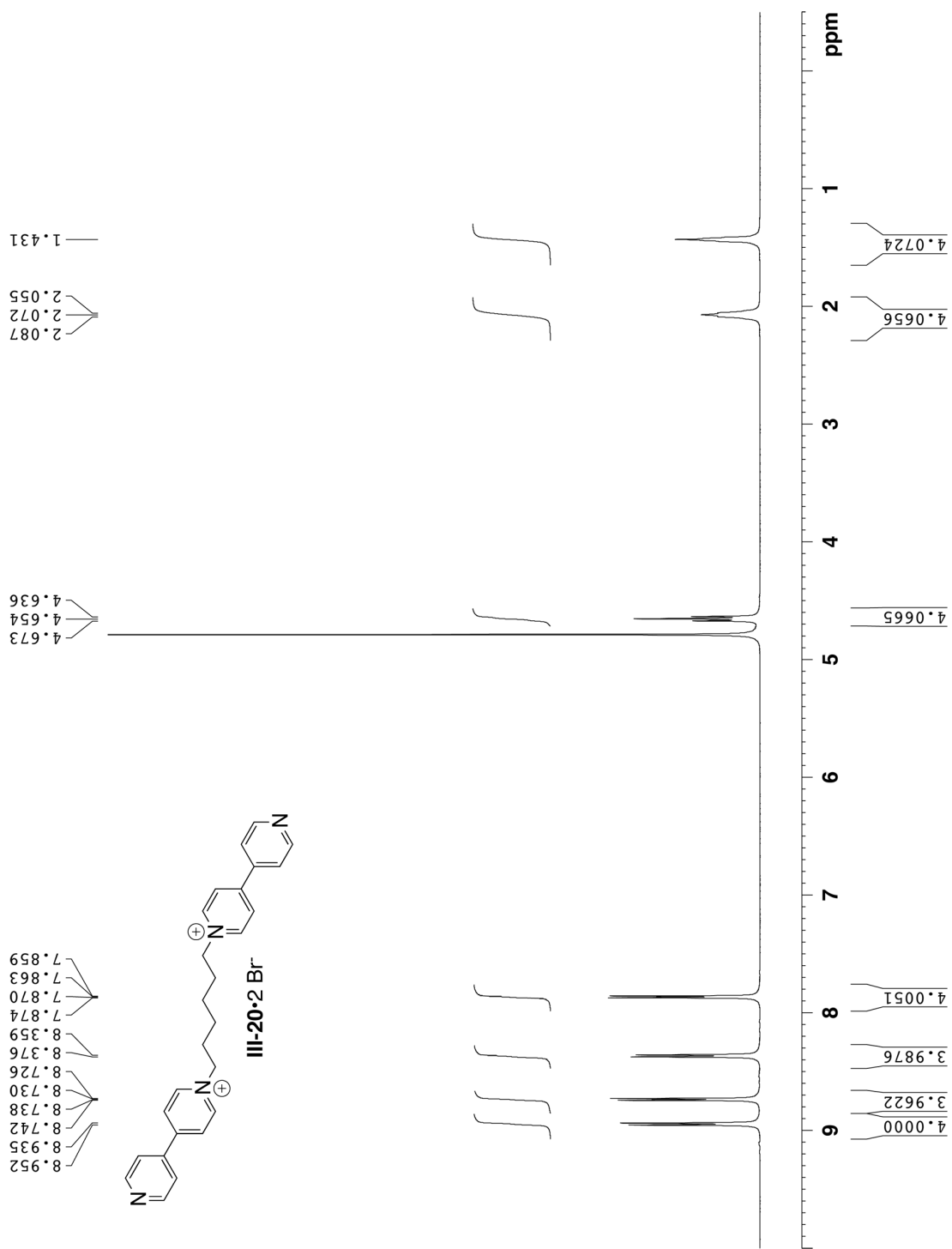


Figure III-S21. ¹H NMR spectrum (400 MHz, D₂O, RT) recorded for compound **III-20 • 2 Br⁻**.

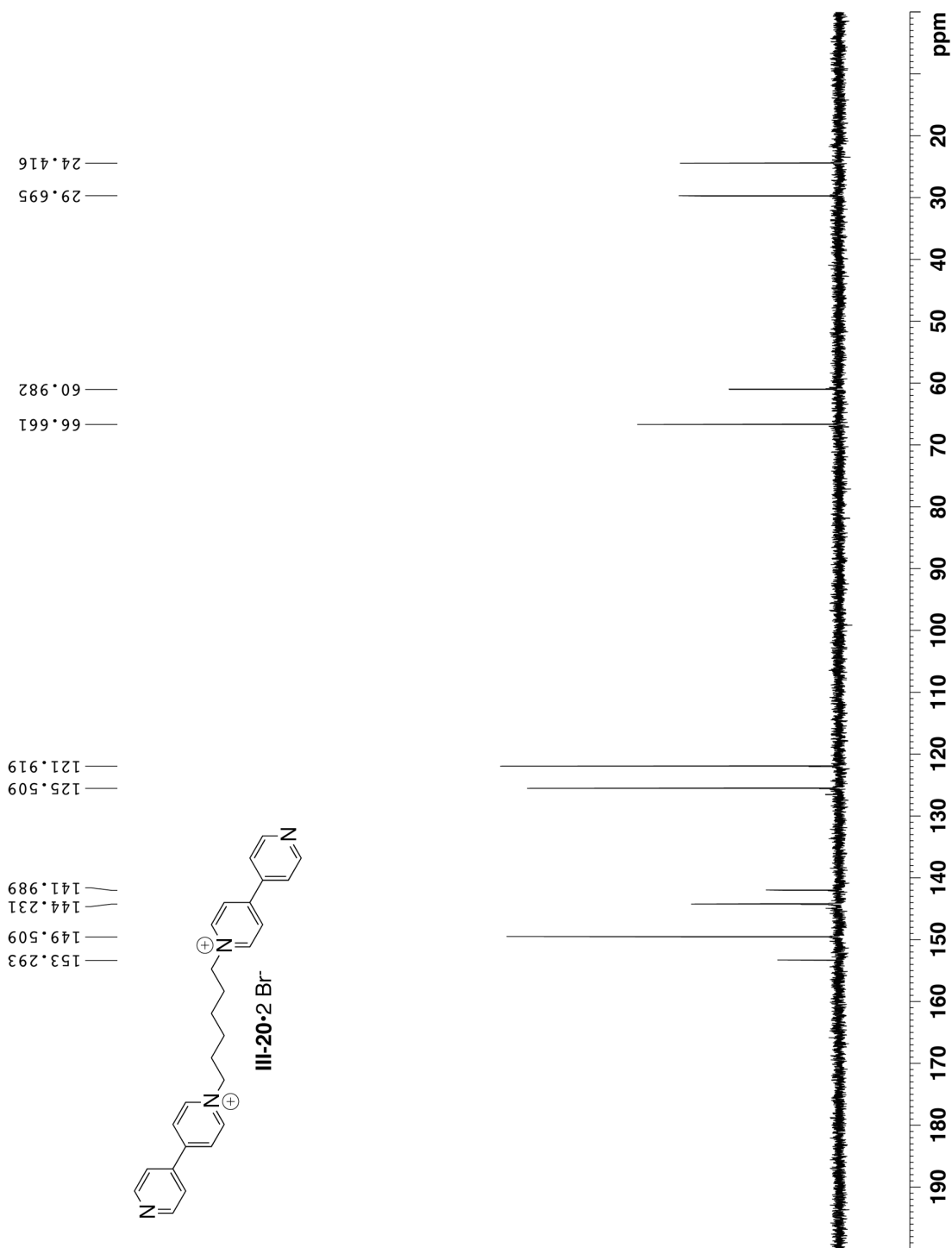


Figure III-S22. ^{13}C NMR spectrum (125 MHz, D_2O , RT, 1,4-dioxane as external standard) recorded for compound **III-20** • 2 Br^- .

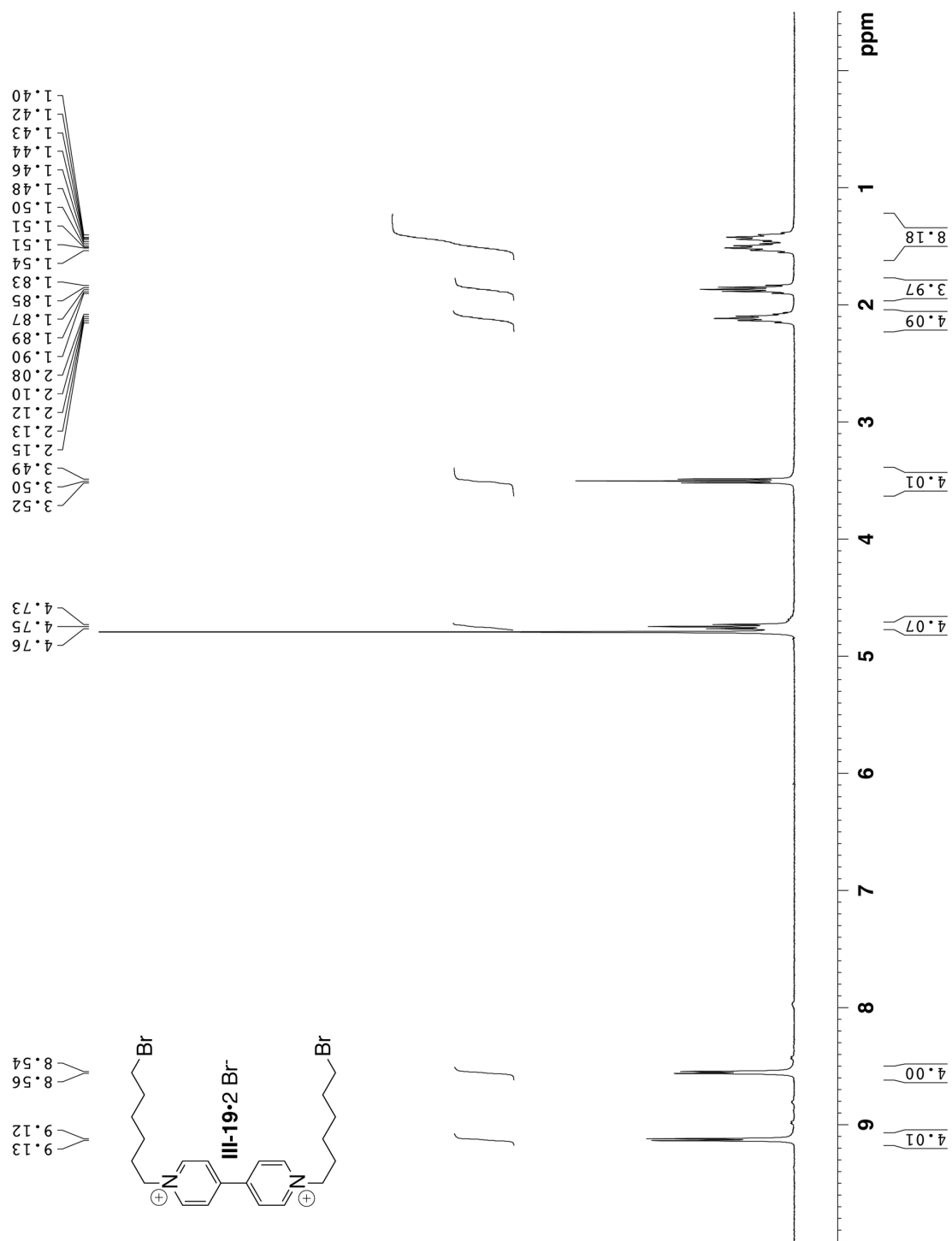


Figure III-S23. ¹H NMR spectrum (400 MHz, D₂O, RT) recorded for compound **III-19 • 2 Br⁻**.

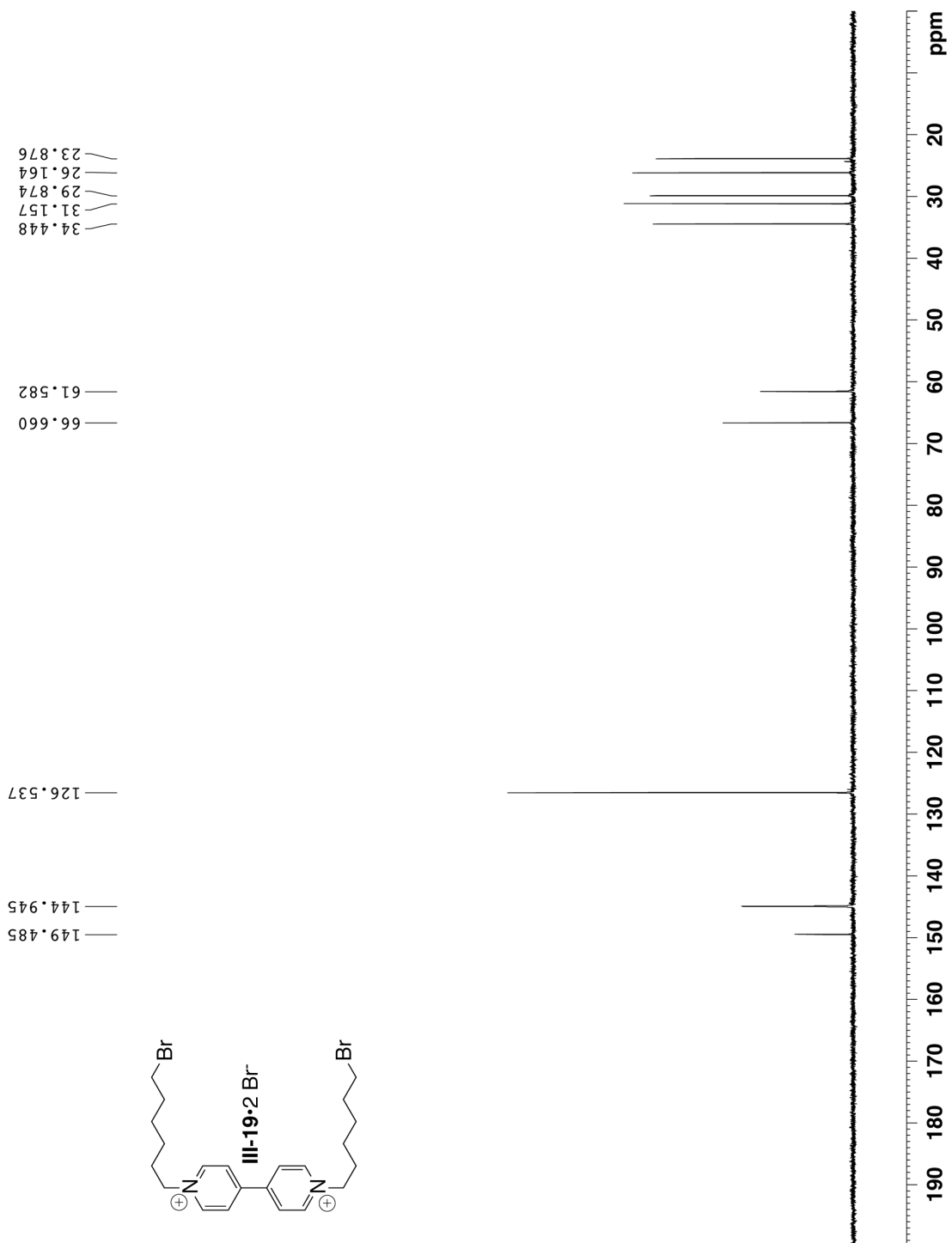


Figure III-S24. ¹³C NMR spectrum (125 MHz, D₂O, RT, 1,4-dioxane as external standard) recorded for compound **III-19 • 2 Br⁻**.

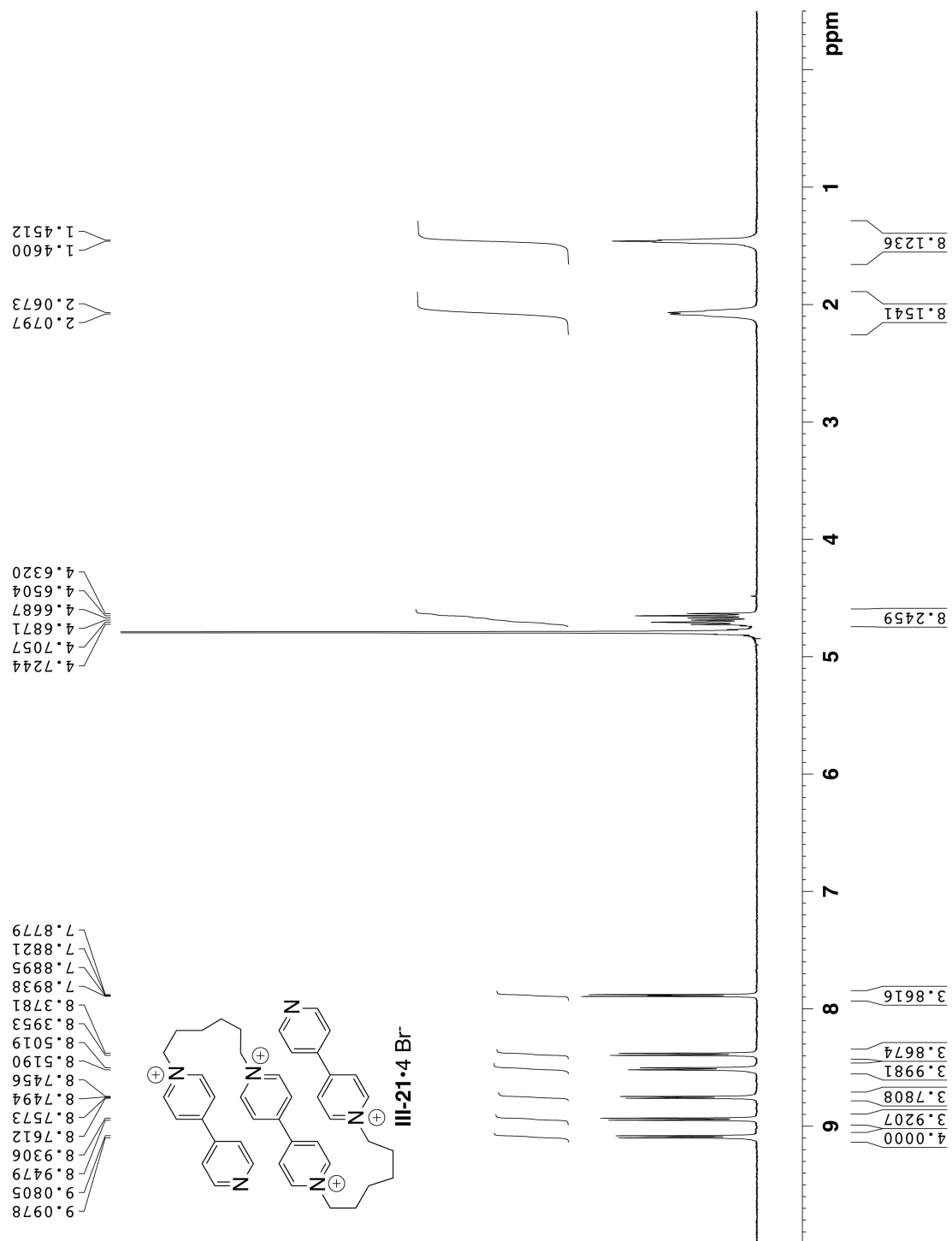


Figure III-S25. ^1H NMR spectrum (400 MHz, D_2O , RT) recorded for compound **III-21** • 4 Br^- .

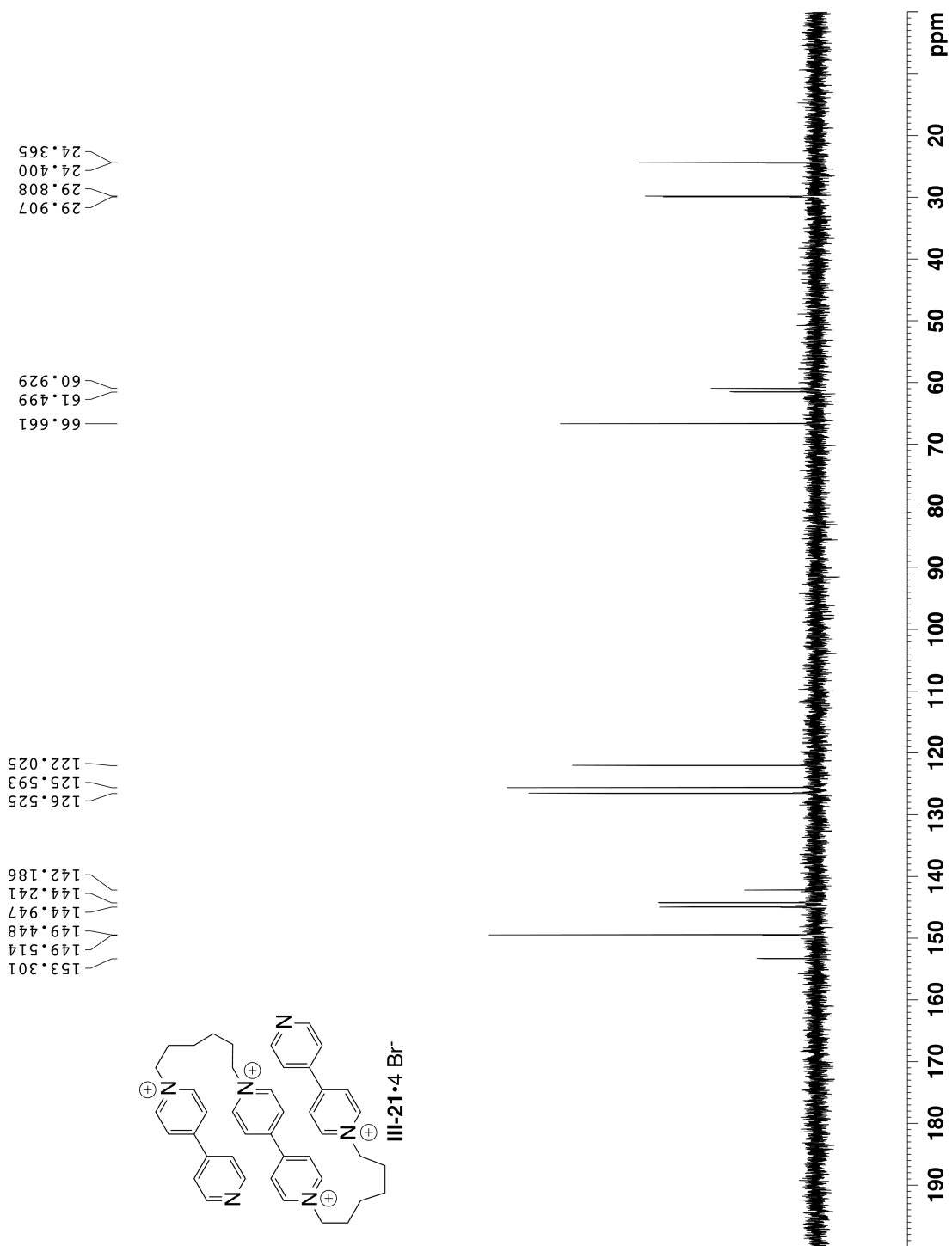


Figure III-S26. ¹³C NMR spectrum (125 MHz, D₂O, RT, 1,4-dioxane as external standard) recorded for compound **III-21 • 4 Br⁻**.

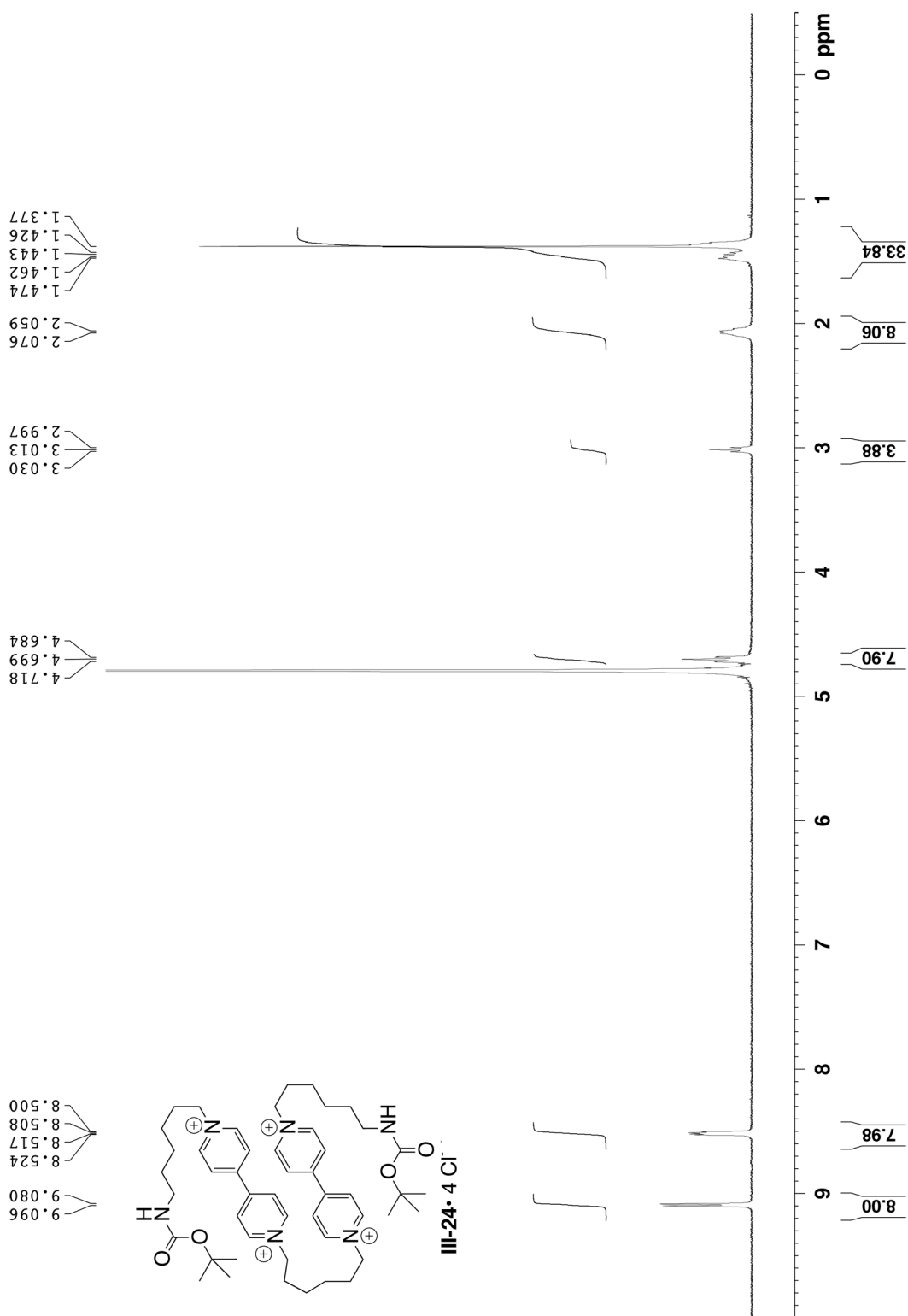


Figure III-S27. ^1H NMR spectra (400 MHz, D_2O , RT) recorded for compound **III-24** • 4 Cl⁻.

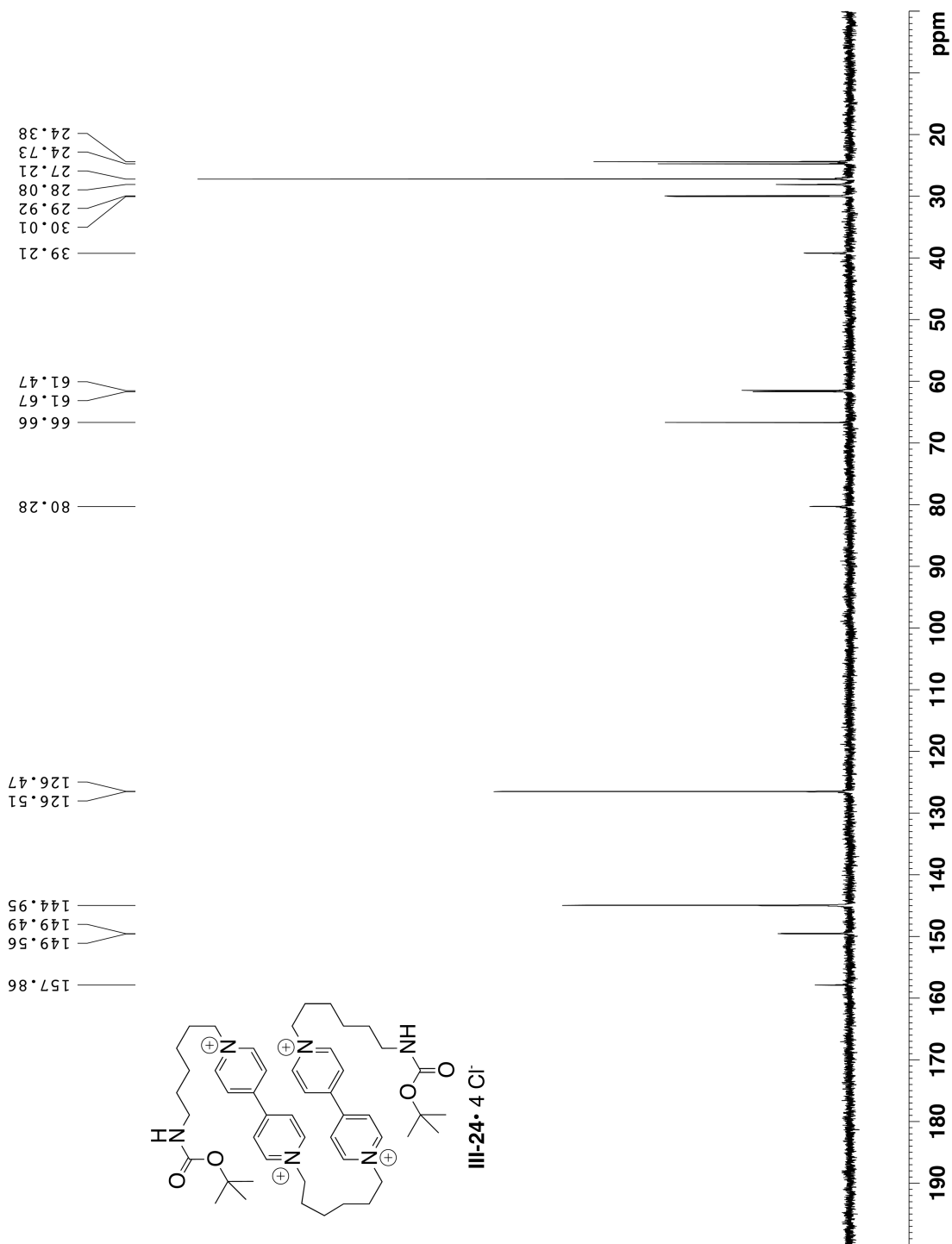


Figure III-S28. ^{13}C NMR spectrum (125 MHz, D_2O , RT, 1,4-dioxane as external standard) recorded for compound **III-24** • 4 Cl⁻.

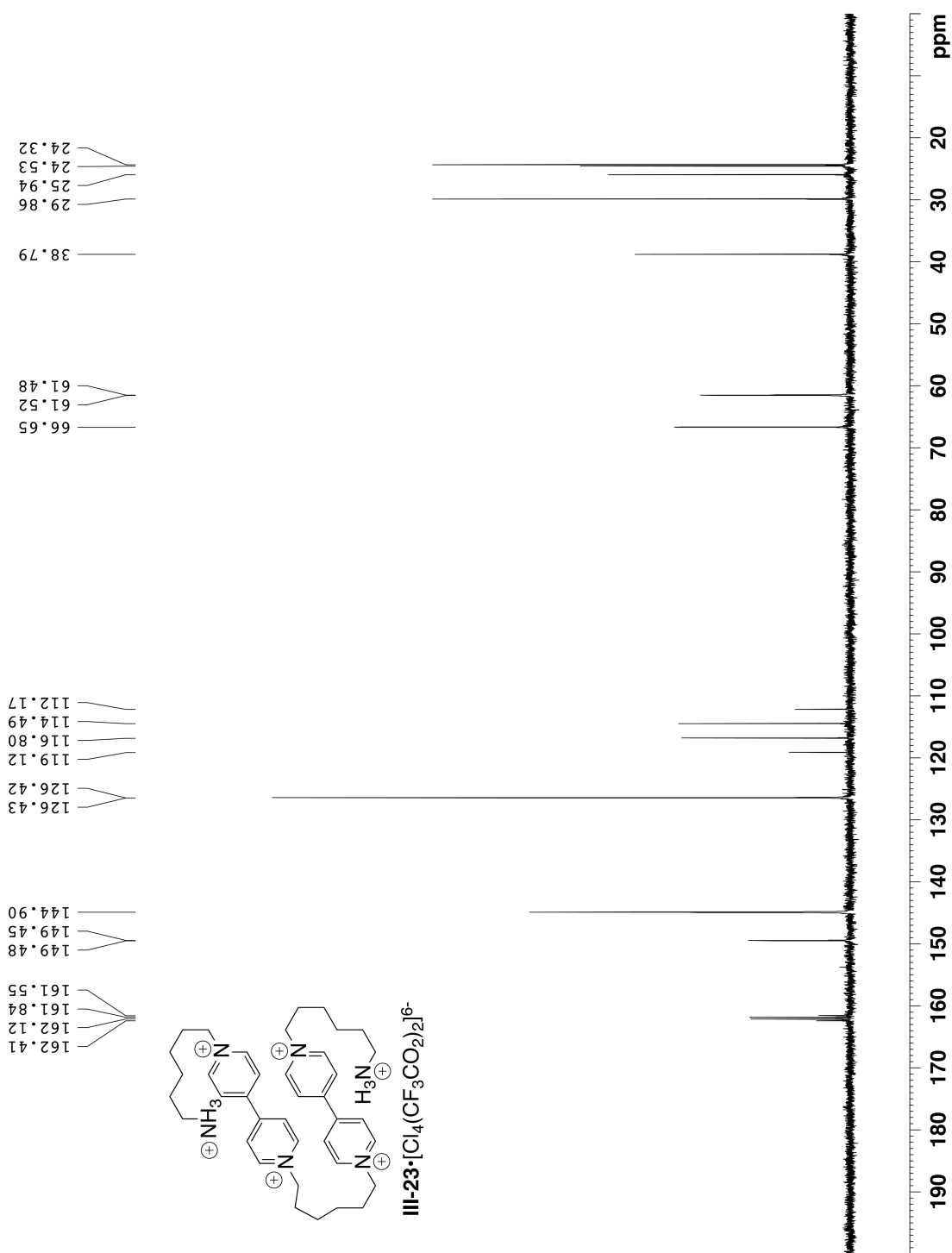


Figure III-S30. ^{13}C NMR spectrum (125 MHz, D_2O , RT, 1,4-dioxane as external standard) recorded for compound **III-22** • $\text{Cl}_4(\text{CF}_3\text{CO}_2)_2^{6-}$.

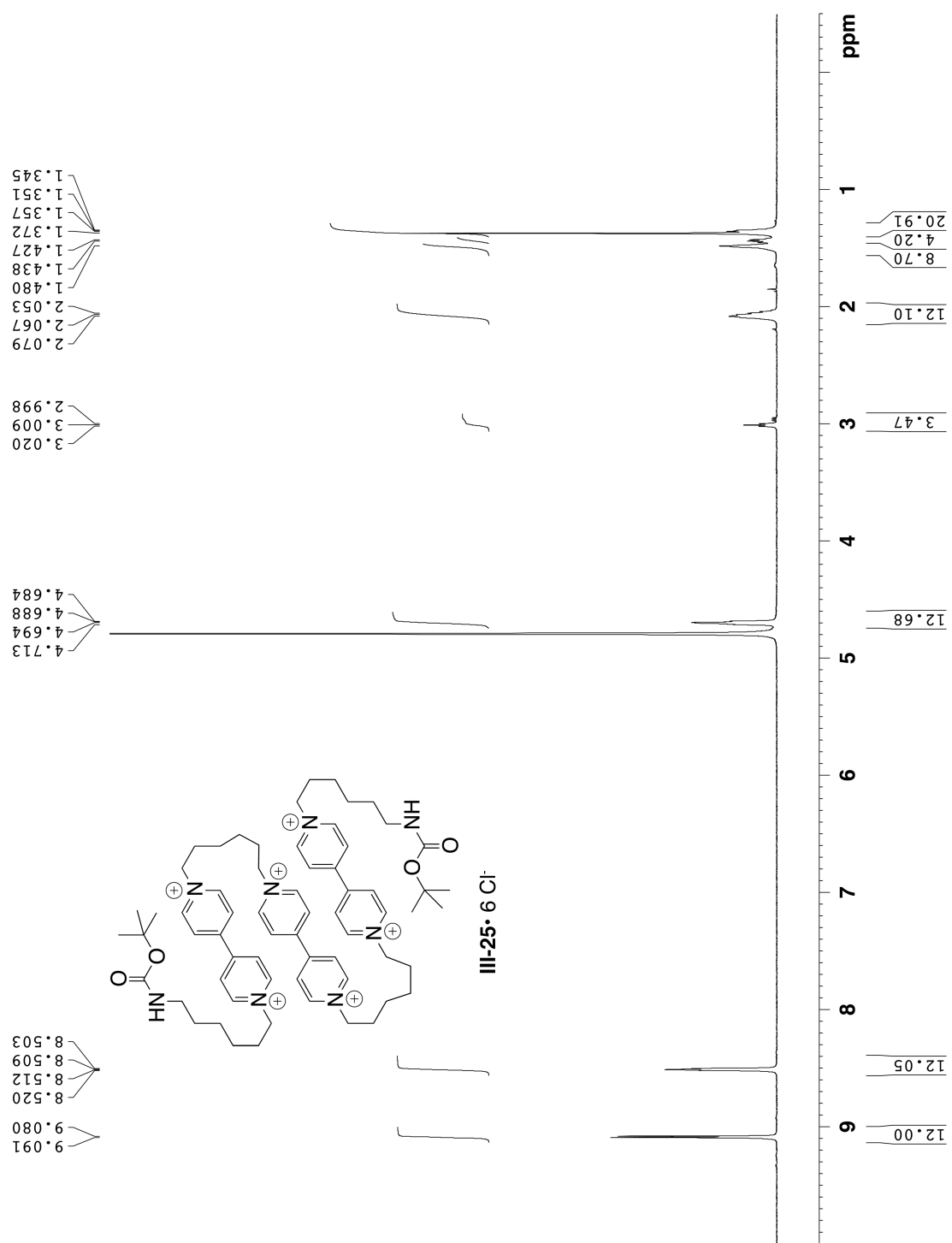


Figure III-S31. ¹H NMR spectra (400 MHz, D₂O, RT) recorded for **III-25 • 6 Cl⁻**.

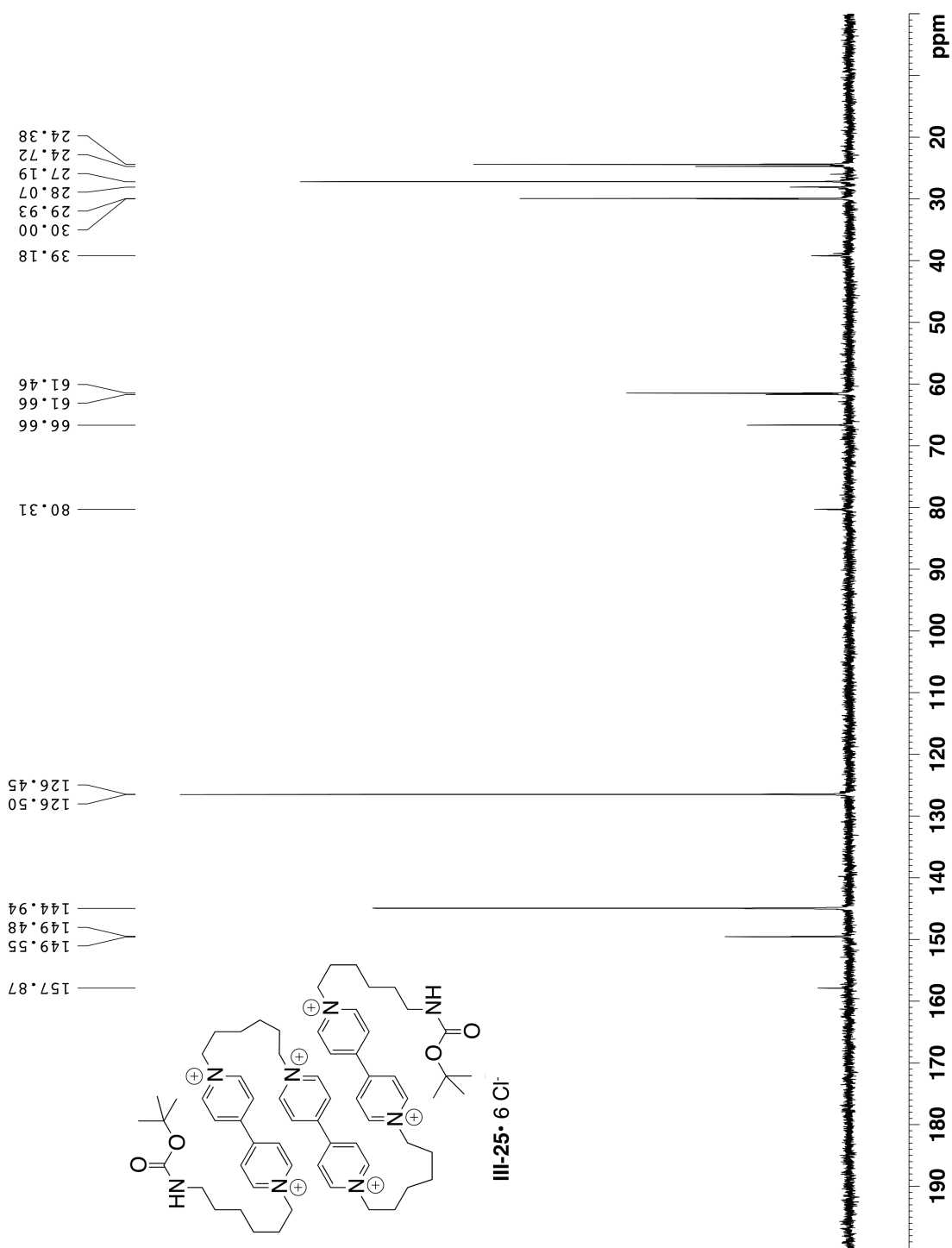


Figure III-S32. ^{13}C NMR spectrum (125 MHz, D_2O , RT, 1,4-dioxane as external standard) recorded for compound **III-25** • 6 Cl^- .

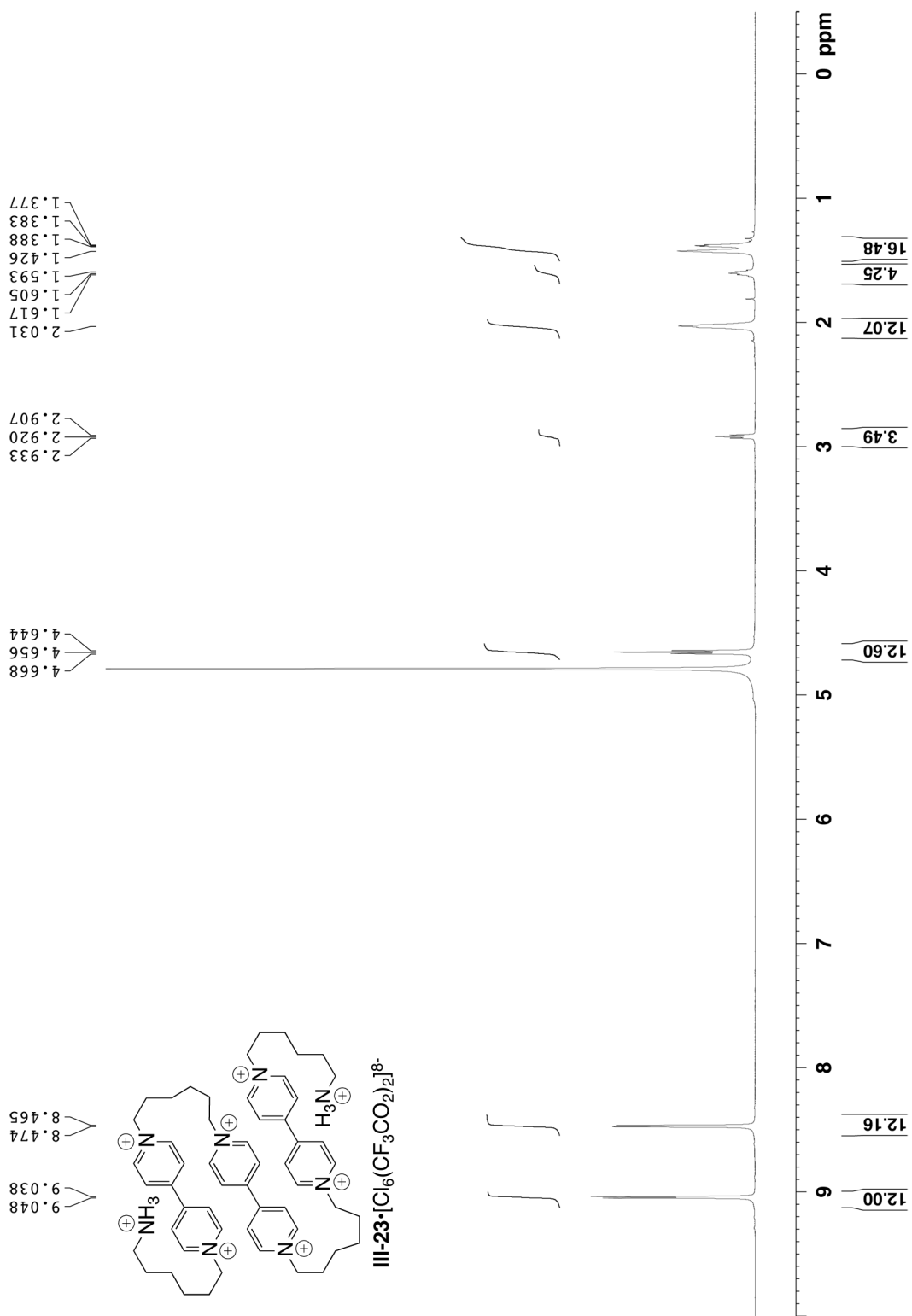


Figure III-S33. ^1H NMR spectra (400 MHz, D_2O , RT) recorded for compound **III-23**· $\text{Cl}_6(\text{CF}_3\text{CO}_2)_2^{8-}$.

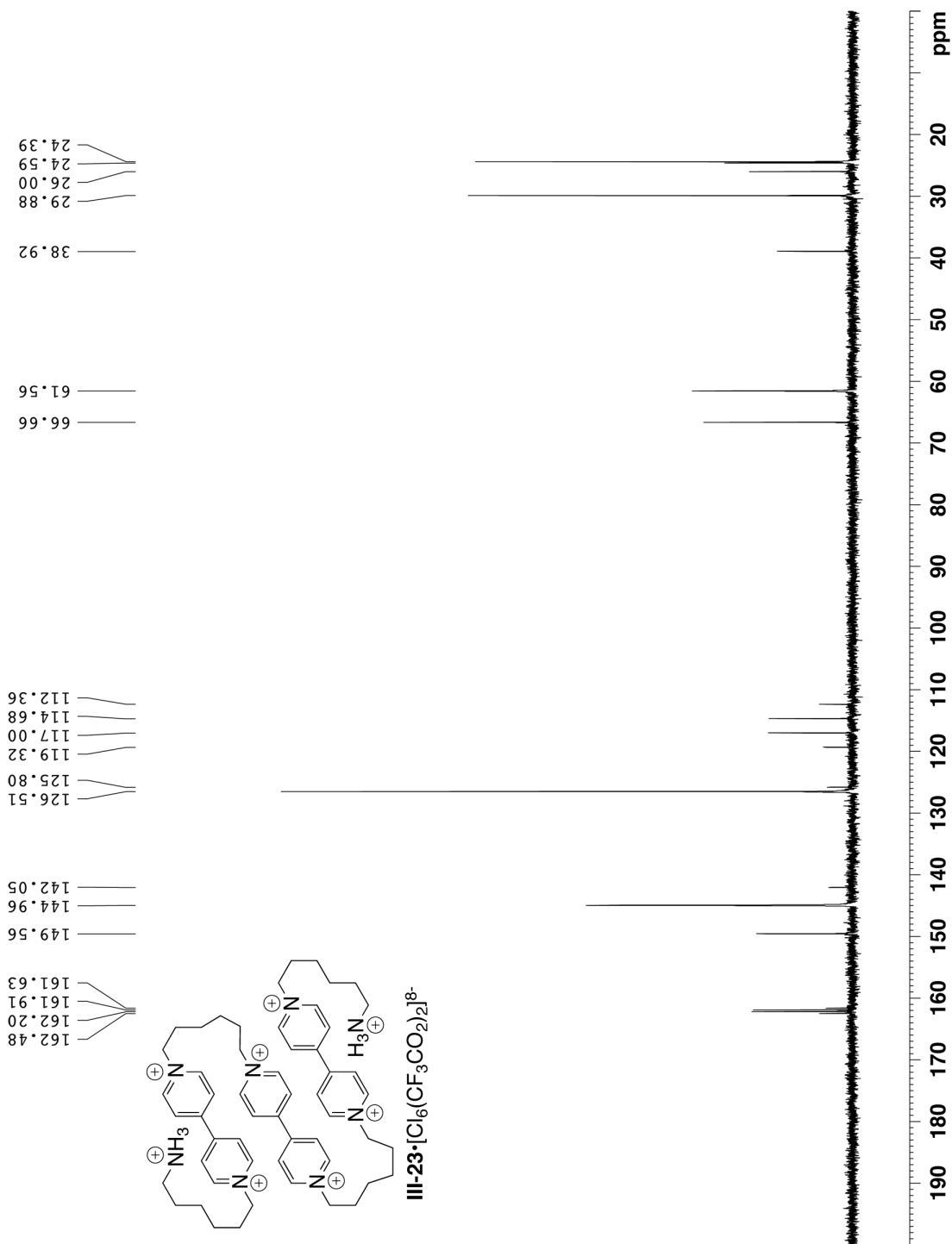


Figure III-S34. ^{13}C NMR spectrum (125 MHz, D_2O , RT, 1,4-dioxane as external standard) recorded for compound **III-23** • $\text{Cl}_6(\text{CF}_3\text{CO}_2)_2^{8-}$.

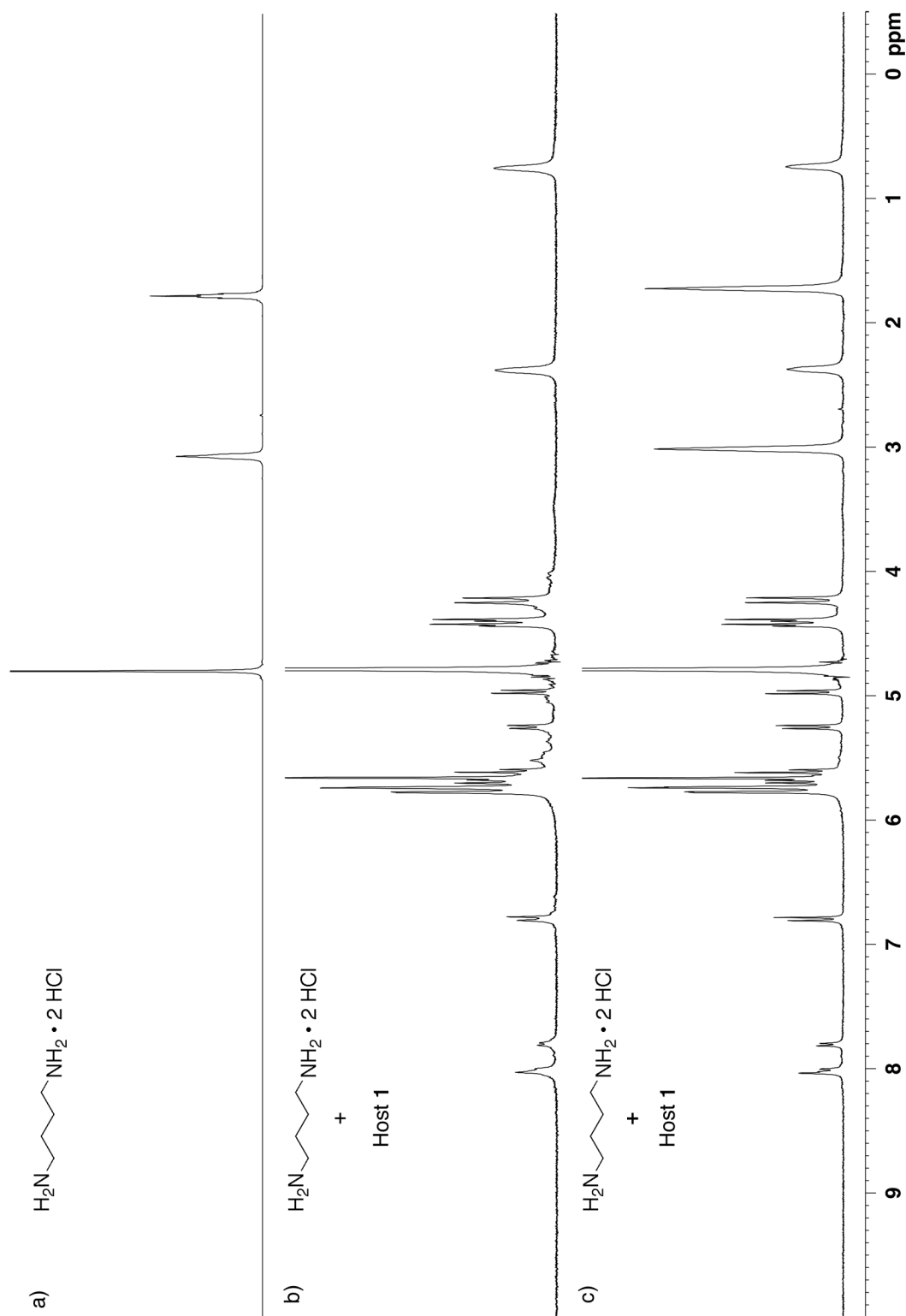


Figure III-S35. ^1H NMR spectra (400 MHz, D_2O , RT) recorded for: a) 1,4-butanediamine dihydrochloride, b) a mixture of 1,4-butanediamine dihydrochloride and **III-1** (2:1 ratio), and c) a mixture of 1,4-butanediamine dihydrochloride and **III-1** (>2:1 ratio).

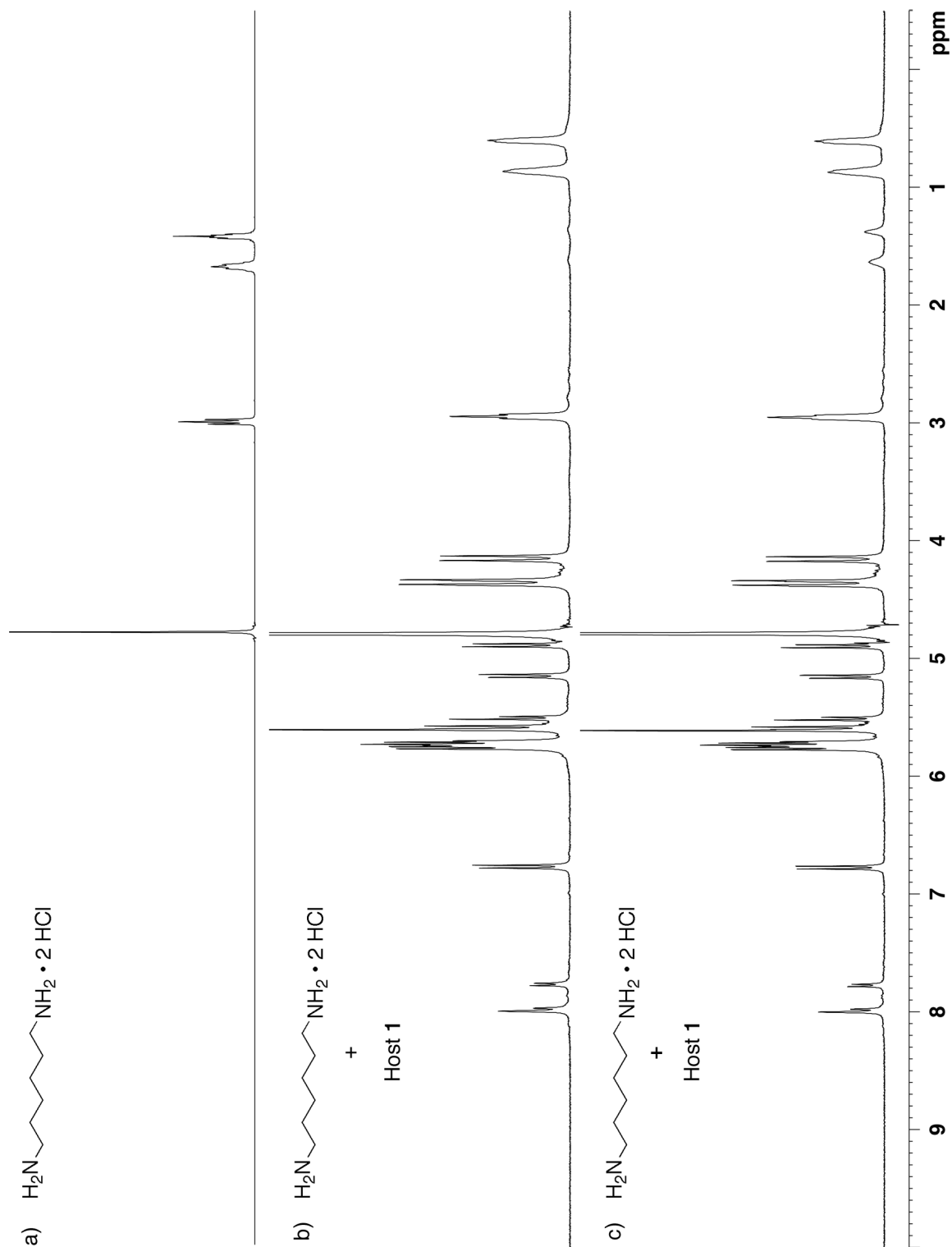


Figure III-S36. ^1H NMR spectra (400 MHz, D_2O , RT) recorded for: a) 1,6-hexanediamine dihydrochloride, b) a mixture of 1,6-hexanediamine dihydrochloride and **III-1** (2:1 ratio), and c) a mixture of 1,6-hexanediamine dihydrochloride and **III-1** (>2:1 ratio).

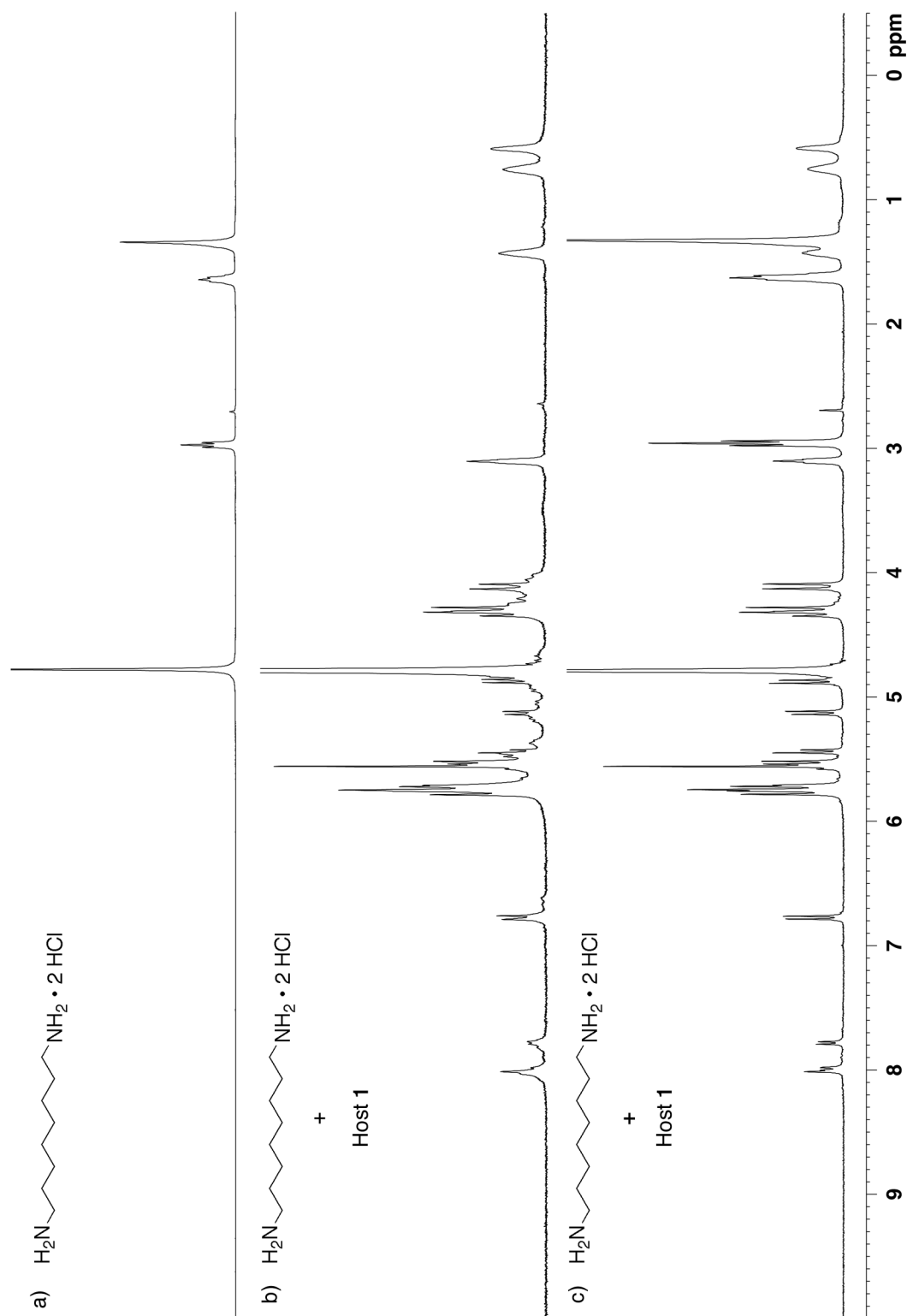


Figure III-S37. ^1H NMR spectra (400 MHz, D_2O , RT) recorded for: a) 1,8-octanediamine dihydrochloride, b) a mixture of 1,8-octanediamine dihydrochloride and **III-1** (2:1 ratio), and c) a mixture of 1,8-octanediamine dihydrochloride and **III-1** (>2:1 ratio).

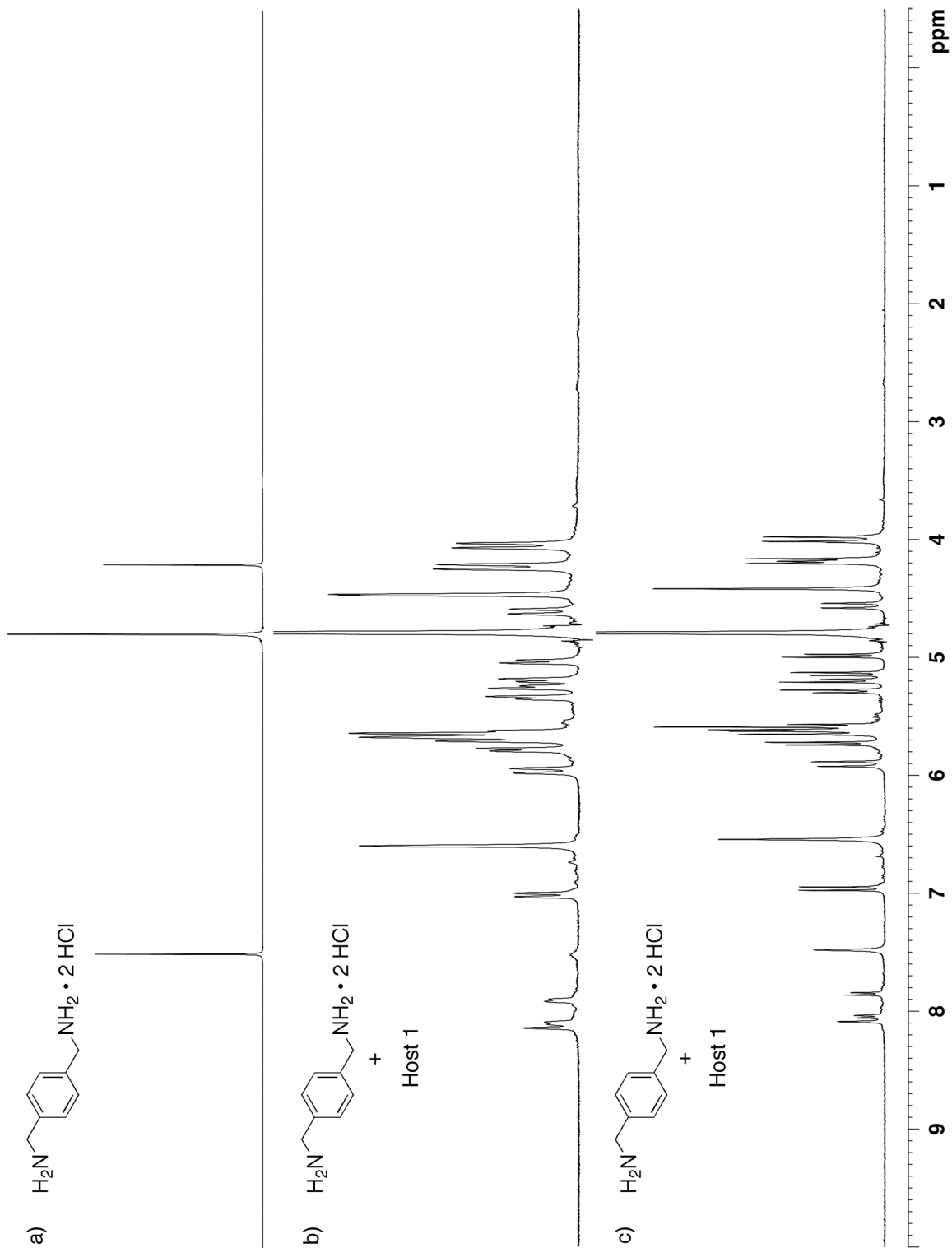


Figure III-S38. ^1H NMR spectra (400 MHz, D_2O , RT) recorded for: a) p -xylenediamine dihydrochloride, b) a mixture of p -xylenediamine dihydrochloride and **III-1** (2:1 ratio), and c) a mixture of p -xylenediamine dihydrochloride and **III-1** (>2:1 ratio).

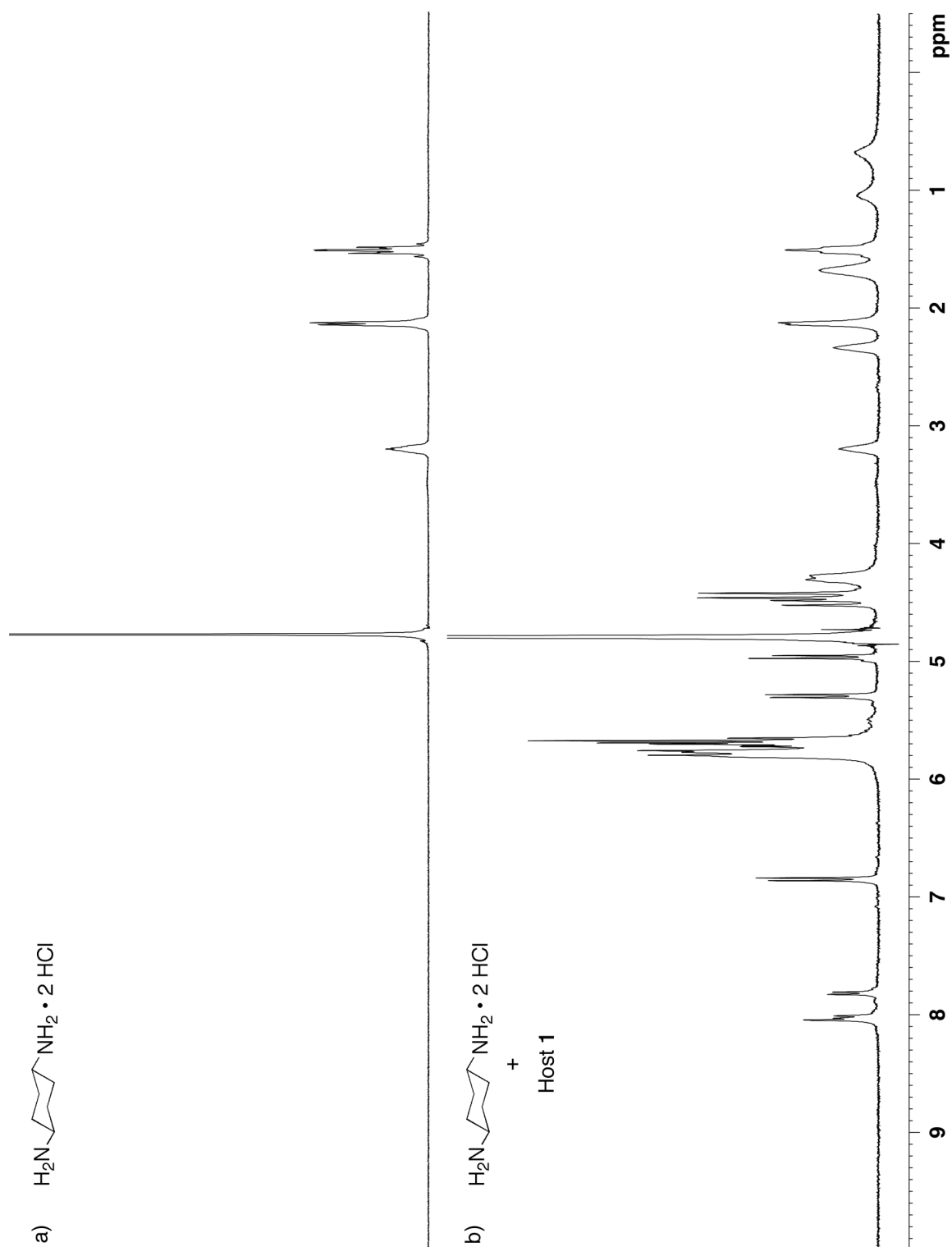


Figure III-S39. ^1H NMR spectra (400 MHz, D_2O , RT) recorded for: a) 1,4-cyclohexanediamine dihydrochloride, and b) a mixture of 1,4-cyclohexanediamine dihydrochloride and **III-1** (2:1 ratio).

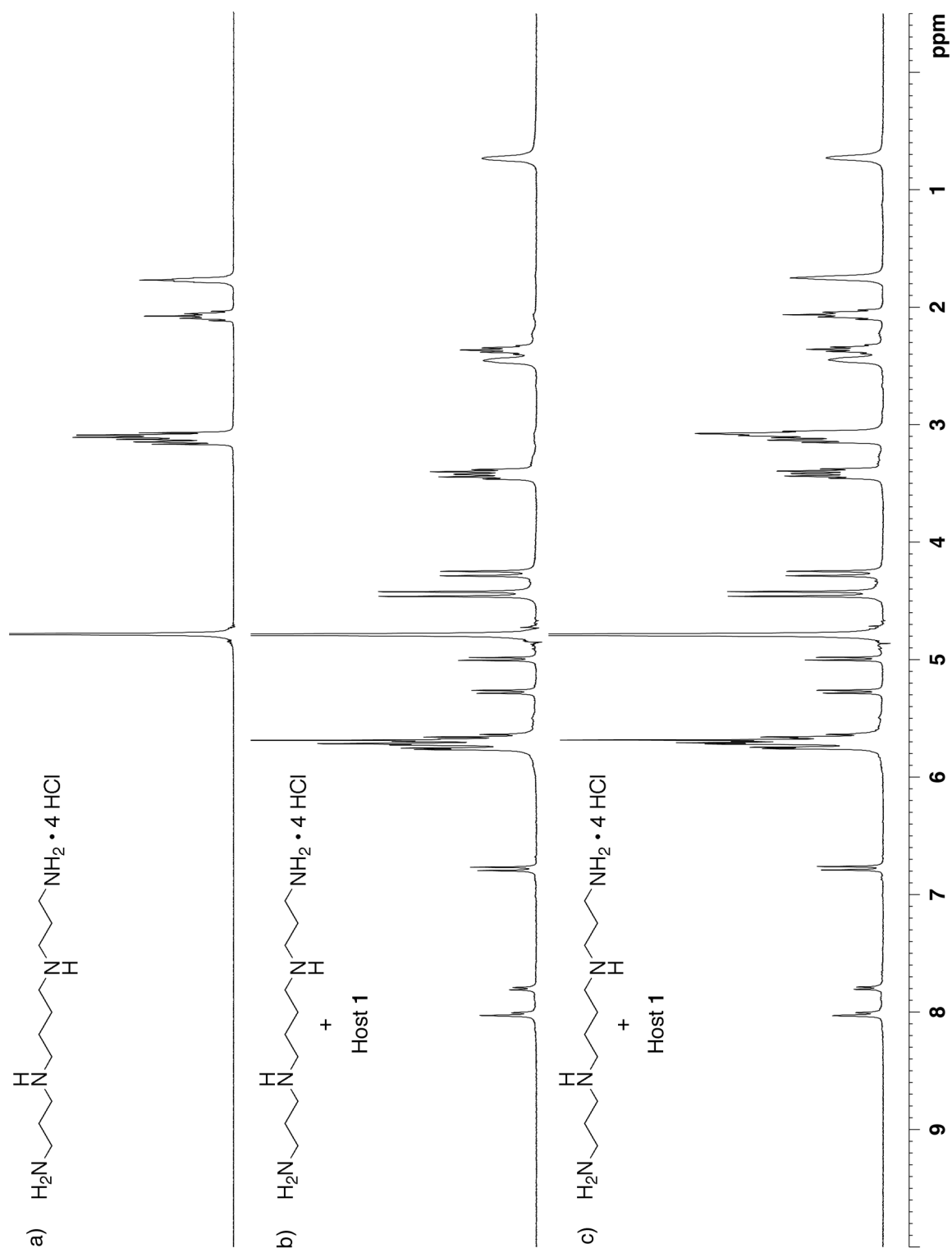


Figure III-S40. ^1H NMR spectra (400 MHz, D_2O , RT) recorded for: a) spermine tetrahydrochloride, b) a mixture of spermine tetrahydrochloride and **III-1** (2:1 ratio), and c) a mixture of spermine tetrahydrochloride and **III-1** (>2:1 ratio).

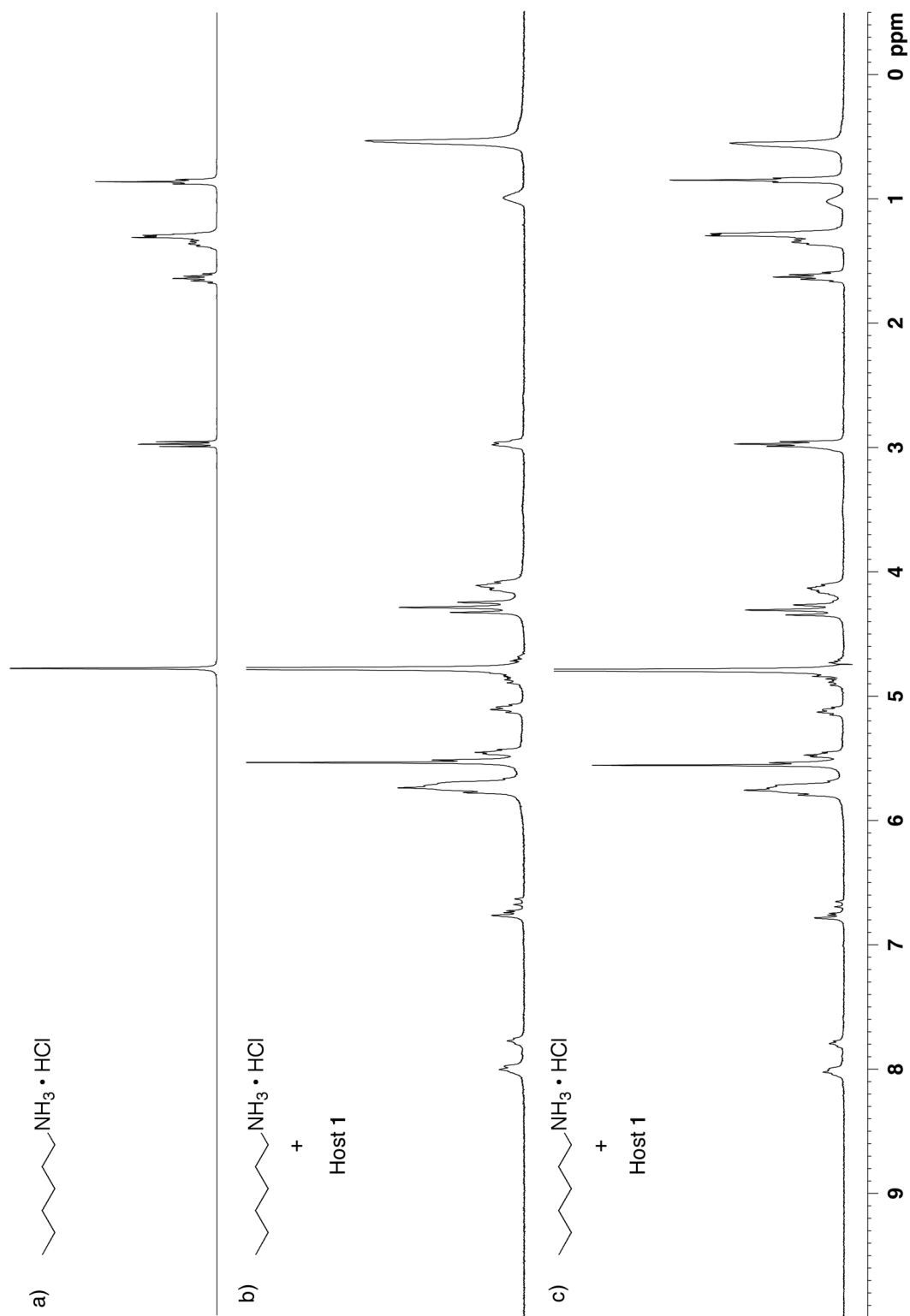


Figure III-S41. ^1H NMR spectra (400 MHz, D_2O , RT) recorded for: a) hexylamine hydrochloride, b) a mixture of hexylamine hydrochloride and **III-1** (2:1 ratio), and c) a mixture of hexylamine hydrochloride and **III-1** (>2:1 ratio).

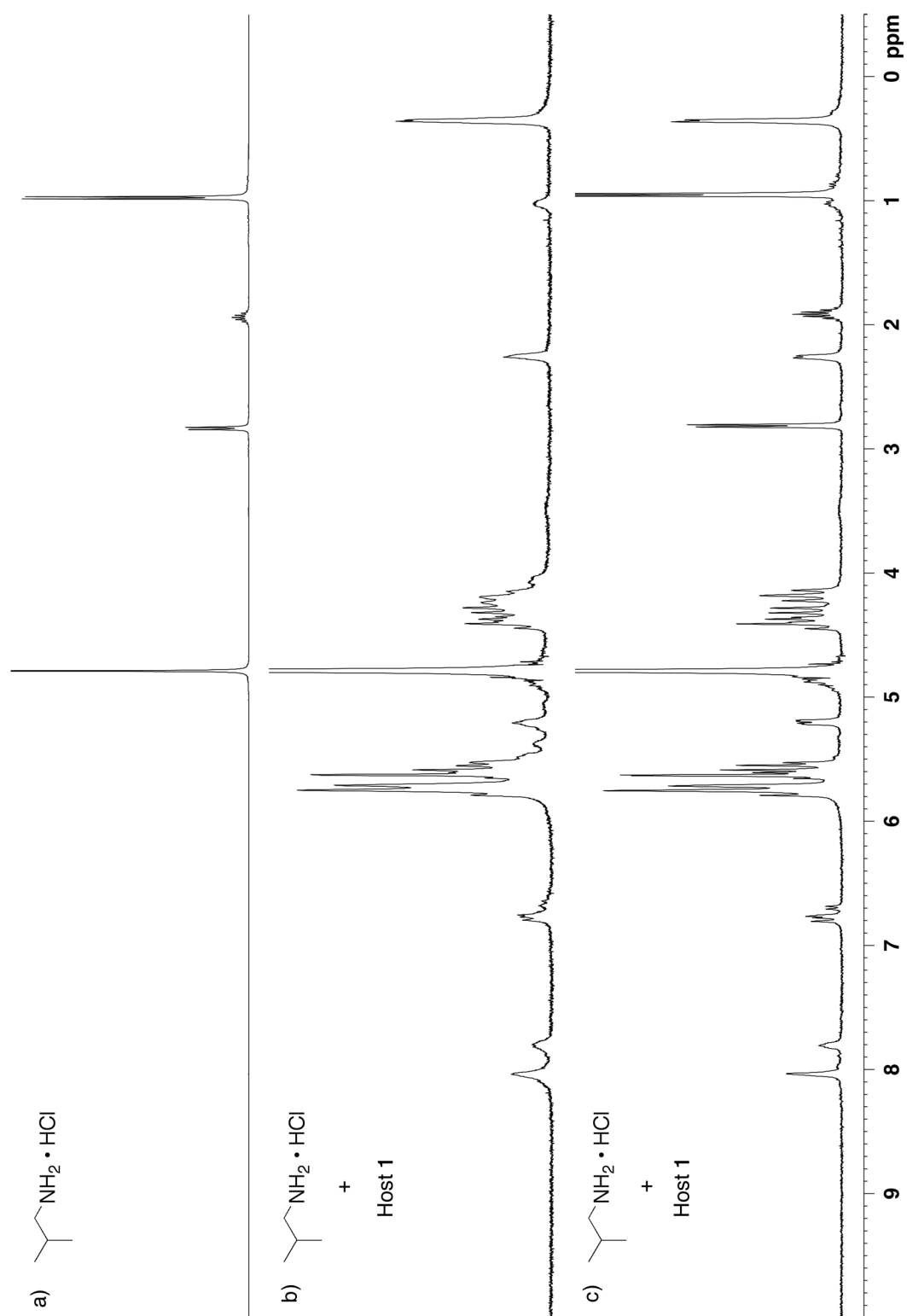


Figure III-S42. ^1H NMR spectra (400 MHz, D_2O , RT) recorded for: a) isobutylamine hydrochloride, b) a mixture of isobutylamine hydrochloride and **III-1** (2:1 ratio), and c) a mixture of isobutylamine hydrochloride and **III-1** (>2:1 ratio).

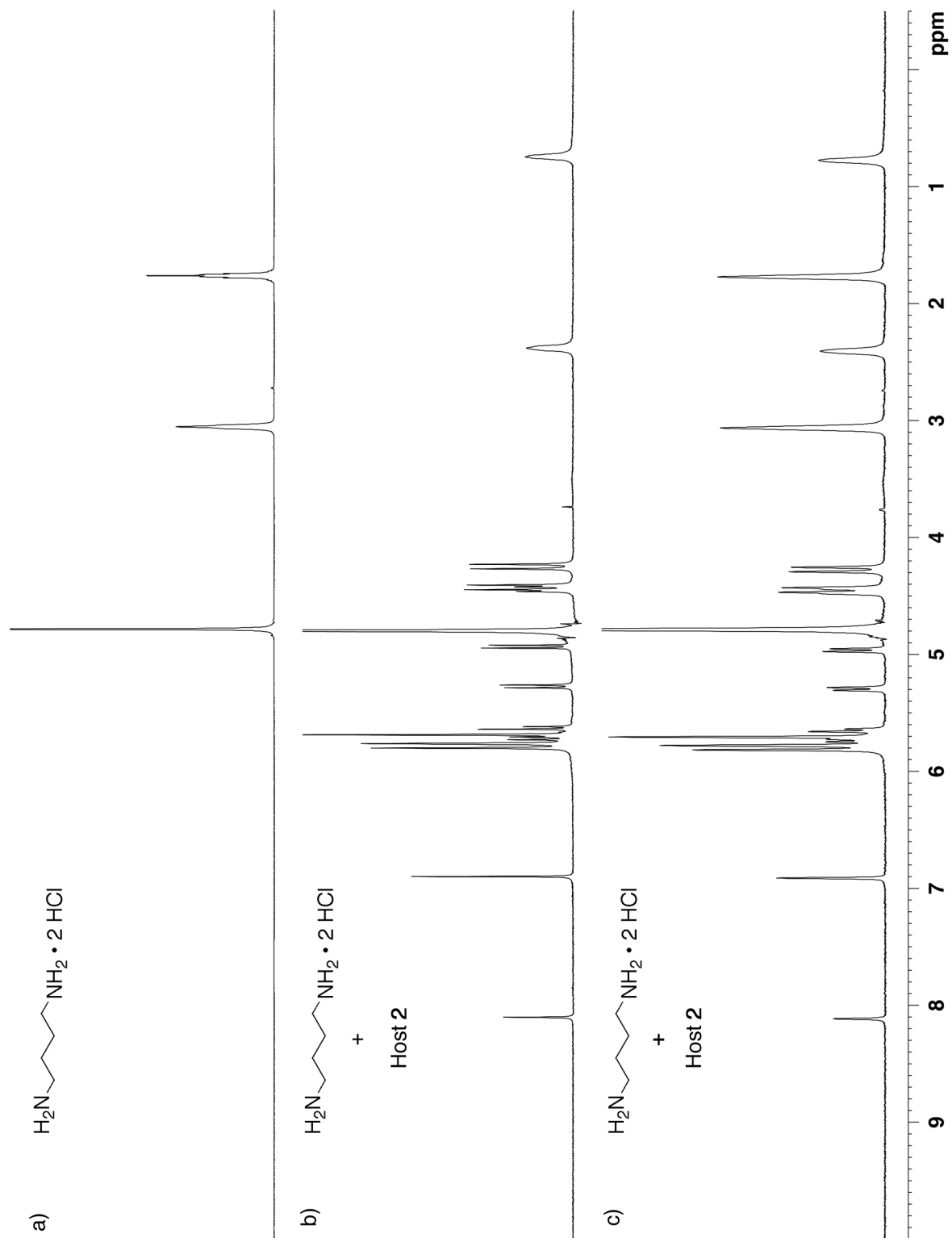


Figure III-S43. ^1H NMR spectra (400 MHz, D_2O , RT) recorded for: a) butanediamine dihydrochloride, b) a mixture of butanediamine dihydrochloride and **III-2** (2:1 ratio), and c) a mixture of butanediamine dihydrochloride and **III-2** (>2:1 ratio).

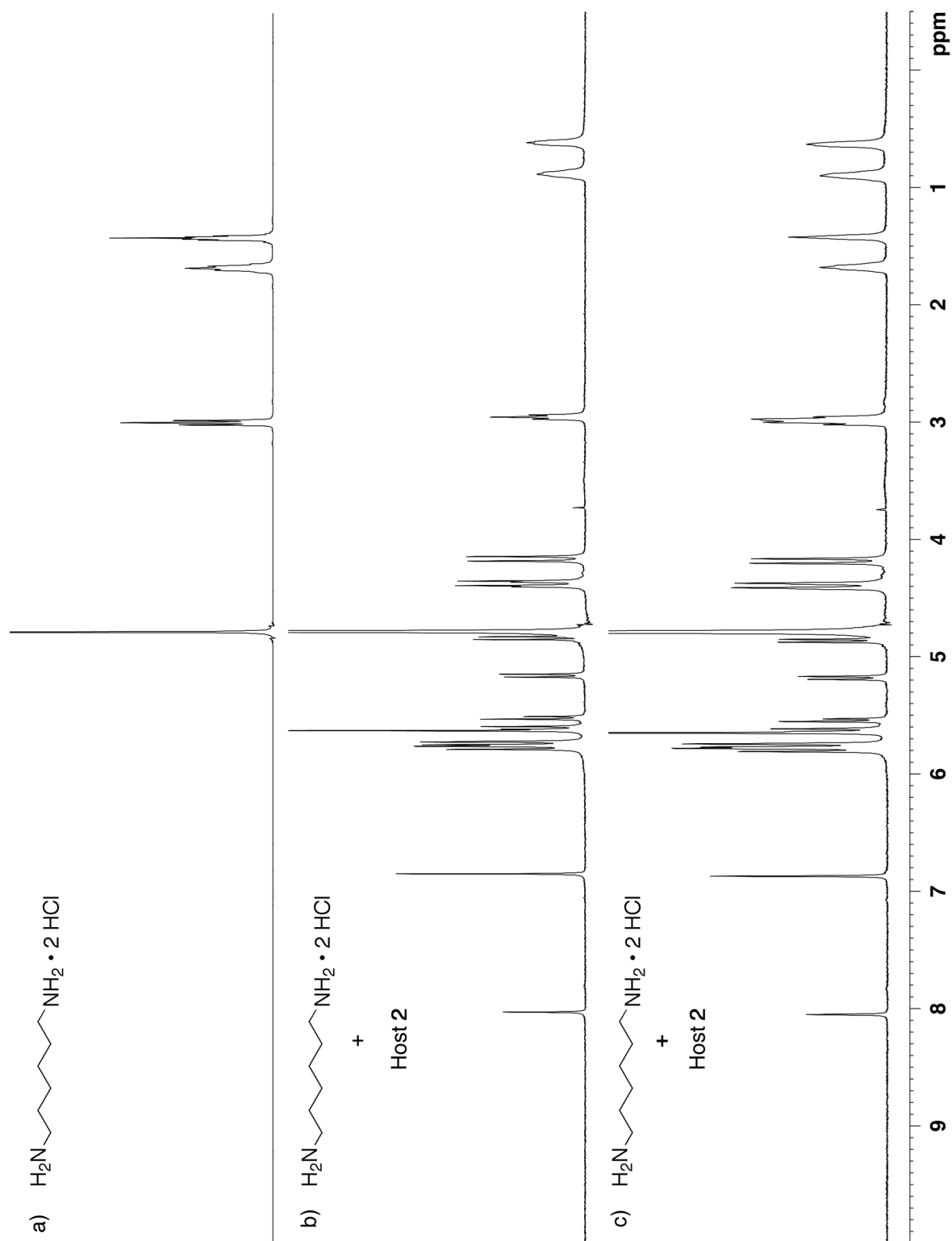


Figure III-S44. ^1H NMR spectra (400 MHz, D_2O , RT) recorded for: a) hexanediamine dihydrochloride, b) a mixture of hexanediamine dihydrochloride and **III-2** (2:1 ratio), and c) a mixture of hexanediamine dihydrochloride and **III-2** (>2:1 ratio).

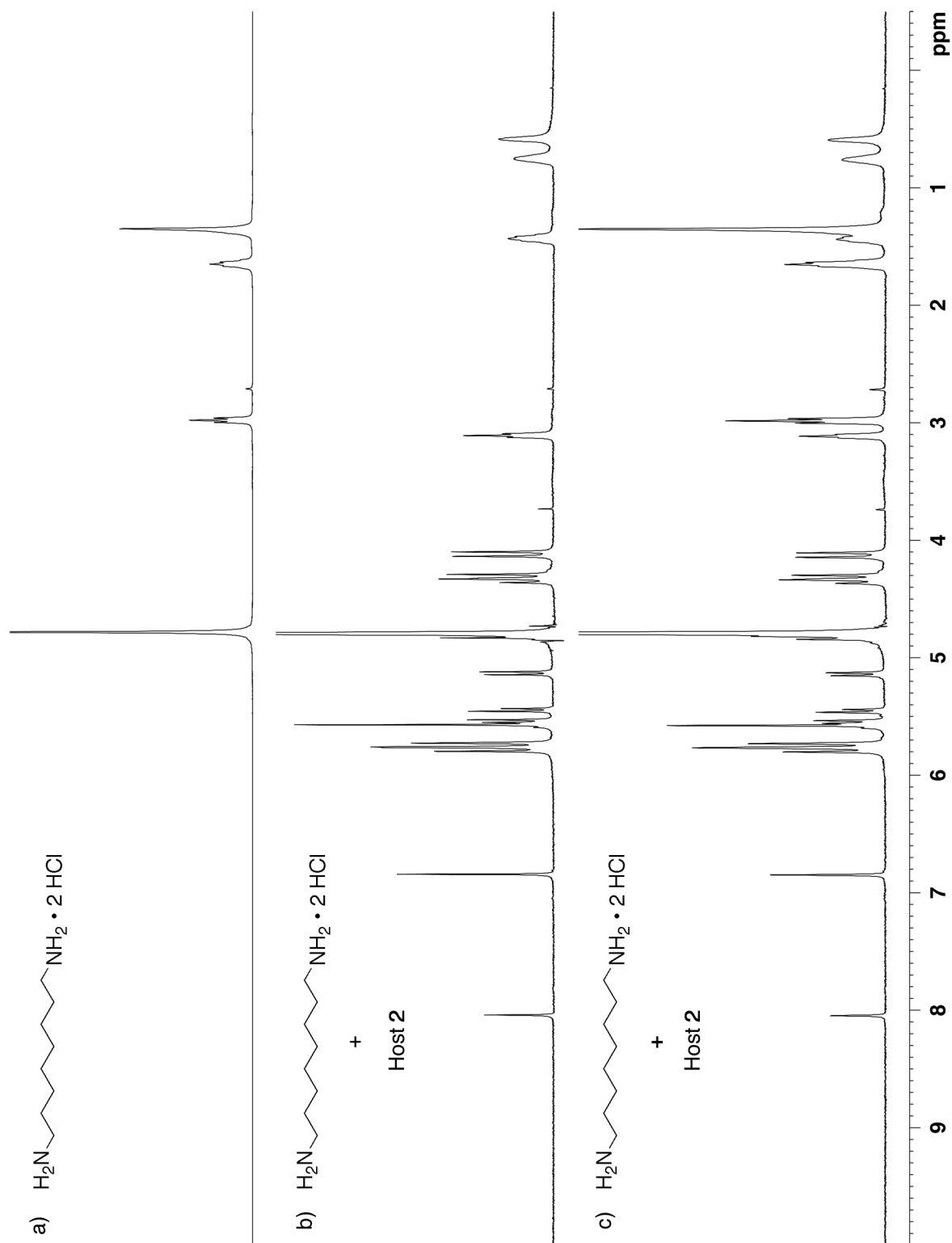


Figure III-S45. ^1H NMR spectra (400 MHz, D_2O , RT) recorded for: a) octanediamine dihydrochloride, b) a mixture of octanediamine dihydrochloride and **III-2** (2:1 ratio), and c) a mixture of octanediamine dihydrochloride and **III-2** (>2:1 ratio).

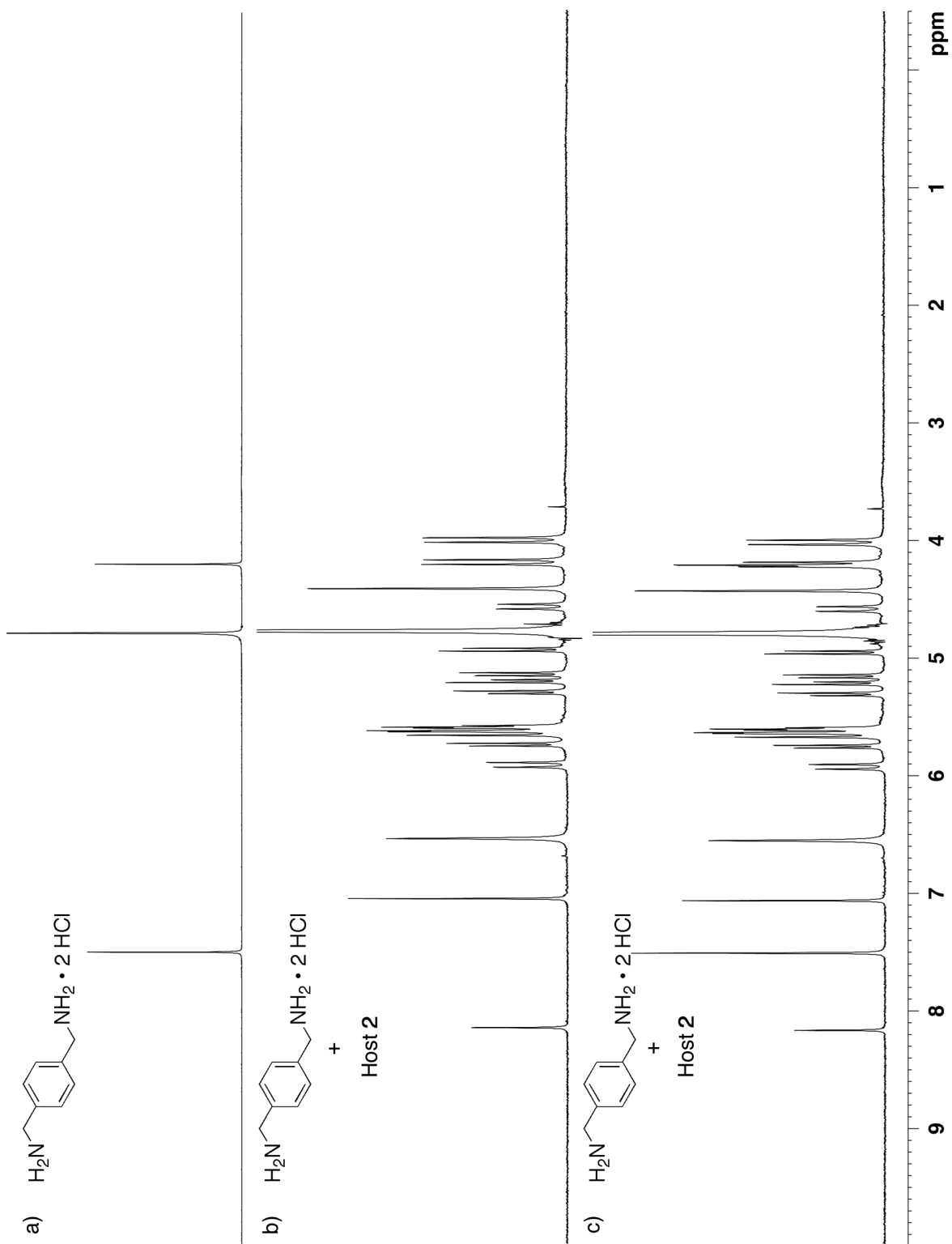


Figure III-S46. ^1H NMR spectra (400 MHz, D_2O , RT) recorded for: a) *p*-xylenediamine dihydrochloride, b) a mixture of *p*-xylenediamine dihydrochloride and **III-2** (2:1 ratio), and c) a mixture of *p*-xylenediamine dihydrochloride and **III-2** (>2:1 ratio).

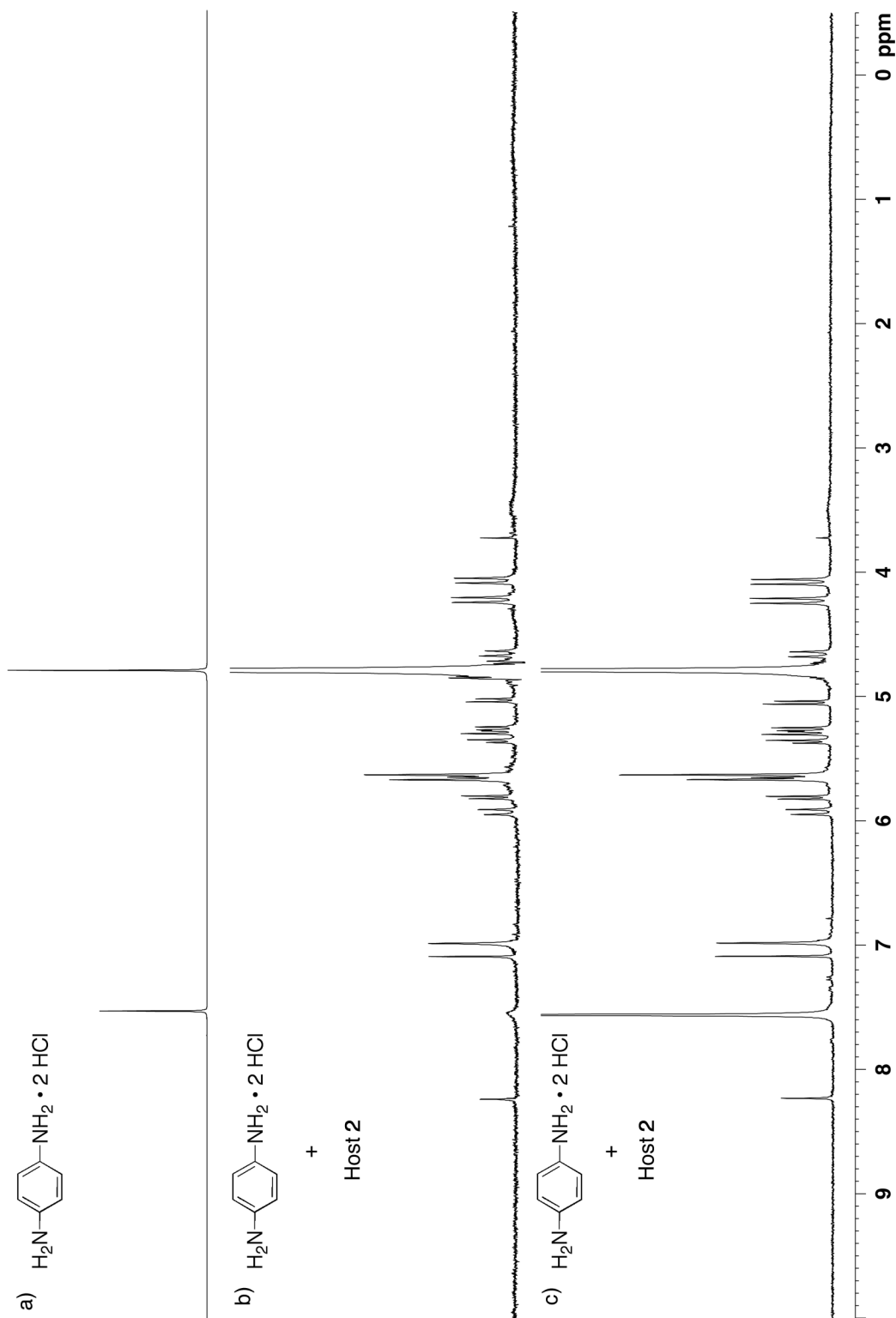


Figure III-S47. ^1H NMR spectra (400 MHz, D_2O , RT) recorded for: a) *p*-phenylenediamine dihydrochloride, b) a mixture of *p*-phenylenediamine dihydrochloride and **III-2** (2:1 ratio), and c) a mixture of *p*-phenylenediamine dihydrochloride and **III-2** (>2:1 ratio).

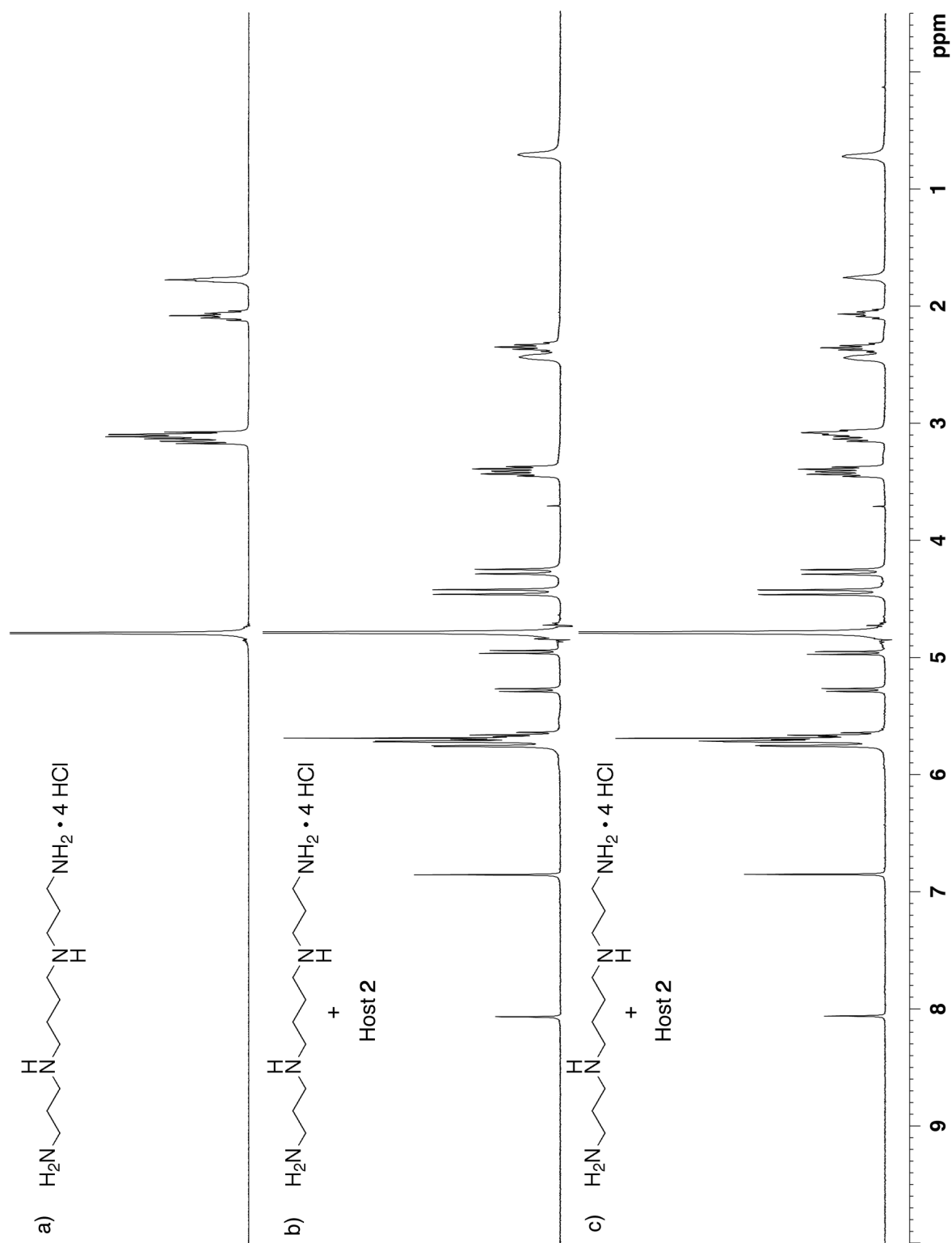


Figure III-S48. ^1H NMR spectra (400 MHz, D_2O , RT) recorded for: a) spermine tetrahydrochloride, b) a mixture of spermine tetrahydrochloride and **III-2** (2:1 ratio), and c) a mixture of spermine tetrahydrochloride and **III-2** (>2:1 ratio).

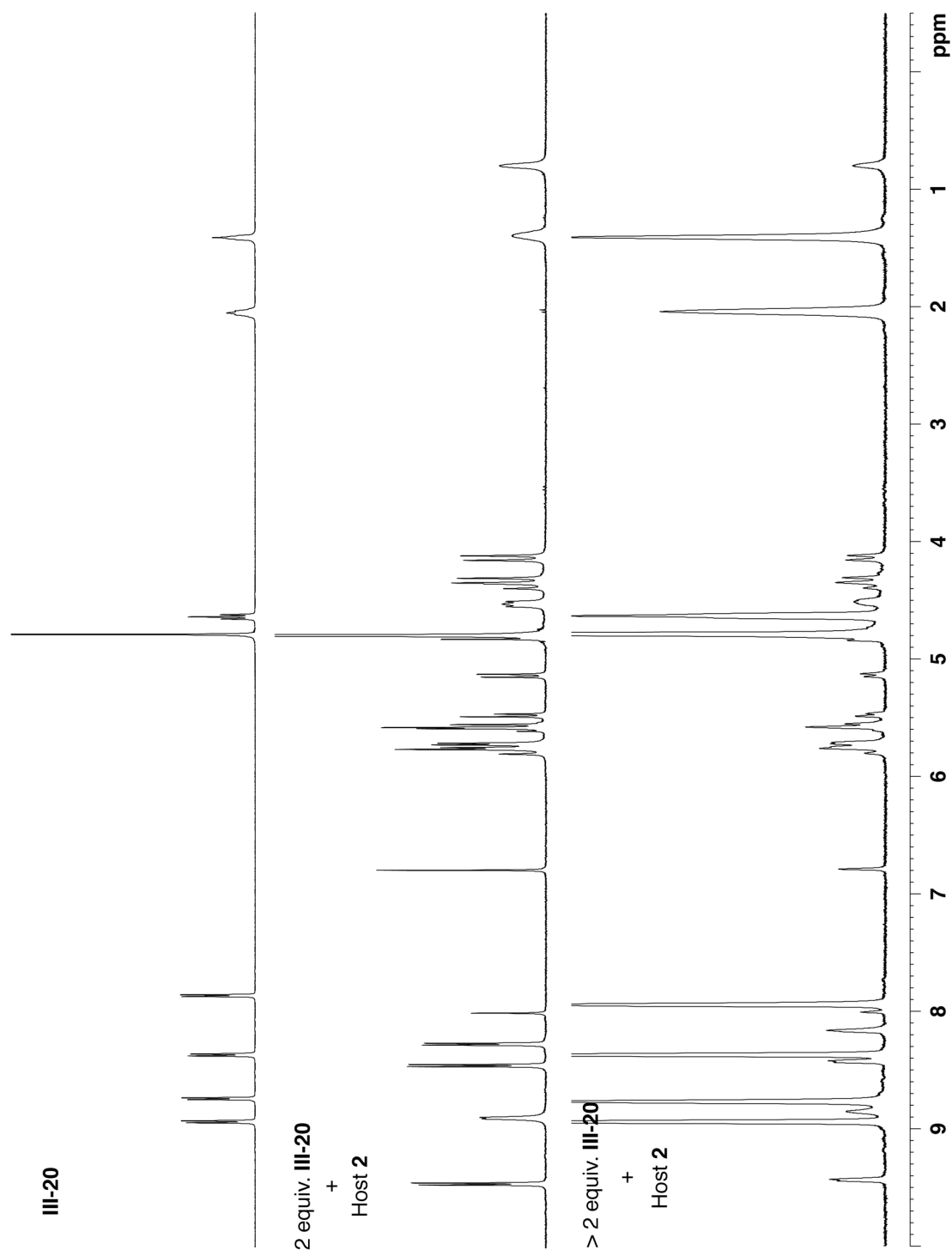


Figure III-S49. ^1H NMR spectra (400 MHz, D_2O , RT) recorded for: a) **III-20** \cdot 2 Br^- , b) a mixture of **III-20** \cdot 2 Br^- and **III-2** (2:1 ratio), and c) a mixture of **III-20** \cdot 2 Br^- and **III-2** (> 2:1 ratio).

Details of the crystal structure of III-1.



A colorless plate-like specimen of $C_{108}H_{163}F_{36}N_{48}O_{86.50}$, approximate dimensions $0.12 \text{ mm} \times 0.40 \text{ mm} \times 0.46 \text{ mm}$, was used for the X-ray crystallographic analysis. The X-ray intensity data were measured on a Bruker Smart APex2, CCD system equipped with a graphite monochromator and a MoK α fine focus sealed tube ($\lambda = 0.71073 \text{ \AA}$). Data collection temperature was 100 K.

The total exposure time was 25.25 hours. The frames were integrated with the Bruker SAINT software package using a narrow-frame algorithm. The integration of the data using a monoclinic unit cell yielded a total of 82943 reflections to a maximum θ angle of 25.00° (0.84 \AA resolution), of which 14974 were independent (average redundancy 5.539, completeness = 99.8%, $R_{\text{int}} = 6.49\%$, $R_{\text{sig}} = 3.82\%$) and 12587 (84.06%) were greater than $2\sigma(F^2)$. The final cell constants of $a = 34.886(5) \text{ \AA}$, $b = 15.865(2) \text{ \AA}$, $c = 15.391(2) \text{ \AA}$, $\beta = 92.500(2)^\circ$, $V = 8510.(2) \text{ \AA}^3$, are based upon the refinement of the XYZ-centroids of 9208 reflections above $20 \sigma(I)$ with $4.428^\circ < 2\theta < 55.41^\circ$. Data were corrected for absorption effects using the multi-scan method (SADABS). The calculated minimum and maximum transmission coefficients (based on crystal size) are 0.9294 and 0.9807.

The structure was solved and refined using the Bruker SHELXTL Software Package, using the space group $P2/c$, with $Z = 2$ for the formula unit, $C_{108}H_{163}F_{36}N_{48}O_{86.50}$. The final anisotropic full-matrix least-squares refinement on F^2 with 953 variables converged at $R_1 = 8.72\%$, for the observed data and $wR_2 = 18.38\%$ for all data. The goodness-of-fit was 1.000. The largest peak in the final difference electron density synthesis was $0.707 \text{ e}^-/\text{\AA}^3$ and the largest hole was $-0.579 \text{ e}^-/\text{\AA}^3$ with an RMS deviation of $0.085 \text{ e}^-/\text{\AA}^3$. On the basis of the final model, the calculated density was 1.640 g/cm^3 and $F(000)$, 4326 e^- .

APEX2 Version 2010.11-3 (Bruker AXS Inc.)
 SAINT Version 7.68A (Bruker AXS Inc., 2009)
 SADABS Version 2008/1 (G. M. Sheldrick, Bruker AXS Inc.)
 XPREP Version 2008/2 (G. M. Sheldrick, Bruker AXS Inc.)
 XS Version 2008/1 (G. M. Sheldrick, *Acta Cryst.* (2008). **A64**, 112-122)
 XL Version 2008/4 (G. M. Sheldrick, *Acta Cryst.* (2008). **A64**, 112-122)
 Platon (A. L. Spek, *Acta Cryst.* (1990). **A46**, C-34)

Table III-S1. Sample and crystal data for UM2160.

| | | |
|------------------------|---------------------------------------|---------------------------|
| Identification code | 2160 | |
| Chemical formula | $C_{108}H_{163}F_{36}N_{48}O_{86.50}$ | |
| Formula weight | 4201.86 | |
| Temperature | 100(2) K | |
| Wavelength | 0.71073 \AA | |
| Crystal size | 0.12 \times 0.40 \times 0.46 mm | |
| Crystal habit | colorless plate | |
| Crystal system | monoclinic | |
| Space group | $P 1 2/c 1$ | |
| Unit cell dimensions | $a = 34.886(5) \text{ \AA}$ | $\alpha = 90^\circ$ |
| | $b = 15.865(2) \text{ \AA}$ | $\beta = 92.500(2)^\circ$ |
| | $c = 15.391(2) \text{ \AA}$ | $\gamma = 90^\circ$ |
| Volume | $8510.(2) \text{ \AA}^3$ | |
| Z | 2 | |
| Density (calculated) | 1.640 Mg/cm^3 | |
| Absorption coefficient | 0.163 mm^{-1} | |
| $F(000)$ | 4326 | |

Table III-S2. Data collection and structure refinement for UM2160.

| | | |
|-------------------------------------|--|--|
| Diffractometer | Bruker Smart Apex2, CCD | |
| Radiation source | fine focus sealed tube, MoK α | |
| Theta range for data collection | 2.15 to 25.00° | |
| Index ranges | -41 ≤ h ≤ 41, -18 ≤ k ≤ 18, -18 ≤ l ≤ 18 | |
| Reflections collected | 82943 | |
| Independent reflections | 14974 [R(int) = 0.0649] | |
| Coverage of independent reflections | 99.8% | |
| Absorption correction | multi-scan | |
| Max. and min. transmission | 0.9807 and 0.9294 | |
| Structure solution technique | direct methods | |
| Structure solution program | SHELXS-97 (Sheldrick, 2008) | |
| Refinement method | Full-matrix least-squares on F ² | |
| Refinement program | SHELXL-97 (Sheldrick, 2008) | |
| Function minimized | $\Sigma w(F_o^2 - F_c^2)^2$ | |
| Data / restraints / parameters | 14974 / 69 / 953 | |
| Goodness-of-fit on F ² | 1.000 | |
| Δ/σ_{\max} | 0.001 | |
| Final R indices | 12587 data; I > 2 σ (I) | R ₁ = 0.0872, wR ₂ = 0.1796 |
| | all data | R ₁ = 0.0967, wR ₂ = 0.1838 |
| Weighting scheme | w = 1/[$\sigma^2(F_o^2) + (0.0100P)^2 + 45.3000P$], P = (F _o ² + 2F _c ²)/3 | |
| Largest diff. peak and hole | 0.707 and -0.579 eÅ ⁻³ | |
| R.M.S. deviation from mean | 0.085 eÅ ⁻³ | |

$$R_{\text{int}} = \frac{\Sigma |F_o^2 - F_o^2(\text{mean})|}{\Sigma [F_o^2]} \quad R_1 = \frac{\Sigma ||F_o| - |F_c||}{\Sigma |F_o|}$$

$$\text{GOOF} = S = \{\Sigma [w(F_o^2 - F_c^2)^2] / (n - p)\}^{1/2} \quad wR_2 = \{\Sigma [w(F_o^2 - F_c^2)^2] / \Sigma [w(F_o^2)^2]\}^{1/2}$$

Bibliography

- (1) Lehn, J.-M. *Angew. Chem. Int. Ed.* **1988**, *27*, 89–112.
- (2) Cram, D. J. *Angew. Chem. Int. Ed.* **1988**, *27*, 1009–1020.
- (3) Pedersen, C. J. *Angew. Chem. Int. Ed.* **1988**, *27*, 1021–1027.
- (4) Comprehensive Supramolecular Chemistry Vol. 1 Molecular Recognition: Receptors for Cationic Guests (Ed.: G. W. Gokel), Pergamon, Oxford, 1996.
- (5) Comprehensive Supramolecular Chemistry Vol. 2 Molecular Recognition: Receptors for Molecular Guests (Ed.: F. Vögtle), Pergamon, Oxford, 1996.
- (6) Comprehensive Supramolecular Chemistry, Vol. 3 Cyclodextrins (Eds.: J. Szejtli, T. Osa), Pergamon, Oxford, 1996.
- (7) Trinh, T.; Cappel, J. P.; Geis, P. A.; McCarty, M. L.; Pilosof, D.; Zwerdling, S. S. Uncomplexed Cyclodextrin Solutions For Odor Control On Inanimate Surfaces. U.S. Patent 5,714,137. Feb. 3, 1998.
- (8) Woo, R. A. M.; Trinh, T.; Cobb, D. S.; Schneiderman, E.; Wolff, A. M.; Rosenbalm, E. L.; Ward, T. E.; Chung, A. H.; Reece, S. Uncomplexed Cyclodextrin Compositions For Odor Control. U.S. Patent Number 6,033,679. Mar. 7, 2000.
- (9) Cameron, K. S.; Clark, J. K.; Cooper, A.; Fielding, L.; Palin, R.; Rutherford, S. J.; Zhang, M.-Q. *Org. Lett.* **2002**, *4*, 3403–3406.
- (10) Adam, J. M.; Bennett, D. J.; Bom, A.; Clark, J. K.; Feilden, H.; Hutchinson, E. J.; Palin, R.; Prosser, A.; Rees, D. C.; Rosair, G. M.; Stevenson, D.; Tarver, G. J.; Zhang, M.-Q. *J. Med. Chem.* **2002**, *45*, 1806–1816.

- (11) Bom, A.; Bradley, M.; Cameron, K.; Clark, J. K.; Van Egmond, J.; Feilden, H.; MacLean, E. J.; Muir, A. W.; Palin, R.; Rees, D. C.; Zhang, M.-Q. *Angew. Chem. Int. Ed.* **2002**, *41*, 266–270.
- (12) Leigh, D. A.; Wong, J. K. Y.; Dehez, F.; Zerbetto, F. *Nature* **2003**, *424*, 174–179.
- (13) Hernández, J. V.; Kay, E. R.; Leigh, D. A. *Science* **2004**, *306*, 1532–1537.
- (14) Castellano, R. K.; Rudkevich, D. M.; Rebek, J. *Proc. Natl. Acad. Sci. USA* **1997**, *94*, 7132–7137.
- (15) Screen, T. E. O.; Thorne, J. R. G.; Denning, R. G.; Bucknall, D. G.; Anderson, H. L. *J. Am. Chem. Soc.* **2002**, *124*, 9712–9713.
- (16) Kay, E.; Leigh, D.; Zerbetto, F. *Angew. Chem. Int. Ed.* **2007**, *46*, 72–191.
- (17) Brunsveld, L.; Folmer, B. J.; Meijer, E. W.; Sijbesma, R. P. *Chem. Rev.* **2001**, *101*, 4071–4098.
- (18) De Greef, T. F. A.; Smulders, M. M. J.; Wolffs, M.; Schenning, A. P. H. J.; Sijbesma, R. P.; Meijer, E. W. *Chem. Rev.* **2009**, *109*, 5687–5754.
- (19) Behrend, R.; Meyer, E.; Rusche, F. *Liebigs Ann. Chem.* **1905**, *339*, 1–37.
- (20) Freeman, W.; Mock, W.; Shih, N. *J. Am. Chem. Soc.* **1981**, *103*, 7367–7368.
- (21) Mock, W.; Shih, N. *J. Org. Chem.* **1986**, *51*, 4440–4446.
- (22) Mock, W. L.; Shih, N. Y. *J. Am. Chem. Soc.* **1989**, *111*, 2697–2699.
- (23) Hoffmann, R.; Knoche, W.; Fenn, C.; Buschmann, H. J. *J. Chem. Soc., Faraday Trans.* **1994**, *90*, 1507–1511.
- (24) Buschmann, H. J.; Mutihac, L.; Jansen, K. *J. Inclusion Phenom. Macrocyclic Chem.* **2001**, *39*, 1–11.

- (25) Day, A. I.; Blanch, R. J.; Arnold, A. P.; Lorenzo, S.; Lewis, G. R.; Dance, I. *Angew. Chem. Int. Ed.* **2002**, *41*, 275–277.
- (26) Kim, J.; Jung, I. S.; Kim, S. Y.; Lee, E.; Kang, J. K.; Sakamoto, S.; Yamaguchi, K.; Kim, K. *J. Am. Chem. Soc.* **2000**, *122*, 540–541.
- (27) Lee, J. W.; Samal, S.; Selvapalam, N.; Kim, H.-J.; Kim, K. *Acc. Chem. Res.* **2003**, *36*, 621–630.
- (28) Wu, A.; Chakraborty, A.; Witt, D.; Lagona, J.; Damkaci, F.; Ofori, M. A.; Chiles, J. K.; Fettinger, J. C.; Isaacs, L. *J. Org. Chem.* **2002**, *67*, 5817–5830.
- (29) Chakraborty, A.; Wu, A.; Witt, D.; Lagona, J.; Fettinger, J. C.; Isaacs, L. *J. Am. Chem. Soc.* **2002**, *124*, 8297–8306.
- (30) Liu, S.; Zavalij, P. Y.; Isaacs, L. *J. Am. Chem. Soc.* **2005**, *127*, 16798–16799.
- (31) Huang, W.-H.; Zavalij, P. Y.; Isaacs, L. *J. Am. Chem. Soc.* **2008**, *130*, 8446–8454.
- (32) Lagona, J.; Mukhopadhyay, P.; Chakrabarti, S.; Isaacs, L. *Angew. Chem. Int. Ed.* **2005**, *44*, 4844–4870.
- (33) Liu, S.; Ruspic, C.; Mukhopadhyay, P.; Chakrabarti, S.; Zavalij, P.; Isaacs, L. *J. Am. Chem. Soc.* **2005**, *127*, 15959–15967.
- (34) Rekharsky, M. V.; Mori, T.; Yang, C.; Ko, Y. H.; Selvapalam, N.; Kim, H.; Sobransingh, D.; Kaifer, A. E.; Liu, S.; Isaacs, L.; Chen, W.; Moghaddam, S.; Gilson, M. K.; Kim, K.; Inoue, Y. *Proc. Natl. Acad. Sci. USA* **2007**, *104*, 20737–20742.

- (35) Huang, W.-H.; Zavalij, P. Y.; Isaacs, L. *Angew. Chem. Int. Ed.* **2007**, *46*, 7425–7427.
- (36) Huang, W.-H.; Zavalij, P. Y.; Isaacs, L. *Org. Lett.* **2008**, *10*, 2577–2580.
- (37) Huang, W.-H.; Liu, S.; Zavalij, P. Y.; Isaacs, L. *J. Am. Chem. Soc.* **2006**, *128*, 14744–14745.
- (38) Jon, S. Y.; Selvapalam, N.; Oh, D. H.; Kang, J.-K.; Kim, S.-Y.; Jeon, Y. J.; Lee, J. W.; Kim, K. *J. Am. Chem. Soc.* **2003**, *125*, 10186–10187.
- (39) Zhao, N.; Lloyd, G. O.; Scherman, O. A. *Chem. Commun.* **2012**, *48*, 3070–3072.
- (40) Lucas, D.; Minami, T.; Iannuzzi, G.; Cao, L.; Wittenberg, J. B.; Anzenbacher, P., Jr.; Isaacs, L. *J. Am. Chem. Soc.* **2011**, *133*, 17966–17976.
- (41) Vinciguerra, B.; Cao, L.; Cannon, J. R.; Zavalij, P. Y.; Fenselau, C.; Isaacs, L. *J. Am. Chem. Soc.* **2012**, *134*, 13133–13140.
- (42) Wittenberg, J. B.; Costales, M. G.; Zavalij, P. Y.; Isaacs, L. *Chem. Commun.* **2011**, *47*, 9420–9422.
- (43) Nally, R.; Isaacs, L. *Tetrahedron* **2009**, *65*, 7249–7258.
- (44) Anderson, S.; Anderson, H. L.; Sanders, J. K. M. *Acc. Chem. Res.* **1993**, *26*, 469–475.
- (45) Lucas, D.; Isaacs, L. *Org. Lett.* **2011**, *13*, 4112–4115.
- (46) Cao, L.; Isaacs, L. *Org. Lett.* **2012**, *14*, 3072–3075.
- (47) Hennig, A.; Bakirci, H.; Nau, W. M. *Nat. Methods* **2007**, *4*, 629–632.
- (48) Chinai, J. M.; Taylor, A. B.; Ryno, L. M.; Hargreaves, N. D.; Morris, C. A.; Hart, P. J.; Urbach, A. R. *J. Am. Chem. Soc.* **2011**, *133*, 8810–8813.

- (49) Urbach, A. R.; Ramalingam, V. *Israel J. Chem.* **2011**, *51*, 664-678.
- (50) Zhao, N.; Lloyd, G. O.; Scherman, O. A. *Chem. Commun.* **2012**, *48*, 3070–3072.
- (51) Kim, H. J.; Heo, J.; Jeon, W. S.; Lee, E.; Kim, J.; Sakamoto, S.; Yamaguchi, K.; Kim, K. *Angew. Chem. Int. Ed.* **2001**, *40*, 1526–1529.
- (52) Jeon, W. S.; Kim, E.; Ko, Y. H.; Hwang, I.; Lee, J. W.; Kim, S.-Y.; Kim, H.-J.; Kim, K. *Angew. Chem. Int. Ed.* **2005**, *44*, 87–91.
- (53) Moon, K.; Grindstaff, J.; Sobransingh, D.; Kaifer, A. E. *Angew. Chem. Int. Ed.* **2004**, *43*, 5496–5499.
- (54) Wang, W.; Kaifer, A. E. *Angew. Chem. Int. Ed.* **2006**, *45*, 7042–7046.
- (55) Rajgariah, P.; Urbach, A. R. *J. Inclusion Phenom. Macrocyclic Chem.* **2008**, *62*, 251–254.
- (56) Reczek, J. J.; Kennedy, A. A.; Halbert, B. T.; Urbach, A. R. *J. Am. Chem. Soc.* **2009**, *131*, 2408–2415.
- (57) Rauwald, U.; Scherman, O. A. *Angew. Chem. Int. Ed.* **2008**, *47*, 3950–3953.
- (58) Liu, Y.; Liu, K.; Wang, Z.; Zhang, X. *Chem. Eur. J.* **2011**, *17*, 9930–9935.
- (59) Uhlenheuer, D. A.; Petkau, K.; Brunsveld, L. *Chem. Soc. Rev.* **2010**, *39*, 2817–2826.
- (60) Uhlenheuer, D. A.; Young, J. F.; Nguyen, H. D.; Scheepstra, M.; Brunsveld, L. *Chem. Commun.* **2011**, *47*, 6798–6800.
- (61) Lee, J.; Samal, S.; Selvapalam, N.; Kim, H.; Kim, K. *Acc. Chem. Res.* **2003**, *36*, 621–630.

- (62) Day, A.; Arnold, A.; Blanch, R.; Snushall, B. *J. Org. Chem.* **2001**, *66*, 8094–8100.
- (63) Jeon, W. S.; Ziganshina, A. Y.; Lee, J. W.; Ko, Y. H.; Kang, J.-K.; Lee, C.; Kim, K. *Angew. Chem. Int. Ed.* **2003**, *42*, 4097–4100.
- (64) Ko, Y. H.; Kim, E.; Hwang, I.; Kim, K. *Chem. Commun.* **2007**, 1305–1315.
- (65) Mock, W. L.; Pierpont, J. J. *Chem. Soc., Chem. Commun.* **1990**, 1509–1511.
- (66) Zhao, J.; Kim, H.; Oh, J.; Kim, S.; Lee, J.; Sakamoto, S.; Yamaguchi, K.; Kim, K. *Angew. Chem. Int. Ed.* **2001**, *40*, 4233–4235.
- (67) Sindelar, V.; Cejas, M. A.; Raymo, F. M.; Chen, W.; Parker, S. E.; Kaifer, A. E. *Chem. Eur. J.* **2005**, *11*, 7054–7059.
- (68) Bush, M. E.; Bouley, N. D.; Urbach, A. R. *J. Am. Chem. Soc.* **2005**, *127*, 14511–14517.
- (69) Wagner, B. D.; Boland, P. G.; Lagona, J.; Isaacs, L. *J. Phys. Chem. B* **2005**, *109*, 7686–7691.
- (70) Young, J. F.; Nguyen, H. D.; Yang, L.; Huskens, J.; Jonkheijm, P.; Brunsveld, L. *ChemBioChem.* **2009**, *11*, 180–183.
- (71) Appel, E. A.; Biedermann, F.; Rauwald, U.; Jones, S. T.; Zayed, J. M.; Scherman, O. A. *J. Am. Chem. Soc.* **2010**, *132*, 14251–14260.
- (72) Kim, K.; Kim, D.; Lee, J. W.; Ko, Y. H.; Kim, K. *Chem. Commun.* **2004**, 848–849.
- (73) Liu, Y.; Yu, Y.; Gao, J.; Wang, Z.; Zhang, X. *Angew. Chem. Int. Ed.* **2010**, *49*, 6576–6579.

- (74) Liu, S.; Zavalij, P. Y.; Lam, Y.-F.; Isaacs, L. *J. Am. Chem. Soc.* **2007**, *129*, 11232–11241.
- (75) Ghosh, S.; Isaacs, L. *J. Am. Chem. Soc.* **2010**, *132*, 4445–4454.
- (76) Kim, C.; Agasti, S. S.; Zhu, Z.; Isaacs, L.; Rotello, V. M. *Nature Chem.* **2010**, *2*, 962–966.
- (77) Mock, W. L.; Irra, T. A.; Wepsiec, J. P.; Adhya, M. *J. Org. Chem.* **1989**, *54*, 5302–5308.
- (78) Tuncel, D.; Steinke, J. H. G. *Macromolecules* **2004**, *37*, 288–302.
- (79) Yang, C.; Ko, Y. H.; Selvapalam, N.; Origane, Y.; Mori, T.; Wada, T.; Kim, K.; Inoue, Y. *Org. Lett.* **2007**, *9*, 4789–4792.
- (80) Ma, D.; Gargulakova, Z.; Zavalij, P. Y.; Sindelar, V.; Isaacs, L. *J. Org. Chem.* **2010**, *75*, 2934–2941.
- (81) Lagona, J.; Fettinger, J. C.; Isaacs, L. *J. Org. Chem.* **2005**, *70*, 10381–10392.
- (82) Miyahara, Y.; Goto, K.; Oka, M.; Inazu, T. *Angew. Chem. Int. Ed.* **2004**, *43*, 5019–5022.
- (83) Svec, J.; Necas, M.; Sindelar, V. *Angew. Chem. Int. Ed.* **2010**, *49*, 2378–2381.
- (84) Taylor, R.; Kennard, O. *Acc. Chem. Res.* **1984**, *17*, 320–326.
- (85) Leeming, S. W.; Anemian, R. M.; Williams, R.; Brown, B. A. Oligomeric Polyacene and Semiconductor Formulation. Int. Patent Number WO 2006/125504 A1. Nov. 30, 2006.
- (86) Schrievers, T.; Brinker, U. H. *Synthesis* **1988**, 330–331.

- (87) Zhao, Y.; Xue, S.; Tao, Z.; Zhang, J.; Wei, Z.; Long, L.; Hu, M.; Xiao, H.; Day, A. *Chin. Sci. Bull.* **2004**, *49*, 1111–1116.
- (88) Samsonenko, D. G.; Virovets, A. V.; Lipkowski, J.; Geras'ko, O. A.; Fedin, V. P. *J. Struct. Chem.* **2002**, *43*, 664–668.
- (89) Bardelang, D.; Udachin, K. A.; Leek, D. M.; Margeson, J. C.; Chan, G.; Ratcliffe, C. I.; Ripmeester, J. A. *Cryst. Growth Des.* **2011**, *11*, 5598–5614.
- (90) Harris, J. M.; Struck, E. C.; Case, M. G.; Paley, M. S.; Yalpani, M.; Van Alstine, J. M.; Brooks, D. E. *J. Polym. Sci. Polym. Chem. Ed.* **1984**, *22*, 341–352.
- (91) Li, J.; Kao, W. J. *Biomacromolecules* **2003**, *4*, 1055–1067.
- (92) Roberts, M. J.; Bentley, M. D.; Harris, J. M. *Adv. Drug Deliver. Rev.* **2012**, *64*, 116–127.
- (93) Cohen, Y.; Avram, L.; Frish, L. *Angew. Chem. Int. Ed.* **2005**, *44*, 520–554.
- (94) Zhu, P.; Yang, H.; Peng, C.; Zhang, X. *Macromol. Chem. Phys.* **2001**, *202*, 1380–1383.
- (95) Ho, D. L.; Hammouda, B.; Kline, S. R. *J. Polym. Sci. Part B: Polym. Phys.* **2002**, *41*, 135–138.
- (96) Linegar, K. L.; Adeniran, A. E.; Kostko, A. F.; Anisimov, M. A. *Colloid J.* **2010**, *72*, 279–281.
- (97) Shimada, K.; Kato, H.; Saito, T.; Matsuyama, S.; Kinugasa, S. *J. Chem. Phys.* **2005**, *122*, 244914.
- (98) Sugimoto, T.; Suzuki, T.; Shinkai, S.; Sada, K. *J. Am. Chem. Soc.* **2007**, *129*, 270–271.

- (99) Ohi, H.; Tachi, Y.; Itoh, S. *Inorg. Chem.* **2004**, *43*, 4561–4563.
- (100) Chou, C.-M.; Lee, S.-L.; Chen, C.-H.; Biju, A. T.; Wang, H.-W.; Wu, Y.-L.; Zhang, G.-F.; Yang, K.-W.; Lim, T.-S.; Huang, M.-J.; Tsai, P.-Y.; Lin, K.-C.; Huang, S.-L.; Chen, C.-H.; Luh, T.-Y. *J. Am. Chem. Soc.* **2009**, *131*, 12579–12585.
- (101) Summers, L. A.; Andriopoulos, N.; Channon, A.-L. *J. Heterocyclic Chem.* **1990**, *27*, 595–598.
- (102) Bonchio, M.; Carraro, M.; Casella, G.; Causin, V.; Rastrelli, F.; Saielli, G. *Phys. Chem. Chem. Phys.* **2012**, *14*, 2710–2717.
- (103) Gothard, C. M.; Bruns, C. J.; Gothard, N. A.; Grzybowski, B. A.; Stoddart, J. F. *Org. Lett.* **2012**, *14*, 5066–5069.
- (104) Choi, S. W.; Ritter, H. *Macromol. Rapid Commun.* **2007**, *28*, 101–108.
- (105) Bhattacharya, P.; Kaifer, A. E. *J. Org. Chem.* **2008**, *73*, 5693–5698.
- (106) Zhu, L.; Lu, M.; Zhang, Q.; Qu, D.; Tian, H. *Macromolecules* **2011**, *44*, 4092–4097.
- (107) Yuan, L.; Wang, R.; Macartney, D. H. *J. Org. Chem.* **2007**, *72*, 4539–4542.
- (108) Hvastkovs, E. G.; Buttry, D. A. *Anal. Chem.* **2007**, *79*, 6922–6926.
- (109) Arduini, A.; Bussolati, R.; Credi, A.; Faimani, G.; Garaudée, S.; Pochini, A.; Secchi, A.; Semeraro, M.; Silvi, S.; Venturi, M. *Chem. Eur. J.* **2009**, *15*, 3230–3242.